TITLE

Physical Analysis of Worn Surfaces

Formed under Extreme Pressure

Lubrication Conditions

A Thesis submitted for the degree of

Doctor of Philosophy

in the University of Aston in Birmingham

by

Richard Charles Coy, B.Sc., M.Sc.

Physics Department

November 1973

Abstract

A considerable amount of work, over the last 20 years, has elucidated some of the reactions that take place on the surfaces of steel worn against steel under extreme pressure lubrication conditions. However, in most studies of the worn surfaces only one or two physical analytical techniques have been used. In this study a comprehensive examination of the surfaces has been attempted using a wide selection of physical techniques.

The surface topography of worn specimens has been examined using both optical and scanning electron microscopy. The distribution of the elements in the wear scars in conjunction with the surface topography has been observed with an electron probe microanalyser. The chemical environment of these elements in the wear scars has been studied with an electron spectrometer for chemical analysis and the crystalline structures formed using glancing angle X-ray diffraction. Metallographic techniques have been used on taper sections (micro-indentation hardness tests and etching) to observe the structures formed below the wear scars in the base metal.

These techniques have been applied to specimens worn under varying loads with two groups of additives (three disulphides and two zinc dithio-phosphates) and two base oils. The role of these additives has been studied under antiwear and extreme pressure conditions using the above techniques of physical analysis and the mechanisms of their action have been explained on the basis of the results obtained in this research.

CONTENTS

Abstract

Contents

CHAPTER 1

INTRODUCTION

1.1 Early Tribological Theory and Practice

The problems arising when surfaces slide upon each other are not
new. Animal and vegetable fats have been used for lubricating surfaces
for the past 4000 years (1) and were used almost exclusively up until the
present century. It was not until the Middle Ages that some of the
fundamental laws of Tribology were propounded. Leonardo da Vinci (2)
clearly recognised the first two laws of friction, that the frictional
force is proportional to load and independent of apparent contact area.
These laws were later rediscovered by Amontons (3) and are now associated
with his name. In the same period Newton (4) discovered the law of
viscous flow and this formed the basis of modern fluid film lubrication
theory. Coulomb (5) confirmed Amontons' laws and added a third, namely,
that the frictional force is independent of sliding velocity.

During the eighteenth century the needs of industrialisation led
to considerable improvements in bearing designs and the need for sealed
lubricated bearings was recognised. The increasing use of steam driven
machinery, with the consequent increase in speeds and loads, meant that a
greater understanding of lubrication was required so that one could design
for improved performance and reliability. Adams (6) showed that opposing
bearing surfaces must be separated by a film of lubricant and that there
must be an adequate supply of the lubricant.

In 1883, Petroff (7) investigated bearing friction using animal,
vegetable and mineral oils and concluded that the friction could be
explained as a hydrodynamic phenomenon. Tower (8), in 1884, provided the

first evidence of pressures in the lubricant film in journal bearings in excess of the ambient pressure. Following Tower's work, Reynolds (9) showed that, by applying hydrodynamic principles of viscous flow to a geometry representative of the clearance space in a journal bearing, the motion of the surface of the shaft would produce pressures in the oil film which could support a considerable load.

Thurston (10) was a pioneer in the field of systematic comparative testing of lubricants and provided some of the early "rule-of-thumb" relationships between safe "load per unit area" and speed. In 1895 Kingsbury (11) compared mineral oil, lard oil and mineral oil containing graphite and observed, for the first time under controlled conditions, the characteristic known as "oiliness". Kapff (12) concluded that some property other than viscosity was influential in determining the friction. The extensive work of Sir William Hardy (13) on boundary lubrication showed how friction phenomena could be explained in terms of an adsorbed layer of the lubricant, or some constituent of the lubricant, on each of the sliding surfaces. The nature of the solid surfaces was also very important.

1.2 Types of Lubrication

Figure 1.1 shows the order of magnitude of the separation of sliding surfaces under different conditions.

HYDRODYNAMIC LUBRICATION

In hydrodynamic lubrication (thick film lubrication) the oil film separates the two sliding surfaces completely. The flow of oil between the bearing surfaces produces a pressure in the oil sufficient to separate the surfaces and the physical properties of the oil (density, viscosity, viscosity index, etc.) determine the loads and speeds which can be used in a particular system.
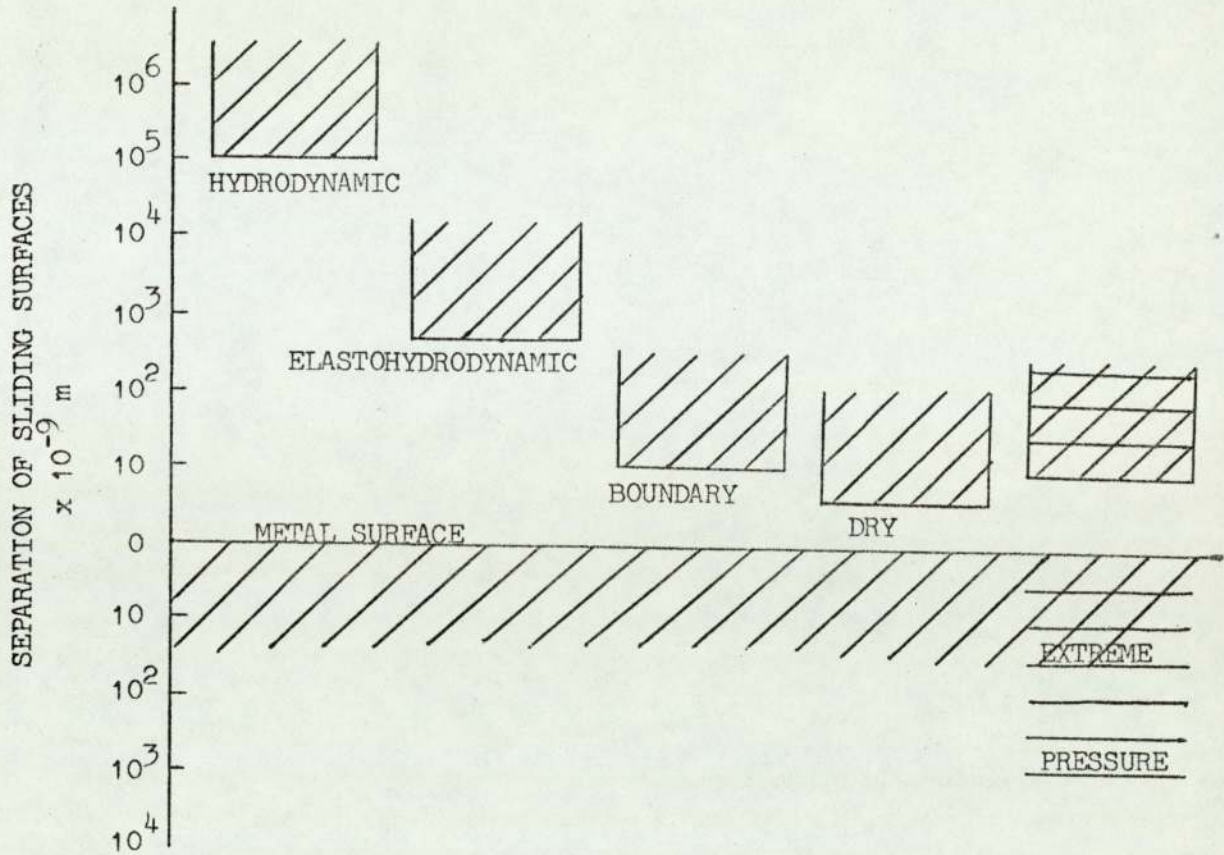
Fig. 1.1

ELASTOHYDRODYNAMIC LUBRICATION

At higher loads elastohydrodynamic lubrication (thin film lubrication) occurs. The high pressures involved increase the viscosity of the lubricant and the mating surfaces, which are in relative motion, undergo elastic deformation in the contact zone. The thickness of the film formed between the deformed surfaces is usually greater than the roughness of the mating surfaces and consequently very little wear takes place. Both the physical properties of the lubricant and the sliding materials have to be considered.

BOUNDARY LUBRICATION

Under boundary or mixed lubrication (the antiwear regime) conditions

an oil film exists between the surfaces, but intermittent penetration of this film by surface asperities occurs. The antiwear (a.w.) additive functions by reacting with the metal asperities to form surface films which aid the oil film in reducing intermetallic contact and wear. Both the physical and chemical properties of the lubricant have to be considered together with the nature of the sliding surfaces.

DRY WEAR

In dry wear the metal surfaces are in contact and asperities are worn off. Usually under mild wear conditions oxides form on the sliding metal surfaces thus separating them and ameliorating the wear, whereas under severe wear conditions metallic contacts continue to take place and high wear rates ensue.

EXTREME PRESSURE LUBRICATION

At very high loads under lubricated conditions the bulk oil film collapses and there is catastrophic wear usually followed by welding of the sliding surfaces. If an extreme pressure (e.p.) additive is present in the oil the break down of the bulk oil film is not followed by welding of the sliding surfaces. The e.p. additive reacts with the metal surface to form an inorganic surface coating which separates the metal surfaces and prevents welding and halts the catastrophic wear process. The physical and chemical properties of the lubricant have to be considered and the nature of the sliding surface.

1.3 The Origins of Extreme Pressure Additives

During the 19th century, serious efforts were made to develop materials for use specifically as lubricants. Until mineral oils became available on a commercial basis, most lubricants were based on animal and vegetable fats. These were often mixed with a wide array of materials, including alkaline soaps, lead compounds, graphite and sulphur, infact

quite a number of what were later to be called "extreme pressure additives".
There was no systematic study of additives until the first part of this
century when tests were developed to screen a wide range of compounds.
These tests are still used, but with a much sounder basis for the choice of
additives.

With the increasing use of the automobile and the more exacting
conditions of lubrication, ordinary oils were no longer sufficient.
"Oiliness" additives (which are now known as boundary lubricants such as
long-chain acids, esters and amines, and natural polar molecules) were used.
The work of Hardy (13) showed that these additives were merely absorbed on
the metal surfaces and, at high loads, they became desorbed. By increasing
the hardness of the sliding members, it was possible to push the breakdown
loads a little higher, but eventually scoring or galling of metal surfaces
took place. This occurred when the real areas of contact reached high
enough pressures and temperatures to weld together. This set an operating
limit, which was extended by using "extreme pressure" lubricants. Some of
these lubricants were tested by Mougey and Almen (14) on what is now called
the "Almen Tester". These "extreme pressure" (e.p.) lubricants contained
compounds which appeared to react chemically with the metal surfaces and
thus separated them so that welding did not occur.

1.4 Previous Use of Physical Analytical Techniques in Lubrication Research

During the 1930's, electron diffraction and X-ray diffraction
techniques were developed sufficiently to be applicable to lubrication
problems. Murison (15) used reflection electron diffraction to analyse
films of polar compounds on metal surfaces. These films were coated on the
metal surface and it was found that the polar molecules oriented themselves
with their carbon chains approximately normal to the surface of the metal.
Clark, Sterrett and Lincoln (16) examined the structures present in the

surface formed when chlorinated paraffin wax was rubbed onto the surface of steel. They used X-ray diffraction and found that again the molecules had their axes approximately normal to the surface and that in some cases the oriented layers were hundreds of molecules thick. Germer and Storks (17) studied stearic acid, and Beeck, Givens and Smith (18) studied a whole range of polar compounds rubbed onto flat metal surfaces, using reflection electron diffraction and they all found oriented films. Finch and Zahoorbux (19) showed that for a long-chain hydrocarbon, the separation of the "layer lines" corresponded to a spacing of 2.54Å, which is the distance between alternate carbon atoms in the aliphatic chain.

In 1941, Simard, Russell and Nelson (20) looked at films formed under extreme pressure conditions using a reflection electron diffraction camera with accelerating voltages between 30 and 40 kV. The additives used were free sulphur, lead napthenate and lead napthenate plus free sulphur. From the dynamic friction experiments they were able to identify Fe_3O_4, $FeOOH$, $PbSO_4$ and PbS in the worn surfaces.

Greenhill (21) used optical interference methods to estimate the thickness of the sulphide films formed on copper when investigating the variation of the coefficient of friction with thickness of the sulphide films. He also used taper-sections across wear tracks, in conjunction with optical micrographs of the tracks, to compare the types of surfaces and surface layers formed using different additives.

Clark, Gallo and Lincoln (22) were the first to use a radioactive tracer technique to study lubrication. They studied sulphurised lubrication additives in "test-tube" type experiments, and although they produced some valuable information they added little to the explanation of extreme-pressure agents on actual rubbing surfaces. It was not until a decade later that Borsoff and Wagner (23), and Loeser, Wiquist and Twiss (24, 25) used radiotracer techniques in test situations. Borsoff and Wagner used a

lubricant with dibenzyl disulphide additive containing radioactive sulphur S^{35}. Gears were operated under controlled conditions with this lubricant and the worn surfaces examined for their radioactivity using a Geiger-Muller (G.M.) counter with a thin window and autoradiographs. Loeser et al also used both radioactive sulphur S^{35} and P^{32} synthesized into Zinc dithio-phosphate molecules. They studied the e.p. films formed on cast iron cams and tappets run in motor oils containing the radioactive Zinc dithiophosphate The amount of radioactive material on the tappets was measured using a thin window G.M. counter and autoradiographs. The Zinc content was measured using X-ray spectroscopy, and ratios of Zn : S : P were measured. Sakurai, Ikeda and Okabe (26) related their radiotracer experiments using S^{35} to the kinetics of the formation of iron sulphide and the rate of wear of prepared radioactive sulphide films. They measured the intensity of radioactivity on the worn surfaces against running time (using a G.M. tube) and related this to their theory of the kinetics of chemical wear.

In 1962 Godfrey (27) used several physical analytical techniques to investigate worn steel surfaces formed in Society of Automotive Engineers (S.A.E.) extreme-pressure tests. He used sulphurised mineral oil and commercial gear oils, and analysed the surfaces using electron diffraction, X-ray diffraction, emission spectroscopy and proton scattering. By using these techniques he was able to show that oxides and sulphides were present down to a depth of several microns below the surface. He also showed that the sulphide was not always crystalline in form, since it was detectable in some cases by proton scattering but not by electron or X-ray diffraction. Using proton scattering Godfrey (27) was able to measure the amount of oxygen in the wear scars. He found that the spinel iron oxide (Fe_3O_4) was a major constituent and iron sulphide (FeS) a minor constituent of the e.p. films examined. He also showed that FeC and Wüstite (FeO) were present in some cases in small amounts.

In 1968 Allum and Forbes (28) applied electron probe microanalysis (E.P.M.A.) to surfaces worn under e.p. conditions. One advantage of the electron probe is that it offers an opportunity to study the distribution of active elements, such as sulphur, within the contact zone in much greater detail than is possible by autoradiography and at the same time it provides an electron image of the topography of the area being analysed. The electrons penetrate to a depth of several microns, depending on their energy and on the material present in the surface, so that the X-rays produced by arresting these electrons can be used to give information about the distribution of the elements with depth. Allum and Forbes (28) analysed scars, worn under oils containing organic sulphur additives, for their sulphur and iron content. The oxygen content was calculated by the difference method. The variation in the sulphur content of scars formed in the 4-Ball tester at loads above and below the initial seizure load (I.S.) was measured for each of the additives and in one case a cross-section of a scar was used to show the distribution of sulphur with depth below the surface. Forbes, Allum and Silver (29) have also studied the load carrying properties of metal dithiophosphates using E.P.M.A.

Scanning electron microscopy has the advantages of high magnification and large depth of field compared with optical microscopy and is an ideal tool for looking at worn surfaces of metals [Czichos and Kirsche (30), Quinn and Woolley (31)].

Electron Spectroscopy for Chemical Analysis (E.S.C.A.) is beginning to be applied to lubrication problems, although there is no actual literature available. Worn surfaces can be observed using a beam of X-rays and the energy of electrons ejected from the surface analysed. The information obtained indicates the chemical environment of the elements in the surface layers. The depth analysed is of the order of 100's of angstroms so that surface layers as well as adsorbed material can be observed.

1.5 Hypotheses Proposed to Explain the Action of Extreme-Pressure Additives

1.5.1 Early Ideas

Mougey and Almen (14) in 1931 developed a simulated gear test machine and used this machine to test a range of additives. They found that the addition of large amounts of sulphur to an oil which already contained lead-soap as an additive, considerably increased the load-carrying capacity of the lead-soap additive. With this information, the fact that flowers of sulphur had long been used to overcome over-heated bearings, and the fact that sulphur oil is used in cutting lubricants, they suggested that sulphur was the active ingredient in successful lead-soap lubricants. They proposed that lubrication at these extreme loads is accomplished by "some medium having properties different from oil as used in ordinary film lubrication". They showed that a fatty oil will carry pressures up to a certain point beyond which a mineral oil will fail and at the point where the fatty oil fails it is necessary to have a substance, such as sulphur, which forms a film on the metal which prevents welding.

Evans (32) suggested that the film rupture strength of a lubricant is associated with a chemical reaction between the lubricant and the bearing metal. This idea of producing a protective film has led to the adoption of active substances containing sulphur, chlorine, phosphorus or selenium and he proposed that these corrosive atoms produce a layer of sulphide etc. which keeps the metal surfaces apart.

Wear prevention agents have been found to be effective through their chemical polishing action according to Beeck, Givens and Williams (33). They suggested that, for instance, additives containing phosphorus form a metal phosphide on the surface which is able to alloy with the metal, lowering the melting point considerably, and by this action, aiding the maintenance of a polished surface. On the other hand, extreme pressure

agents should be corrosive in the sense of preventing polishing and should form a high melting point reaction product that does not form a low melting alloy with the metal.

The electron diffraction studies of Simard, Russell and Nelson (20) showed that for lead napthenate plus free sulphur additive, iron oxides and hydrates, lead sulphate and sulphide, were formed on iron surfaces. They state that the appearance of iron oxide and lead sulphate showed that oxygen must be included in considering the reactions of e.p. lubricants.

1.5.2 Mechanisms of action of disulphides as extreme pressure agents

Prutton, Turnbull and Dloughy (34) suggested that the reaction mechanism for disulphides and iron was:-

$$R_2S_x + Fe \longrightarrow FeS + R_2S_{x-1}$$
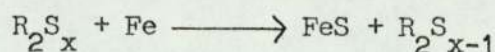
They were unable to ascertain whether there is a splitting of the additive on the iron surface to give sulphur before reaction with the iron.

Hamilton and Woods (35) deduced, from reaction rates and e.p. lubricant tests, that the overall reaction of an aliphatic disulphide could be represented by

$$RSSR + 2Fe \; (or \; 2Fe^{++} + 4e) \longrightarrow 2FeS + Hydrocarbon \; (RR?)$$
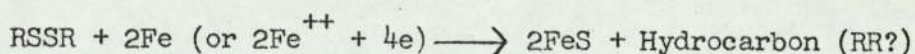
Davey and Edwards (36), on the evidence of 4-Ball lubrication tests, put forward a reaction mechanism for disulphides on steel consisting of three steps. The first involved an adsorbed layer formed under mild loading, viz.:

$$R-S-S-R + Fe \longrightarrow Fe:S \underset{S-R}{\overset{R}{<}}$$
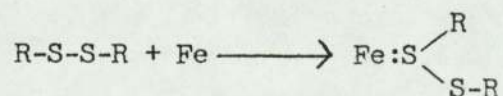
The second involves the formation of an iron mercaptide layer, namely:

$$Fe:S \underset{S-R}{\overset{R}{<}} \longrightarrow Fe \underset{S-R}{\overset{S-R}{<}}$$
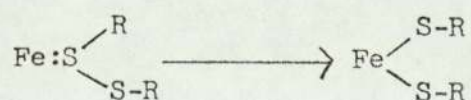
which will function in a similar manner to a soap film formed from a fatty-acid under boundary-lubrication conditions. Under very severe loading, the

mercaptide film breaks down to form ferrous sulphide, as shown below:-

$$Fe \begin{matrix} \nearrow S-R \\ \searrow S-R \end{matrix} \longrightarrow FeS + R-S-R$$
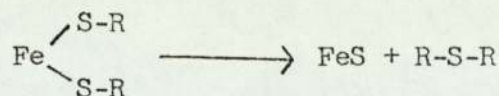
This material has good "anti-seizure" or e.p. properties. Llopes, Gamboa, Arizmendi and Minana (37) showed that the speed of reaction of sulphides was in the order

$$R-S-R \ \langle \ R-S-S-R \ \langle\!\langle \ R-S-H \ \langle \ R-S_3-R \ \langle \ R-S_4-R$$
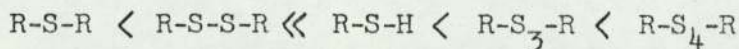
in nitrogen, but that air enhanced the reactivity of mono- and disulphides whilst suppressing the mercaptan and higher sulphide reactions. Llopes et alia (37) proposed the following for the disulphide reaction:-

$$R-S-S-R \longrightarrow 2RS$$

$$2RS + 2Fe \longrightarrow 2Fe-S-R \longrightarrow FeS_x + R_2S$$
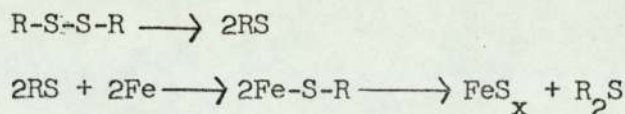
and that oxygen increased the radical formation. Toyoguchi, Takai and Kato (38) attributed the higher reactivity to oxidation of iron.

From S.A.E. extreme pressure tests with sulphurised mineral oil, Godfrey (27) showed that the major compound on the worn surfaces was Fe_3O_4 whilst FeS was a minor constituent. He suggested that the sulphur catalysed the formation of iron oxides. Greenhill (21) found that FeS films were not very good lubricants on their own and Sakurai, Ikeda and Okabe (26) found that iron sulphide films seemed to absorb polar compounds more actively than iron oxide and suggested a possible mechanism:

$$FeS + RSSR \longrightarrow Chemisorption$$

$$\begin{matrix} \diagdown & \overset{\oplus}{} & \overset{\ominus}{} & \diagup \\ & Fe & - & S \\ & \vdots & & \vdots \\ & S & - & S \\ \diagup & \underset{\ominus}{} & \underset{\oplus}{} & \diagdown \\ R & & & R \end{matrix}$$
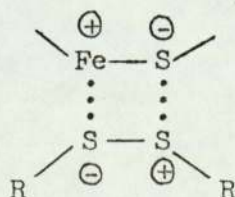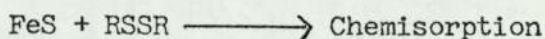
Allum and Ford (39) demonstrated that the e.p. activity of mono- and disulphides depended on the strength of the C-S bond, the order of

increasing activity being:-

diphenyl $<$ di-n-butyl $<$ di-sec-butyl $<$ di-tert-butyl $<$ dibenzyl

whereas Allum and Forbes (40) showed that, for mixed lubrication (anti-wear)

the order of increasing activity was:-

di-tert-butyl $<$ di-n-butyl $<$ di alkyl $<$ dibenzyl $<$ diphenyl

which followed the ease of scission of the S-S bond to form an iron

mercaptide layer. Forbes and Reid (41) carried out adsorption experiments

on iron powder and confirmed an earlier proposed mechanism for the load-

carrying action of organo-sulphur compounds as e.p. additives and indicated

the temperatures at which organo-disulphides function as e.p. additives.

Their hypothesis for the action of mono- and disulphides can be simply

shown as follows:-

$$
\begin{array}{ccccccc}
R & R & & R & & R & \\
| & | & & | & & | & \\
S-S & \longrightarrow & S & S & \longrightarrow & S & S \quad + 2R \longrightarrow \text{alkane, olefin, etc.}\\
\end{array}
$$

Fe surface

Anti-wear region   e.p. region
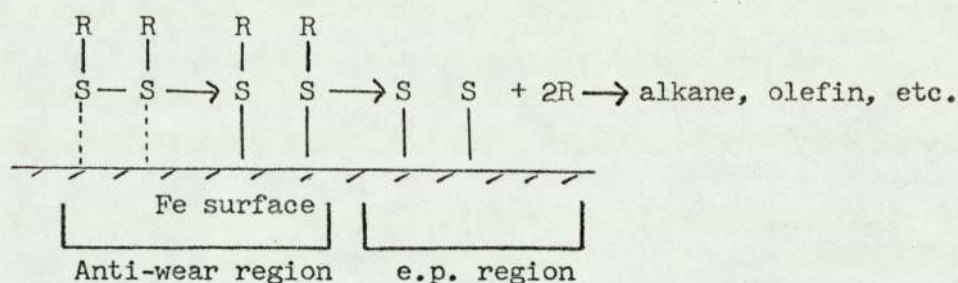
1.5.3 Mechanism of action of Zinc Dithiophosphates as extreme pressure agents

Zinc Dithiophosphate additives exhibit good extreme pressure,

antiwear, antioxidant, detergent and corrosion inhibition properties. There

have been many studies of the action of the Zinc Dithiophosphates since the

early 1950's, but the detailed mechanism of their action is still not

completely understood.

In a series of publications Loeser et alia (42,43,24,25) studied

the action of Zinc Dithiophosphate using radioactive tracers and X-ray

spectroscopy techniques. They were unable to identify any definite chemical

compounds on worn surfaces of cams and tappets. However, the relative

number of the three types of atom in the film did differ from that of the additive, $Zn\left[(RO)_2PSS\right]_2$, where the ratio of Zn : P : S is 1 : 2 : 4. They found that generally the films were low in sulphur content and that the amount of zinc, and particularly phosphorus, increased more rapidly than sulphur both with running time and load. These films were not easily worn off and they hypothesised that the mechanism of action of Zinc Dithiophosphate appeared to be related to chemical reactions of additive decomposition products with metal surfaces to form solid films that reduced wear under extreme-pressure conditions. They also found that the sulphur content of the film was highly localised to contact areas subjected to high pressures. Furthermore, sulphur-printing showed the presence of metal sulphides.

Larson (44) used Zn^{65}, P^{32} and S^{35} radiotracers to study films formed by Zinc Dithiophosphates on copper-lead bearings. He proposed that "the end result of zinc dithiophosphate decomposition involves stripping three or more of the alkyl groups and $1\frac{1}{2}$ sulphur atoms from the molecule leaving a largely inorganic residue." Furey (45) suggested that the phosphorus in the films could be present in the following forms; (a) physically adsorbed zinc dithiophosphate, (b) thermal decomposition products of the additive, (c) varnish or lacquer deposits containing physically or chemically bound phosphorus and (d) metal/phosphorus reaction products. In the discussion of this paper Antler (46) suggested that zinc oxide, zinc sulphide, zinc phosphide and zinc phosphate as well as more complex inorganic compounds could be formed from zinc dithiophosphates. He also suggested that if the divalent metal oxide ZnO was formed initially as a decomposition product, this could react with α-Fe_2O_3 to form the spinel $ZnO.Fe_2O_3$ which may give relatively low friction and wear in the same way as the spinel iron oxide (Fe_3O_4).

Bennett (47) used interference microscopy on worn surfaces to show that zinc dithiophosphate produced an increase in small-scale roughness

which resulted from a reaction of additive decomposition products with the metal surface. Asseff (48) of the Lubrizol Corporation, proposed mechanisms for the decomposition of zinc dithiophosphate. The general structure of zinc dithiophosphates is:-

where the R's represent a variety of alkyl and alkylaromatic radicals. When the R group is a secondary alkyl radical, decomposition of the dithiophosphate may be caused by the instability of the activated hydrogen atoms on the beta carbon atoms. Thus:-

The strong acid formed could react with iron to form the corresponding iron salt and further decomposition of the remaining secondary alkyl radical would result in the formation of a second acid group that could also attack the iron surface. Similarly, if R is a primary alkyl radical as shown below:-

decomposition would be at a higher temperature and follow the same pattern.
If R is an aromatic radical
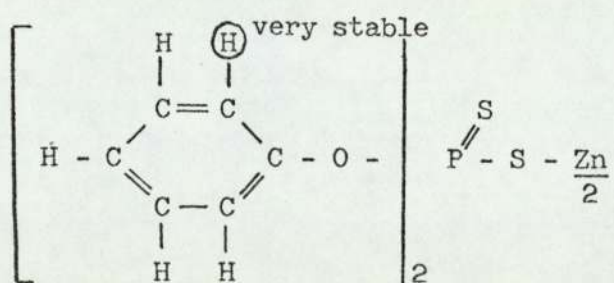
cleavage of the aromatic ring would be necessary if the same mechanism
applied and this would be unlikely because of the large energy required.
These differences in zinc dithiophosphate molecules are reflected in their
behaviour as additives.

Reflection infra red spectroscopy, in conjunction with electron
diffraction and X-ray fluorescence, was used by Francis and Ellison (49) to
determine the structure of films formed on metals using zinc dithiophosphates.
They showed that zinc dithiophosphate molecules, $ZnSO_4$ and zinc thiophosphate
were formed on metal surfaces immersed in the additive plus white oil. For
surfaces rubbed with zinc dithiophosphates, PO_4^{-3} ions were present on the
surface. They also suggested that the oxidation property of zinc dithio-
phosphate was related to sulphate formation.

Gallopoulos (50) examined critically the mechanism proposed by
Feng, Perilstein and Adams (51) for the decomposition of zinc dithiophosphates.
This is stated briefly below:

(i) Acid and olefin formation
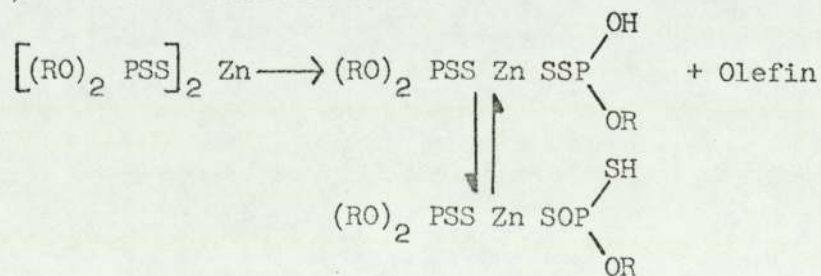
(ii) H_2S liberation - Anhydride formation

$$2(RO)_2 \; PSSZnOP \overset{SH}{\underset{OR}{<}} \longrightarrow$$

$$(RO)_2 PSSZnS - \overset{\overset{O}{\parallel}}{\underset{\underset{OR}{\mid}}{P}} - S - \overset{\overset{O}{\parallel}}{\underset{\underset{OR}{\mid}}{P}} - SZnSSP(OR)_2 + H_2S$$
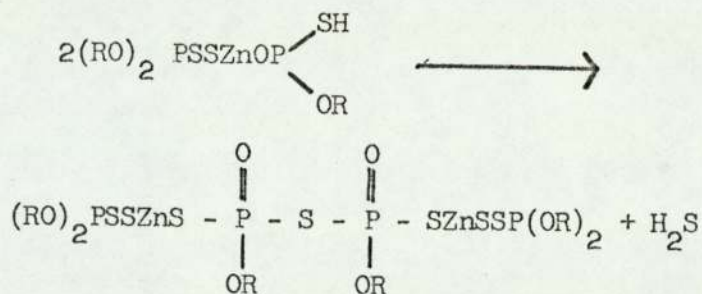
(iii) Formation of a polymer with structure

$$\left[- \overset{\overset{O}{\parallel}}{\underset{\underset{OR}{\mid}}{P}} - S - Zn - S - \overset{\overset{O}{\parallel}}{\underset{\underset{OR}{\mid}}{P}} - S \right]_n$$
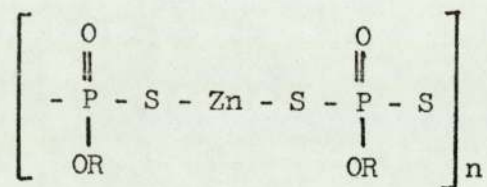
He concluded that this mechanism was inconsistent with the experimental data.

Rowe and Dickert (52) showed that for metal dithiophosphates of varying alkyl group structure and metal cation, antiwear activity can be correlated with the thermal stability of the additive. In a later paper, on the role of additive adsorption on wear, Rowe (53) showed that zinc dithiophosphate was either adsorbed in an oriented manner with a configuration similar to that which it would have in the crystalline state or decompose rapidly to form reaction products with the surface.

Allum and Forbes (29, 54) concluded that the factors determining antiwear and extreme pressure activity are different and that the metal used in the dithiophosphate has a greater effect on the load-bearing characteristics than the alkyl group. From their E.P.M.A. work they determined the amounts of Zn, P and S in the wear scars and found that there was less sulphur in the scar in the antiwear region than in the extreme pressure region.

Barton, Klaus, Tewksbury and Strang (55) showed that both zinc and phosphorus containing impurities of the same relative polarity were present

in zinc dithiophosphate. They proposed that these polar impurities were preferentially adsorbed onto the metal surface and acted in the lubrication mechanism in place of the zinc dithiophosphate molecules. They suggested that acid phosphates were the active impurities as had been suggested by several researchers (56, 57, 58) for the mechanism involved with tricresyl phosphate. Barton, Klaus, Tewksbury and Strang proposed the following mechanism:-

(i) preferential adsorption of polar zinc and phosphorus impurities onto the metal surface,

(ii) asperity contacts produce high temperatures,

(iii) chemical reaction of impurities with the metal to produce a metal phosphate surface film.

1.6 Summary of the Present Position in e.p. Research and an Outline of the Research Carried Out in this Investigation

1.6.1 The Disulphides

The mechanism of action of disulphides in the e.p. region is determined by the scission of the C-S bond rather than the S-S bond as is the case in the antiwear region. The greater the energy density in the sliding contact the greater the speed of the reaction. The speed of the reaction may well depend on the nature of the metal surface and in particular the oxide layer and/or the oxygen available. Godfrey (27) showed that a film of Fe_3O_4 does not have e.p. lubricating properties nor does a film of pure FeS, but the presence of both in the surface layers of the metal is the prerequisite for high load-carrying capacity. Llopes et al (37) showed that oxygen increased the reactivity of disulphides and suggested that the oxygen tended to enhance the sulphurisation reaction, whereas Toyoguchi, Takai and Kato (38) attributed the higher reactivity to oxidation of iron. The detailed mechanism of the action of disulphides under highly loaded sliding conditions and the reasons for bearing such high loads have not

been fully explained.

1.6.2 Zinc dithiophosphate additives

The mechanisms of action of zinc dithiophosphates must be complex and depend on a number of factors, some of which are unknown. Because of their good antiwear characteristics, some form of adsorption of polar compounds seems likely at lower loads, but in the e.p. region it is possible that phosphates and sulphides are formed which protect the under-lying metal. It is also possible that complex oxides with the spinel structure are formed in conjunction with the above compounds and that the role of oxygen in both disulphide and zinc dithiophosphate additives is important.

1.6.3 Outline of research carried out in this investigation

In this investigation three sulphur additives, diphenyl, di-tert-butyl and dibenzyl disulphide, two zinc dithiophosphate compounds, a commercial additive (Lubrizol 1395) and a pure compound zinc dibutyl-phosphorodithioate (ZDP) were used as additives in two base oils (a white oil and a mineral oil). In all cases except the Lubrizol 1395 (where the sulphur content was not known accurately) the same sulphur concentration was used in the oil-plus-additive blends. Tests were conducted on a Shell 4-Ball Machine using both the conventional 4-Ball geometry and a 1-ball-on-3-flats geometry, sliding EN31 steel on EN3ŧ steel. A limited number of tests were also carried out using lead and phosphor-bronze on EN31 steel.

Several physical analytical techniques were used to obtain as much information as possible about the nature of the worn surfaces. Topographical information was obtained by systematically observing the wear scars using optical and scanning electron microscopy. In some cases, estimates of the thickness of the surface films were made where the worn surface had cracked revealing the film edge on. The types of surfaces found gave a good

indication of the way in which they were formed. Also the surface films changed with load as well as additive indicating changing mechanisms of lubrication.

E.P.M.A. gave quantitative and qualitative values for the concentration of the elements in the surface film together with topographical data on their distribution relative to the type of surface features. The depth of penetration of the "probing" electrons below the surface could be varied by changing the electron accelerating potential. By a difference technique, applied to the correction of the raw data, the oxygen and carbon concentration was indirectly determined.

Glancing-angle X-ray diffraction provided information about the structure of the surface films. The resolution of this technique was good since the iron provided an internal standard. A systematic study of the structures present in the wear scars showed up variations in composition both with additive and load. Micro-indentation hardness tests of the surface of the scars and the unworn regions plus hardness tests on taper sections through the scars provides information about the surface films and the underlying structures in the steel.

E.S.C.A. was used to study the top few hundred angstroms of the films to gain knowledge of the chemical environment of the elements present in the additives.

Using this wide range of physical analytical techniques, a broad picture of the action of disulphides and zinc dithiophosphate additives was obtained. As a result of this investigation a more comprehensive explanation of the action of these typical e.p. agents was proposed.

As part of the industrial research programme of this Co-operative Award in Science and Engineering, a limited study of the action of several additives on lead-and phosphor-bronze run against steel was carried out at Shell Research Limited, Thornton, Cheshire. A review of this additional (but related) work is given in the Appendix.

C H A P T E R   2

EXPERIMENTAL DETAILS

2.1   The 4-Ball Machine and Test Procedures

2.1.1 The 4-Ball Machine

The test rig used was a Shell 4-ball machine (Figure 2.1) kindly donated to the University by Shell Research Limited for this project. This type of machine is used for assessing lubricants (59, 60). The apparatus was used primarily to form specimens under conditions comparable to those described in other published works. In this way the results of the physical analyses of the wear scars can be related to other studies.

A $\frac{1}{2}$ inch diameter steel ball is rotated at 1500 r.p.m. under load in the cavity formed by three other similar balls clamped in a cup containing the lubricant to be tested. The range of loading used in these experiments was from 70 Kgf to 220 Kgf in steps of 10 Kgf, and 220 Kgf up to 440 Kgf in steps of 20 Kgf, depending upon whether a weight of 10 or 20 Kg was placed on the load arm.

The friction arm on the ball cup was attached with a chain to a spring-loaded pointer which pressed against a paper-covered, rotating drum to measure the frictional force.

Figure 2.2 shows a typical log-log plot of scar diameter versus applied load.

The region AB is referred to as the antiwear (a.w.) region. The wear scars are of the same order of diameter as that given by the Hertz line which represents the diameters of the contact areas under static loading conditions. BC is the initial seizure (I.S.) region. Here there is a momentary breakdown of the lubricating film which is recognised by a sudden
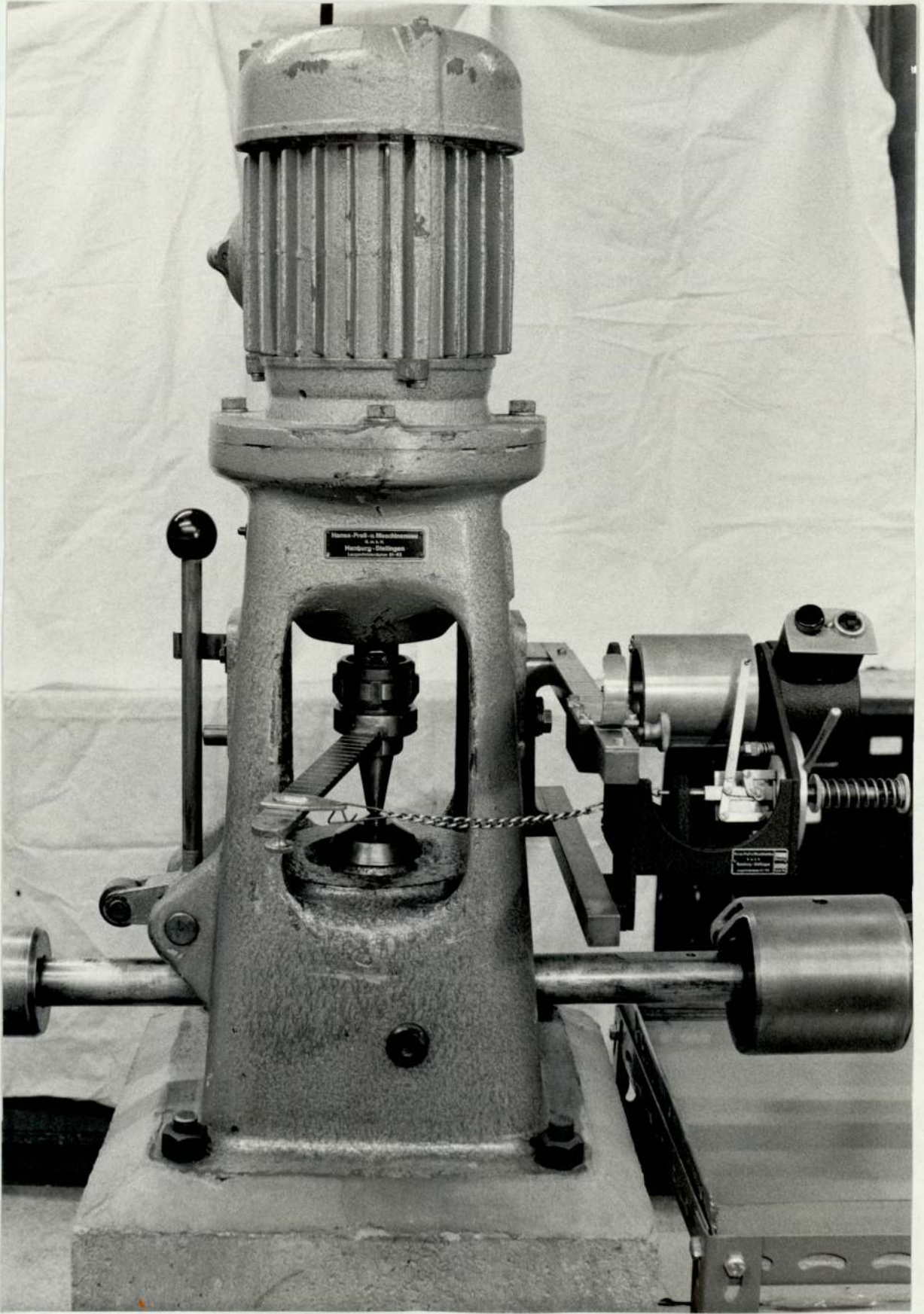
FIG.2.1   4-BALL MACHINE

increase in the measured scar diameter and a momentary deflection on the friction trace. CD is the extreme pressure (e.p.) region and is characterised by seizure or welding at the start of the test and by large wear scars.
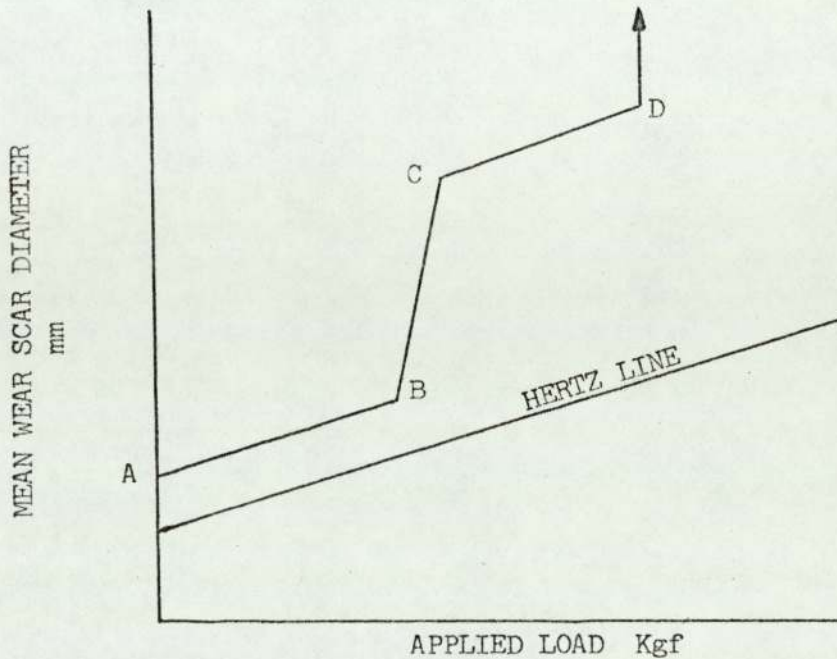
Figure 2.2

2.1.2 Extending the load range

As the lowest load that could be applied was 70 Kgf, the loading arm was modified to extend the range down to 15 Kgf. A cylindrical load cell (Figure 2.3) with 8 resistive strain gauges, fixed alternately parallel and at right angles to the circumference, were connected to form a Wheatstone Bridge (Figure 2.4). To calculate the thickness of the cylinder wall of the load cell, it was assumed that the maximum load was 300 Kgf (660 lb) and that the strain ϵ_L had to be less than 0.01% ($\Delta L/L < 10^{-4}$). From basic elasticity formulae r_1, the external diameter can be obtained, namely:-

$$E = \frac{stress}{strain} = \frac{660}{\pi(r_1{}^2 - r_2{}^2)} \cdot \frac{1}{10^{-4}} \qquad \ldots (2.1)$$

STRAIN GAUGES
MOUNTED AROUND
CIRCUMFERENCE
OF CYLINDER

CAP

r_2 r_1
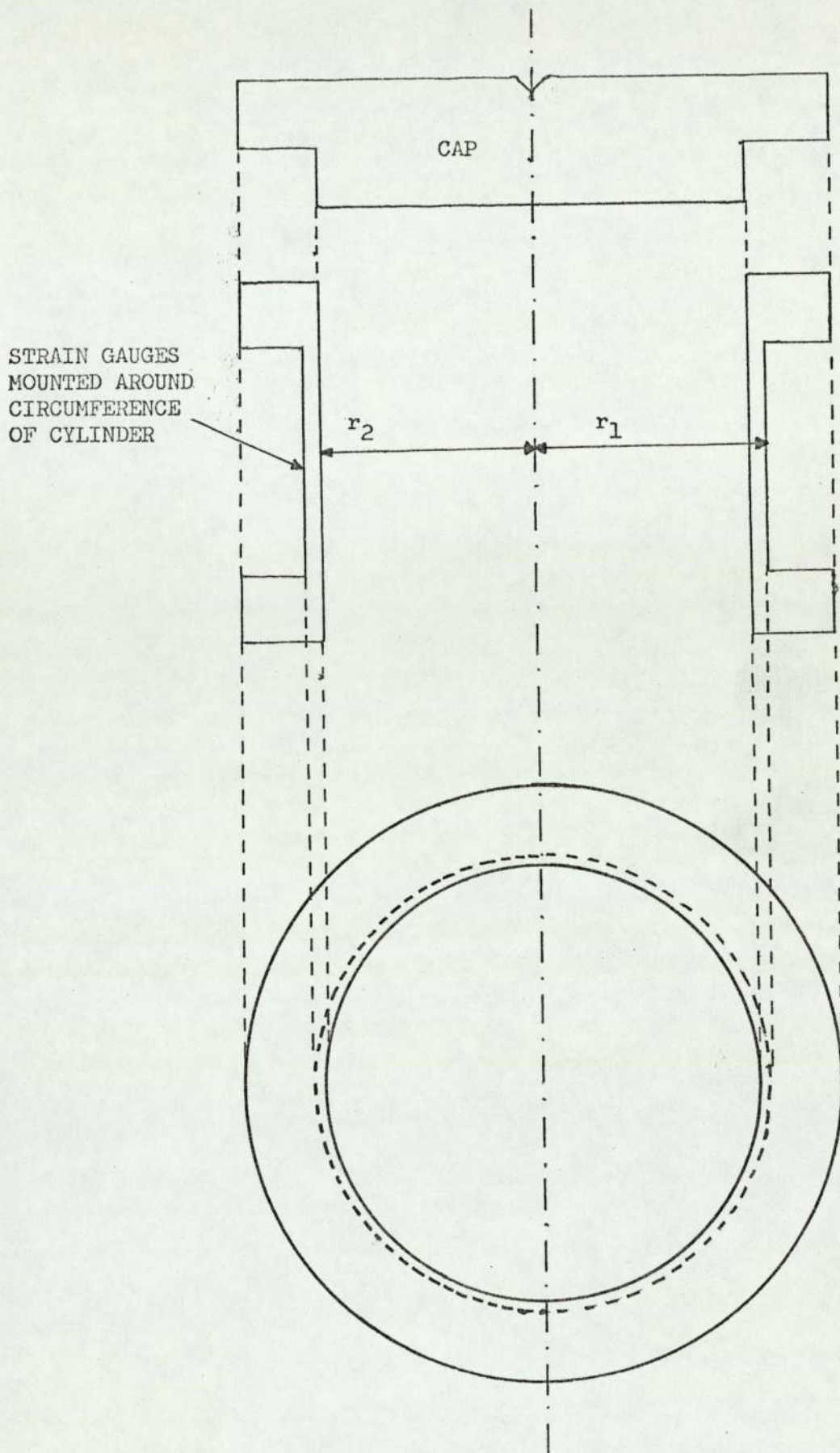
FIG.2.3 CYLINDRICAL LOADCELL

SCALE 2.1 MATERIAL EN24 STEEL

POTENTIOMETER

1 MΩ
BALANCING
RESISTANCE

10 V STABILISED
SUPPLY
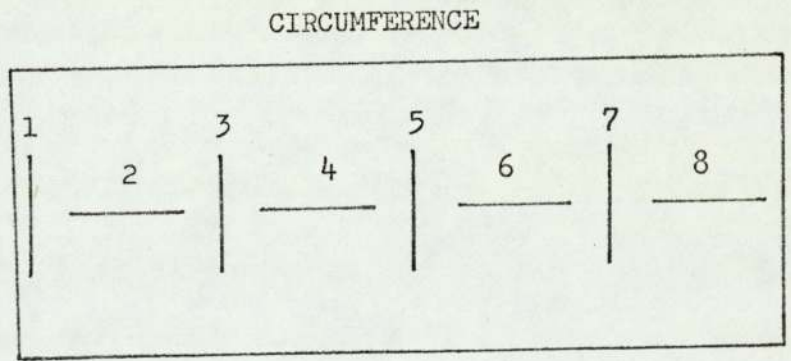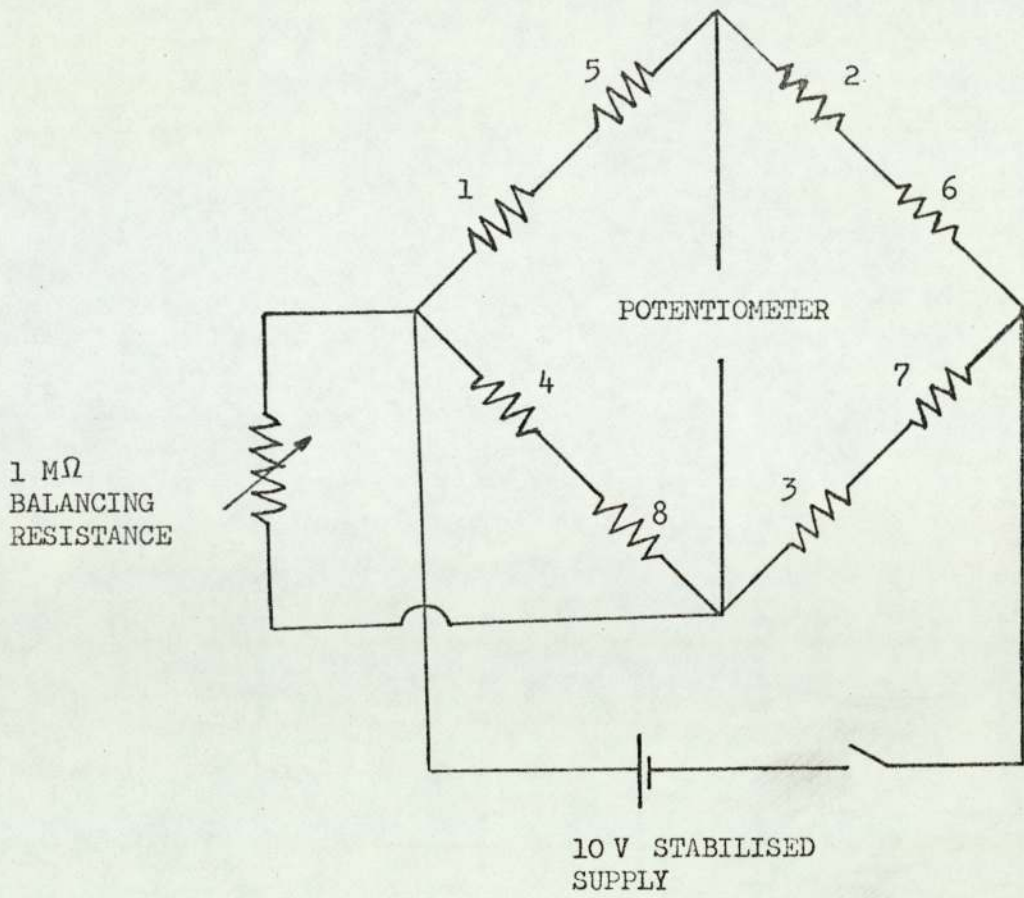
CIRCUMFERENCE

FIG.2.4   STRAIN GAUGES PARALLEL AND AT RIGHT ANGLES TO
CIRCUMFERENCE CONNECTED TO FORM WHEATSTONE BRIDGE

r_2 is the internal diameter and E is the Young's Modulus (equal to 3.027 x 10^7 lbs in^{-2} for EN24 steel). The internal diameter (r_2) was fixed at 0.69 ins so that it fitted onto the base plate of the 4-ball machine in the position of the ball race. From equation (2.1) r_1 = 0.74 ins which gives a wall thickness of 0.05 ins for the strain to be less than 0.01% up to 300 Kgf load. The strain gauges were Techni-Measure type FLA-6, 6mm x 2.2mm, nominal resistance 120 ohms. The change in voltage with strain is given by:-

$$\frac{\Delta V}{V} = \left(\frac{1 + \nu}{2}\right) . G . \varepsilon_L \qquad \qquad ...(2.2)$$

where

ν = Poissons Ratio (0.3)

G = Gauge factor (2.1)

ε_L = Strain (10^{-4})

ΔV = Change in Voltage

V = 10 volt stabilised supply

which gives ΔV = 1.36 millivolts at 300 Kgf. The load cell was calibrated on a hydraulic press up to 300 Kgf, readings were taken several times both loading and unloading, and a mean value obtained. Figure 2.5 is a plot of load versus ΔV showing that up to 200 Kgf, the loads as indicated on the 4-ball machine are accurate but, at higher loads, the actual load applied is less than the load indicated. Using a 4 Kgf load as a counterbalance, the 4-ball loading was reduced so that the range 15 Kgf upwards in steps of 10 Kgf (Figure 2.6) was obtained.

2.1.3 The 3-Flats Holder

Initially all the tests were conducted using 4-ball geometry. Unfortunately, these specimens were not a suitable size for analysis in the electron probe. Furthermore, it was extremely difficult to spark-erode relevant portions of the ball bearings in order to get specimens of the correct size. An alternative was to use 1/4" x 1/4" rollers which are,
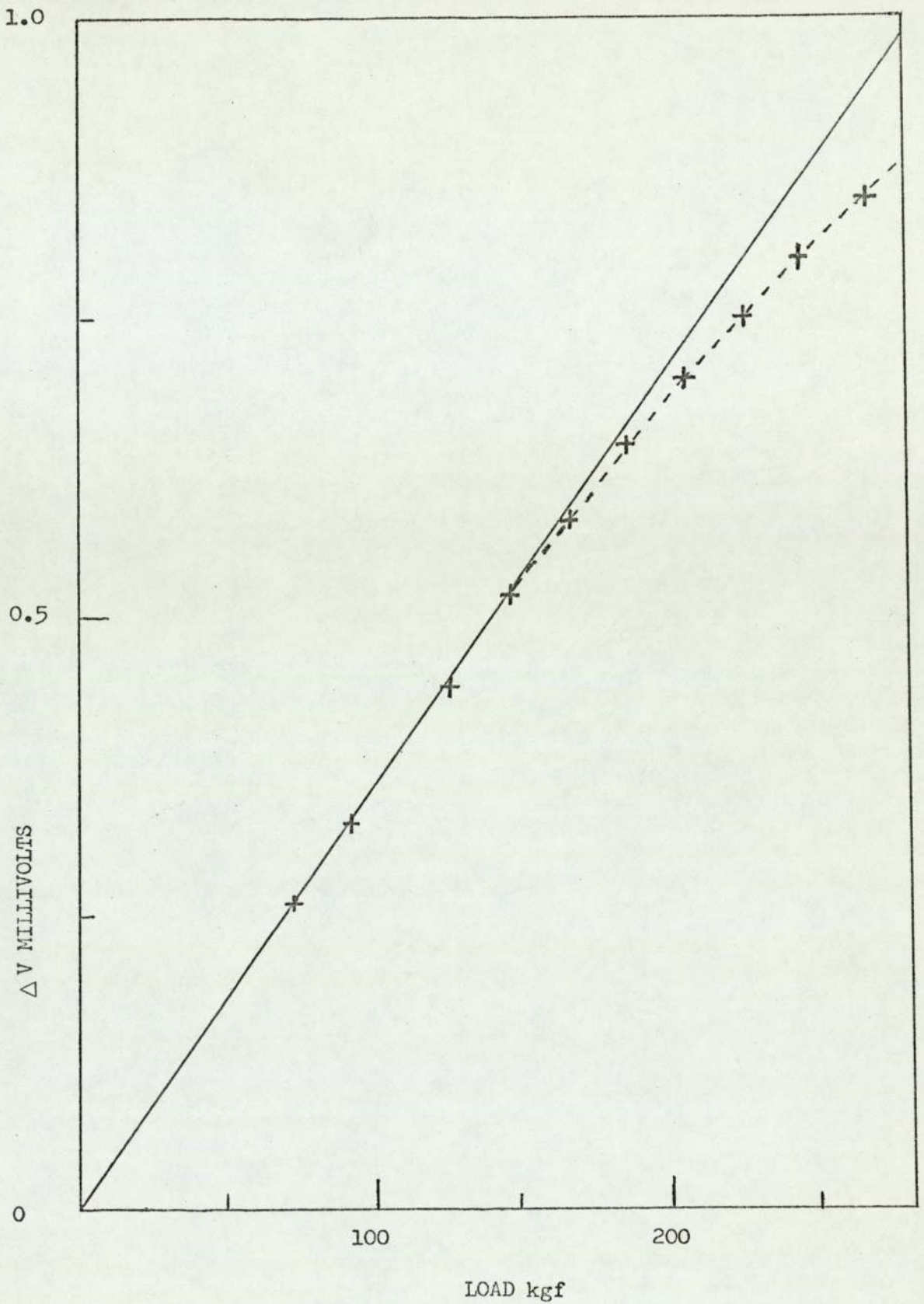
FIG.2.5   LOAD VERSUS △V

  (a)   FULL LINE — CALIBRATION CURVE FOR LOAD CELL

  (b)   DASHED LINE (+) NOMINAL 4-BALL LOAD VERSUS △V
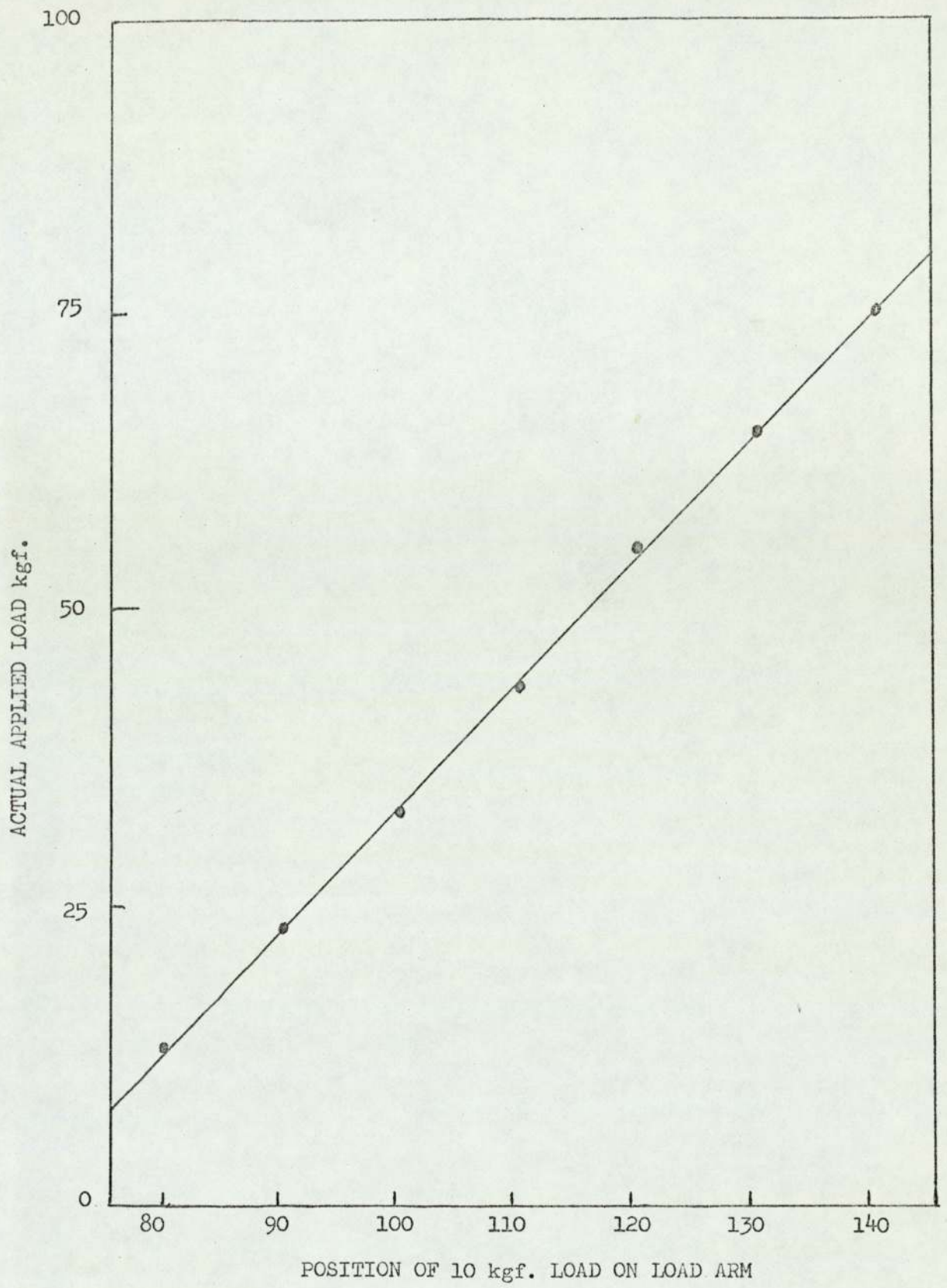
FIG.2.6   ACTUAL APPLIED LOAD WHEN 4 kgf. COUNTERBALANCE IS USED

in fact, small enough to be analysed in the electron probe. Figure 2.7 illustrates the final design for a 3-flats holder. The flat faces of the steel rollers are placed uppermost in the three slots in the holder and when the locking-nut clamps it in place in the ball-cup, the silver steel cone locks the rollers in position. The first design used grub screws to lock the rollers in position, but the screws were continually seizing through lack of lubrication because the cleaning process degreased the threads. The flat faces of the rollers were arranged in the holder so that the top rotating ball rested at the centre of their faces and tangent to them.

2.1.4 Cleaning procedures

The balls and rollers were first washed in petroleum ether and dried. They were then placed in a water cooled vapour-bath containing boiling (40-60°C boiling point) petroleum ether for about two hours. The balls and rollers were wrapped in tissues and stored in a desiccator ready for use the following day.

All the removable parts of the 4-ball machine were cleaned in the vapour-bath before and after use and allowed to cool to room temperature. The parts were assembled without touching the clean surfaces by hand. The used balls and rollers were cleaned in the vapour-bath, packed in cotton wool in test tubes and stored in a desiccator.

2.1.5 The 4-ball test procedure

At the start of a series of tests the motor rotating the upper ball was run for several minutes to warm up. A clean holder was taken and 3 clean balls (or flats) clamped into place and a clean ball put in the chuck on the end of the drive shaft. About 20ml of the oil blend under test was poured into the cup and the load was applied. The friction arm was connected and the motor switched on for one minute. When the test was completed the

EN31 STEEL BALL

EN24 STEEL HOLDER

EN31 STEEL ROLLER

SILVER STEEL CONE
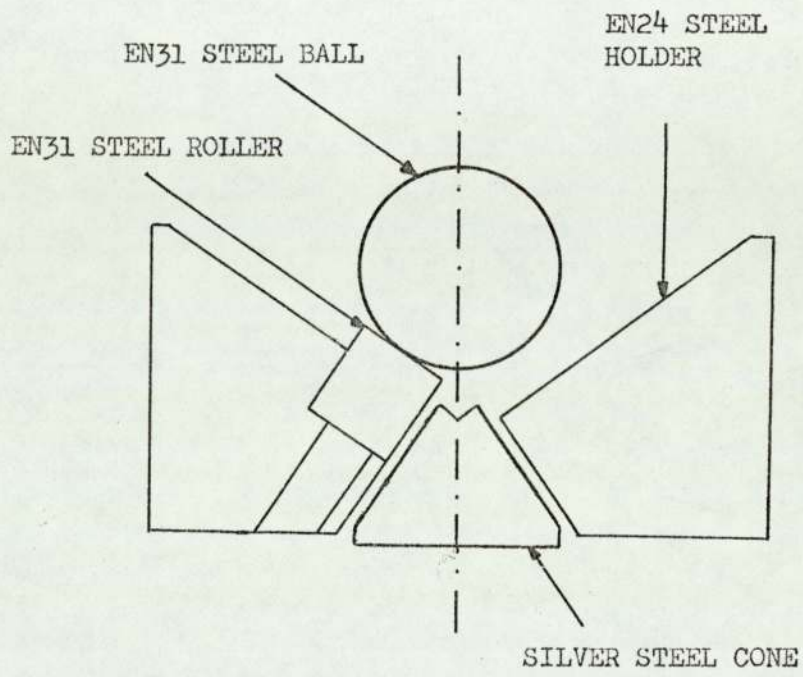
FIG.2.7   3-FLATS HOLDER

diameter of the scars on each of the lower test specimens was measured, using a travelling microscope, parallel and at right angles to the direction of sliding and a mean value obtained. The balls and rollers were cleaned and stored.

Tests were conducted from 15 Kgf load upwards until welding occurred. The mean wear scar diameter was plotted against load on a log - log graph.

2.2 Materials

2.2.1 Balls and rollers

The balls were obtained from Shell Research Limited and carried the Skefco specification RB 12.7 III E212 balls for 4-ball machine testing. The composition of EN31 steel is:

Element	Percentage
C	0.9 - 1.2
Si	0.10 - 0.35
Mn	0.30 - 0.75
S	0.050 max.
P	0.050 max.
Cr	1.00 - 1.60
Ni	0.1
Fe	Balance

The hardness of the balls was 835 ± 10 V.P.N. (30 Kgf load). The rollers were $1/4$ " x $1/4$" EN31 steel obtained from Ransome Hoffmann and Pollard Ltd. The hardness was 855 ± 10 V.P.N. (30 Kgf load). The ends of the rollers were used and these had a scratched appearance and were not as smooth as the cylindrical face. Talysurfs of the flat faces showed a c.l.a. of approximately 0.015μm.

When a ball presses on to another ball, or upon a flat surface,

both surfaces deform elastically until the load is supported. The diameter
(D) of the contact of a ball on a ball, and a ball on a flat, were
calculated using Hertzian theory (61) and the Hertz line plotted for the
two types of geometry on the graphs of mean wear scar diameter versus load.
The following equations were used to calculate the Hertzian diameters:-

$$D_{ball} = 2 \times 1.103 \left(\frac{NR}{2E}\right)^{1/3} \quad \text{Ball on Ball}$$

$$D_{flat} = 2 \times 1.109 \left(\frac{NR}{E}\right)^{1/3} \quad \text{Ball on Flat}$$

where N = normal load = 0.4082 P, where

P = applied load on the 4-ball machine

R = radius of ball (6.35mm)

E = Young's modulus (2.125×10^4 Kg/mm^2).

Using these values the Hertzian diameters are:-

$$D_{ball} = 8.73 \times 10^{-2} P^{1/3} \quad ; \quad D_{flat} = 11.00 \times 10^{-2} P^{1/3}$$

2.2.2 Oils

Two oils were used throughout the tests,

(a) Risella 29, a highly refined white oil containing mainly saturated
cyclic hydrocarbons with side chains and less than 100 p.p.m. sulphur.
This oil has been specially refined to reduce the level of sulphur
compounds and polar materials.

(b) HVI 55 consists mainly of saturated cyclic hydrocarbons with side
chains, iso-paraffins and some aromatic compounds. This oil contains
sulphur (to the extent of 1% weight sulphur), and polar compounds.

The properties of these oils are presented in Table 2.1.

2.2.3 Additives

Two groups of additives were used in the tests.

(a) This group consists of 3 disulphides. Disulphides are used both in

Table 2.1

Properties of Risella 29 (SPL 758/70) and HVI (SPL 77/65) oils

PROPERTY	RISELLA 29	HVI
Appearance	Clear	Clear yellow
Colour (ASTM)	0.0	1.5
Specific gravity at 60°F	0.881	0.867
Kinematic viscosity at 100°F c/s	50.50	21.79
Kinematic viscosity at 210°F c/s	6.40	4.13
Viscosity Index	78	99
Neutralisation value (mg KOH/gm)	<0.05	<0.05
Pour Point (°F)	-20	+15
Sulphur content (% wt)	<0.01	~1.0
Aromatic content (% wt)	7.53	-

extreme pressure lubrication and in metal cutting oils. The three

compounds used in the tests are:-

(i) Dibenzyl Disulphide (DBDS), $C_{14}H_{14}S_2$, structure
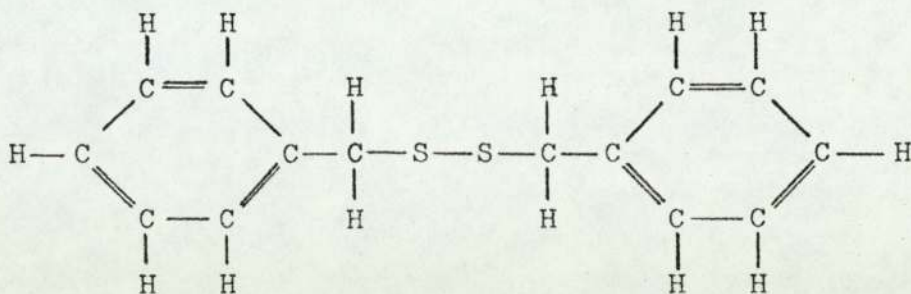
Molecular weight 246.4 and supplied by British Drug Houses.

(ii) Diphenyl Disulphide (DPDS), $C_{12}H_{10}S_2$, structure
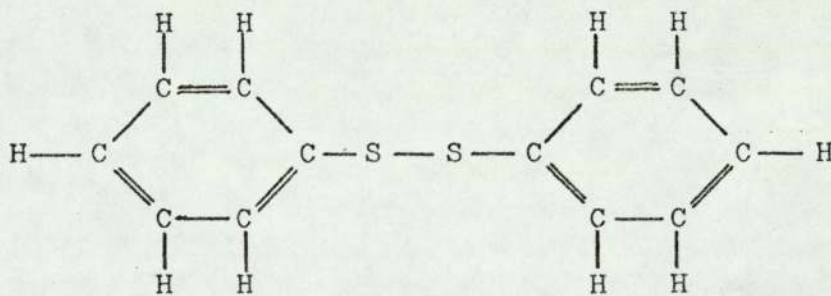
Molecular weight 218.3 and supplied by Hopkins and Williams.

(iii) Di-tert-butyl Disulphide (DTBDS), $C_8H_{18}S_2$, structure
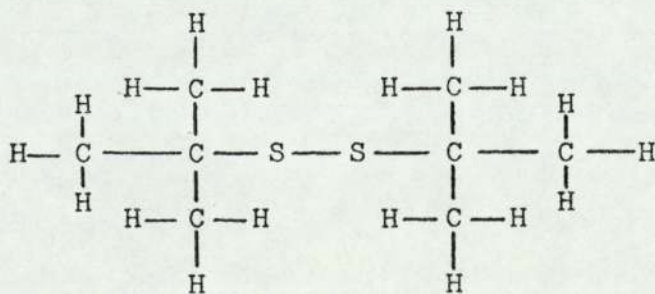
Molecular weight 178.2, provided by Shell Research Limited and 99.1% pure,

the main impurities being di-n-butyl disulphide and di-tert butyl

trisulphide.

(b) This group consists of 2 zinc dithiophosphates, a commercial blend and a pure compound. This class of compounds is used extensively in lubricants for their a.w., e.p., anti-oxidant, detergent and corrosion inhibition properties.

(i) <u>Pure Zinc Dithiophosphate (ZDP)</u>, $C_{16}H_{36}O_4S_4P_2Zn$, structure
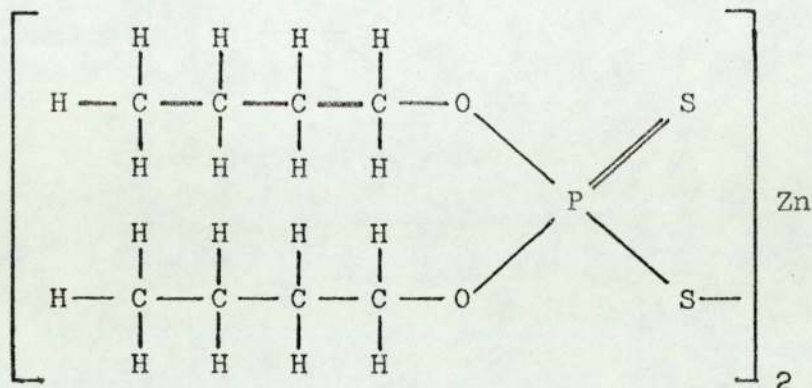
Molecular weight 547.8 (kindly supplied by Shell Research Limited). Analysis showed 11.8% zinc compared to 11.9% theoretically and infra red analysis was consistent with the above structure. No free SH groups were detected.

(ii) <u>Lubrizol 1395</u> (supplied by Shell Research Limited) is a blend of zinc dithiophosphate with oil. The molecules consist of mixed n- and iso- C_4 and C_5 alkyl groups. The decomposition temperature is about 200°C.

1.0% by weight of dibenzyl disulphide was used at a concentration of 0.265% weight sulphur (4.06 millimoles per 100 gms of blend). This sulphur concentration was used with all the additives (0.886% weight DPDS, 0.723% weight DTBDS and 1.112% weight ZDP) except Lubrizol 1395 where 1% weight was used, the sulphur content being approximately 0.2% weight. Dibenzyl and diphenyl disulphide are powders and the oil had to be heated to about 60°C until the additive dissolved.

2.3 <u>The Analysis of the Worn Surfaces using X-Ray Diffraction</u>

The glancing angle, edge-irradiated X-ray diffraction technique of Isherwood and Quinn (62) was used to analyse the surface films formed during

sliding. Most of the analyses were conducted on specimens from the e.p. regions as the patterns from the scars formed at loads below initial seizure were similar to that of an unworn ball.

A worn $\frac{1}{2}$" diameter ball was placed on the goniometer of a conventional single crystal, cylindrical rotation camera of 3cm radius. The wear scar was aligned so that the general surface of the wear scar was at about 20° to the incident X-ray beam (Figure 2.8) and the edge of the wear scar exactly in the centre of the cylindrical camera. Thus, effectively, the area irradiated was 0.25mm in diameter when using a 0.5mm diameter collimator. A Cobalt X-ray tube (300 watts) with an iron filter and a 0.5mm collimator was used to produce a fine beam of Co $K\alpha$ X-rays to irradiate the specimens. With this fine collimator well resolved diffraction patterns were obtained.

Quinn (63) has shown that the transmitted component arises mainly from the surface films whereas the reflected component arises mainly from the bulk of the material. Thus α-Fe lines from the bulk material tend to be broad while those from the surface films are fine and have line widths much less than that of the incident beam.

The α-Fe lines 110, 200, 211, 220 were used as the internal standard of the film. Assuming the 'd' values for these lines a graph of 2θ against distance along the film (Figure 2.9) can be used to obtain the 'd' values for all the other lines.

As a 300 watt tube and a fine collimator were used the exposure times required were found to be long, varying between 60 and 100 hours. Several specimens from the e.p. region of each series of tests were analysed using this technique.

A number of standard specimens were used to facilitate indexing of the films obtained from worn specimens. Two flat faces intersecting at 90° were ground on an unworn ball and the resultant edge irradiated. After
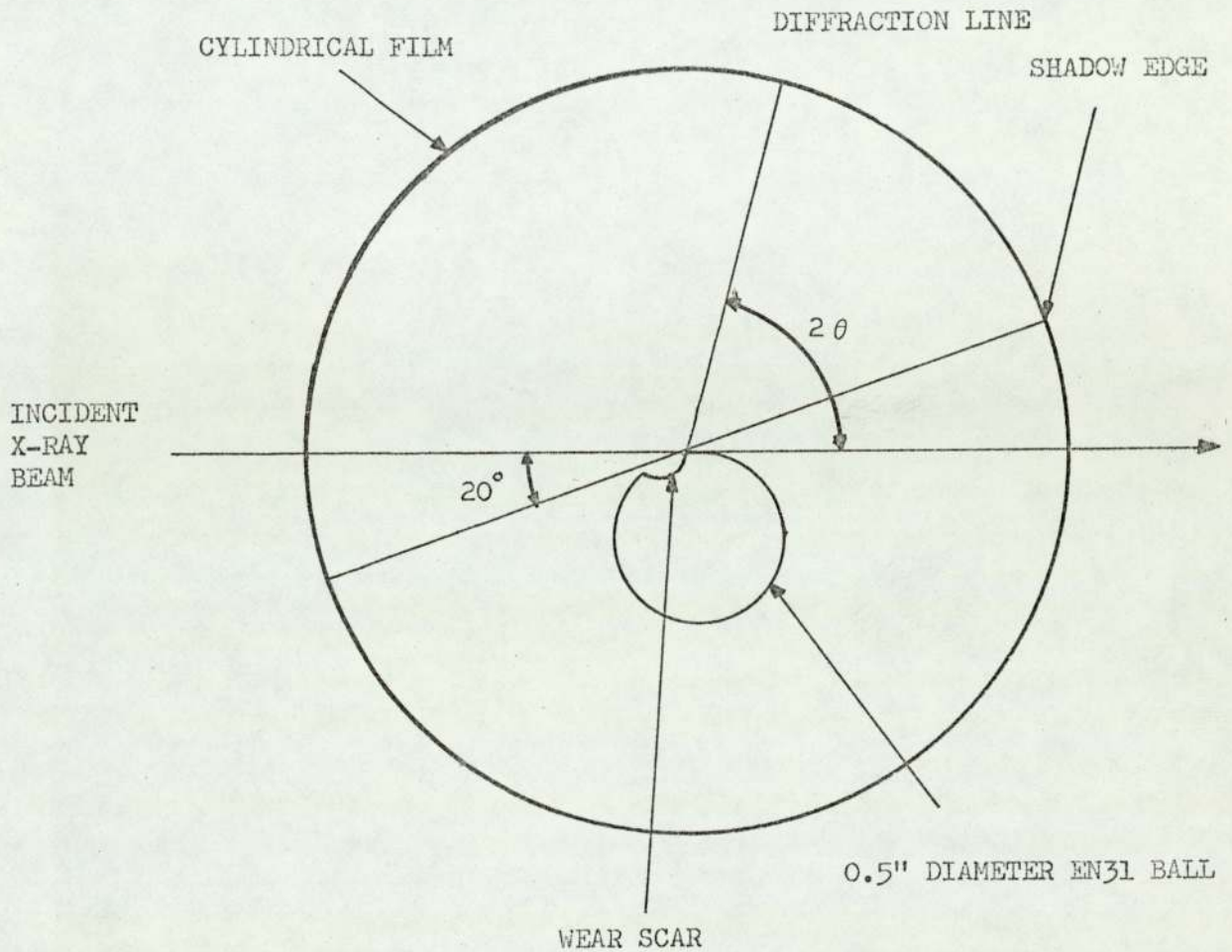
FIG.2.8 Diagram of the irradiation geometry used for
obtaining the glancing-angle, edge-irradiated
x-ray diffraction patterns (wear scar size
exaggerated for the sake of illustration)
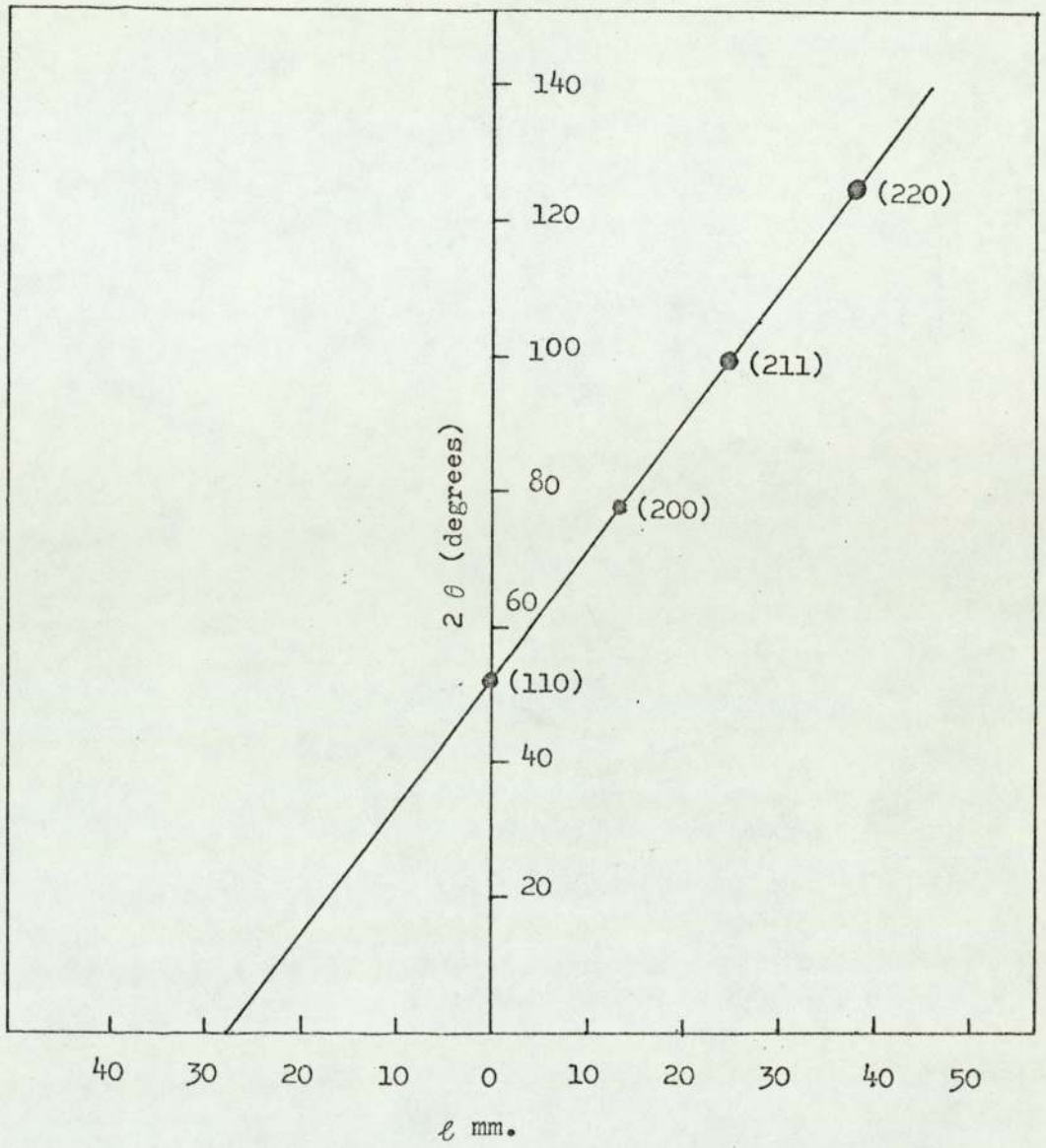
FIG.2.9 GRAPH OF 2θ AGAINST DISTANCE ALONG THE FILM 'ℓ' mm.

obtaining an X-ray diffraction pattern this ball was etched with 2% Nitol
and again irradiated. This etching process exposed the carbides. A piece
of technical grade FeS was broken from a stick and the clean broken edge
irradiated producing an FeS pattern from a specimen of similar geometry to
that of the worn balls. Finally specimens formed with each of the base
oils as lubricants were irradiated to obtain standard patterns.

2.4 Electron Probe Microanalysis of Worn Surfaces

2.4.1 Introduction

The wear scars formed on the flat faces of the rollers were
analysed using a Cambridge Instruments Microscan Mark II electron probe
microanalyser. A beam of electrons impinging on a solid surface interact
with the atoms and loose energy. Some of this energy is given off as
characteristic X-radiation from the elements present in the solid. These
X-rays can be analysed using crystal spectrometers (crystals of Gypsum or
Lithium Fluoride) and the elements identified. The intensity of the X-rays,
from the specimen relative to the intensity from standards indicates the
concentration of the elements in the specimen. In the Microscan II a
collimated beam of monochromatic electrons hits the specimen normally and
two spectrometers are mounted on either side of the specimen at a take off
angle of 20°. The electron beam can be rastered over the surface of the
specimen and a back scattered electron image of the surface observed as
well as an area distribution of the elements from the X-rays.

In accurate quantitative analysis the specimen and the comparison
standard must be as smooth and flat as possible. Unfortunately the surfaces
of wear scars are by no means flat and smooth. With this in mind, any
corrections applied to the results must be regarded as improving the overall
accuracy within the constraints of the surface roughness errors.

2.4.2 Operating Procedures

A specimen was placed in the probe and observed in the optical microscope. The specimen was aligned so that the wear tracks lay diagonally across the field of view for maximum electron contrast or with the wear tracks horizontal for maximum X-ray sensitivity. When the tracks are diagonally across the field of view the back scattered electrons are collected at right angles to the tracks thus giving the best contrast. When the tracks are horizontal the X-rays are collected parallel to the wear tracks so that there is less absorption of the X-rays by the specimen.

The analysis of the worn surfaces consisted of several parts:

(i) A visual display of the topography and the element distributions.

(ii) Spot analyses over the wear scars.

(iii) Area analyses over the wear scars.

(iv) Area analyses at various electron accelerating potentials.

2.4.3 Visual Displays

At 20kV accelerating potential the area observed at minimum magnification is approximately 0.5mm square. A polaroid camera was used to record the electron image and the element distributions. Exposure times of 2 to 5 minutes for iron, and 30 minutes for the other elements were used. The element distributions represent the average element content over the depth of penetration of the electron beam. The amounts of each element present cannot be directly related to the "whiteness" of the film as there are a considerable number of factors to be considered (for example, scattering cross sections, absorption, etc.).

2.4.4 Spot Analysis

To obtain information about the concentration of the elements

spot analyses were conducted at several points over the surface of the wear scar, front, rear, centre and sides, at least 5 points on each scar. The crystal in the spectrometer was rotated until the ratemeter indicated maximum counts at the relevant Bragg angle for a particular element. For high accuracy at least 10,000 counts are necessary and for low counting rates this means long counting times. Carbon contamination and electronic instability affect the accuracy of long counting times, thus for low concentrations the accuracy is lower than at higher concentrations. Five separate counts of 10 seconds were obtained for each point and the crystal rotated off the peak to obtain the background count rate.. Keeping all conditions constant counts were obtained on the standard in the same way. The count rates were corrected for background and counter deadtime and the ratio

$$K = \frac{(\underline{\text{Peak c/s - Background c/s + Deadtime c/s}})_{specimen}}{(\text{Peak c/s - Background c/s + Deadtime c/s})_{standard}}$$

obtained for each spot analysis.

Using a computer programme, corrections for absorption, fluorescence and atomic number provided results of the corrected weight percentage of each element present in the surface.

The correction factor (64) is

$$C_m = K_m \frac{f(\chi)_{m_{SP}}}{f(\chi)_{m_{ST}}} \cdot \left(\frac{1}{1+\gamma_m}\right) \cdot \frac{1}{N_m}$$

where C_m = correct percentage of element m.

K_m = measured percentage of element m.

$f(\chi)_{m_{SP}}$ = absorption correction for specimen.

$f(\chi)_{m_{ST}}$ = absorption correction for standard.

γ_m = fluorescence correction.

N_m = atomic number correction.

Elements with atomic numbers less than sodium cannot be detected on the Microscan II. The oxygen and carbon content of the scars can be estimated by using a method of differences.

The computation is an iterative process and by assuming that the difference between the total percentage of the elements measured and 100% is oxygen and carbon , corrected percentages including oxygen and carbon can be obtained.

2.4.5 Area Analysis

Using spot analysis of the wear scars did not appear to give a representative picture of the surfaces. The wear scars are not flat so the signal may be enhanced or reduced by surface effects. To overcome this problem area analyses of the scars were used instead. An area of 150μm x 150μm was scanned. The analysis was conducted in the same way as for spot analysis. The peak count rate was obtained from a line scan through the centre of the area so that the error in Bragg angle was similar on each side. This error was the same for the standard and thus the corrections applied to spot analysis are equally applicable to area analysis. The areas were scanned at the highest scan speed to minimise the effect of variation in the number of scans per counting time. The wear tracks were aligned horizontally so that the X-rays were collected parallel to the tracks. As the take-off angle for the X-rays was only 20° at high loads, when quite deep scars were produced, the count rates close to the front and rear edges of the scar may be affected. Because of the slope of the scar surface, surface constituents will appear more abundant whereas substrate constituents will appear reduced as the beam will not penetrate to such a great depth below the surface. Also the edge of the scar may absorb some of the X-rays.

2.4.6 Area Analysis at different Electron Accelerating Potentials

In order to obtain some idea of the distribution of the elements with depth, the accelerating potential was altered to obtain varying electron penetration. It was impossible to return to the same spot on the surface at each accelerating potential unless the surface was marked in some way. A number of wear scars were marked with micro-hardness indentations 50μm apart in two lines at right angles. Using these indentations as markers the same area (150μm square) was observed at each accelerating potential (15, 20 and 25kV) by adjusting the magnification. The standards were also scanned at each value of accelerating potential and at the same magnification so that quantitative analyses could be obtained.

2.5 The Application of Scanning Electron Microscopy to the Worn Surfaces

2.5.1 Introduction

A Cambridge Instruments Stereoscan Mark 2A was used to obtain information about the surface topography of the wear scars. The specimens, both balls and rollers, were mounted on 0.5" diameter metal stubs with adhesive and a strip of high conductivity paint was applied to the side of the specimen and onto the stub so that the specimen could conduct away electrons absorbed from the beam. If the specimen is not conducting and a charge of electrons builds up the electron beam will be deflected near the surface of the specimen and a poor image will be obtained. Back scattered electrons are collected by a scintillation counter and a visual display of the surface is produced on a cathode ray tube. Specimens can be rotated, tilted and moved in the x, y and z directions. All the specimens were observed at normal incidence as it was only possible to observe the balls in this position because of their size.

2.5.2 Specimen Analysis

Balls and rollers from each series of tests were observed. First,

a low magnification picture was taken and then higher magnification pictures
of representative areas and areas of special interest were observed. The
balls and rollers were placed so that the wear tracks ran from side to side
in the field of view to give maximum contrast. Where possible the front of
the wear scar was always on the left hand side.

A problem that occurred, particularly with specimens formed at
high loads, was the build up of electrons on the surface films because of
their poor conductivity or their lack of adhesion to the bulk of the material.
With much reduced contrast these surface details could still be observed.

2.6 Optical Microscopy

Balls and rollers from each series of tests were observed at a
variety of magnifications on a Reichert microscope and interesting features
described and photographed.

A limited number of specimens from the e.p. region of the tests
were prepared so that taper sections through the films could be observed. A
film of Aluminium was evaporated over the worn end of the rollers as a
protective coating and the roller stuck onto the centre of a $1\frac{1}{4}$ " diameter
disc. The disc was tapered at an angle of $11\frac{1}{2}°$ approximately. The roller
and disc were placed in a press and covered with granular, conducting plastic
and a mount formed under pressure. When the disc was removed the end of the
roller was covered with clear plastic. The roller was then ground down
keeping the top surface of the mount parallel to the base until half the
wear scar was exposed so that a magnification of 5 was obtained for the taper
section. The rollers had been mounted so that the wear tracks ran parallel
to the exposed taper section. These specimens were then observed in both
the etched and unetched condition and hardness measurements taken across the
surfaces.

2.7 Electron Spectroscopy for Chemical Analysis

A limited amount of analysis was conducted on an AEI machine at Shell Research Limited. An area of approximately 10mm x 2mm is irradiated with Aluminium Kα radiation under a vacuum of approximately 10^{-9} Torr and electrons are emitted from the top 100 or so angstroms. These electrons pass through a double focusing spectrometer, the energy of the electrons indicating which type of atom they originated from and the chemical environment of the atom.

A specimen holder was manufactured to take $\frac{1}{4}$" x $\frac{1}{4}$" rollers. The end of the rollers were masked with 0.003 inch thick platinum foil with a small hole exposing the wear scar. The spectra obtained from scars formed at low loads in the a.w. region were compared with those formed in the e.p. region. Gold foil masks 0.005 inches thick were also used to cover the unworn parts of the roller.

2.8 Micro-indentation Hardness Tests

A small number of scars were used to measure the hardness of the surface films. Microhardness indentations were made using applied loads of 100 and 300 gms depending on the hardness of the film. The measurements were taken on smooth areas of the scars where possible. Also the measurements were taken in the centre of the scars where the surfaces were approximately normal to the direction of the applied load. Hardness tests were also conducted on the taper sections to give some indication of the hardness of the subsurface structures.

C H A P T E R   3

THE 4-BALL MACHINE TESTS

3.1 Results Using Base Oils

Standard one minute tests using both ball on ball and ball on flat geometries, were carried out with Risella 29 and HVI oils as lubricants. Figures 3.1 and 3.2 show the graphs of mean wear scar diameter in millimetres (mm) versus load in kilogrammes (Kgf) for the two oils. The white oil (Risella 29) seized at 45 and 55 Kgf for ball on ball and ball on flat geometries respectively. Using HVI oil seizure occurred at 55 and 110 Kgf for ball on ball and ball on flat geometries. The HVI oil, especially for ball on flat geometry showed some extreme pressure activity whereas Risella 29 showed no such action. For the ball on flat geometry with HVI oil, initial seizure varied between 45 and 65 Kgf and final seizure between 80 and 110 Kgf. In the other three tests there was little variation in final seizure.

The differences observed between the tests run with the two geometries may be explained by several factors. The surface finish of the flat faces of the rollers was not as good as that of the balls, as the cylindrical faces were the highly polished parts of the rollers, the flat ends having a polished face covered with fine scratches. The geometry of a ball on a flat surface is different to that of a ball on a ball and affects the running conditions, for example the heat dissipation and the rate of wear.

3.2 Results with Sulphur Additives

The results of tests carried out with oils containing 1% by weight
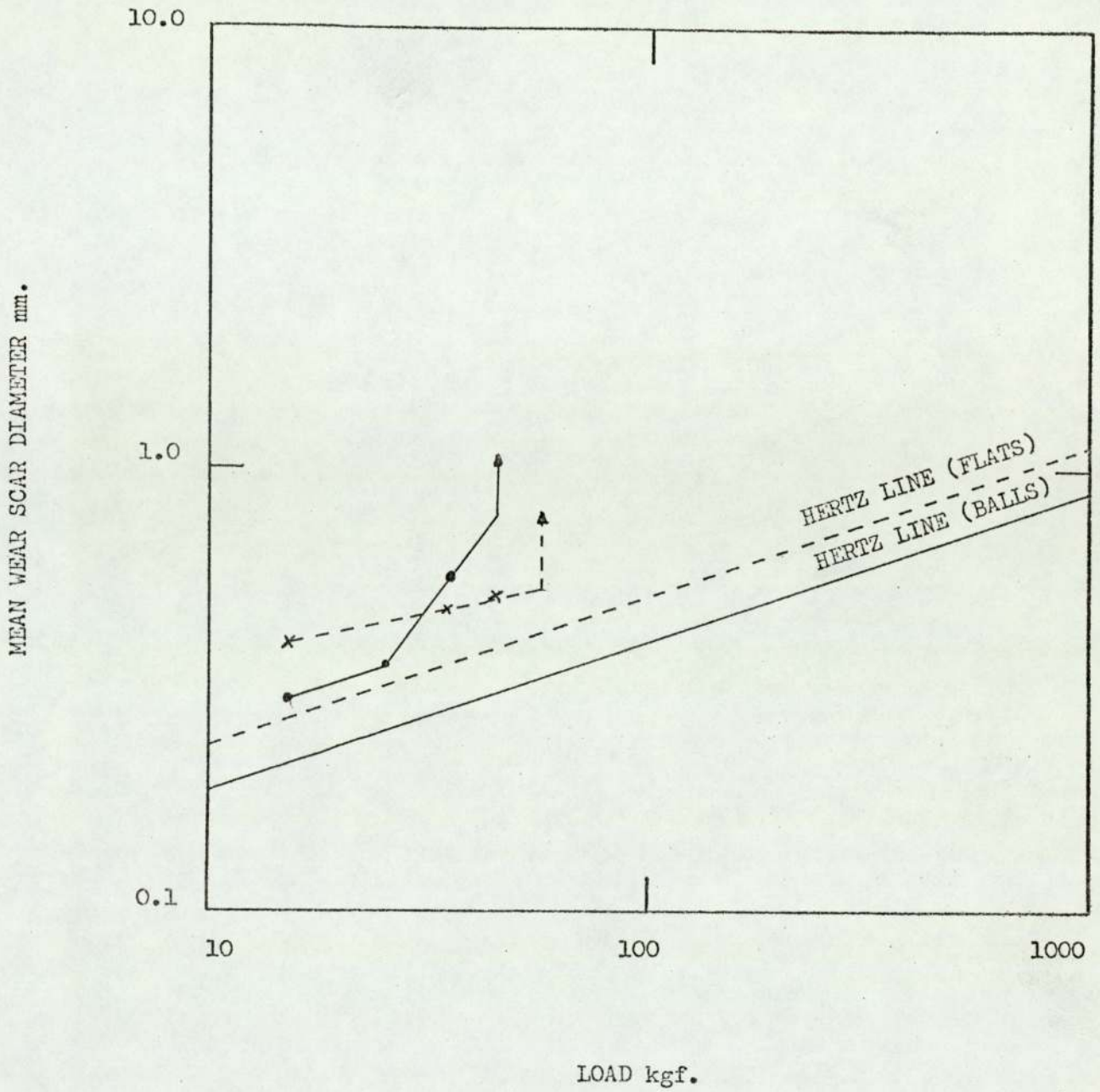
FIG. 3.1 LOAD VERSUS MEAN WEAR SCAR DIAMETER.

LUBRICANT: RISELLA 29 OIL

•——— 4 Ball Geometry

x — — — 1-Ball-on-3-Flats Geometry
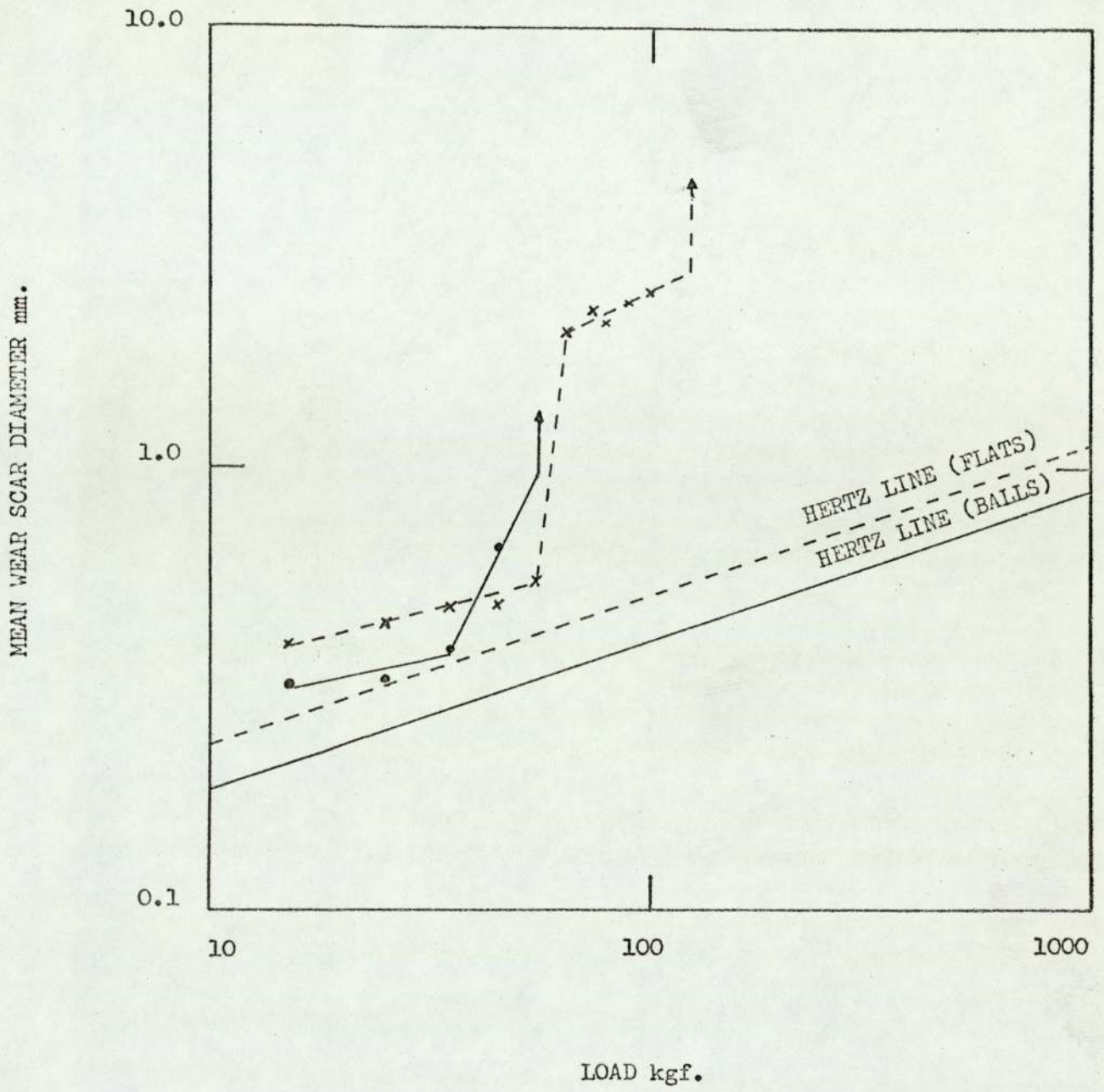
FIG. 3.2   LOAD VERSUS MEAN WEAR SCAR DIAMETER.

LUBRICANT: HVI OIL

•———   4-Ball Geometry

✕ – – –   1-Ball-on-3-Flats Geometry

of Dibenzyl Disulphide are plotted in Figures 3.3 and 3.4. There is a considerable range to the distribution of the points between 55 and 160 Kgf. Above and below these values the wear scar diameters were similar in all the tests with DBDS. The onset of initial seizure varied from 45 Kgf up to 70 Kgf. At low loads before initial seizure (in the anti-wear region), the graphs are approximately parallel to and slightly above their respective Hertz lines indicating that the area of contact due to elastic deformation has been increased by wearing of the surfaces. The gradient of the lines after initial seizure (in the e.p. region) for all the tests is greater than the Hertz lines.

The graphs obtained from tests using 4-ball geometry have a second step after initial seizure lying between the a.w. and e.p. regions. This occurred using both oils. There were points above and below these lines which fell on continuations of the lines drawn through the points in the a.w. and e.p. regions. This second step was not apparent using Risella 29 and ball on flat geometry although up to 80 Kgf points were falling on the continuation of the a.w. line. Using HVI oil and ball on flat geometry there was a broad distribution above 55 Kgf through which a straight line was drawn as the best fit. The graphs all have final seizure loads of 260 Kgf except for HVI oil and ball on flat geometry which seized at 220 Kgf. They all have initial seizures around 55 Kgf.

When 0.886% by weight of Diphenyl Disulphide was used as additive the graphs of load versus wear scar diameter (Figures 3.5 and 3.6) have final seizure loads around 180 Kgf, considerably below those using Dibenzyl Disulphide. Using Risella 29 as base oil initial seizure occurred at 55 and 65 Kgf for ball on ball and ball on flat geometries respectively. Final seizure occurred at 180 Kgf in both cases. When HVI oil was used initial seizure occurred at 55 Kgf for ball on ball and at 35 Kgf for ball on flat.
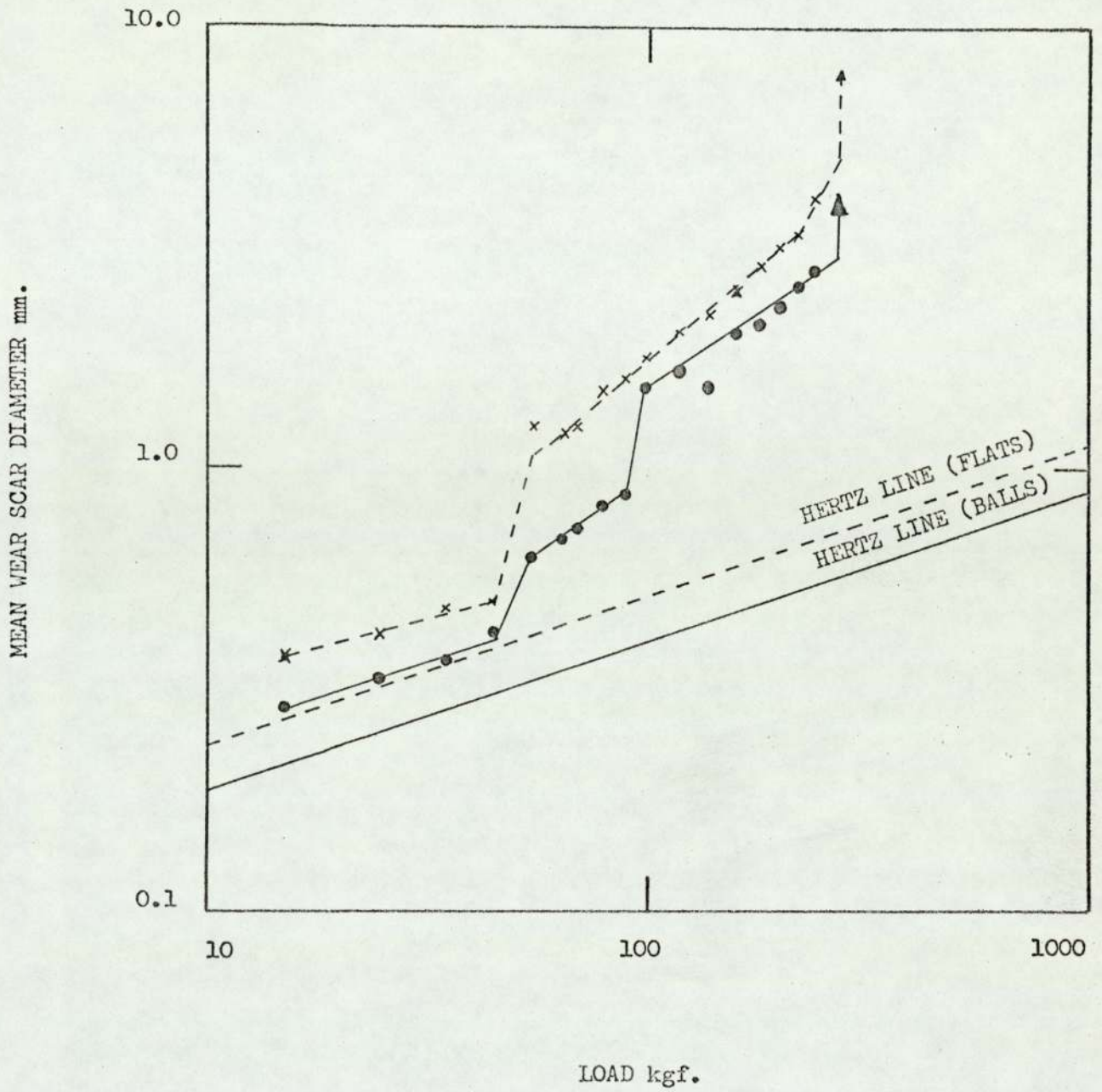
FIG. 3.3   LOAD VERSUS MEAN WEAR SCAR DIAMETER.

LUBRICANT: RISELLA 29 + 1.0%wt DBDS

•———   4-Ball Geometry

x————   1-Ball-on-3-Flats Geometry
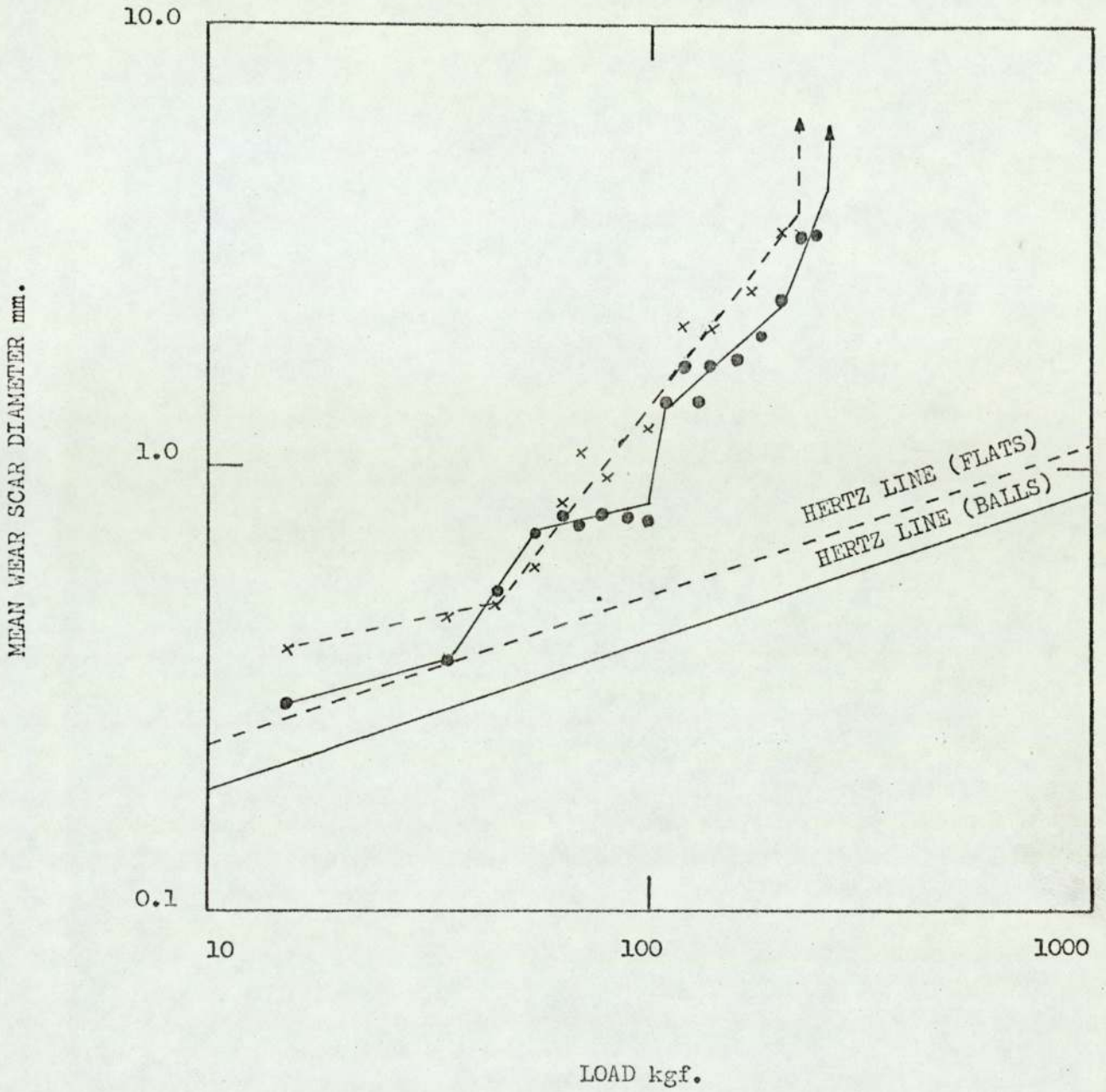
FIG. 3.4   LOAD VERSUS MEAN WEAR SCAR DIAMETER.

LUBRICANT: HVI + 1.0%wt DBDS

●——— 4-Ball Geometry

X——— 1-Ball-on-3-Flats Geometry
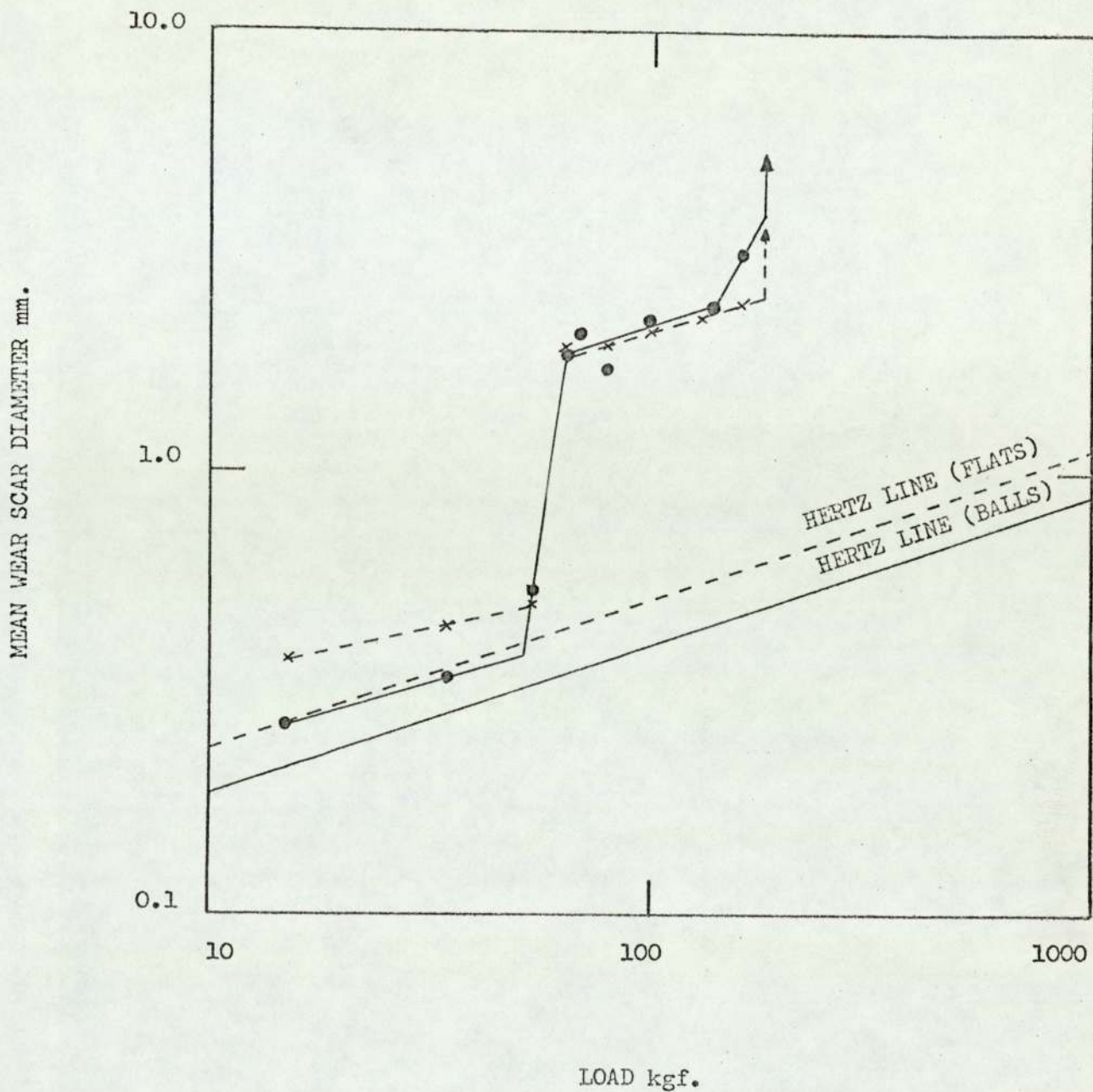
FIG. 3.5   LOAD VERSUS MEAN WEAR SCAR DIAMETER.

LUBRICANT: RISELLA 29 + 0.886%wt DPDS

●———   4-Ball Geometry

✗————   1-Ball-on-3-Flats Geometry
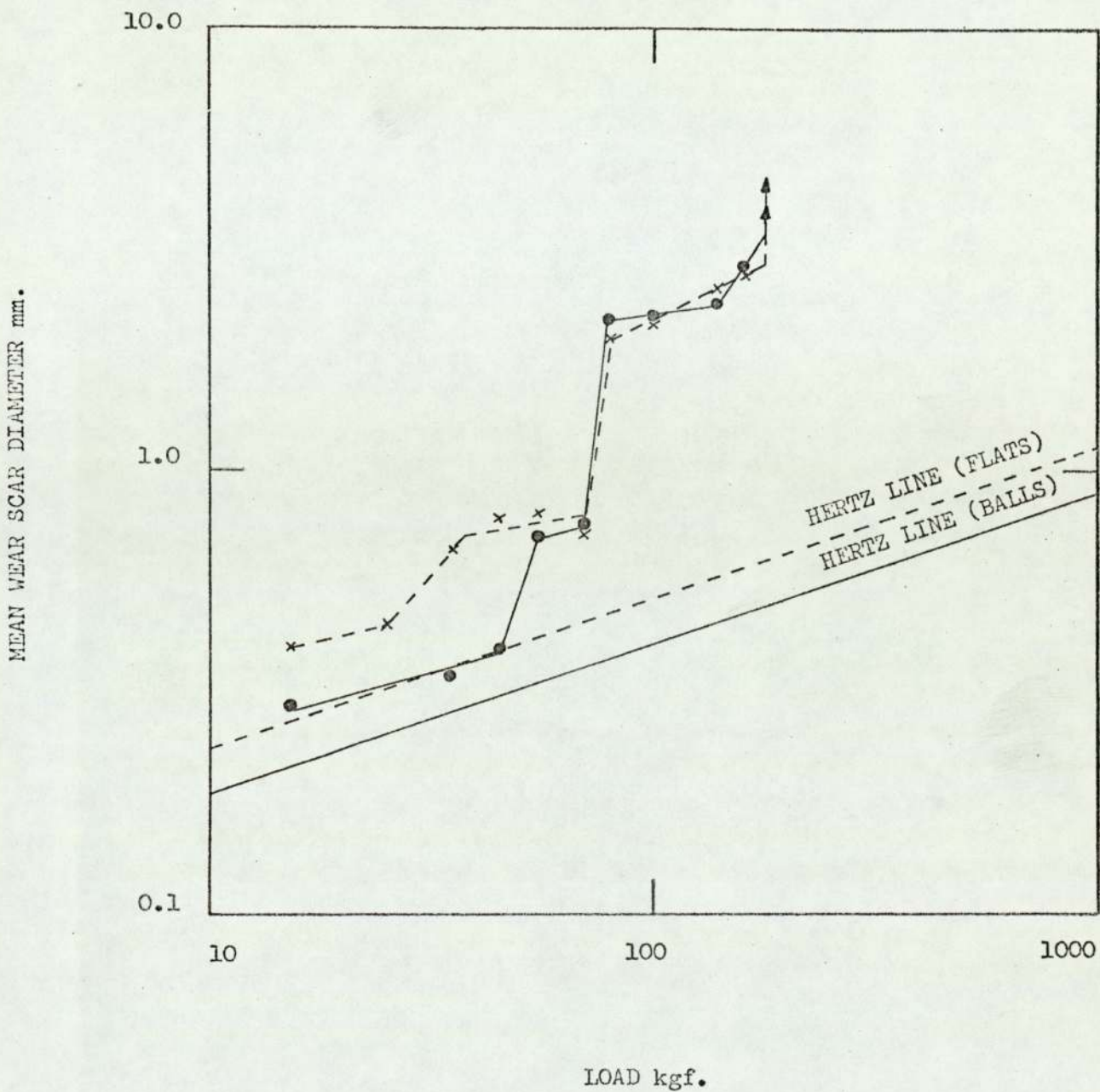
FIG. 3.6   LOAD VERSUS MEAN WEAR SCAR DIAMETER.

LUBRICANT: HVI + 0.886%wt DPDS

●———   4-Ball Geometry

×—-—-—   1-Ball-on-3-Flats Geometry

Final seizure was at 180 Kgf in both tests. There are wear scars of intermediate size in both tests with HVI oil. These results have a much smaller spread than those obtained with DBDS as additive. Variations in wear scar diameter only occurred around initial seizure where scars of intermediate size were obtained. The transition to the e.p. region appeared at 65 or 70 Kgf on all occasions. Before initial seizure the gradient of the graphs follow the Hertz lines indicating that the wear rates are similar when the load is increased. The fact that the intermediate step only occurs when HVI oil was used suggests that competition for the metal surface between the additive molecules and the polar compounds in the oil was taking place. This could lead to a partial breakdown of the film initially causing some wear and a reduction in the pressure. This reduction in pressure would allow the film to be re-established and protection of the metal surface to continue so that a low wear rate was again obtained. When the conditions became too severe, complete breakdown occurred and extreme pressure effects were observed.

The graphs of load versus wear scar diameter (Figures 3.7 and 3.8) using 0.723% by weight of Di-tert-butyl Disulphide as additive are similar to those obtained using Dibenzyl Disulphide. Initial seizure occurred at slightly lower loads (45 Kgf) using DTBDS than using DBDS. This was followed by an intermediate step up to 80 Kgf and then on to the e.p. region where final seizure occurred between 220 and 260 Kgf. The behaviour of DTBDS seemed much more predictable than that of DBDS. In the a.w. region the wear scar diameters at 15 Kgf were quite large indicating that a considerable amount of wear had taken place. As the loads were increased the wear scar diameters approached the Hertzian diameters showing that the wear rate was decreasing with increasing load up to initial seizure. The graphs for the two geometries, ball on ball and ball on flat, are very similar, showing that for this additive, the different surface finishes and
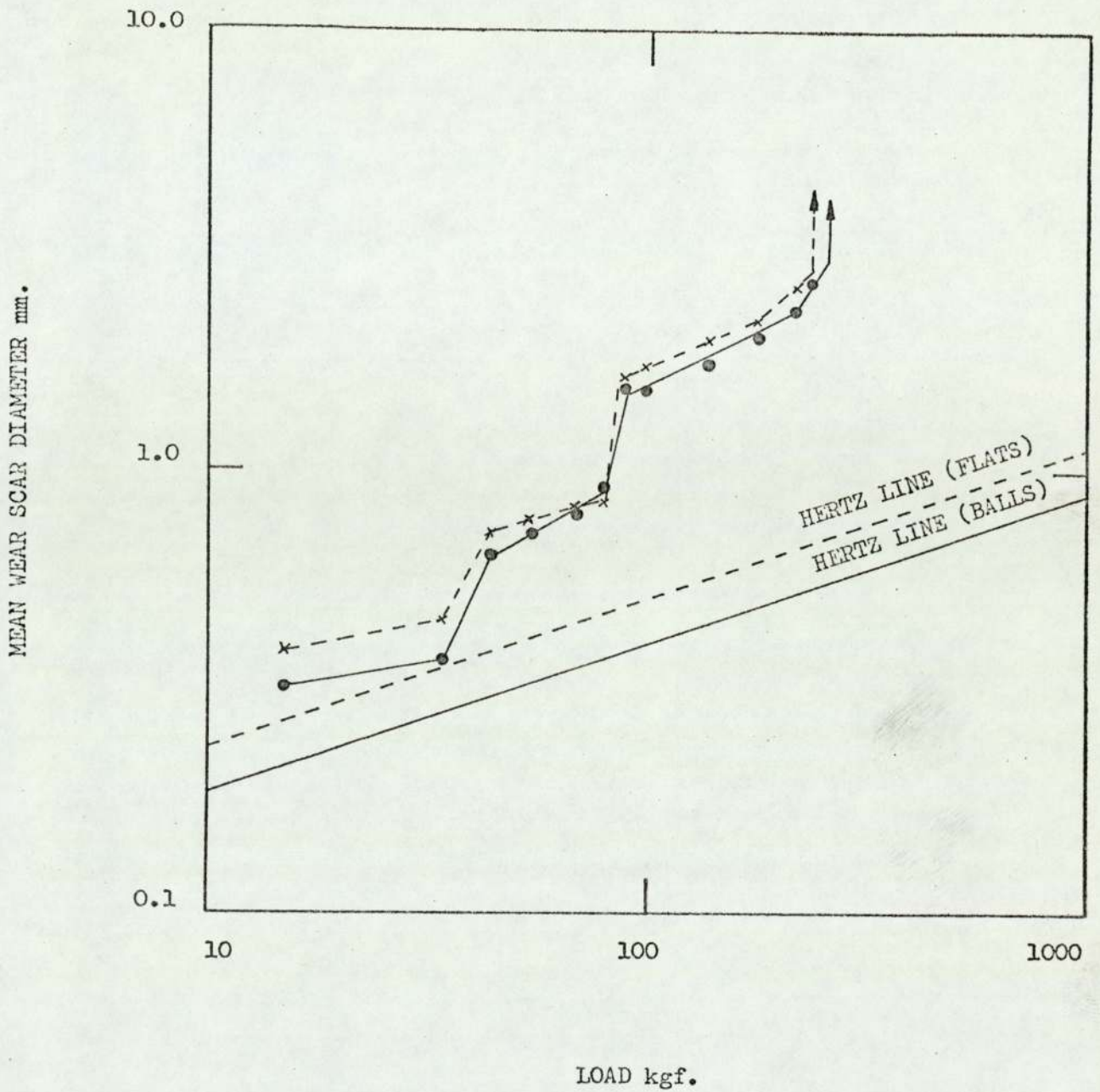
FIG. 3.7   LOAD VERSUS MEAN WEAR SCAR DIAMETER.

LUBRICANT: RISELLA 29 + 0.723%wt DTBDS

     ●———   4-Ball Geometry

     x————   1-Ball-on-3-Flats Geometry
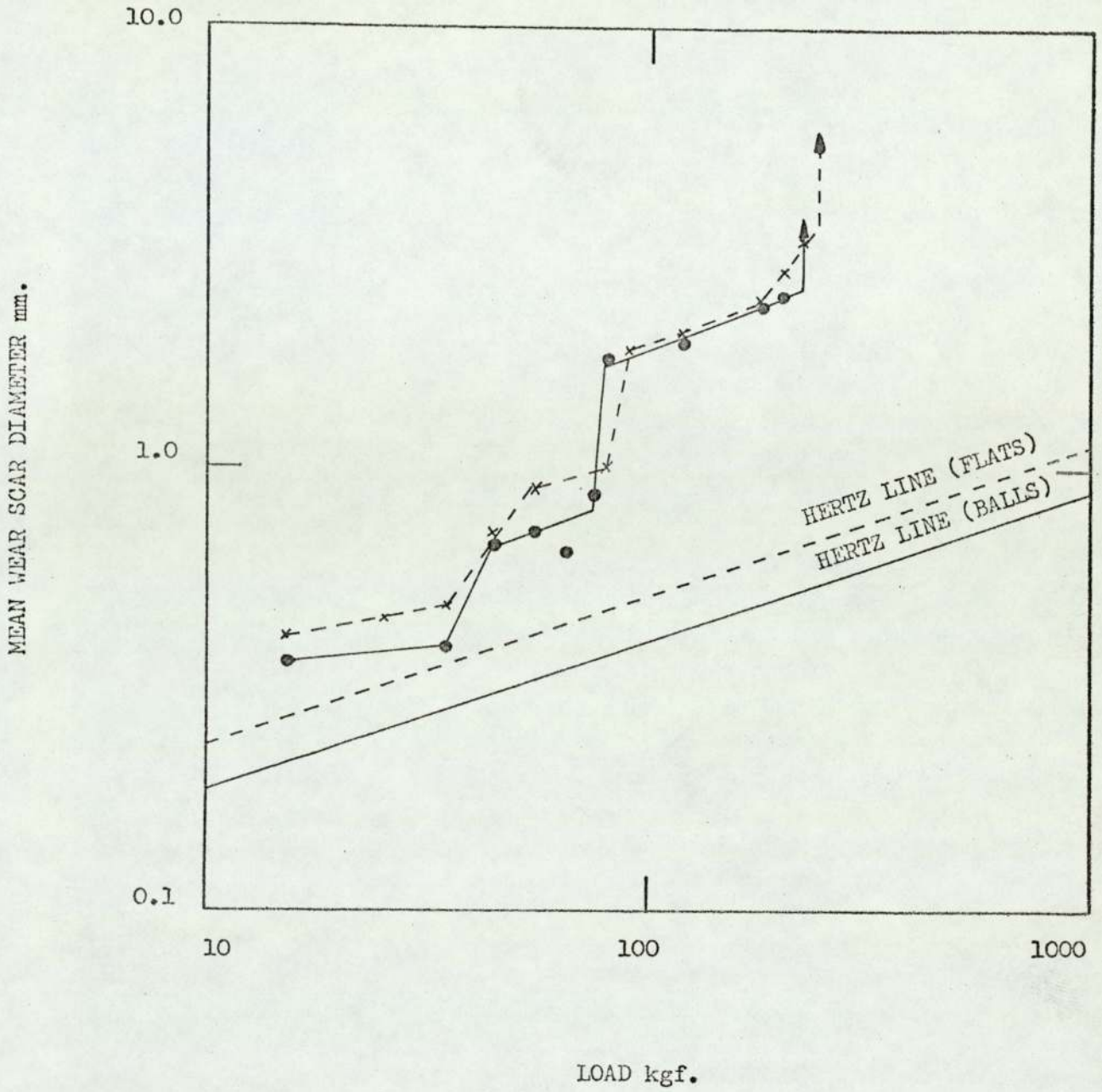
FIG. 3.8   LOAD VERSUS MEAN WEAR SCAR DIAMETER.

LUBRICANT: HVI + 0.723%wt DTBDS

- ●——— 4-Ball Geometry
- ✗ – – – 1-Ball-on-3-Flats Geometry

geometries have very little effect on the overall performance of the additive.

3.3 Results with Zinc Dialkyldithiophosphate Additives

Using 1.112% by weight of pure Zinc Dibutylphosphorodithioate (ZDP) as additive the initial seizure load on the 4-ball machine tests was increased considerably over those obtained using sulphur additives. Figures 3.9 and 3.10 show these results. When Risella 29 was used as base oil initial seizure occurred at 100 and 90 Kgf for ball on ball and ball on flat geometries respectively and final seizure occurred at 140 Kgf in both cases. The gradients of the lines in the a.w. region are less than the Hertz lines showing that the wear rates are low. When HVI oil is used similar results are obtained for ball on ball geometry, initial seizure occurring at 100 Kgf and final seizure at 160 Kgf. However, when the ball on flat results are compared there is an obvious difference in the load range 35 to 90 Kgf. In this region using HVI oil wear scar diameters lying on two distinct lines were obtained. Points on the a.w. line and the intermediate line were obtained at the same loads. This difference may be due to the competition for the surface, between the polar compounds in the HVI oil and the active molecules in the ZDP additive, reducing the effective-ness of the film. If this is combined with the poorer surface finish of the flat ends of the rollers less effective boundary lubrication would occur. The final seizure load using HVI oil was slightly higher than that obtained using Risella 29 and may possibly be due to the e.p. activity of the base oil as indicated by the tests conducted on the base oils alone (HVI oil has ~1% sulphur). The extreme pressure activity of this additive is very limited in extent as indicated by the low final seizure loads.

Figures 3.11 and 3.12 show the results of 4-ball machine tests using 1.0% by weight of Lubrizol 1395 as additive. The initial seizure load
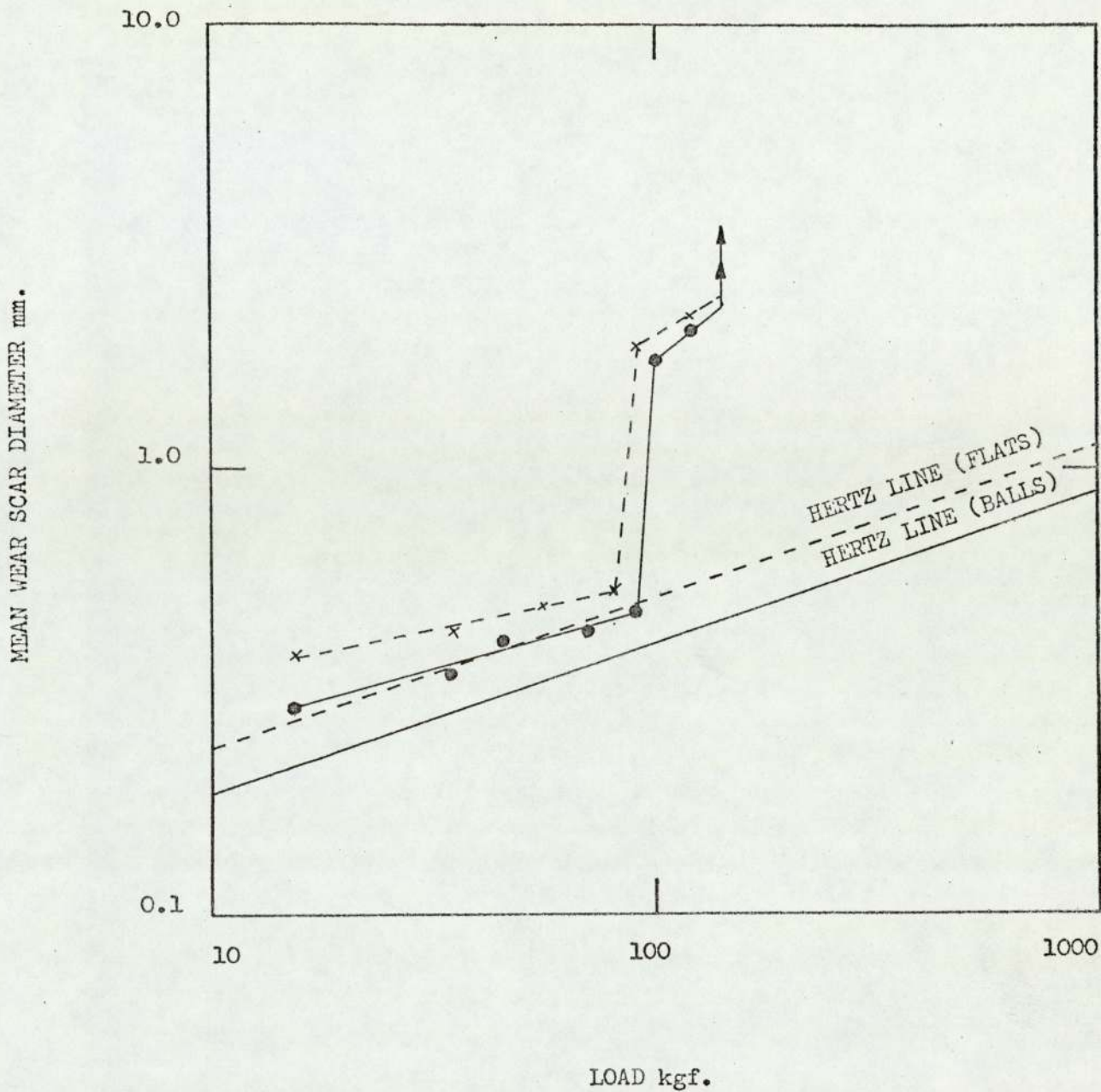
FIG. 3.9   LOAD VERSUS MEAN WEAR SCAR DIAMETER.

LUBRICANT: RISELLA 29 + 1.112%wt ZDP

●——————   4-Ball Geometry

✗ — — —   1-Ball-on-3-Flats Geometry
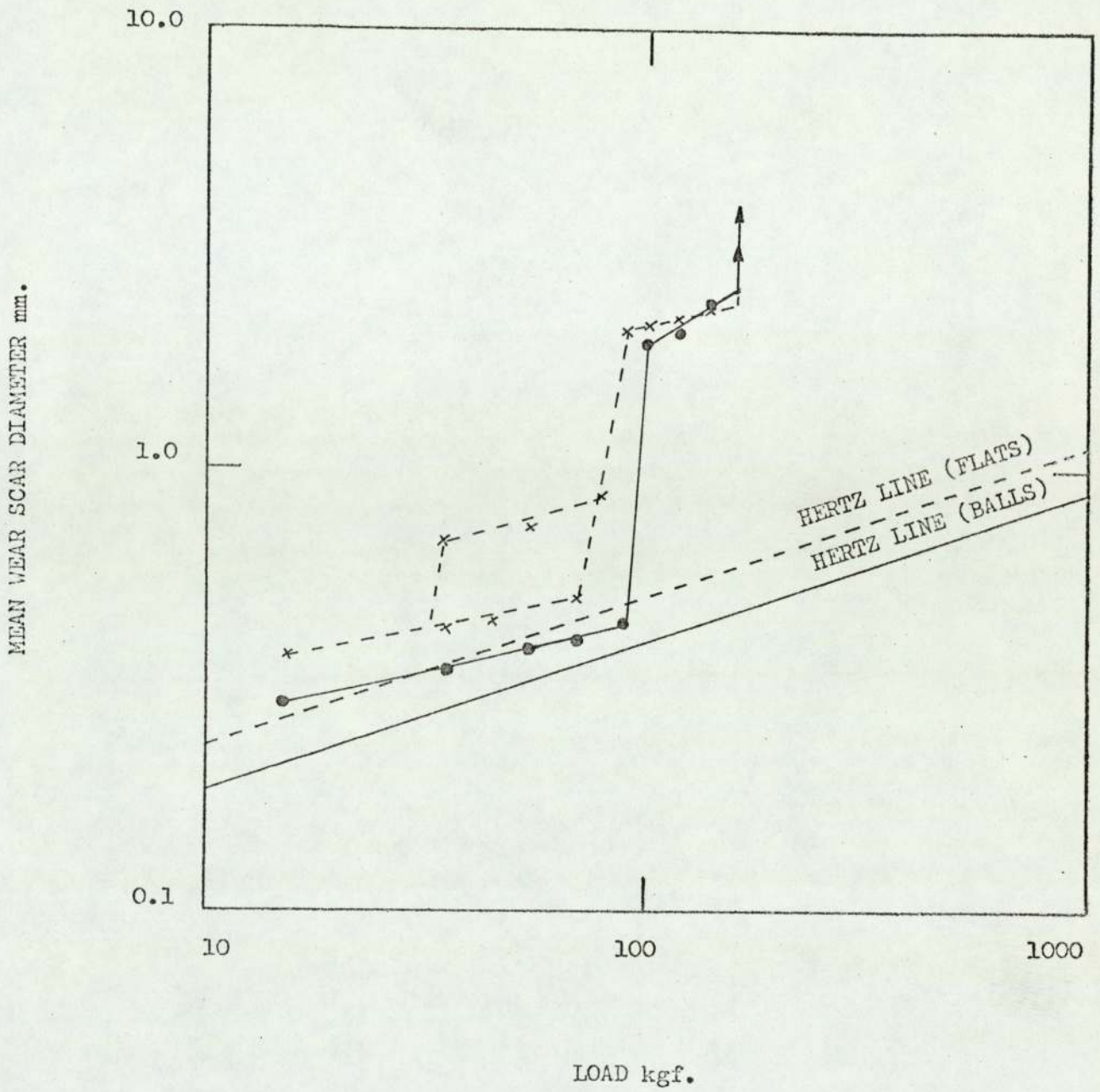
FIG. 3.10   LOAD VERSUS MEAN WEAR SCAR DIAMETER.

LUBRICANT: HVI + 1.112%wt ZDP

●————   4-Ball Geometry

✗————   1-Ball-on-3-Flats Geometry
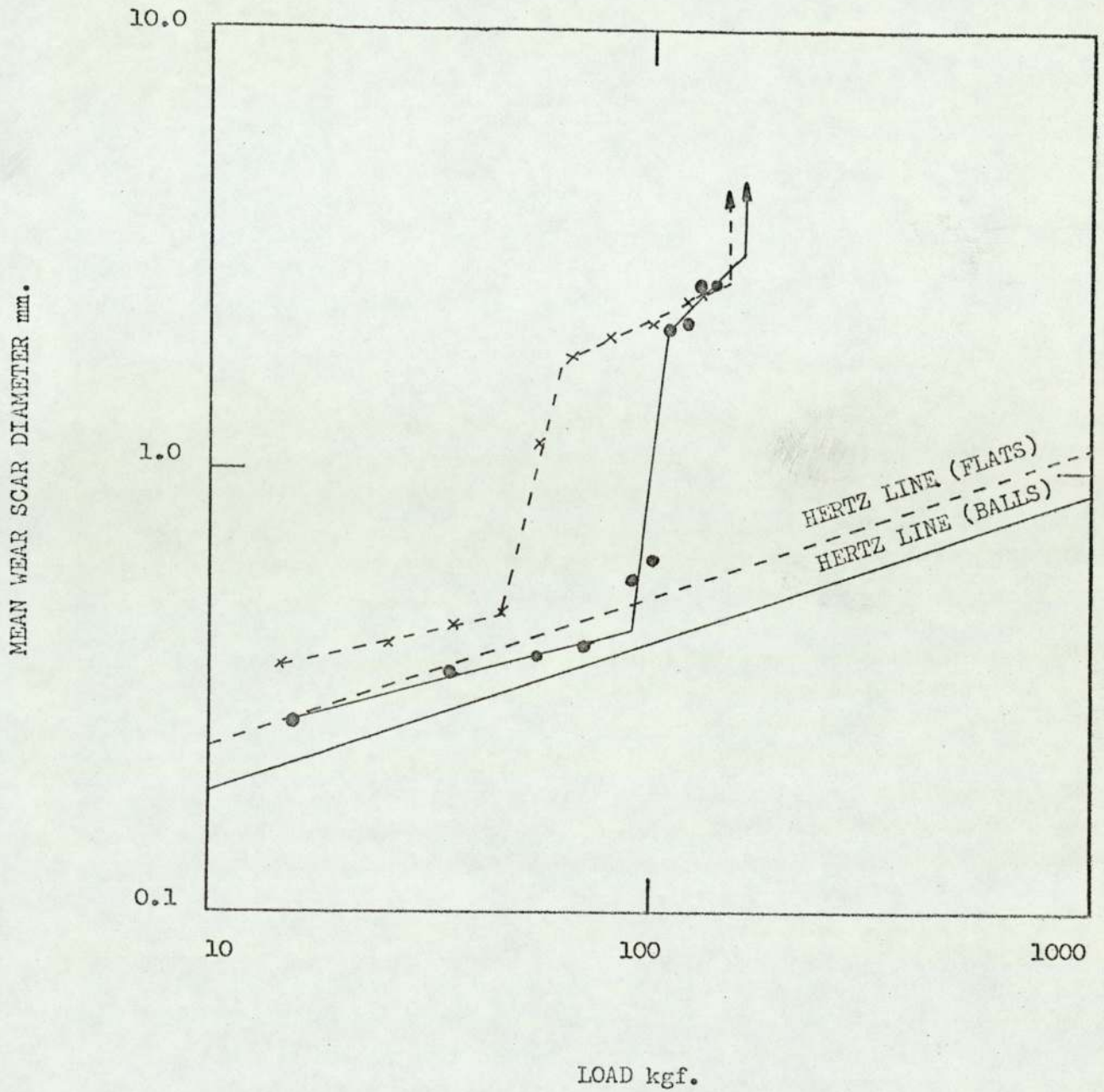
FIG. 3.11   LOAD VERSUS MEAN WEAR SCAR DIAMETER.

LUBRICANT: RISELLA 29 + 1.0%wt LUBRIZOL 1395

● ——————   4-Ball Geometry

✗ — — —   1-Ball-on-3-Flats Geometry
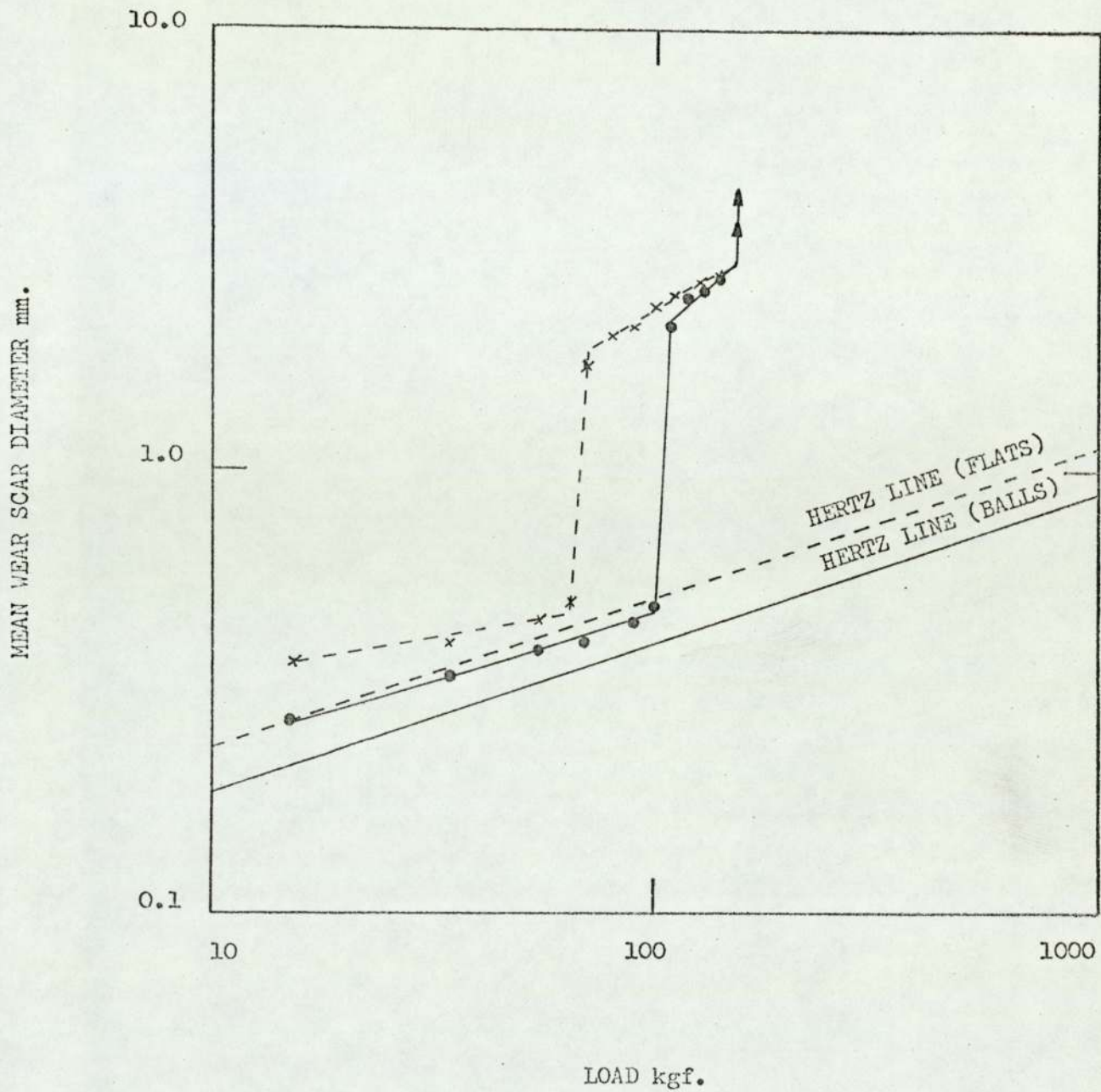
FIG. 3.12   LOAD VERSUS MEAN WEAR SCAR DIAMETER.

LUBRICANT: HVI + 1.0%wt LUBRIZOL 1395

●————   4-Ball Geometry

✕————   1-Ball-on-3-Flats Geometry

for ball on ball geometry was 110 Kgf for both base oils but for the ball on flat geometry the initial seizure loads were lower at 55 and 70 Kgf for Risella 29 and HVI base oils respectively. The slopes of the lines in the a.w. region were less than that of the Hertz lines indicating low wear rates similar to those obtained using pure ZDP additive. The difference in the results for ball on ball and ball on flat geometries is similar for both base oils and must be attributed to the surface finish of the rollers. If a thin protective layer was formed on a rough surface it may not be sufficient to afford protection to the metal surfaces. The tests using Lubrizol 1395 as additive show that it has a limited e.p. activity similar to that of pure ZDP.

3.4 Summarizing Remarks

The base oils seize at low loads, HVI oil having some limited e.p. activity. The sulphur additives have similar initial seizure loads ($\sim$ 55 Kgf) and DBDS and DTBDS give similar wear graphs, DTBDS being more predictable in behaviour. These two additives give a high seizure load. DPDS has a much poorer e.p. activity than the other two sulphur additives. In the a.w. region the graphs for the sulphur additives are approximately parallel to the Hertz lines except for DTBDS which has a high wear rate at 15 Kgf. There are differences between the graphs both due to base oils and geometry. The two ZDP additives gave very similar results. The initial seizure loads are high ($\sim$ 100 Kgf) but the final seizure loads are lower than the poorest sulphur additive (DPDS). The ball on flat results, particularly when using Lubrizol 1395 as additive, have lower initial seizure values than those obtained with a ball on ball configuration. This may be due to the poorer surface finish of the flat ends of the rollers compared to the finish on the balls.

In the following chapters (4 to 7) the specimens formed in the 4-ball tests were analysed using various physical techniques.

C H A P T E R   4

ANALYSIS OF THE WORN SURFACES USING
GLANCING-ANGLE X-RAY DIFFRACTION

4.1   X-Ray Diffraction Analysis of Standards

Several standards were used as comparisons for the diffraction
patterns obtained from worn specimens. Cobalt $K\alpha$ radiation was used in all
the analyses. A solid specimen of FeS, broken from a stick of technical
grade material, was irradiated for 12 hours at a glancing angle of 15°. The
α-Fe lines were used as internal standard and the results of the analyses
are presented in Table 4.1. The α-Fe lines were quite broad, consequently
small variations in the 'd' values obtained from each film required the
results to be presented in total so that allowances for these differences
can be made. In two columns of the table, the 'd' values from cards
4 - 0832 FeS (ordered) and 11 - 151 FeS (Troilite) of the ASTM card index
are presented for reference. The edge of the specimen acts as a cut-off
for 'd' values above about 3Å, consequently the higher 'd' values are
missing from all the specimens that have been analysed. Table 4.1 contains
examples of all the patterns referred to in the text of this chapter.

Two flat surfaces were ground on a ball so that they intersected
at 90° to form a sharp edge. The ball was then etched with 2% Nitol to
expose the carbides. The edge so formed was irradiated at an angle of 20°
for 70 hours. The resultant diffraction pattern contained 15 lines other
than α-Fe. These lines were compared with the 'd' values from the ASTM
card number 6-0688 Fe_3C (Cementite) and good agreement was obtained (see
Table 4.1). An unetched, unworn ball irradiated for 70 hours gave 12 lines
other than α-Fe, which again were identified as cementite Fe_3C.

Table 4.1

Left axis label: **'d' VALUES, Å**

α-Fe$_2$O$_3$ (13-534) d	I/I₁	Fe$_3$O$_4$ (11-614) d	I/I₁	FeS (4-0832) d	I/I₁	FeS (11-151) d	I/I₁	Fe$_3$C (6-0688) d	I/I₁	FeS Specimen	Etched Ball	Unworn Ball	HVI 45Kgf	HVI+DBDS 55Kgf	RIS+DBDS 90Kgf	RIS+DBDS 140Kgf	HVI+DBDS 200Kgf	RIS+DBDS 200Kgf	RIS+DBDS 200Kgf	RIS+DBDS 200Kgf	HVI+DBDS 220Kgf	RIS+DBDS 220Kgf	RIS+DTBDS 100Kgf	RIS+DTBDS 180Kgf	RIS+DTBDS 240Kgf	HVI+DTBDS 180Kgf	RIS+DTBDS 200Kgf	RIS+DPDS 160Kgf	HVI+DPDS 140Kgf	HVI+DPDS 160Kgf	HVI+DPDS 140Kgf	RIS+ZDP 120Kgf	HVI+ZDP 120Kgf	RIS+LUB1395 90Kgf	RIS+LUB1395 140Kgf	HVI+LUB1395 100Kgf	HVI+LUB1395 140Kgf
3.68	25			4.85	40	5.4	20																														
						4.74	10																														
		2.97	70	2.98	90	2.98	40			2.98							3.00	2.99	2.99	2.98	3.05	2.99	2.98	3.00	2.99						2.97						
				2.93	50					2.91									2.89		2.96		2.91														
2.69	100			2.67	90	2.66	60			2.66							2.67	2.66	2.66	2.67	2.67	2.65	2.66	2.67	2.66		2.63	2.63	2.65								
																					2.61																
Standards																																					
2.51	50	2.53	100	2.52	30	2.52	10	2.54	5	2.54							2.52	2.54	2.54	2.54	2.54	2.55	2.52			2.53		2.54	2.53	2.53							
										2.48								2.46				2.48				2.49											
		2.42	10																																		
						2.38	65				2.383	2.38	2.38	2.38	2.38	2.39	2.38	2.38	2.38	2.39	2.38	2.38	2.39	2.38	2.38		2.37	2.38	2.39	2.39	2.37	2.38	2.38	2.38	2.38	2.39	2.38
										2.29								2.30						2.28	2.30	2.30											
2.20	30					2.26	25				2.257	2.26	2.26	2.26	2.26	2.27	2.26	2.24	2.26	2.27	2.26	2.27	2.27	2.26	2.25	2.24	2.26	2.26	2.27	2.27	2.24	2.26	2.24	2.26	2.24	2.27	2.26
						2.20	25				2.203	2.20	2.20		2.20	2.22	2.212	2.21	2.21	2.22	2.22	2.20															
				2.15	50	2.14	10			2.15								2.165			2.17			2.22	2.21	2.20	2.20	2.20				2.22	2.20	2.21	2.22	2.20		2.20	2.22
				2.14	50																																
						2.09	100	2.09	100	2.097	2.10	2.10	2.10	2.10	2.10	2.11		2.10	2.097	2.11	2.09	2.09	2.09	2.11	2.12	2.17	2.14										2.11
		2.096	70															2.093	2.082								2.09	2.09	2.09	2.09	2.06	2.06			2.09	2.09		2.09
2.07	2					2.06	70			2.027	2.063	2.06				2.07		2.06	2.055	2.066	2.06		2.07	2.07	2.06	2.06	2.07	2.06			2.04	2.06	2.07		2.06	2.07	2.07
						2.02	60			2.027	2.027	2.027	2.027	2.027	2.027	2.027	2.027	2.027	2.027	2.027	2.027	2.027	2.027	2.027	2.027	2.027	2.027	2.027	2.027	2.027	2.027	2.027	2.027	2.027	2.027	2.027	2.027
						2.01	100																														2.00
						1.97	55			1.97	1.964	1.97	1.97	1.97	1.97	1.987	1.97	1.97	1.97	1.98	1.98	1.97	1.98	1.98	1.97	1.97	1.98	1.98	1.97	1.97	1.97	1.97	1.98	1.97	1.97	1.98	1.97
										1.94								1.91		1.92		1.95	1.93	1.91	1.94												
				1.95	50	1.923	30																														
				1.92	60																																
1.837	40					1.87	30			1.89	1.878	1.87	1.87	1.87	1.87	1.875	1.87	1.87	1.87	1.88	1.87	1.86	1.87	1.88	1.87	1.86	1.87	1.87	1.87	1.86	1.87	1.87		1.87	1.87
						1.85	40			1.85	1.85	1.85	1.85	1.85	1.857		1.85	1.85	1.86	1.85	1.84		1.84	1.85	1.85	1.85	1.85	1.85					1.85	1.80	1.85
										1.797							1.81			1.80	1.81	1.81	1.80	1.80	1.81	1.80	1.80	1.80	1.80	1.79	1.79	1.79	1.81			
				1.75	60	1.748	10	1.76	15	1.76		1.76	1.76		1.76	1.77	1.76	1.76	1.76	1.76	1.76	1.75	1.76	1.76	1.76	1.76	1.76	1.76	1.75	1.76	1.76		1.76	1.75	1.76
		1.712	60	1.72	90	1.72	50			1.73							1.72	1.72	1.73	1.73	1.72	1.73	1.72	1.72	1.72	1.73	1.72										
1.691	60					1.68	15								1.68	1.686	1.68	1.68	1.68	1.69	1.68	1.68	1.69	1.69	1.68	1.67	1.67	1.68		1.68	1.69	1.68	1.68	1.68	1.67	1.68	1.68
																							1.65														
1.634	4			1.64	60	1.634	30			1.64						1.65	1.64	1.64	1.64	1.63		1.64	1.65	1.63	1.62	1.63	1.64	1.64	1.63		1.63				1.63	1.64	1.64
				1.62	40																																
1.596	16	1.614	85	1.60	40	1.595	5	1.61	7	1.606					1.58	1.59	1.59	1.59	1.59	1.59	1.58	1.59			1.58	1.59	1.58	1.58	1.58	1.58	1.59	1.59	1.58	1.59	1.51	1.58
								1.58	20																												
				1.50	50	1.501	5			1.51						1.52	1.51	1.51	1.51	1.51	1.51			1.52	1.51	1.50	1.51	1.50	1.50	1.51		1.51		1.50	1.51	1.51
1.484	35	1.483	85	1.49	50					1.48						1.46				1.46						1.46											
				1.47	60					1.46																											
1.452	35			1.46	50	1.469	30											1.45				1.45														
				1.44	60	1.445	20																													
				1.42	50	1.422	5			1.43	1.433	1.433		1.433	1.433	1.433	1.433	1.4332	1.433	1.433	1.433	1.433	1.433	1.433	1.433	1.433	1.433	1.433	1.433	1.433	1.433	1.433	1.433	1.433	1.433	1.433
																										1.428											
																1.40	1.41	1.40									1.41		1.41							1.41
1.349	4	1.327	20	1.34	40	1.331	40			1.34					1.34		1.35	1.33	1.34	1.33	1.33	1.33	1.35	1.34	1.33	1.32	1.33	1.36			1.325			1.33	1.33	1.31
				1.33	80	1.320	10			1.31																											
1.310	20			1.32	50			1.33	25	1.298								1.29																			
				1.28	40	1.284	5			1.277	1.268	1.27			1.266		1.277	1.27		1.28	1.275	1.278			1.26	1.26		1.27	1.27	1.275	1.27				1.26	1.27
1.258	8	1.264	10	1.27	40	1.271	5																														
1.213	4	1.211	20	1.23	40	1.224	20			1.230	1.215	1.22			1.214	1.219	1.22	1.22	1.22	1.22	1.25	1.22	1.22	1.22	1.22	1.22	1.20	1.22	1.22	1.22		1.22	1.21	1.22	1.22
																					1.21																
1.187	8			1.19	40	1.188	10			1.190									1.19	1.19	1.19			1.18	1.21	1.19											
						1.179	10																														
1.160	10			1.18	40					1.170	1.170	1.170	1.170	1.170	1.170	1.170	1.170	1.170	1.170	1.170	1.170	1.170	1.170	1.170	1.170	1.170	1.170	1.170	1.170	1.170	1.170	1.170	1.170	1.170	1.170	1.170
1.141	12					1.135	20			1.14							1.146	1.15	1.15	1.14				1.15	1.15		1.15			1.15							1.15
1.100	14	1.1214	30			1.119	40			1.122	1.125	1.125			1.127	1.127	1.127	1.126	1.13	1.13	1.125	1.13	1.13	1.13	1.13	1.13	1.13	1.12	1.13	1.12		1.13	1.12	1.13	1.13
						1.108	30			1.11						1.107	1.11	1.10	1.11	1.12	1.104	1.11	1.10	1.11	1.11	1.10	1.11	1.10	1.11	1.10		1.10	1.10	1.11
		1.092	60			1.091	10			1.096	1.081	1.08			1.082						1.09	1.09															
1.053	18	1.049	40			1.054	30			1.06	1.057							1.05	1.06						1.06		1.09	1.09	1.09	1.09	1.09		1.08	1.08
											1.037											1.039				1.045	1.04	1.04	1.04	1.04				1.03	1.04
				1.024	10					1.032																										
										1.018	1.0134	1.0134	1.0134	1.0134	1.0134	1.0134	1.0134	1.0134	1.0134	1.0134	1.0134	1.0134	1.0134	1.0134	1.0134	1.0134	1.0134	1.0134	1.0134	1.0134	1.0134	1.0134	1.0134	1.0134	1.0134	1.0134	1.0134
										1.000																											
0.989	10	0.989	10			0.994	20			0.991			0.991	0.989		0.991	0.986	0.993	0.992			0.996	0.982		0.992				0.992					0.987	0.993

Included in the standards are patterns obtained from worn specimens formed when only the base oils were used as lubricants. These patterns were very similar to those of the etched and unworn specimens.

For completeness ASTM cards 13-534, α-Fe_2O_3 and 11-614 Fe_3O_4 are included in Table 4.1 under the standards section.

4.2 X-Ray Diffraction Analysis of Surfaces formed using Sulphur Additives

Glancing angle X-ray diffraction patterns from specimens worn under lubricants containing sulphur additives were obtained with exposure times between 70 and 100 hours. All the specimens analysed showed that up to initial seizure loads ($\sim$ 55 Kgf) there was very little difference between the three additives DBDS, DPDS and DTBDS. The patterns were very similar to that obtained from an unworn ball. The wear scars formed below initial seizure were approximately the same size as the X-ray beam. This indicates that there was insufficient surface material on the wear scars to form a diffraction pattern and/or the surface film was not crystalline.

The X-ray diffraction patterns of scars formed at loads between initial seizure and 100 Kgf show an increasing amount of iron carbide Fe_3C. The intensities of the Fe_3C lines were greater than the intensities of the Fe_3C lines obtained from an etched ball indicating that the iron carbide is a wear product.

Patterns obtained from wear scars formed with DPDS as additive between 100 Kgf load and final seizure (160 Kgf) continued to show increasing amounts of cementite. The intensities of the Fe_3C lines on the diffraction patterns obtained from scars formed at loads of 160 Kgf with DPDS as additive are similar to the intensities of the α-Fe lines showing that Fe_3C is present in similar quantities as α-Fe in the wear scars. There were no detectable differences in the diffraction patterns formed when either of the two base oils was used with DPDS additive.

Between loads of 100 Kgf and final seizure (~240 Kgf) the amounts of iron carbide detected by X-ray diffraction, when DBDS and DTBDS additives were used, were less than the amounts detected with DPDS as additive. For these two additives iron sulphide, FeS was identified from diffraction patterns of wear scars formed above 100 Kgf in amounts increasing with increasing load. Also very small amounts of iron oxides, α-Fe_2O_3 (haematite) and Fe_3O_4 (magnetite) were detected. Over 30 lines other than α-Fe lines were obtained in most of the diffraction patterns. These patterns are quite distinct from the other patterns obtained from worn balls as can be seen from Table 4.1. They show that large amounts of FeS, and small amounts of iron oxides, are formed under e.p. conditions using DBDS and DTBDS and that only small amounts of Fe_3C are formed. Again no differences due to base oil were detected.

4.3 X-Ray Diffraction Analysis of Surfaces formed with Zinc Dialkyldithiophosphate Additives

Several worn specimens using both ZDP and Lubrizol 1395 as additive in both types of oil were analysed using X-ray diffraction. Those specimens formed at loads below initial seizure (~100 Kgf) produced diffractio patterns very similar to the pattern of an unworn ball. About 10 lines, other than α-Fe were indexed as Fe_3C. The surface films must be too thin to produce diffraction patterns and / or are not crystalline in form.

When scars formed in the e.p. region were analysed using glancing angle X-ray diffraction 10 to 14 lines other than α-Fe lines were obtained when ZDP was the additive and over 20 lines were obtained when Lubrizol 1395 was the additive. These lines were all indexed as Fe_3C. The intensities of the Fe_3C lines when ZDP was the additive were greater than the intensities obtained from an etched ball showing that some Fe_3C was a wear product. When Lubrizol 1395 was used the Fe_3C intensities were considerably greater than those obtained from an etched ball, indicating that considerable

amounts of Fe_3C were produced in the wear process. However, these intensities were not as great as those observed when DPDS additive was used.

No differences due to type of base oil were observed.

4.4 Summarizing Remarks

Comparing all the results presented in Table 4.1, it is clearly shown that in most cases the surface films formed on the wear scars are too thin and / or are non-crystalline and do not reveal any information using glancing angle X-ray diffraction. The amounts of iron carbide detected in scars formed at loads below initial seizure with all the additives were similar to the amounts found in an unworn ball and hence cannot be attributed to the wear processes.

After initial seizure wear scars formed with DPDS as additive showed increasing amounts of Fe_3C with increasing load. However, the wear scars formed with DBDS and DTBDS as additives in the e.p. region showed increasing amounts of FeS and small amounts of iron oxides being formed but only a small increase in the amounts of Fe_3C.

The Zinc Dialkyldithiophosphate additives were not detected in the wear scars. In the e.p. region increasing amounts of Fe_3C were detected, Lubrizol 1395 producing more than ZDP.

The iron carbides detected in all the wear scars, formed under e.p. conditions, may come from the Fe_3C in the steel being worn away less quickly than the steel and / or chemical reaction with the carbon in the lubricants at the elevated temperatures occurring during sliding.

C H A P T E R   5

ELECTRON PROBE MICROANALYSIS OF THE WORN SURFACES

5.1   E.P.M.A. of Surfaces Worn with Sulphur Additives

5.1.1 Qualitative Area Analyses of the Worn Surfaces

Figure 5.1(a) is a photograph of the electron image representing an area approximately 0.6mm x 0.6mm of the wear scar formed with HVI + 0.886% DPDS as lubricant, on the flat end of a roller at a load of 15 Kgf. Pits and depressions appear as dark areas and peaks as light areas, thus topographical features are clearly discernible. Figures 5.1(b) and (c) are the iron and sulphur X-ray images respectively. Element radiation appears as bright spots on the photograph and thus a high concentration of spots corresponds to a high concentration of the element, hence the X-ray images show the distribution of the elements within the wear scar. Since the overall intensities of the X-ray images depends on several factors, including exposure time, caution must be exercised when comparing the different photographs. For example, Figure 5.1(b) was exposed for 5 minutes and Figure 5.1(c) for 30 minutes. The amount of sulphur was insufficient ($\sim$2%) to affect the iron X-ray picture as Figure 5.1(b) shows a uniform distribution of iron. The distribution of the sulphur is confined to the wear scar and has streaks across it which follow the direction of sliding. The black dot on the right of Figure 5.1(a) is a foreign particle. The thick dark lines crossing Figure 5.1(a) are scratches on the surface of the roller and have only partially been worn away in the wear scar. The scratches that pass through the scar appear as dark lines in the sulphur X-ray image (Figure 5.1(c)) and this suggests that the film containing

(a) ELECTRON IMAGE

→

SLIDING DIRECTION

100 μ m
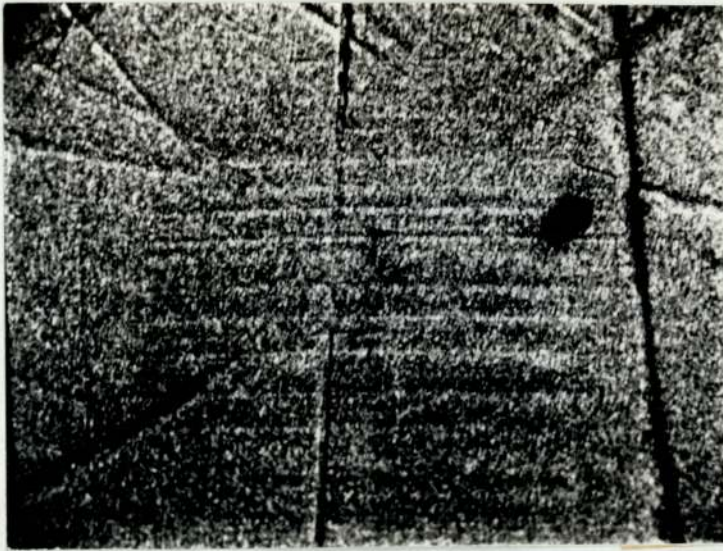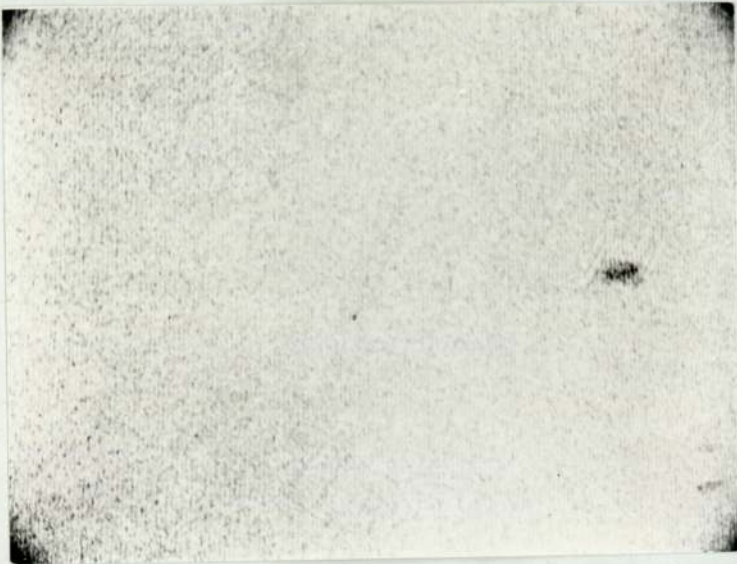
(b) IRON X-RAY IMAGE
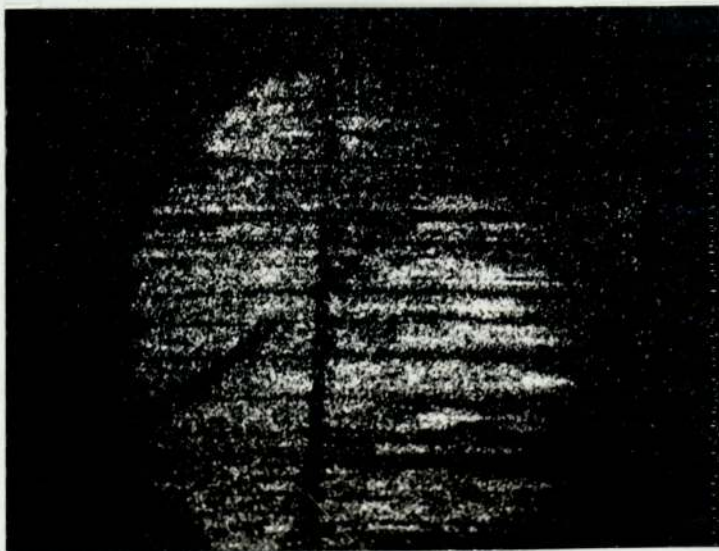
(c) SULPHUR X-RAY IMAGE

FIG. 5.1   LUBRICANT: HVI + DPDS

LOAD: 15 Kgf

sulphur has only been formed to any depth in the load bearing areas. Similar scars were obtained at this load using the other sulphur additives and the other base oil.

As the load is increased the surface scratches on the rollers are worn away completely within the wear scars leaving finely scored surfaces. The distribution of the sulphur in the films varies from wear scar to wear scar.

On some of the scars the sulphur in the film was concentrated in one or two areas. This is illustrated in Figures 5.2(a), (b) and (c), which represent the electron image and the iron and sulphur X-ray images respectively, of a scar formed with Risella 29 + 0.723% DTBDS as lubricant at a load of 35 Kgf. The two dark areas on the right of Figure 5.2(a) are debris. The sulphur X-ray image (Figure 5.2(c)) shows that they contain a high sulphur concentration. Apart from these two particles the sulphur is concentrated within the scar and has an uneven distribution.

On other tests the sulphur was distributed evenly over the surface of the wear scar. Figures 5.3(a), (b) and (c) show the electron image and the iron and sulphur X-ray images respectively of a scar formed at a load of 45 Kgf with Risella 29 + 1% DBDS as lubricant. The finely scored surface of Figure 5.3(b) is mirrored by the sulphur distribution in Figure 5.3(c). The sulphur is mainly confined to the wear scar and is streaked in the direction of sliding. The black dot on the left of Figure 5.3(a) is a foreign particle.

After initial seizure the distribution of sulphur on the surface of the wear scars changed radically. All three sulphur additives did not give similar sulphur contents over the whole e.p. range. DBDS and DTBDS additives continued to give similar distributions and concentrations but DPDS as additive gave only small amounts of sulphur from initial seizure through to final seizure. Before initial seizure the scars had an extensive cover of sulphur and the surfaces were smooth. Immediately after initial seizure all

(a) ELECTRON IMAGE

→

SLIDING DIRECTION

100 μ m
├───┤
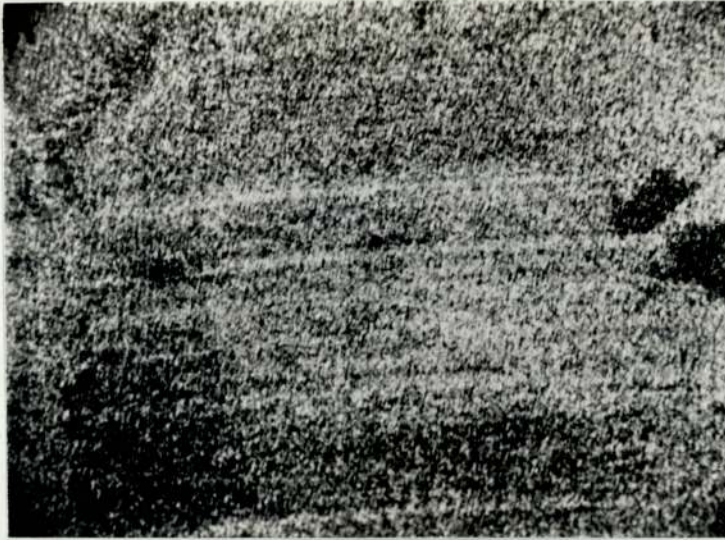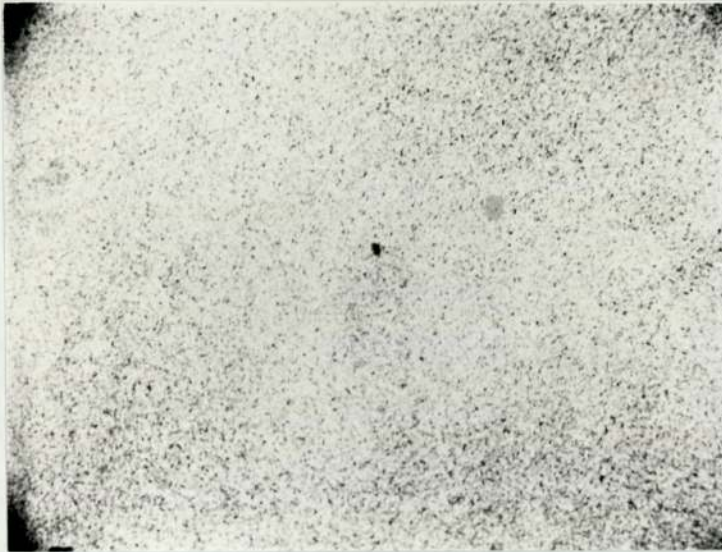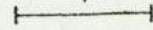
(b) IRON X-RAY IMAGE

(c) SULPHUR X-RAY IMAGE

FIG. 5.2   LUBRICANT: RISELLA 29 + DTBDS

LOAD: 35 Kgf

(a) ELECTRON IMAGE

SLIDING DIRECTION

100 μ m
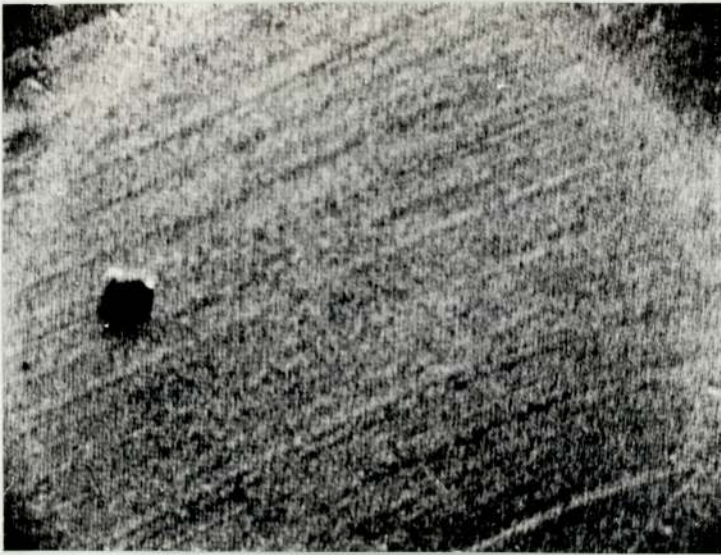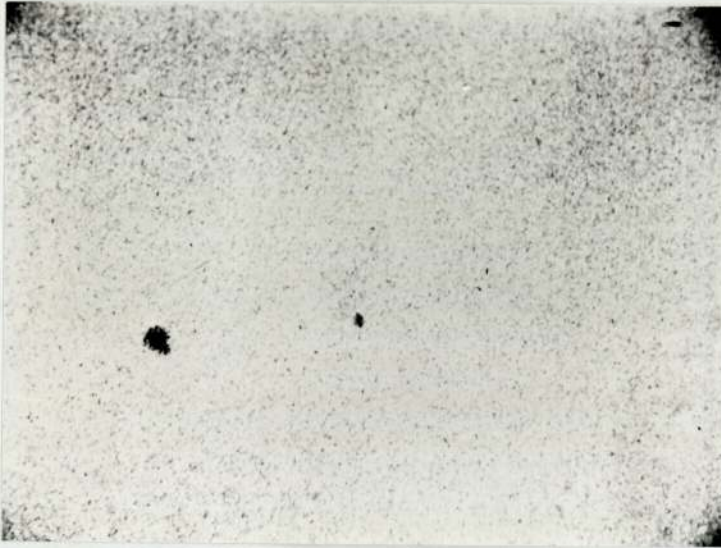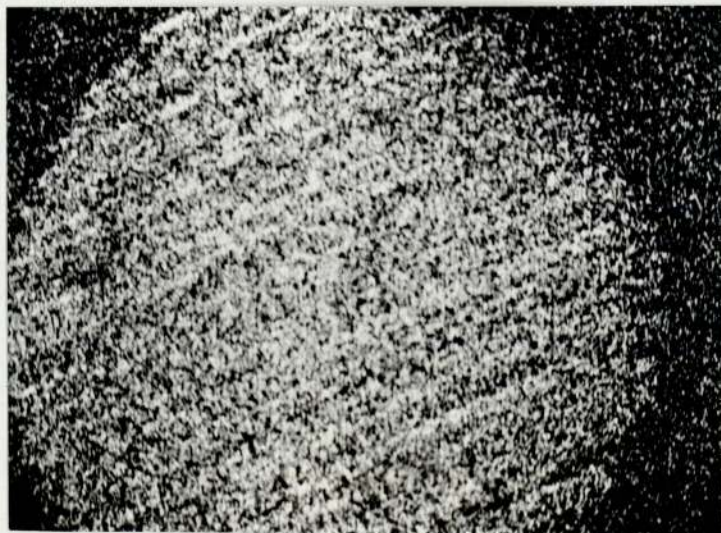
(b) IRON X-RAY IMAGE

(c) SULPHUR X-RAY IMAGE

FIG. 5.3   LUBRICANT: RISELLA + DBDS

LOAD: 45 Kgf

the scars contained very little sulphur and had similar sulphur distributions.
Figures 5.4(a), (b) and (c) represent the electron image and the iron and
sulphur X-ray images respectively of part of a scar formed at a load of
65 Kgf with HVI + 1% DBDS as lubricant. The sulphur is concentrated in the
pitted rough areas of the scar and there is very little sulphur in the
smooth tracked regions. This indicates that the sulphur is in debris
deposited in these areas and that in the real areas of contact the film is
removed very quickly during sliding and does not afford the same protection
that was given to the worn surface before initial seizure took place.

When the load is increased further the amount of sulphur in the
scars formed with DBDS and DTBDS as additives increased especially in the
tracked areas, whereas with DPDS the increase was very small. The electron
image and the iron and sulphur X-ray images respectively, are shown in
Figures 5.5(a), (b) and (c) of a tracked area of a wear scar formed at a
load of 140 Kgf with Risella 29 + 0.723% DTBDS as lubricant. The light
tracks of Figure 5.5(a) are the raised areas of contact and from Figure 5.5(c)
these have the highest sulphur concentrations. The iron X-ray image
(Figure 5.5(b)) has thin dark streaks where the highest sulphur concentrations
occur showing that thick sulphur containing films have been formed. At the
same load using DPDS as additive very little sulphur was detected and a
different type of surface was formed. This will be illustrated in Chapter 6.

At even higher loads using DBDS and DTBDS as additives thick films
of iron sulphide were observed. These films appear to be formed in the load
bearing areas. Figures 5.6(a), (b) and (c) show the electron image and the
iron and sulphur X-ray images respectively of part of a scar formed with
HVI + 0.723% DTBDS as lubricant at a load of 220 Kgf. The surface is
covered with cracks at right angles to the direction of sliding. The area
with these cracks is light and is therefore a raised track. Figure 5.6(c)
shows that this is the area with the highest sulphur concentration, the dark

(a) ELECTRON IMAGE

⟶
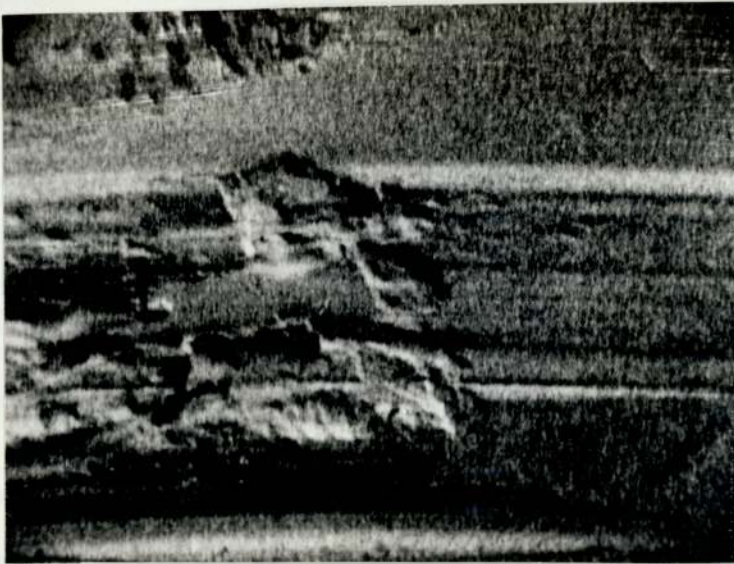
SLIDING DIRECTION

100 μ m
⊢————⊣
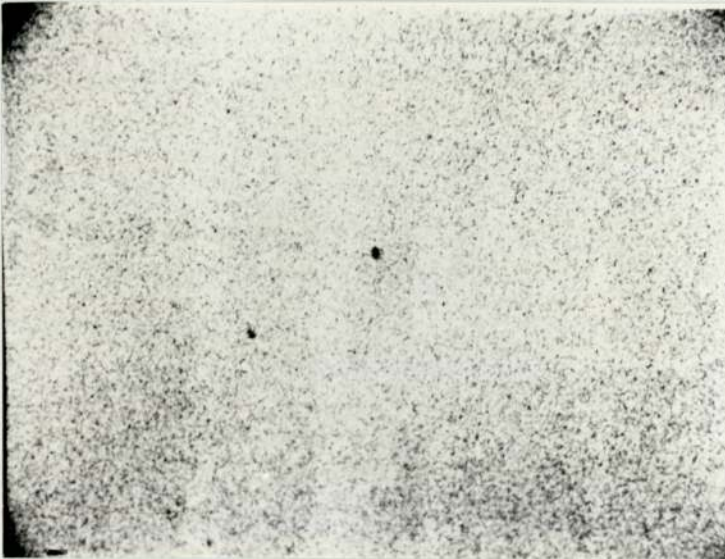
(b) IRON X-RAY IMAGE

(c) SULPHUR X-RAY IMAGE

FIG. 5.4   LUBRICANT: HVI + DBDS

LOAD: 60 Kgf

(a) ELECTRON IMAGE

→

SLIDING DIRECTION

100 μ m
|——|

(b) IRON X-RAY IMAGE

(c) SULPHUR X-RAY IMAGE

FIG. 5.5   LUBRICANT: RISELLA 29 + DTBDS

LOAD: 140 Kgf

(a) ELECTRON IMAGE

⟶
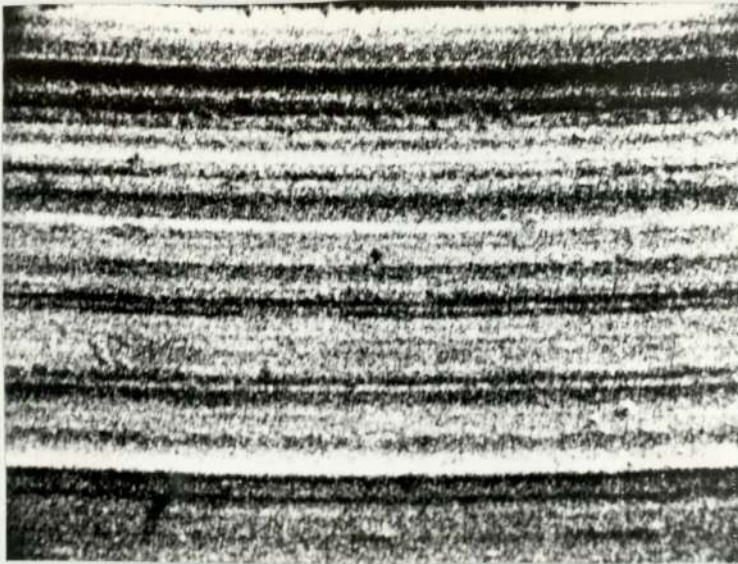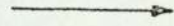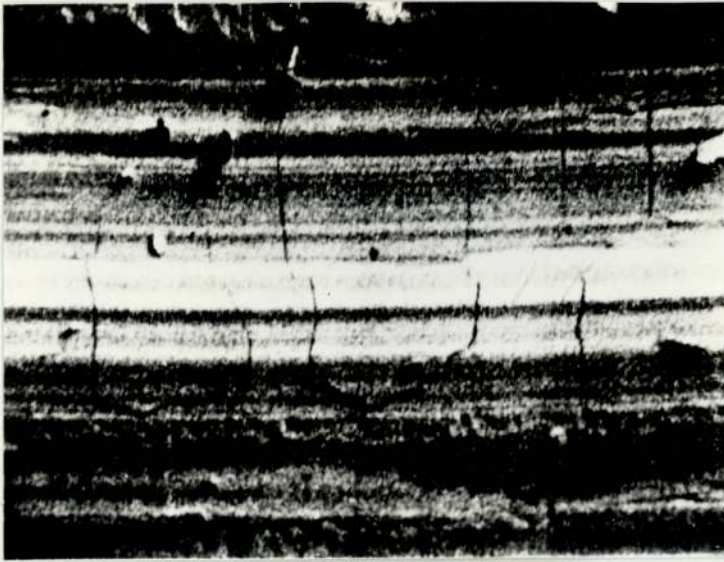
SLIDING DIRECTION

$100 \, \mu \, m$
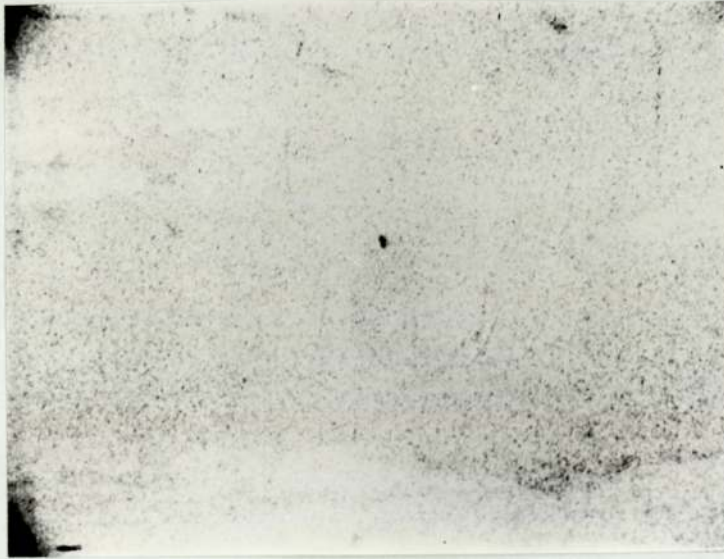
(b) IRON X-RAY IMAGE
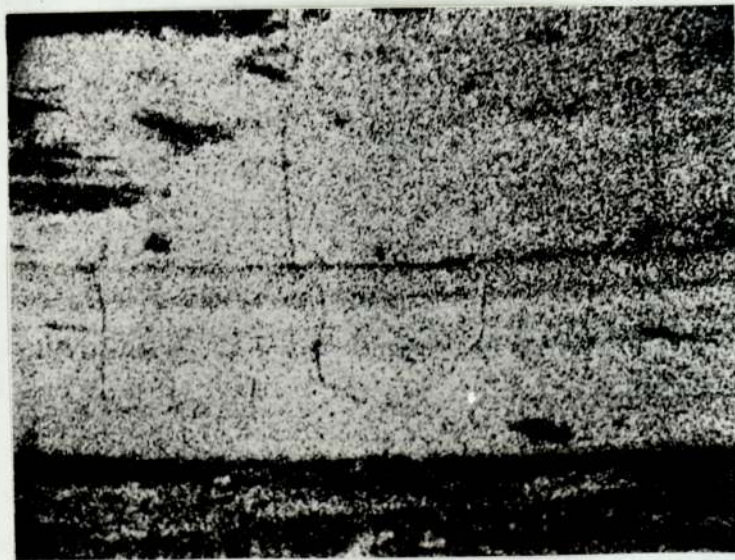
(c) SULPHUR X-RAY IMAGE

FIG. 5.6   LUBRICANT: HVI + DTBDS

LOAD: 220 Kgf

area at the bottom of Figure 5.6(a) being lower and having a lower sulphur content. When this film breaks up it leaves rough areas covered with debris. This is illustrated in Figures 5.7(a), (b) and (c), which represent the electron image and the iron and sulphur X-ray images respectively of part of a wear scar formed at a load of 200 Kgf with Risella 29 + 1% DBDS as lubricant. The top left area of Figure 5.7(a) is rough and covered with debris and has a high sulphur content. The tracked areas have lateral cracks crossing them and show how these areas break up to leave a rough area covered with debris. The iron X-ray image varies in intensity. This means that the sulphur concentration is high. The dark areas on the iron X-ray image correspond to the brightest areas on the sulphur X-ray image.

5.1.2 Quantitative Area Analyses of the Worn Surfaces

Each specimen was analysed for its sulphur and iron content using area analysis (150μm x 150μm), several areas on each scar being analysed. There was a considerable spread in the amounts of iron and sulphur (and oxygen and carbon by difference) within the wear scars. The results of area analyses of wear scars formed at loads of 15,35,45,55,65,80,100,140, 180 and 220 Kgf with Risella 29 + 1% DBDS are plotted in Figure 5.8. The limits on the bars represent the maximum and minimum percentages of iron and sulphur observed at each load when the results have been corrected and oxygen and carbon are assumed to be the difference between 100% and the sum of the iron and sulphur percentages. The dotted line shows the average of the combined oxygen and carbon percentage.

Up to 45 Kgf there is between 2 and 7% sulphur, 1 and 10% oxygen and carbon, and 85 and 97% iron in the scars. At, and just after, the initial seizure load of 55 Kgf the amount of sulphur decreases to between 1 and 2% and from then onwards increases with increasing load. The amounts of iron, and consequently oxygen and carbon, vary widely around initial

(a) ELECTRON IMAGE

SLIDING DIRECTION

100 μ m
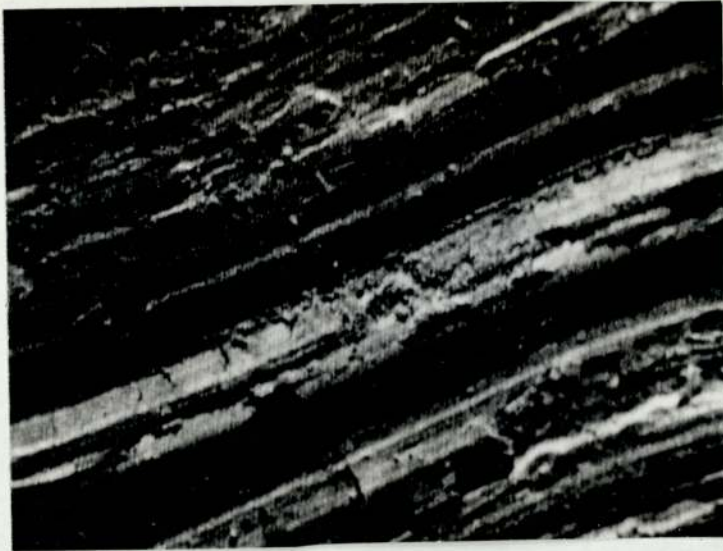
(b) IRON X-RAY IMAGE
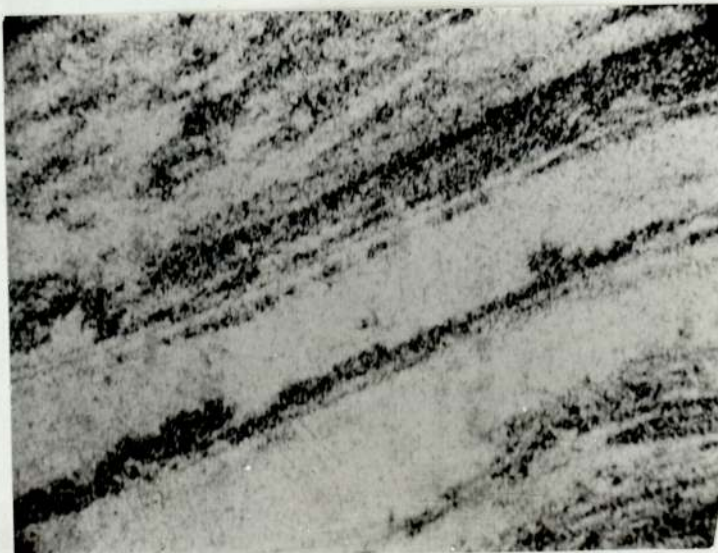
(c) SULPHUR X-RAY IMAGE

FIG. 5.7   LUBRICANT: RISELLA + DBDS

LOAD: 200 Kgf
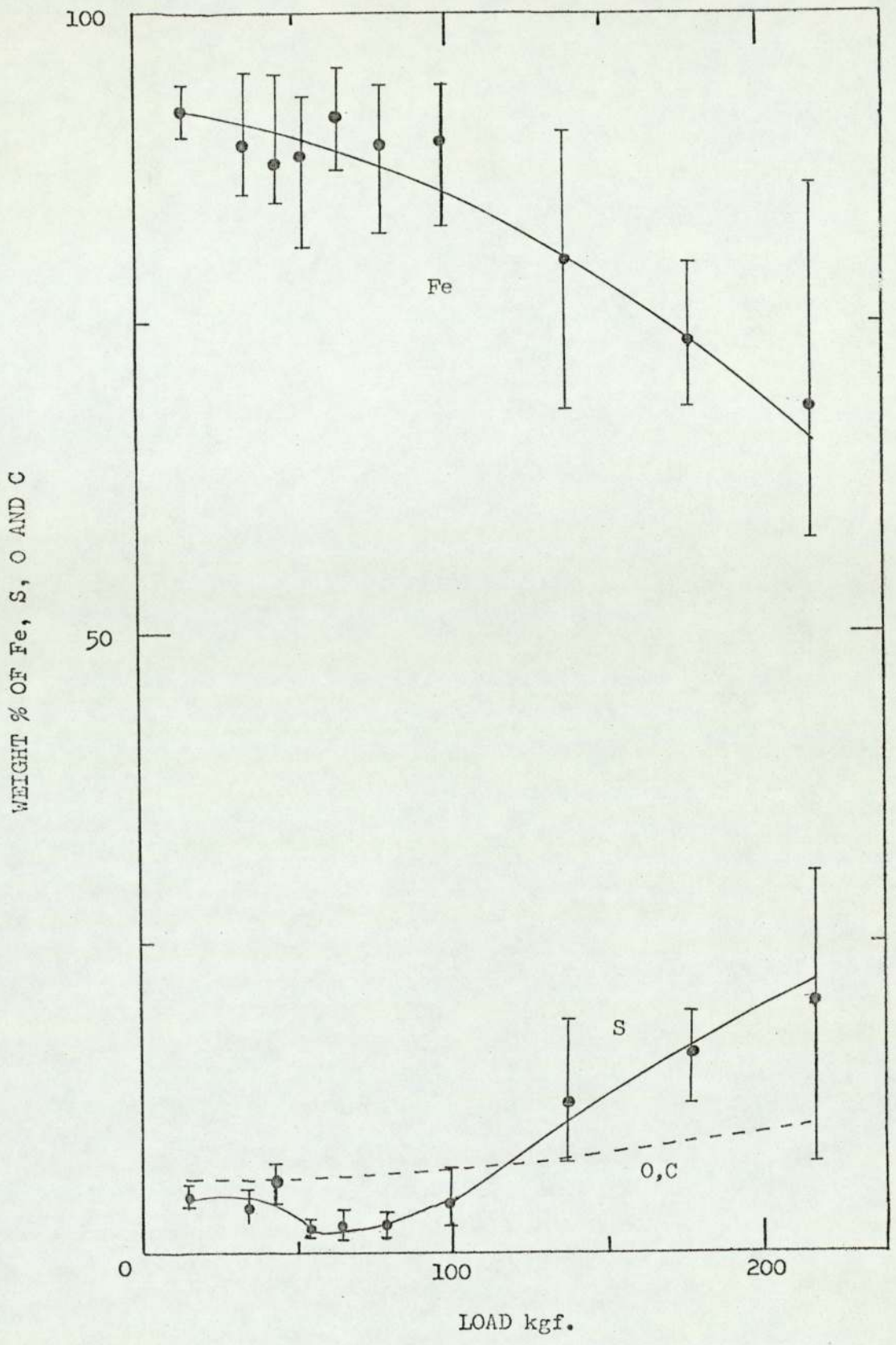
FIG.5.8 VARIATION OF WEIGHT % OF Fe, S, O and C WITH

LOAD.

LUBRICANT: RISELLA 29 + 1% DBDS
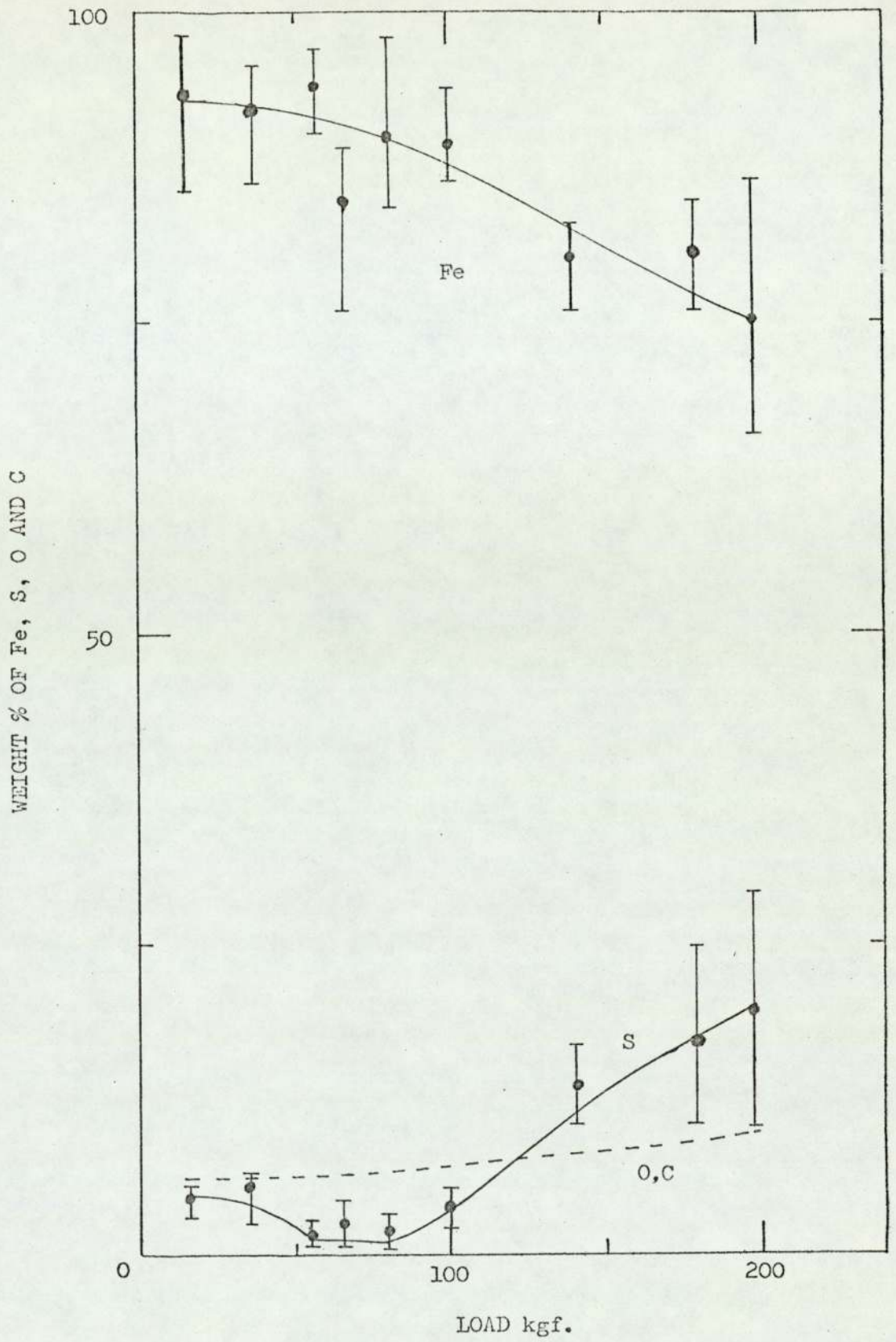
FIG.5.9 VARIATION OF WEIGHT % OF Fe, S, O and C WITH
LOAD.
LUBRICANT: HVI + 1% DBDS

seizure. The overall trend is for the oxygen and carbon content to vary between 1 and 15% above initial seizure and for the iron content to slowly decrease until at 220 Kgf it varies between 60 and 85%. At the highest load the sulphur content varies between 8 and 30%.

Similar analyses were conducted on the specimens formed using HVI + 1% DBDS. Area analyses obtained at 15,35,55,65,80,100,140,180 and 200 Kgf are plotted in Figure 5.9. The variation of sulphur content was very similar being between 2 and 7% in the a.w. region, falling to 1 to 2% at initial seizure and increasing to between 10 and 30% at 200 Kgf. The iron, oxygen and carbon percentages again show large fluctuations around initial seizure. The iron percentages fell with increasing load until at 200 Kgf the range was between 67 and 88%. The oxygen and carbon varied between about 1 and 10% over the whole load range.

When similar analyses were carried out using DTBDS as additive there were differences in the graphs at low loads. In Figure 5.10 the results of area analyses of scars formed at loads of 15,35,45,70,90,140,180 and 220 Kgf with Risella 29 + 0.723% DTBDS as lubricant are presented. The sulphur content of the scars before initial seizure varied between 0.5 and 4% and was lower than with DBDS as additive. The change after initial seizure was less pronounced than in Figure 5.8. However, as the load increased the sulphur content of the scars increased at a similar rate until at a load of 220 Kgf there was between 9 and 30% sulphur and between 61 and 84% iron. The difference (oxygen and carbon) varied between 0 and 14% over the whole load range. When HVI + 0.723% DTBDS was the lubricant, analyses at loads of 15,35,45,80,120,180 and 220 Kgf (Figure 5.11) showed that the amount of sulphur in the scars before initial seizure was lower than the results with Risella 29 + 0.723% DTBDS. In the a.w. region between 0.3 and 1.4% sulphur was detected. In the intermediate region, between loads of 45 and 80 Kgf, 0.6 to 2.0% sulphur was found. At higher loads in the e.p.
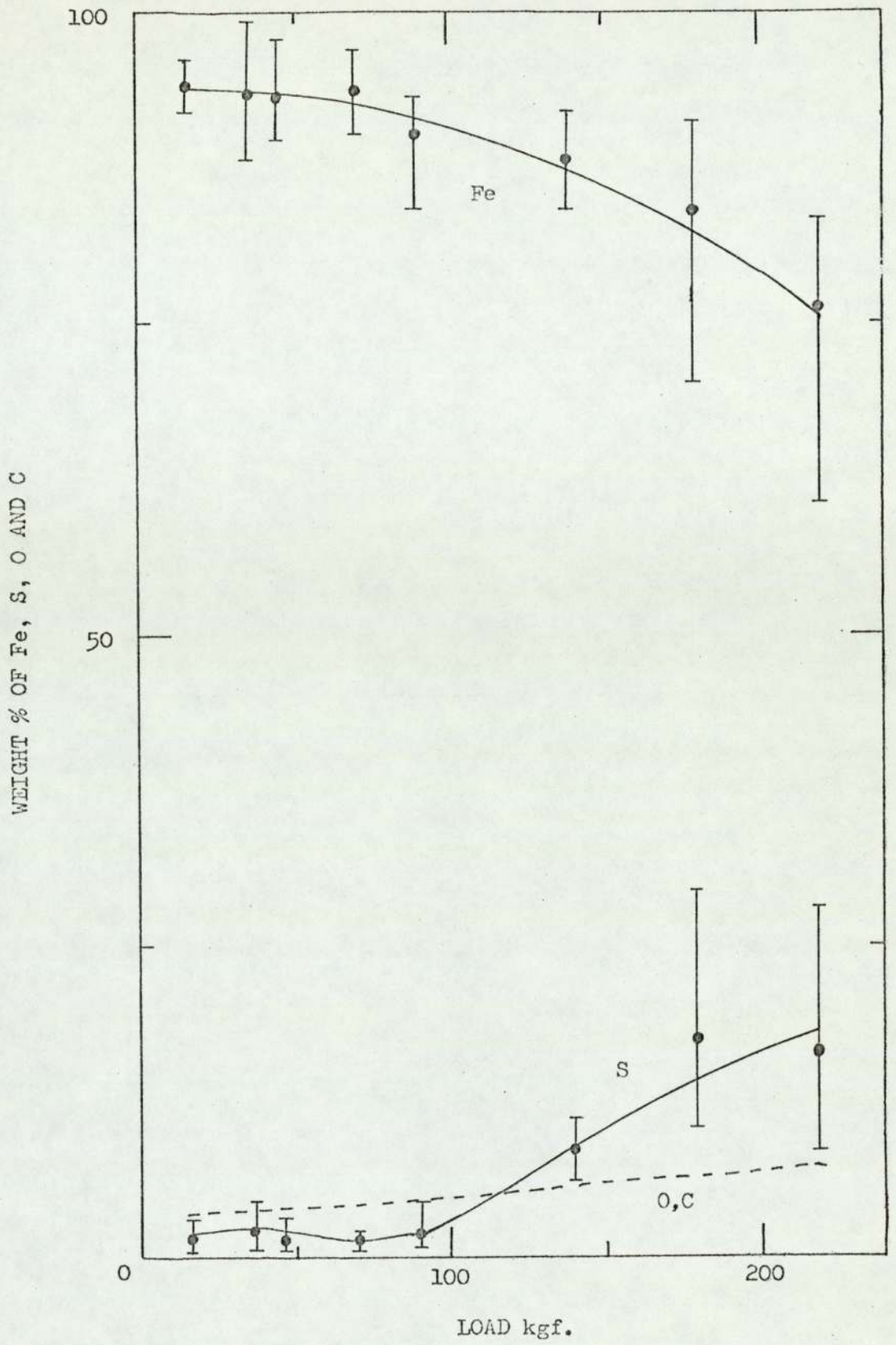
FIG. 5.10 VARIATION OF WEIGHT % OF Fe, S, O and C WITH

LOAD.

LUBRICANT: RISELLA 29 + 0.723% DTBDS
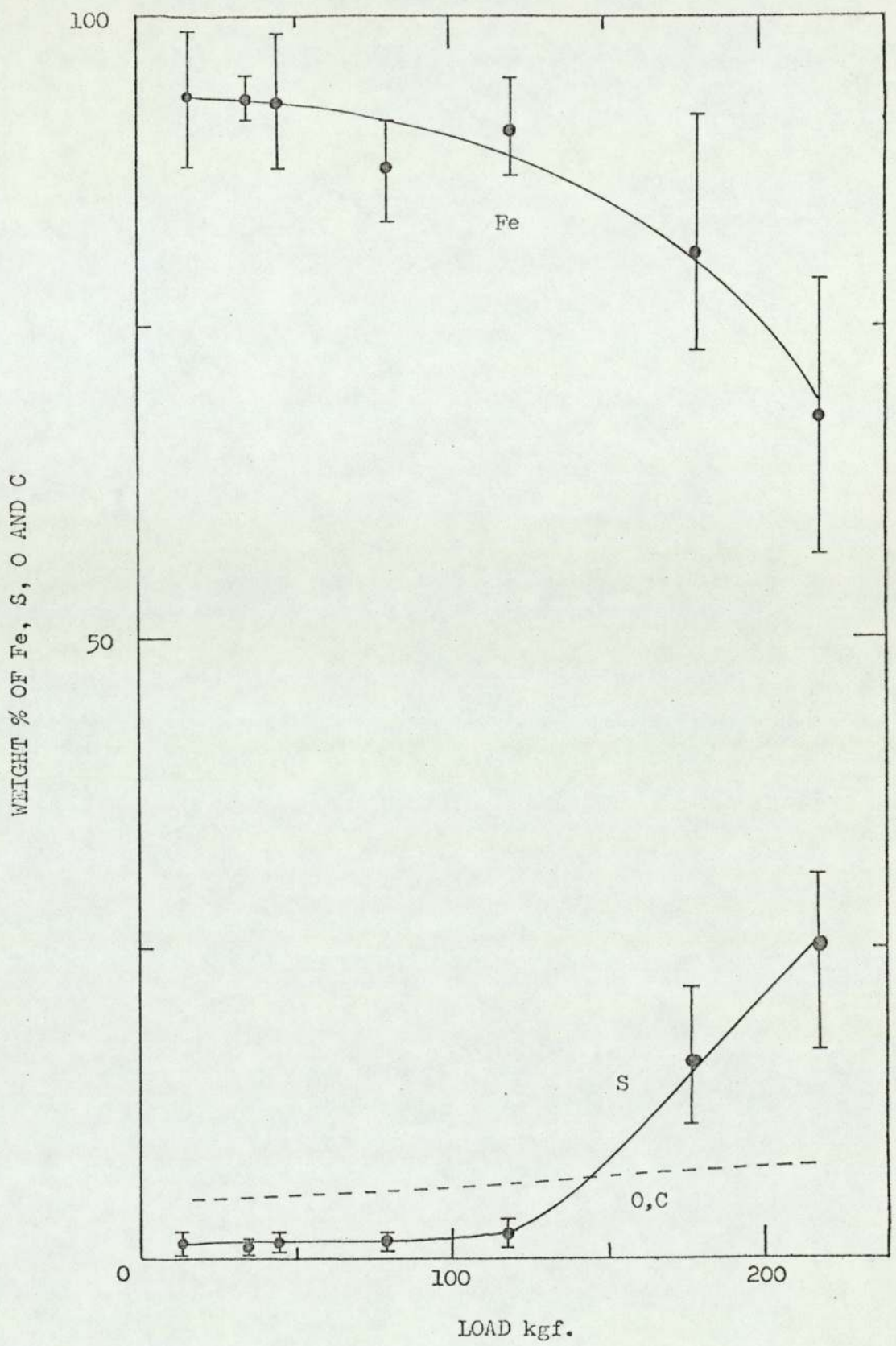
FIG.5.11 VARIATION OF WEIGHT % OF Fe, S, O and C WITH

LOAD.

LUBRICANT: HVI + 0.723% DTBDS

region similar amounts of sulphur to those obtained with Risella 29 + 0.723% DTBDS were observed (between 17 and 30%). The quantities of oxygen and carbon varied between 0 and 14% over the whole load range, averaging around 5% at most loads.

The third sulphur additive, DPDS, behaved in a different manner to that of DBDS and DTBDS. Area analyses of wear scars formed at loads of 15, 35,55,65,70,100,130 and 160 Kgf with Risella 29 + 0.886% DPDS are presented in Figure 5.12. In the a.w. region, before initial seizure, the amount of sulphur varied between 2 and 6%, the iron between 87 and 98% and the balance between 0 and 10%. These were similar to the distributions found with Risella 29 + 1% DBDS in the a.w. region. After initial seizure the amount of sulphur dropped and only rose to between 3 and 5% at 160 Kgf. This is a much lower percentage than was obtained with the other two sulphur additives. It appears that the rate of reaction of DPDS is not sufficient to maintain a film under increasingly severe conditions. The final seizure load is lower than for DBDS and DTBDS. These two additives must have a faster reaction rate to afford protection up to much higher loads. When HVI + 0.886% DPDS is used the results of area analyses of specimens formed at loads of 15,25, 35,45,55,70,80,100,140 and 160 Kgf (Figure 5.13) show that there is less sulphur in the a.w. region than when using the other base oil. The sulphur content varies between 1.5 and 4.5% up to initial seizure, drops to around 2% after initial seizure and at higher loads in the e.p. region varies between 1 and 14%. Some of this sulphur at the higher loads may come from the 1% sulphur in HVI oil. The oxygen and carbon content varied more with HVI oil than with Risella 29, occasionally around 20% was calculated by difference.

5.13 Depth Analyses of Selected Specimens

The surfaces of selected wear scars were marked with microhardness indentations 50μm apart to form two intersecting lines at right angles to
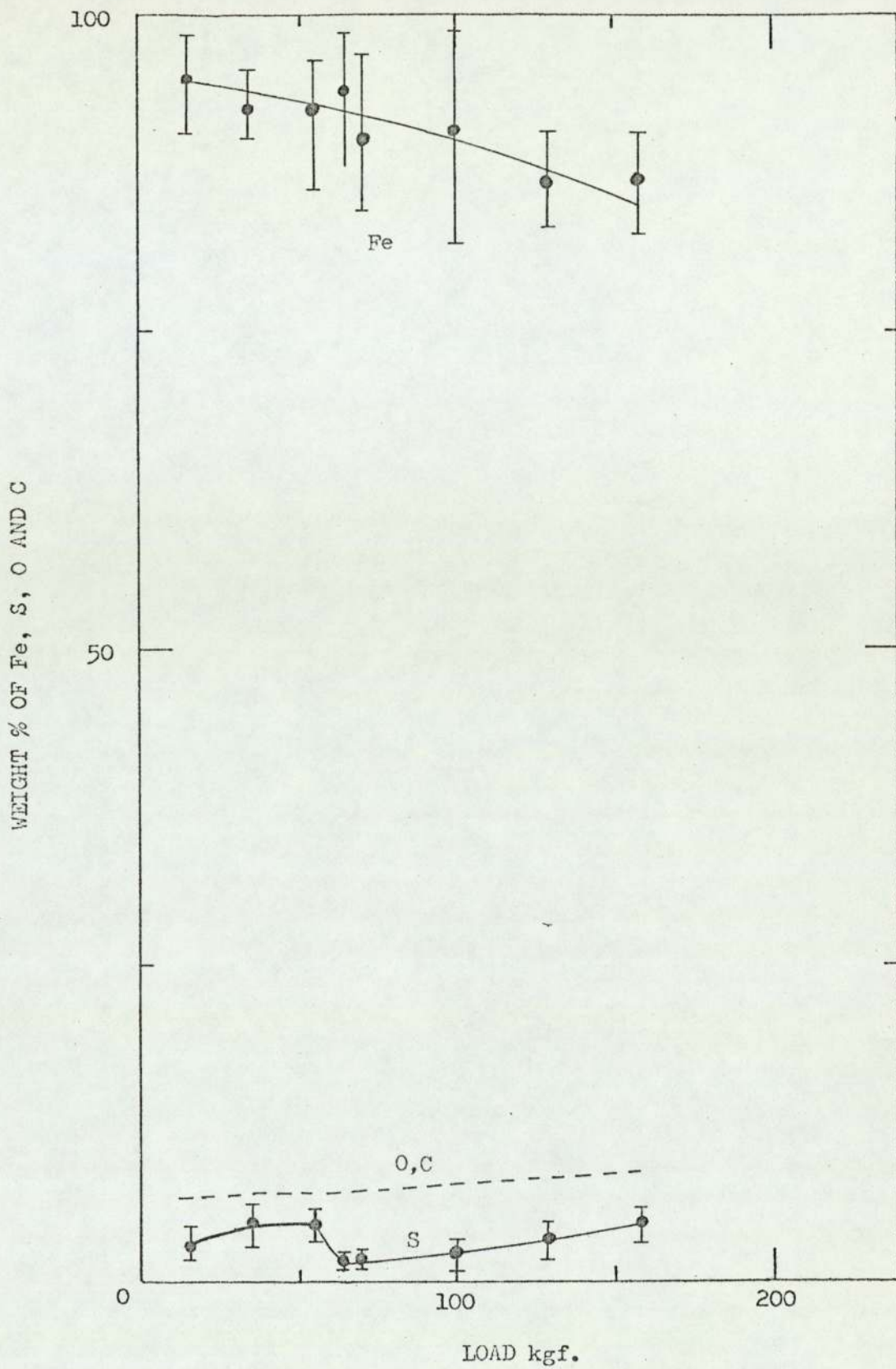
FIG.5.12 VARIATION OF WEIGHT % OF Fe, S, O and C WITH

LOAD.

LUBRICANT: RISELLA 29 + 0.886% DPDS
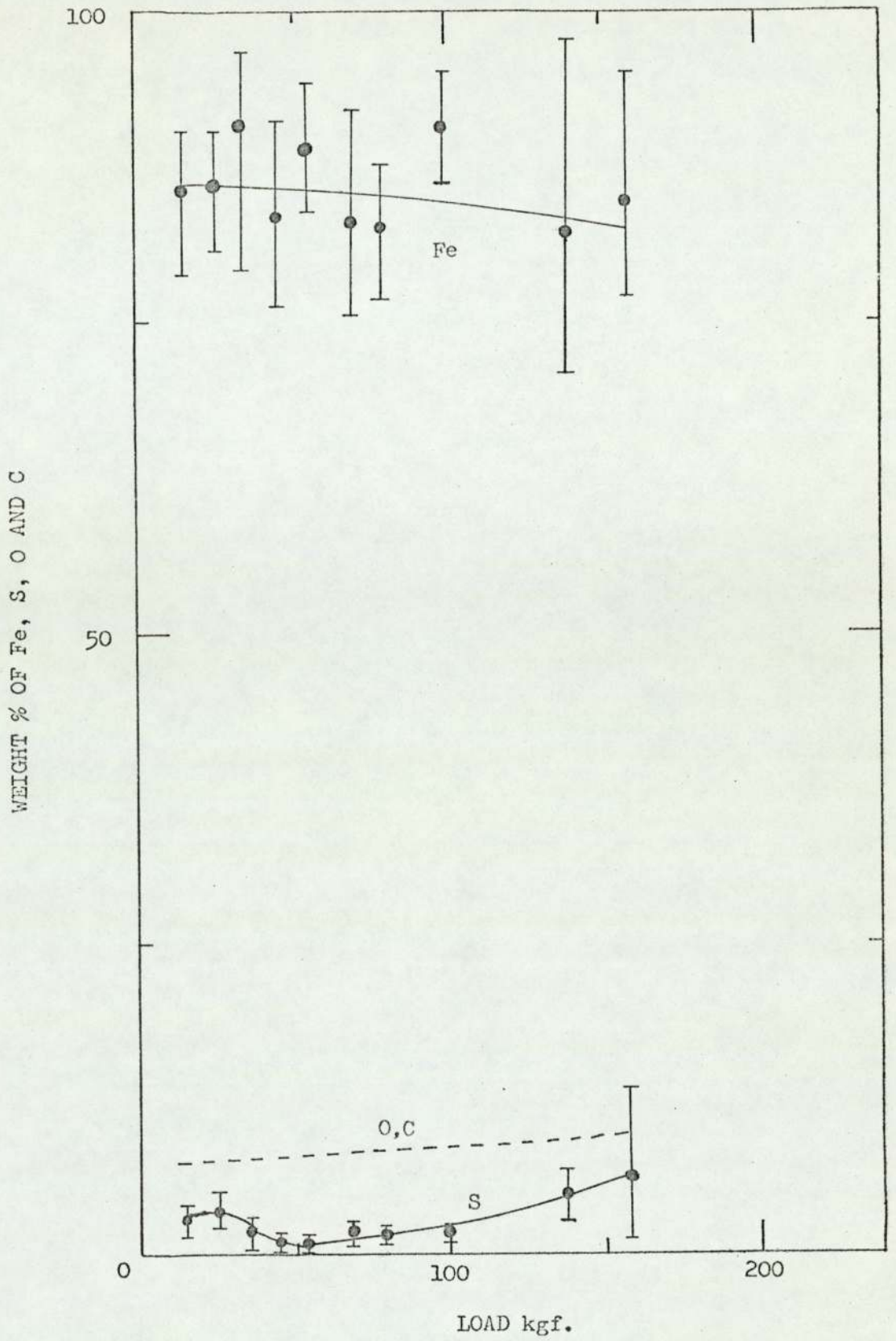
FIG.5.13 VARIATION OF WEIGHT % OF Fe, S, O and C WITH

LOAD.

LUBRICANT: HVI + 0.886% DPDS

each other. In this way a specified region was observed at different
accelerating potentials and the magnification was adjusted so that the same
area was observed each time (150μm x 150μm). The concentrations of iron,
sulphur, and by difference oxygen and carbon, were obtained at 15, 20 and
25 KV electron accelerating potentials. The mass absorption coefficient for
sulphur X-rays in FeS is approximately 850 and the density of FeS is 4.6
gms/cm^3. The take-off angle for the X-rays on this instrument is 20°.
Using this data sulphur X-rays generated at a depth of 2μm below the surface
have their emergent intensities reduced by more than 90% due to absorption
in the FeS. Thus there is very little contribution to the measured intensity
of the sulphur X-rays below this depth.

Table 5.1 shows the results obtained on scars formed at loads of
70, 100, 140 and 180 Kgf with Risella 29 + 0.723% DTBDS as lubricant and
Table 5.2 shows the results on scars formed at 80, 120 and 200 Kgf with HVI +
0.723% DTBDS as lubricant. At the lower loads there is little change in the
sulphur concentration with changing electron accelerating potential. This
is consistent with a thin film of FeS on the surface where the beam
penetration is much greater than the film thickness. At higher loads the
percentages of sulphur obtained at 20 and 25 KV are similar and less than
those obtained at 15 KV. This suggests that at 15 KV most of the electrons
are stopped within a thick FeS layer but that at 20 and 25 KV the electron
beam goes through the FeS film and the increased penetration of the electrons
does not produce more sulphur X-rays that can be collected by the spectrometer.
Using a graph produced by Birks (65) of electron range versus energy, the
effective range of electrons is 0.7, 0.9 and 1.4 mg/cm^2 (1.5, 2 and 3μm in
FeS) at 15, 20 and 25 KV accelerating potentials respectively. The effective
range corresponds to an absorption of over 99% of the electrons. For the
specimen worn with HVI + 0.723% DTBDS at 200 Kgf (Table 5.2) the percentages
of sulphur at 20 and 25 KV were similar showing that the total number of

Table 5.1

Area Analyses of Selected, Marked Specimens at Different Electron Accelerating Potentials using Risella 29 + 0.723% DTBDS as Lubricant

Load, Kgf	KV	%Fe	%S	%O,C
70	15	97.5	0.6	1.9
	20	98.3	0.5	1.3
	25	98.1	0.5	1.4
100	15	90.2	4.2	5.5
	20	93.3	3.6	3.1
	25	94.9	2.8	2.3
140	15	88.3	9.4	2.3
	20	90.2	7.7	2.1
	25	95.2	6.7	-0.9
180	15	88.4	5.1	6.5
	20	91.5	4.1	4.4
	25	94.9	3.8	1.3

Table 5.2

Area Analyses of Selected, Marked Specimens at Different
Electron Accelerating Potentials using HVI + 0.723% DTBDS
as Lubricant

Load, Kgf	KV	%Fe	%S	%O,C
	15	88.5	1.6	10.0
80	20	93.4	1.3	5.3
	25	93.3	1.1	5.6
	15	90.3	1.6	8.1
120	20	92.1	1.4	6.5
	25	93.8	1.0	5.2
	15	75.7	22.2	2.2
200	20	73.8	18.7	7.6
	25	77.9	18.5	3.6

sulphur X-rays collected in both cases were approximately the same. A
similar effect was noticed with Risella 29 + 1.0% DBDS at 200 Kgf where the
sulphur percentages were 18.8, 16.5 and 15.2 at 15, 20 and 25 KV respectively.
This suggests that up to a depth of the order of 2μm there is a high
concentration (∼20%) of sulphur at these high loads and that beyond that
order of depth, absorption is so great that no further increase in
concentration will be recorded at higher electron accelerating potentials.

Similar results were obtained when DBDS was the additive, but this
technique was not attempted with DPDS as additive because of the larger
errors involved when low sulphur concentrations are used.

5.2 E.P.M.A. of Surfaces Worn with Zinc Dialkyldithiophosphate Additives

5.2.1 Qualitative Area Analyses of the Worn Surfaces

Figures 5.14 (a), (b), (c), (d) and (e) show the electron image
and the iron, sulphur, phosphorus and zinc X-ray images respectively of a
wear scar formed at a load of 35 Kgf with Risella 29 + 1.112% ZDP as
lubricant. The sulphur distribution is very closely associated with the
dark areas of the scar, there being little outside these regions. The zinc
and phosphorus distributions are very similar in appearance and extend over
most of the wear scar. The close association of the zinc and phosphorus
distributions suggests that they are bound together in some way, whereas the
sulphur appears to have a separate action. Similar results were obtained
using HVI + 1.112% ZDP as lubricant where the scars fell on the a.w. line
close to the Hertz line (see Figure 3.10). When intermediate wear scar
diameters were obtained the surfaces were pitted and the distribution of the
elements on the surface was different. Figures 5.15 (a), (b), (c), (d) and
(e) show the electron image and the iron, sulphur, phosphorus and zinc X-ray
images respectively of part of a wear scar formed at a load of 55 Kgf with
HVI + 1.112% ZDP as lubricant. Most of the high concentrations of sulphur,
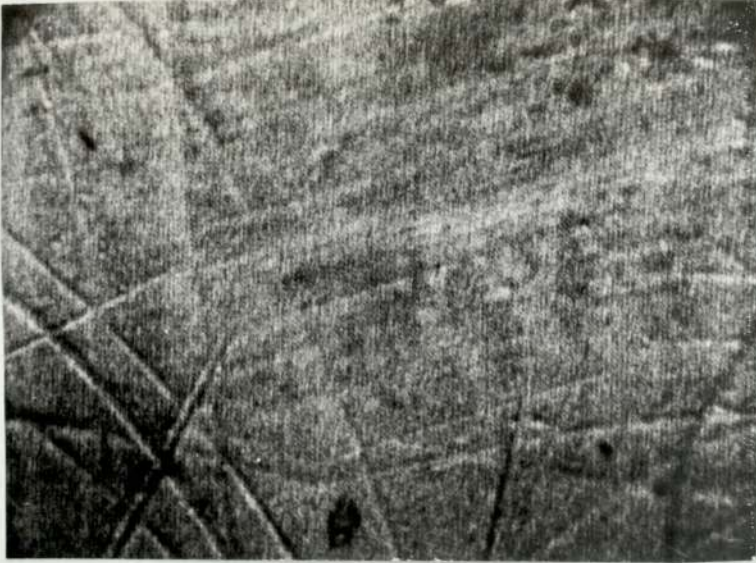
(a) ELECTRON IMAGE

SLIDING DIRECTION
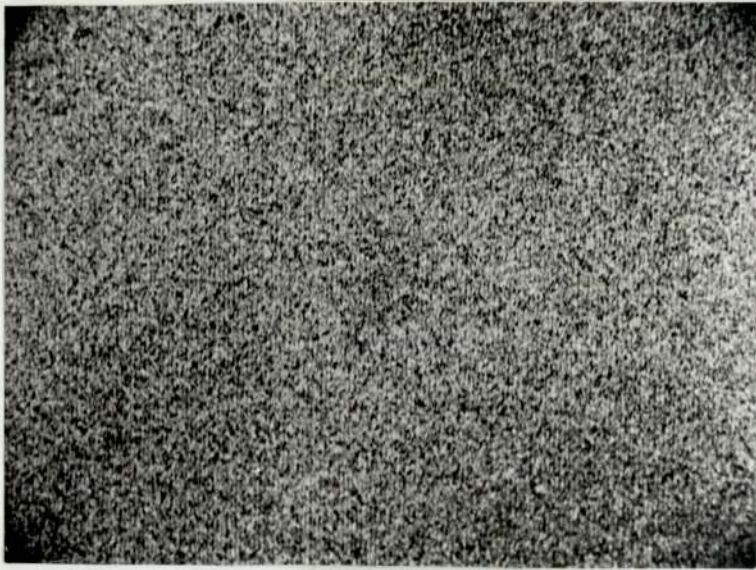
100 μ m
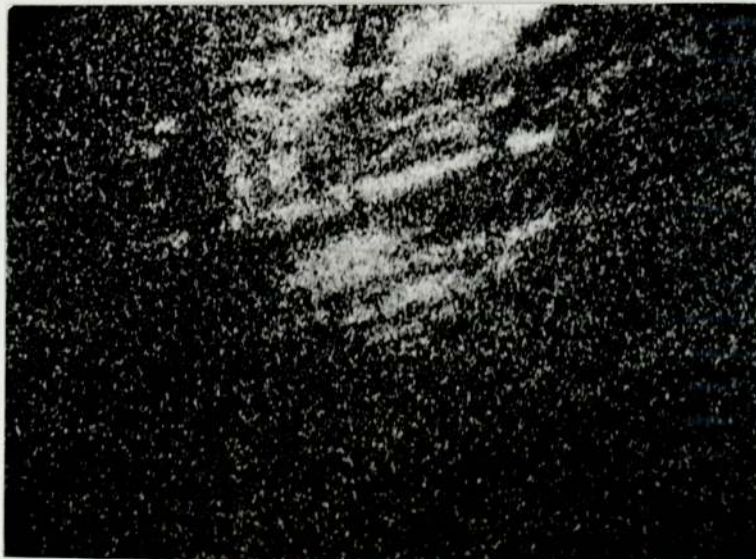
(b) IRON X-RAY IMAGE

(c) SULPHUR X-RAY IMAGE

FIG. 5.14   LUBRICANT: RISELLA 29 + ZDP

LOAD: 35 Kgf
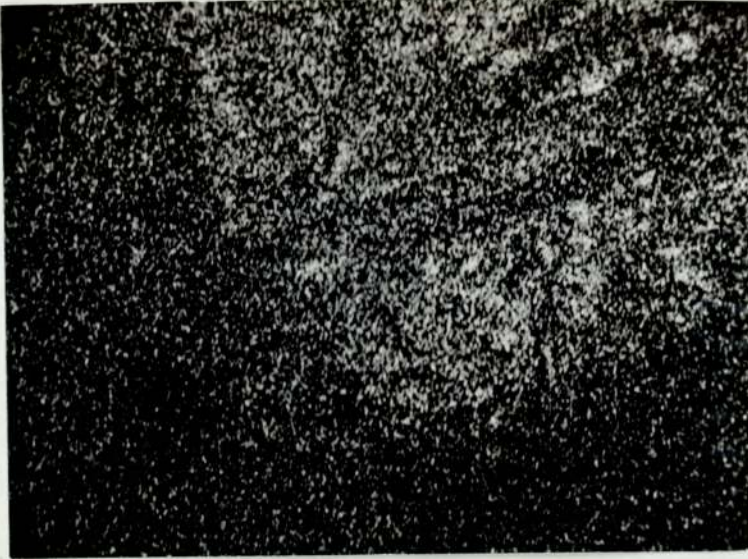
(d) PHOSPHORUS X-RAY
    IMAGE
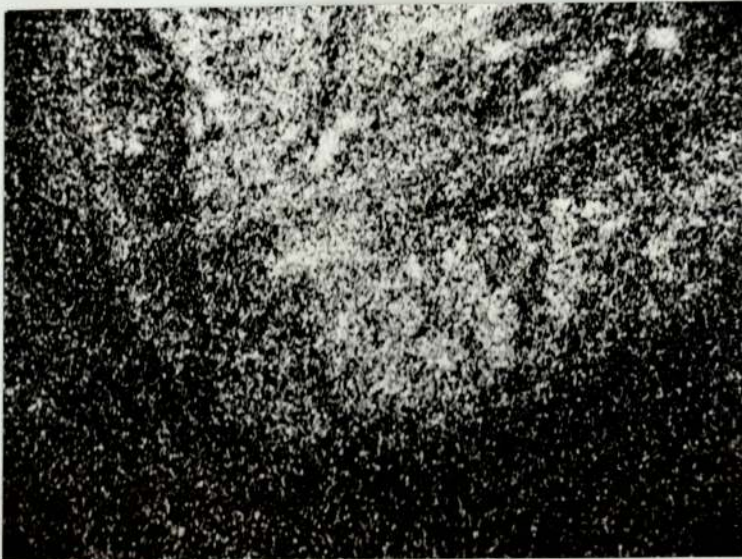
(e) ZINC X-RAY IMAGE

FIG. 5.14

(a) ELECTRON IMAGE

←————

SLIDING DIRECTION

100 μ m
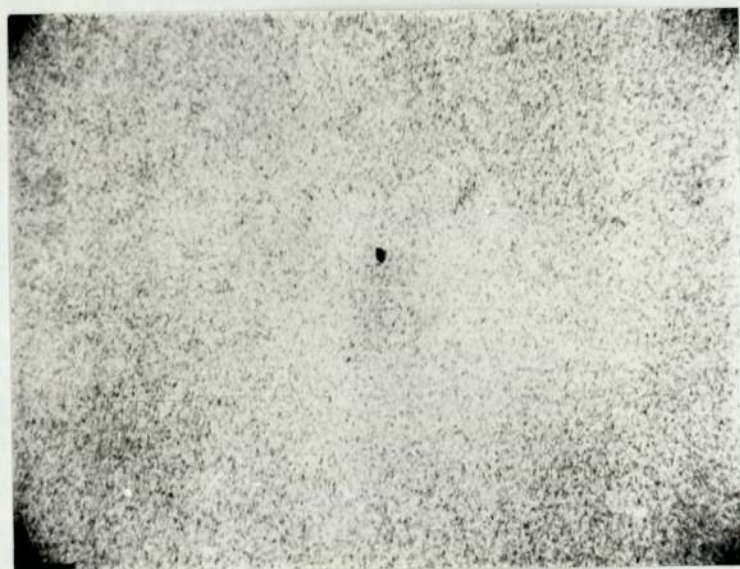
(b) IRON X-RAY IMAGE
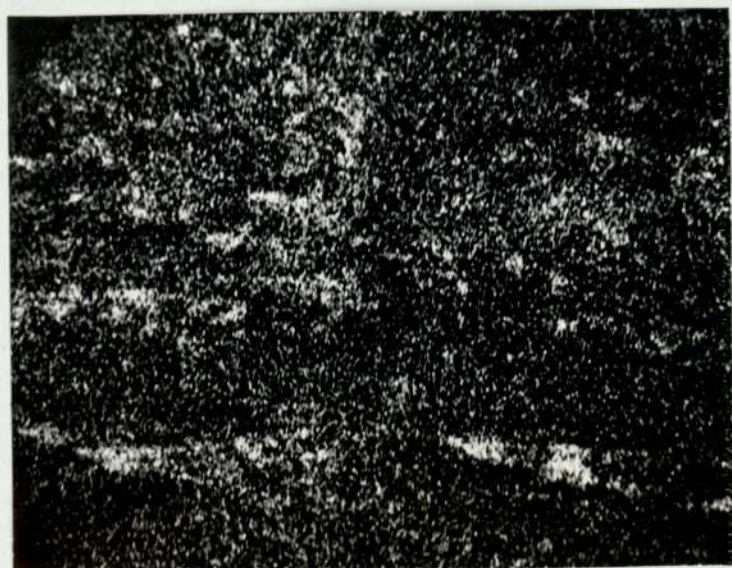
(c) SULPHUR X-RAY IMAGE

FIG. 5.15   LUBRICANT: HVI + ZDP

LOAD: 55 Kgf
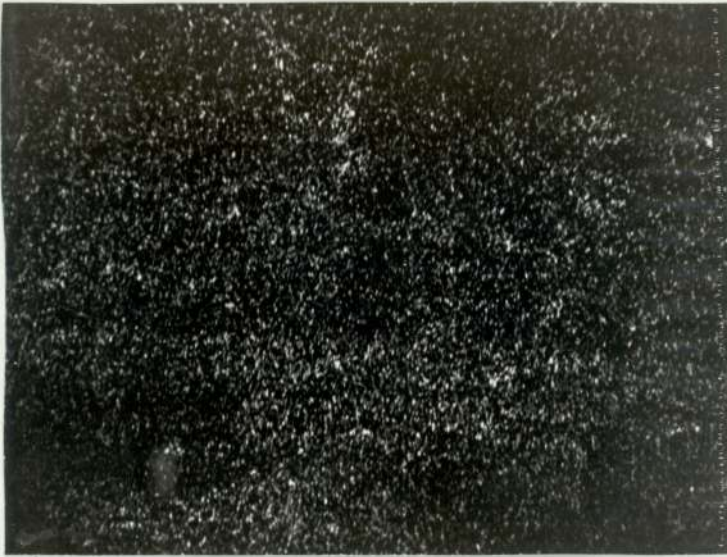
(d) PHOSPHORUS X-RAY IMAGE
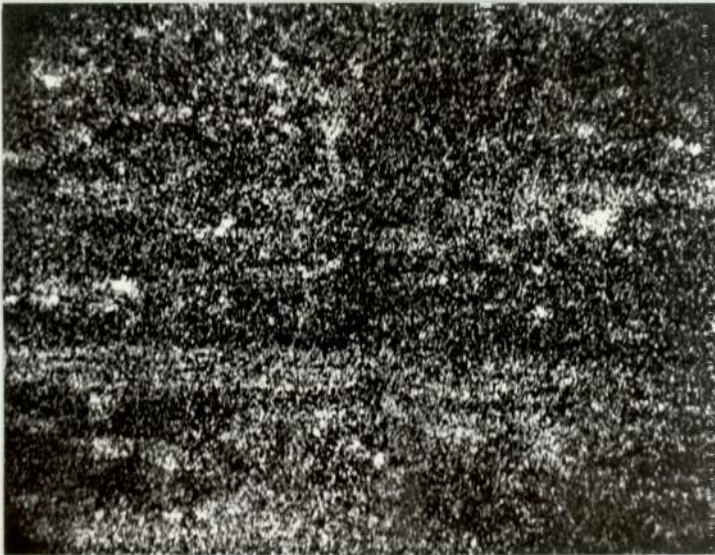
(e) ZINC X-RAY IMAGE

FIG. 5.15

phosphorus and zinc coincide with pitted areas on the electron image. Two streaks of high phosphorus and zinc content can be associated with raised, smooth areas on the electron image. The concentrations of the elements in the pitted area may be attributed to debris deposited there or reactions with the fresh metal exposed when the pits were formed.

When Lubrizol 1395 was used as additive similar distributions of the elements were observed in the a.w. region. Figures 5.16 (a), (b), (c), (d) and (e) show the electron image and the iron, sulphur, phosphorus and zinc X-ray images respectively of a scar formed at a load of 65 Kgf with HVI + 1.0% Lubrizol 1395 as lubricant. The highest sulphur concentrations are again associated with the blackened areas of the wear scar. The phosphorus and zinc distributions are similar and cover most of the scar. A surface scratch on the roller running diagonally across the wear scar has a high sulphur concentration but it appears as a dark line across both the phosphorus and zinc X-ray images. This again indicates that the zinc and phosphorus act together and the sulphur separately.

Once initial seizure had occurred the distribution of the elements changed. Figures 5.17 (a), (b), (c), (d) and (e) show the electron image and the iron, sulphur, phosphorus and zinc X-ray images respectively of an area in the centre of a scar formed at a load of 120 Kgf with HVI + 1.112% ZDP as lubricant. The highest concentrations of sulphur, phosphorus and zinc are associated with a smooth, tracked area. The streaks of sulphur along the edges of this area indicates that the sulphur has reacted with the surface in the load bearing region. Very little phosphorus was detected in the e.p. scars. The results were similar for both base oils.

When Lubrizol 1395 was used the same sort of distribution was observed. Figures 5.18 (a), (b), (c), (d) and (e) show the electron image and the iron, sulphur, phosphorus and zinc X-ray images respectively of part of a wear scar formed at a load of 130 Kgf with Risella 29 + 1.0%

(a) ELECTRON IMAGE

→
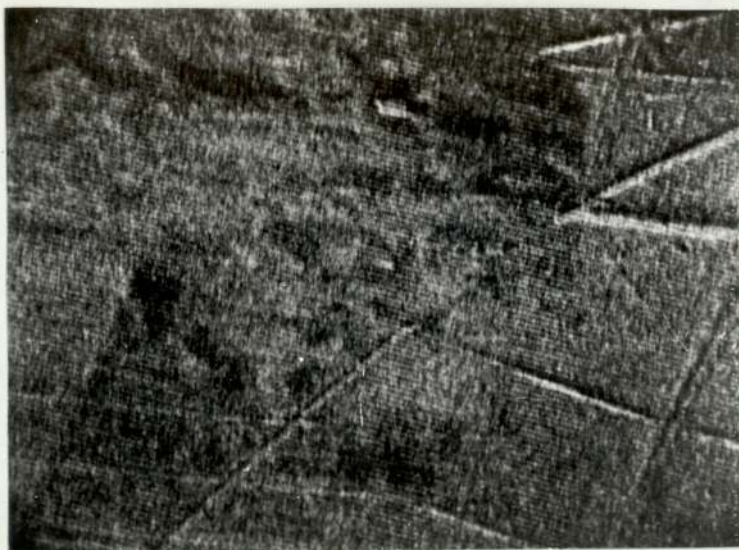
SLIDING DIRECTION
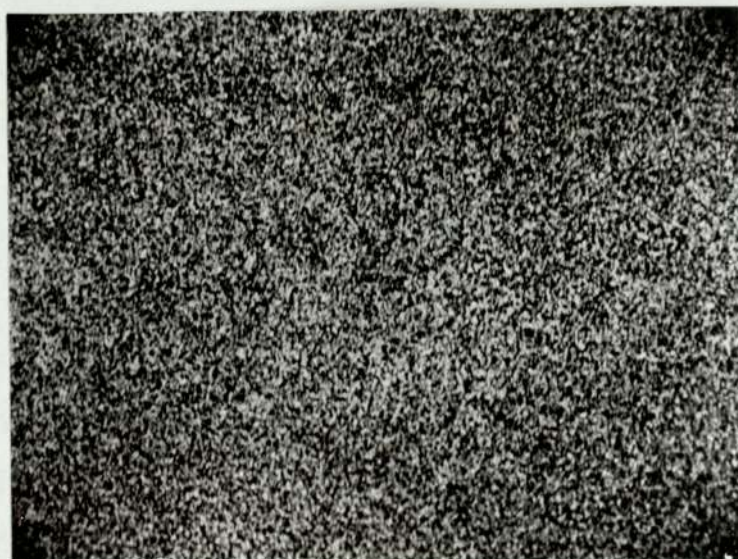
100 μ m

(b) IRON X-RAY IMAGE

(c) SULPHUR X-RAY IMAGE

FIG. 5.16   LUBRICANT: HVI + LUBRIZOL 1395

LOAD: 65 Kgf

(d) PHOSPHORUS X-RAY
    IMAGE
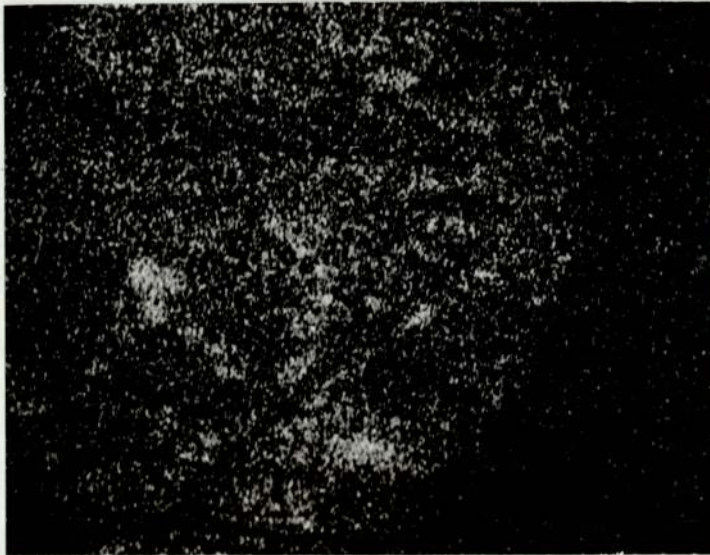
(e) ZINC X-RAY IMAGE

FIG. 5.16
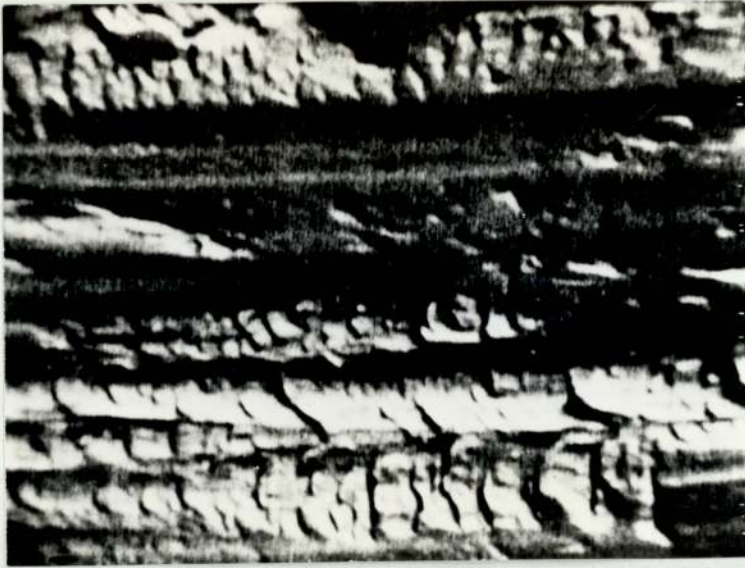
(a) ELECTRON IMAGE

SLIDING DIRECTION

100 μ m
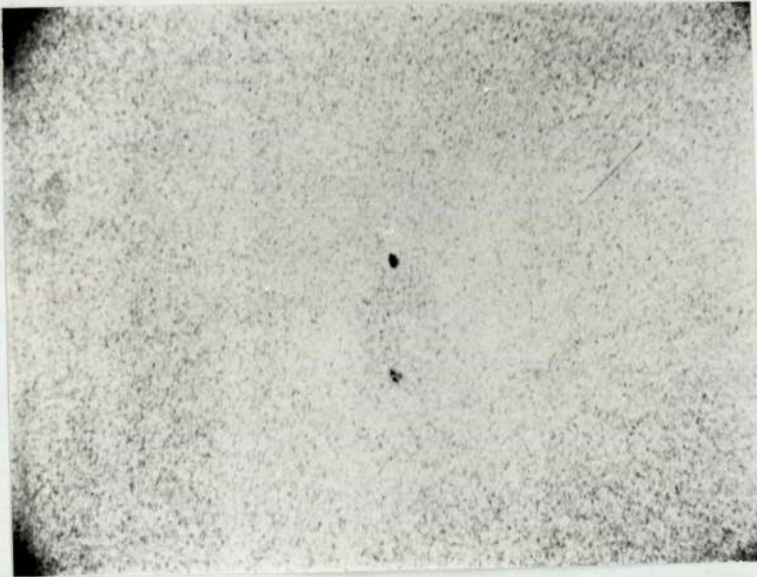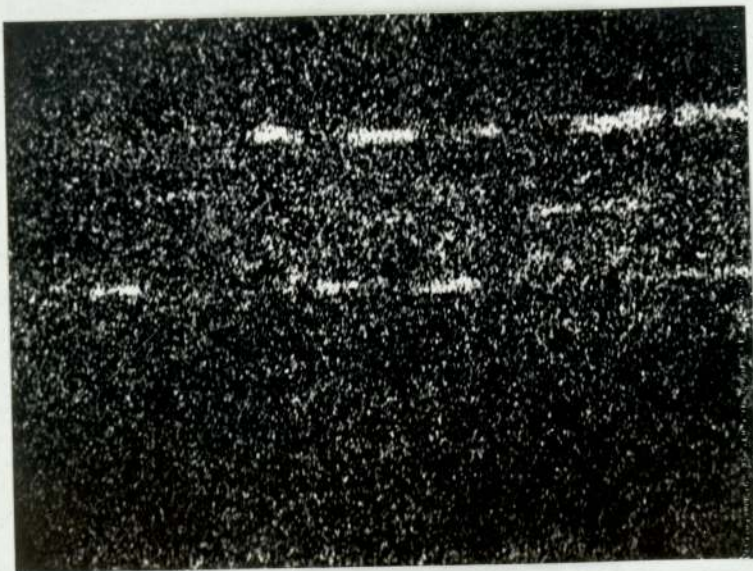
(b) IRON X-RAY IMAGE

(c) SULPHUR X-RAY IMAGE

FIG. 5.17   LUBRICANT: HVI + ZDP

LOAD: 120 Kgf

(d) PHOSPHORUS X-RAY
    IMAGE

(e) ZINC X-RAY IMAGE

FIG. 5.17

(a) ELECTRON IMAGE

SLIDING DIRECTION

100 μ m
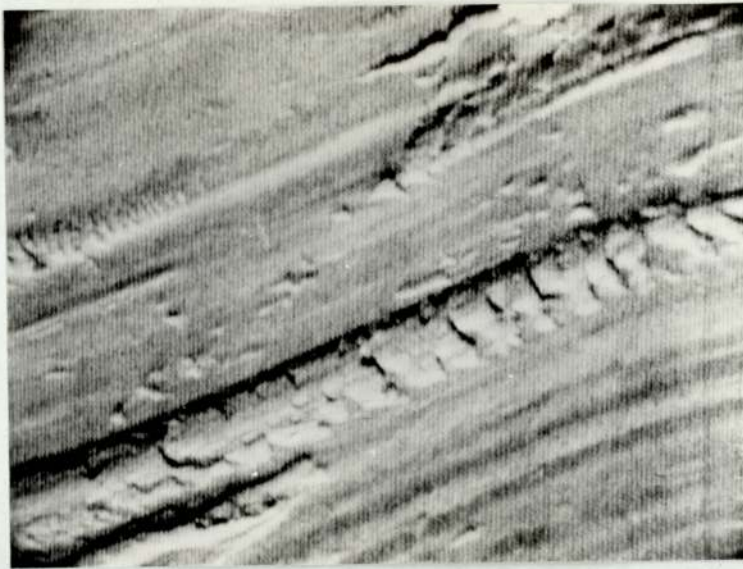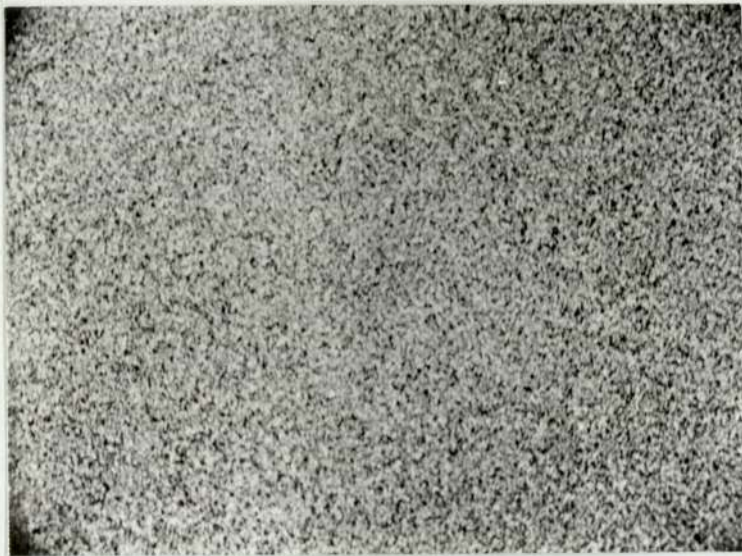
(b) IRON X-RAY IMAGE
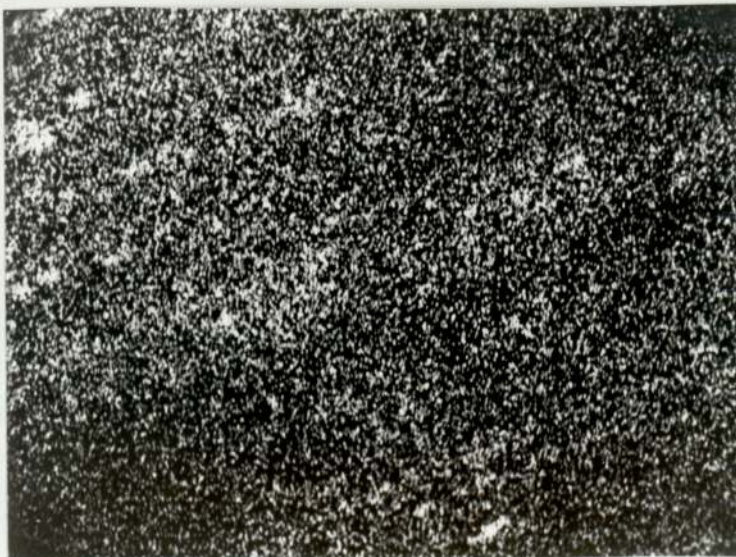
(c) SULPHUR X-RAY IMAGE

FIG. 5.18   LUBRICANT: RISELLA 29 + LUBRIZOL 1395

LOAD: 130 Kgf
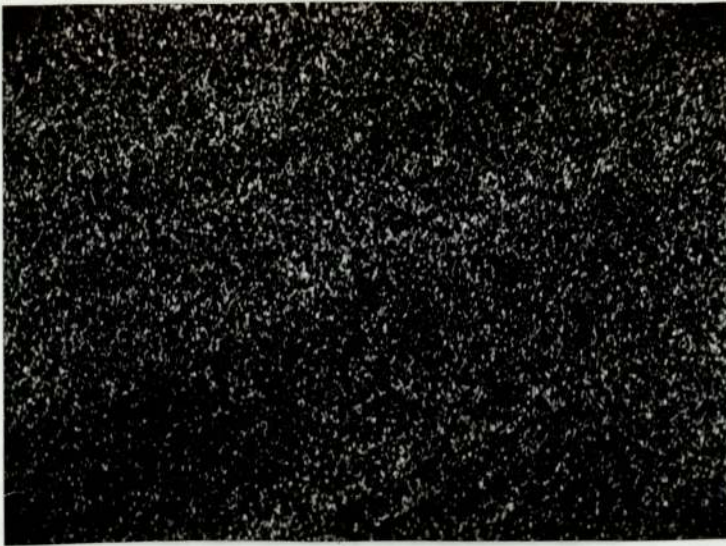
(d) PHOSPHORUS X-RAY
IMAGE

(e) ZINC X-RAY IMAGE

FIG. 5.18

Lubrizol 1395. These results in the e.p. region show different distributions to those obtained in the intermediate region when HVI + 1.112% ZDP was used as lubricant. There the concentrations of the elements was associated with the pitted areas and not with the smooth tracked regions.

5.2.2 Quantitative Area Analyses of the Worn Surfaces

The quantities of sulphur, phosphorus and zinc detected on the wear scars using these additives were always low and varied both with load and within each wear scar. The count rates were low and consequently the errors involved were large, being as high as $\pm$ 50% for the lowest count rates. Table 5.3(a) shows the average values of iron, sulphur, phosphorus, zinc and by difference oxygen and carbon, at loads of 15, 55 and 120 Kgf. using Risella 29 + 1.112% ZDP as lubricant. The variations in the amounts of each element are such that no definite conclusions can be drawn. The indications from the atomic ratios are that the amount of sulphur increased in the e.p. region while the amount of phosphorus decreased. The zinc content was similar in both regions. Similar variations were obtained when using HVI + 1.112% ZDP as lubricant. The results for specimens in the intermediate region were similar to those in the e.p. region.

Table 5.3(b) shows the average values obtained when Risella 29 + 1.0% Lubrizol 1395 was the lubricant involved at loads of 15, 45, 65 and 130 Kgf. The same sort of results were obtained when HVI base oil was used with Lubrizol 1395. Again the variations in the amounts of the elements was such that no definite trends could be established. It was not possible to assess whether there were systematic changes in the atomic ratios of the element when comparing the results from the a.w. and e.p. regions.

From the X-ray images it was apparent that for different areas within one scar the ratio of the elements, particularly between sulphur and the other two elements phosphorus and zinc will vary because of their different spatial distributions. This may in part explain the wide

Table 5.3

Average Element Contents of Area Analyses of Specimens Worn
with (a) Risella 29 + 1.112% ZDP and (b) Risella 29 + 1.0%
Lubrizol 1395 as Lubricant (20 KV Accelerating Potential)

(a)

Load	Average Weight percent in scar of					Atomic Ratio in scar of		
Kgf	Fe	Zn	P	S	O,C	Zn	P	S
15	90.9	0.3	0.7	0.2	7.9	1	4.9	1.4
55	85.5	0.4	0.7	1.0	12.4	1	3.7	5.1
120	89.3	0.4	0.4	1.0	8.9	1	2.1	5.1

(b)

Load	Average Weight percent in scar of					Atomic Ratio in scar of		
Kgf	Fe	Zn	P	S	O,C	Zn	P	S
15	90.3	1.3	1.8	0.7	5.9	1	2.9	1.1
45	87.8	3.4	2.4	1.7	4.8	1	1.5	1.0
65	87.5	1.0	0.8	2.6	8.3	1	1.7	5.3
130	88.4	1.0	0.8	0.9	8.9	1	1.7	2.0

variations observed in Tables 5.3 (a) and (b).

5.3 Summarizing Remarks

Specimens formed with DBDS and DPDS additives gave similar sulphur percentages (2-7%) in the a.w. region, while those formed with DTBDS as additive gave lower values (1-4%). The sulphur was confined to the wear scars and had uniform or patchy distributions. There tended to be more sulphur detected in the a.w. region when Risella 29 base oil was used. After initial seizure the amounts of sulphur dropped to a minimum and increased with increasing load in the e.p. region when DBDS and DTBDS additives were used. When DPDS additive was used the amount of sulphur observed in the e.p. region increased by a small amount only, the increase being greater when HVI oil was used. Around initial seizure most of the sulphur was detected in the pitted, rough areas of the scars but as the load was increased the highest concentrations of sulphur were found in the tracked regions. Depth analyses did not add a great deal of information about the sulphur distribution. They did show that at high loads the sulphur was distributed to a depth of a few microns.

When zinc dialkyldithiophosphate additives were used the zinc and phosphorus had similar spatial distributions in the a.w. region, the sulphur being separate. Quantitative results showed wide variations in the percentages of the elements but generally there was more sulphur detected in the e.p. region than the a.w. region and the reverse for phosphorus, there being similar amounts of zinc in both regions.

C H A P T E R   6

SCANNING ELECTRON MICROSCOPY OF THE WORN SURFACES

6.1 The Topography of the Surfaces Worn with Sulphur Additives

6.1.1 The Anti-Wear Region

Studies of wear scars formed on balls and rollers with the
scanning electron microscope show how the surface topography varies with
load and additive. The scars on the balls and rollers were, in general,
similar at equivalent loads, that is at equivalent positions on the graphs
of load versus wear scar diameter. Unless otherwise stated all the S.E.M.
photographs are of wear scars formed on balls using an electron accelerating
potential of 20 KV.

When no additive was used the wear scars formed with Risella 29
oil look clean and do not have a visible surface film on them. Figure 6.1
shows the wear scar formed at a load of 45 Kgf with Risella 29 as lubricant
on the flat surface of a roller. However, when HVI base oil was used the
surfaces of the scars look discoloured. Figure 6.2 shows the scar formed
at a load of 35 Kgf lubricated with HVI oil. The central strip is covered
with a film which looks darker and rougher than the two outside regions of
the scar.

When the sulphur additives were used the wear scars were again
covered with a visible surface film. Figure 6.3 shows a wear scar formed
at a load of 15 Kgf with HVI + 0.723% DTBDS as lubricant. The scars are
very smooth and covered with fine tracks parallel to the direction of sliding.
This photograph is typical of the surfaces obtained in the a.w. region when
sulphur additives were used.
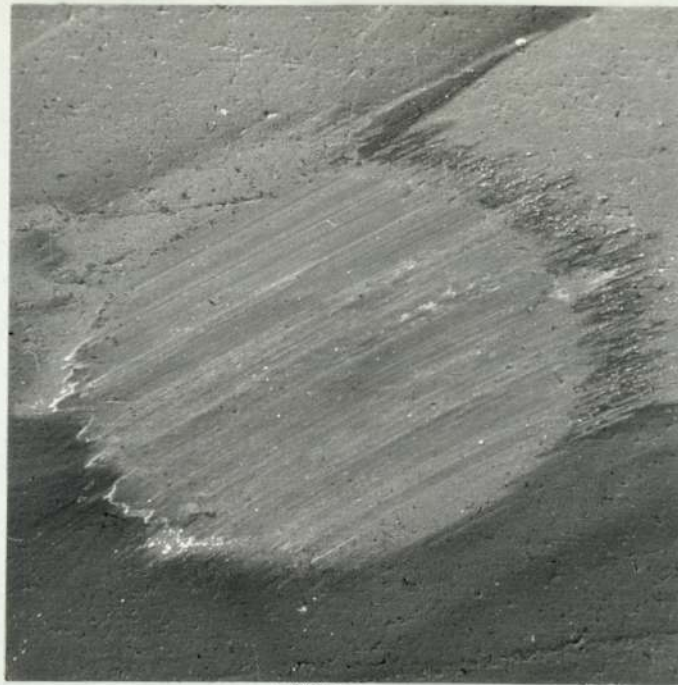
SLIDING
DIRECTION

100μm

FIG. 6.1

LUBRICANT: RISELLA 29 (Flat)

LOAD: 45 Kgf
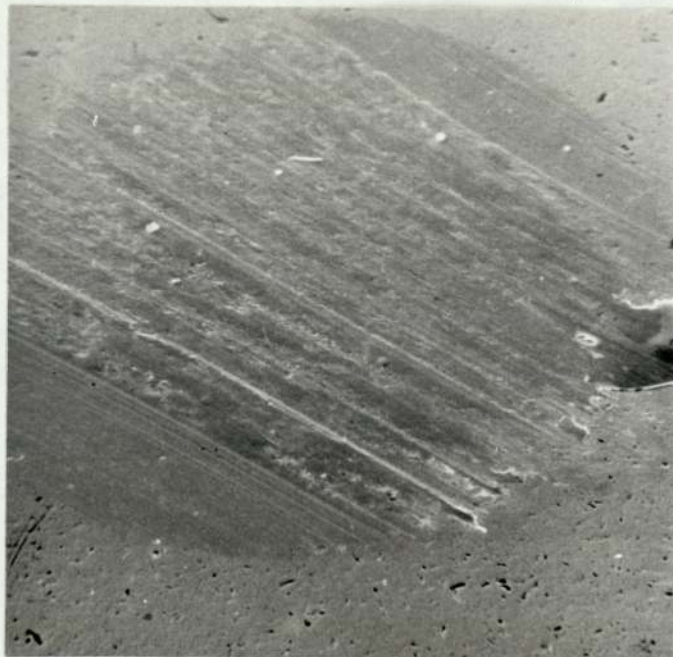
SLIDING
DIRECTION

50μm

FIG. 6.2

LUBRICANT: HVI

LOAD: 35 Kgf

SLIDING
DIRECTION

50μm

FIG. 6.3

LUBRICANT: HVI + DTBDS

LOAD: 15 Kgf

SLIDING
DIRECTION

100μm
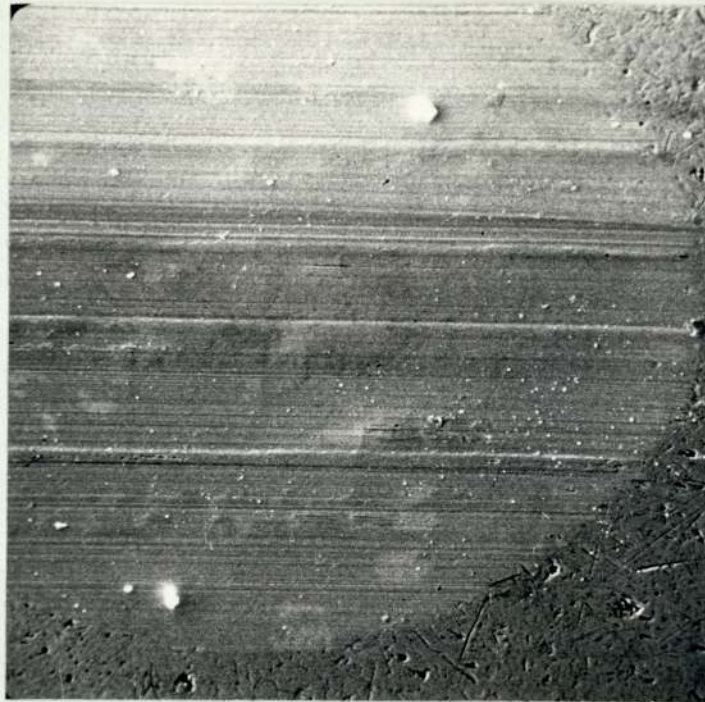
FIG. 6.4

LUBRICANT: RISELLA 29 + DPDS

LOAD: 55 Kgf

6.1.2 The Extreme Pressure Region

At initial seizure the surfaces formed with the two base oils plus sulphur additives were different. When Risella 29 plus sulphur additive was used flaked, deeply grooved surfaces were formed. Figure 6.4 shows the scar formed with Risella 29 + 0.886% DPDS at a load of 55 Kgf. Large areas of the centre and trailing edge of the scar surface are breaking off leaving pitted areas of exposed metal. When HVI plus sulphur additives were used the surfaces were still pitted in the centre and towards the trailing edge but they were much less extensive. Also the scars are more finely scored. This is illustrated in Figure 6.5 which shows a scar formed at a load of 55 Kgf with HVI + 1.0% DBDS as lubricant.

As the load is increased the differences in the form of the wear scars due to the type of base oil disappear and differences due to the type of additive bcome apparent. The wear scars formed with DBDS and DTBDS additives have similar topographies but those surfaces formed with DPDS additive are different. At 100 Kgf with HVI + 0.886% DPDS as lubricant scars are formed with smooth and rough areas. This is illustrated in Figure 6.6. The rough areas have plate like structures which could be due to localised welding between the stationary ball and the upper rotating one. The weld must be broken immediately if seizure is not to take place and hence strips of metal are pulled out one after the other as the welds are broken. Figure 6.7 shows a similar structure formed on a scar at a load of 45 Kgf with only Risella 29 oil as lubricant. This type of surface structure appears to be formed by mechanical action when there is no additive or when the chemical reaction of the additive is insufficient to afford good protection of the sliding surfaces. In contrast to these surface topographies Figure 6.8 shows part of a wear scar formed with Risella 29 + 1.0% DBDS as lubricant at the same load of 100 Kgf. When DBDS and DTBDS additives are used the scars formed at this load are characterised by fine grooves forming

SLIDING
DIRECTION

100μm
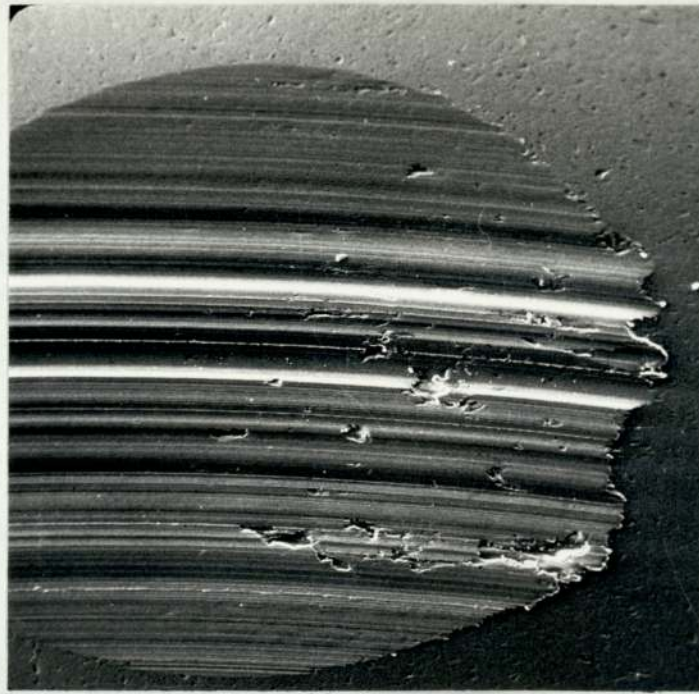
FIG. 6.5

LUBRICANT: HVI + DBDS

LOAD: 55 Kgf

SLIDING
DIRECTION

10μm
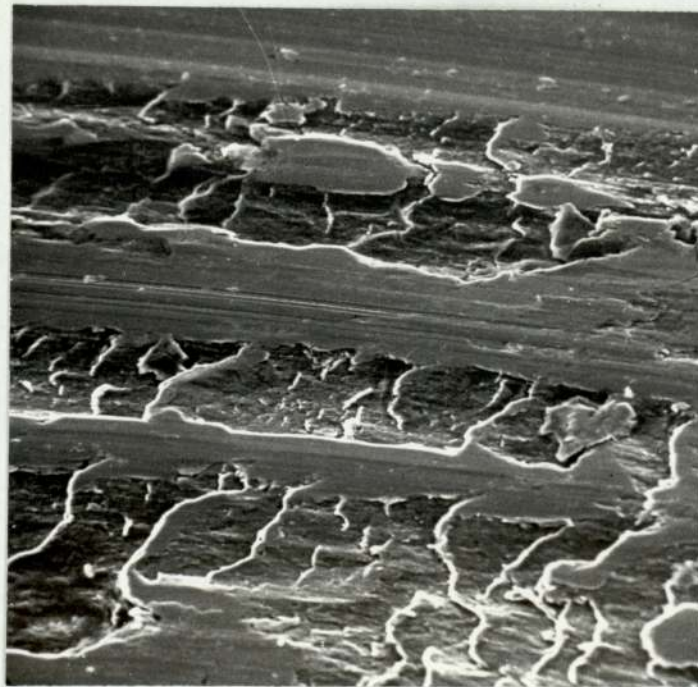
FIG. 6.6

LUBRICANT: HVI + DPDS

LOAD: 100 Kgf

SLIDING
DIRECTION

50μm

FIG. 6.7

LUBRICANT: RISELLA 29

LOAD: 45 Kgf

SLIDING
DIRECTION

100μm

FIG. 6.8

LUBRICANT: RISELLA 29 + DBDS

LOAD: 100 Kgf

a smooth surface. There are very few rough areas and no indications of welding between the sliding surfaces.

At 160 Kgf, just before final seizure with DPDS as additive, the surfaces look extremely rough with only a small percentage of the total area of the scars being smooth. Figure 6.9 shows part of a scar formed with Risella 29 + 0.886% DPDS as lubricant at this load. Whole regions of the scar appear to have been torn out of the surface and welding has taken place extensively. It is apparent that the additive has not given the sliding surfaces sufficient protection and this mode of wear cannot be sustained, hence seizure occurs.

When DBDS and DTBDS additives are used the evidence points in the opposite direction, that is the higher the load the greater the chemical action of the additive and the greater the protection afforded to the sliding surfaces. Figure 6.10 shows an area in the centre of a wear scar formed with HVI + 1.0% DBDS as lubricant at a load of 170 Kgf. The surface has broken up in places leaving fine debris on the scar (bottom left) and raised islands remain as part of the load bearing film. The topography of this type of scar indicates that the additive reacts with the metal to form iron sulphide which breaks up under the applied load leaving debris and fresh metal to react with the additive. Figure 6.11 is an area of a scar formed at 200 Kgf with Risella 29 + 1.0% DBDS as lubricant. The lateral cracks indicate that the mode of destruction of the reacted layer is stress cracking of the film.

When applying a microhardness indentor to the surface of the wear scars to carry out depth analyses on the electron probe the surface film broke up in places on wear scars formed at high loads. Figure 6.12 shows how these indentations affected the surface of a scar formed at a load of 200 Kgf with HVI + 0.723% DTBDS as lubricant on a roller. Cracks spread out

SLIDING
DIRECTION

50μm

FIG. 6.9

LUBRICANT: RISELLA 29 + DPDS

LOAD: 160 Kgf

SLIDING
DIRECTION

10μm

FIG. 6.10

LUBRICANT: HVI + DBDS

LOAD: 170 Kgf

SLIDING
DIRECTION

50μm

FIG. 6.11

LUBRICANT: RISELLA 29 + DBDS

LOAD: 200 Kgf
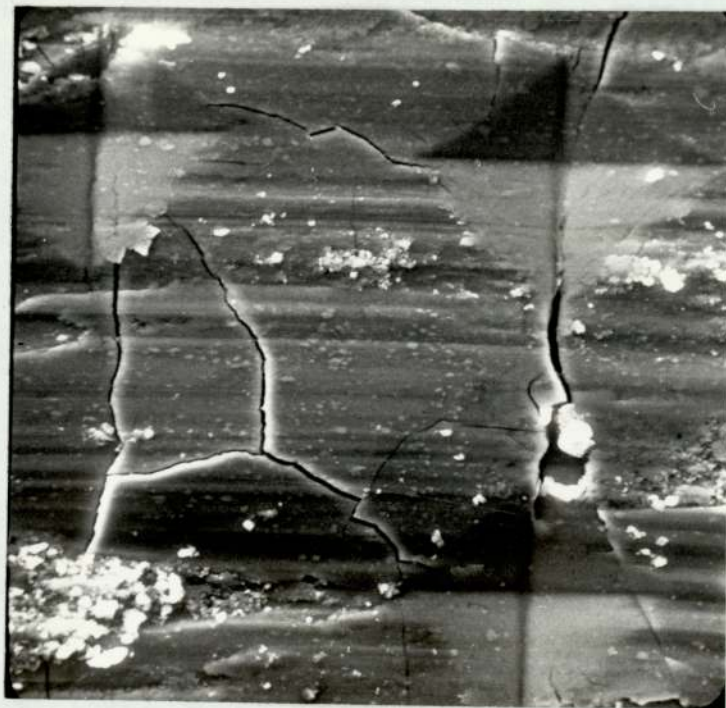
SLIDING
DIRECTION

10μm

FIG. 6.12

LUBRICANT: HVI + DTBDS (Flat)

LOAD: 200 Kgf

from the corners of the indentations. Figure 6.13 shows the edge of the reacted layer on the scar when part of the surface broke away. The thickness of the film exposed was estimated to be 2 to 4 microns.

6.2 The Topography of the Surfaces Worn with Zinc Dialkyldithiophosphate Additives

6.2.1 The Anti-Wear Region

The surfaces formed with pure ZDP and Lubrizol 1395 additives in the a.w. region are extremely smooth and covered with fine grooves. The scars are similar for both the additives and with both base oils. The main characteristic of the surfaces is the presence of dark discolourations covering most of the central area of the scars. Figure 6.14 shows a scar formed at a load of 15 Kgf with HVI + 1.112% ZDP as lubricant. These dark discolourations are associated with concentrations of phosphorus, zinc and particularly sulphur when observed with the electron probe. The evidence from Figure 6.15, which illustrates part of the film formed on a wear scar at a load of 35 Kgf with Risella 29 + 1.112% ZDP as lubricant, suggests that the film is quite thick and sits on top of the metal surface. These films are thicker than those obtained in the a.w. region using the sulphur additives and give good protection to the metal surfaces up to loads around 100 Kgf.

6.2.2 The Extreme Pressure Region

In the e.p. region the wear scars have smooth and rough areas similar to the surfaces formed with DPDS additive. Figure 6.16 shows part of the scar formed at a load of 120 Kgf with HVI + 1.0% Lubrizol 1395 as lubricant. This print is very similar to Figure 6.6 and indicates that localised welding has taken place. The smooth areas have a thin visible film which contains sulphur phosphorus and zinc when observed with the electron probe.

SLIDING
DIRECTION

1 μm

FIG. 6.13

LUBRICANT: HVI + DTBDS (Flat)

LOAD: 200 Kgf

SLIDING
DIRECTION

50μm
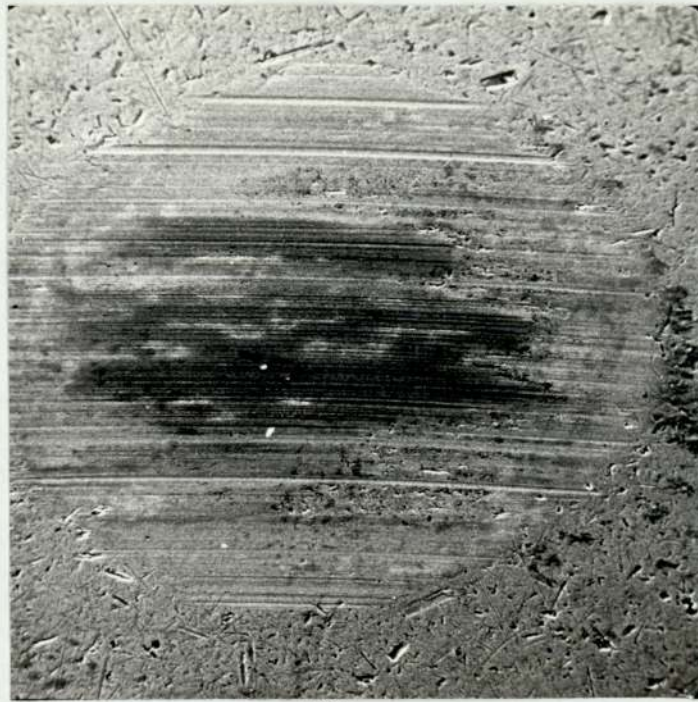
FIG. 6.14

LUBRICANT: HVI + ZDP

LOAD: 15 Kgf

SLIDING
DIRECTION

1μm
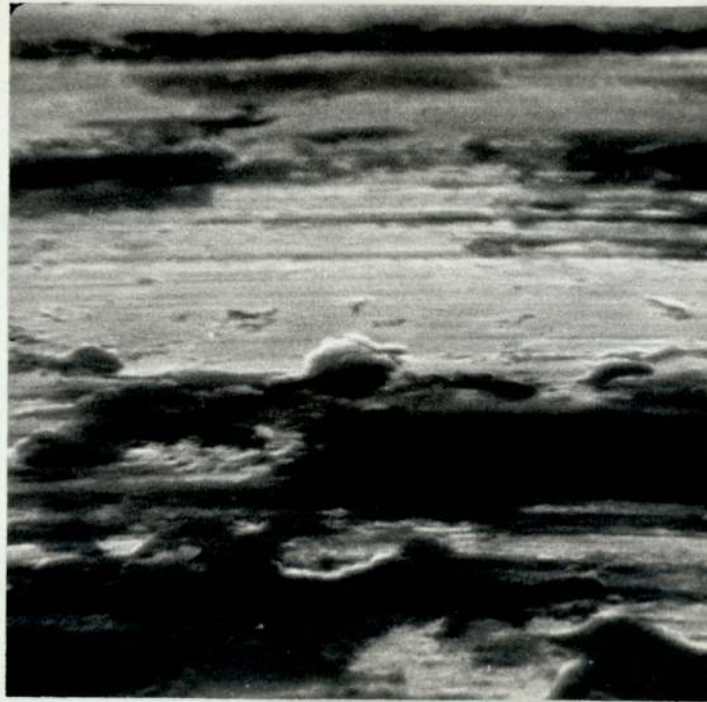
FIG. 6.15

LUBRICANT: RISELLA 29 + ZDP

LOAD: 35 Kgf

SLIDING
DIRECTION

10μm
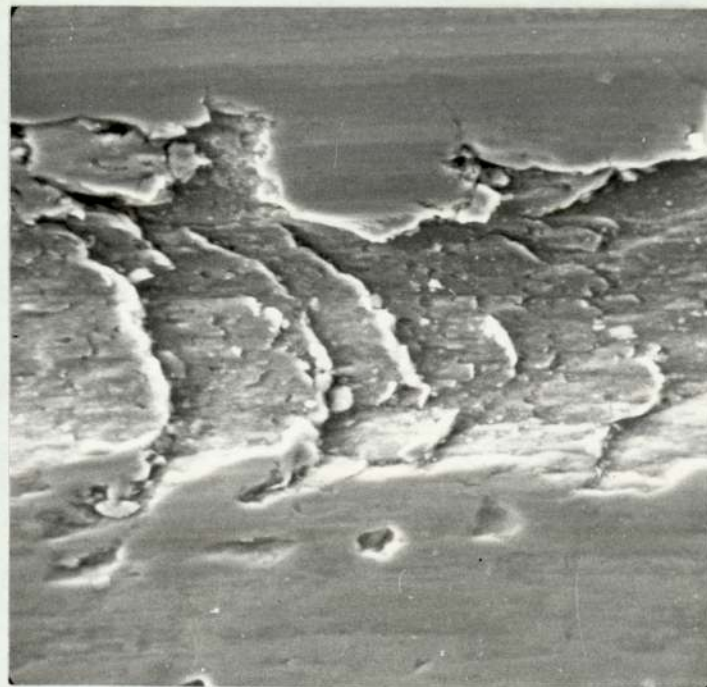
FIG. 6.16

LUBRICANT: HVI + ZDP

LOAD: 120 Kgf

6.3 Summarizing Remarks

When HVI oil was used as lubricant a visible film was formed on the scars similar to those formed when sulphur additives were used in the a.w. region. These scars are finely scored. At initial seizure the scars are pitted and differences due to base oil are apparent. At higher loads DPDS additive affords little protection and rough, welded surfaces occur. When DBDS and DTBDS are used the surfaces are covered with a thick reacted film which cracks up at higher loads revealing that the thickness of the film is of the order of 2 to 4 microns.

When zinc dialkyldithiophosphate additives were used thick films covering most of the scars were observed and these afforded good protection in the a.w. region up to 100 Kgf. However, these two additives gave very little protection in the e.p. region and scars similar to those obtained with DPDS additive were obtained.

C H A P T E R   7

OTHER PHYSICAL TECHNIQUES

7.1   Micro-indentation Hardness Tests on the Surfaces of Selected Wear Scars

The hardness of both the unworn and worn regions of selected rollers were obtained on a Leitz Miniload Tester. A load of 300 gms was used except when the surfaces were very soft and a smaller load (100 gms) was necessary to stop the surface film cracking. The central areas of the scars were tested so that the load was applied approximately normal to the surface and the diagonals of the indentations were similar in length. Several indentations both on and off the wear scars were made on each specimen and mean values obtained. The results were corrected for the small loads used. The Leitz Miniload Tester Handbook suggests adding 1.1μm to the mean length of the diagonals before looking up the hardness value in the tables. This correction was applied to the results.

Table 7.1 shows the hardness values obtained from the selected specimens. The hardness values off the wear scars vary between 875 and 1000 V.P.N. except in the e.p. region when DBDS and DTBDS additives were used, when the hardness decreased from 1000 to 550 V.P.N. as the load was increased. These hardness values are high compared to the macro-indentation tests which gave values around 850 V.P.N. for both balls and rollers. The instrument was not directly calibrated, only a standard correction was made so no direct comparison can be made with the macro-indentation tests. As all the micro-indentation tests were conducted on the same instrument and the same correction applied, comparison can be made between the results obtained from the various specimens recorded in Table 7.1. When rollers worn with DPDS, ZDP and Lubrizol 1395 additives were tested the hardness values obtained on

Table 7.1

Micro-Indentation Hardness Results (V.P.N.)

(Leitz Miniload Tester – 300gm load)

LUBRICANT	RIS + DBDS		RISELLA 29+DTBDS		HVI + DTBDS		RISELLA 29+DPDS		HVI + ZDP		RISELLA 29 + LUBRIZOL 1395	
	HARDNESS VPN		HARDNESS VPN		HARDNESS VPN		HARDNESS VPN		HARDNESS VPN		HARDNESS VPN	
LOAD Kgf	ON SCAR	OFF SCAR	ON SCAR	OFF SCAR	ON SCAR	OFF SCAR	ON SCAR	OFF SCAR	ON SCAR	OFF SCAR	ON SCAR	OFF SCAR
15			875	940								
35			960	960	775	960	920	920	840	930	920	920
45	815	900	780	965	875	960			810	920	840	1000
55	730	900	870	965								
70			575	965	735	1000	860	920				
80	690	960										
100			560		650	920			810	880		
120			560	820			875	875			920	920
140	560	820										
180				735								
200	560	820			375	550						

the wear scars were similar to those obtained off the scars over the whole load range. However, when rollers worn with DBDS and DTBDS additives were tested the hardness on the scars decreased with increasing load in the e.p. region and the values were less than those taken off the scars. This suggests that a soft layer is required to protect the rubbing surfaces under e.p. conditions. At 200 Kgf load with DTBDS as additive the film cracked when a 300 gm load was used suggesting that at room temperature the film was brittle.

7.2   Micro-indentation Hardness Tests on Taper Sections of Selected Specimens

A number of rollers were mounted in thermosetting plastic at an angle of 11.5° to the surface of the mount and ground down to expose half the wear scar which then formed a taper section with a depth magnification of x5. The taper sections were polished and etched with 2% Nitol so that the structures of the underlying material could be observed. Micro-indentation hardness tests using a Vickers microscope and 100 gm applied load were made on the taper sections. A calibration curve was obtained from a set of materials of varying hardness tested on a macro-indentation tester and on the Vickers micro-indentation hardness tester. All the results presented have been corrected from this calibration graph.

Figure 7.1 shows a taper section through a scar formed on a roller at a load of 180 Kgf with HVI + DBDS as lubricant. The wear scar has been covered with clear plastic prior to grinding and polishing so that the surface of the wear scar is visible. A light coloured layer has been formed under the scar, which is thick at the leading edge of the scar and disappears towards the trailing edge. Above this layer a thin, darker film has been formed in the centre of the scar and below the light layer a darker area of tempered martensite has been formed. Below this area of tempered martensite the lighter ordinary martensite can be seen. Figure 7.2 shows a series of photographs of the structures formed below the front half of the wear scar
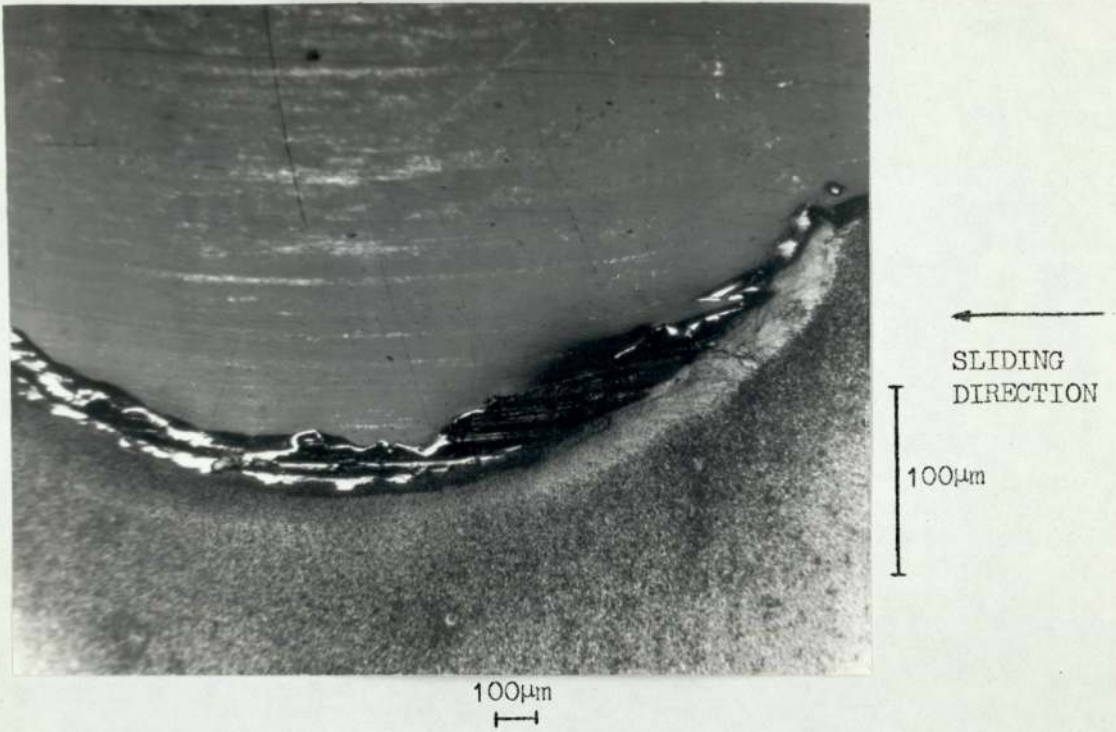
FIG. 7.1 TAPER SECTION

LUBRICANT: HVI + DBDS
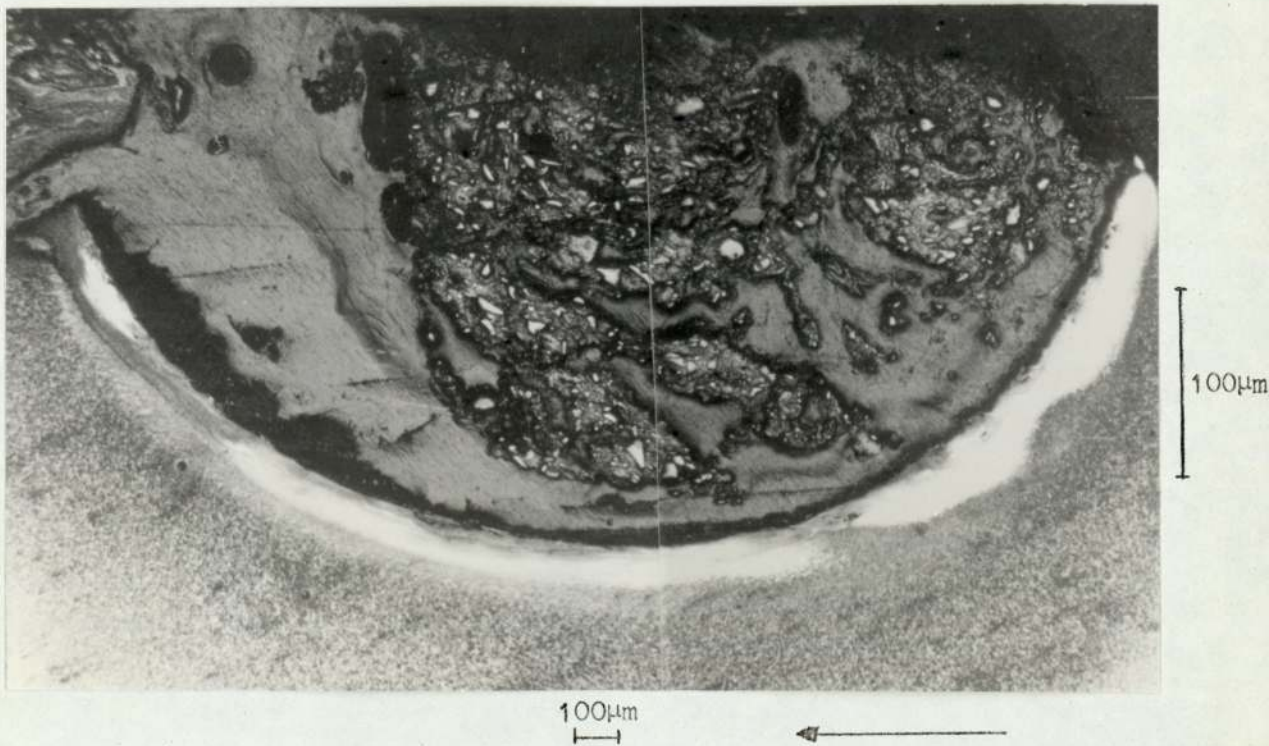
LOAD: 180 Kgf

FIG. 7.3 TAPER SECTION   SLIDING DIRECTION

LUBRICANT: HVI + DPDS

LOAD: 140 Kgf

FIG. 7.2   TAPER SECTION

LUBRICANT: HVI + DBDS

LOAD: 180 Kgf

20μm

20μm

SLIDING DIRECTION
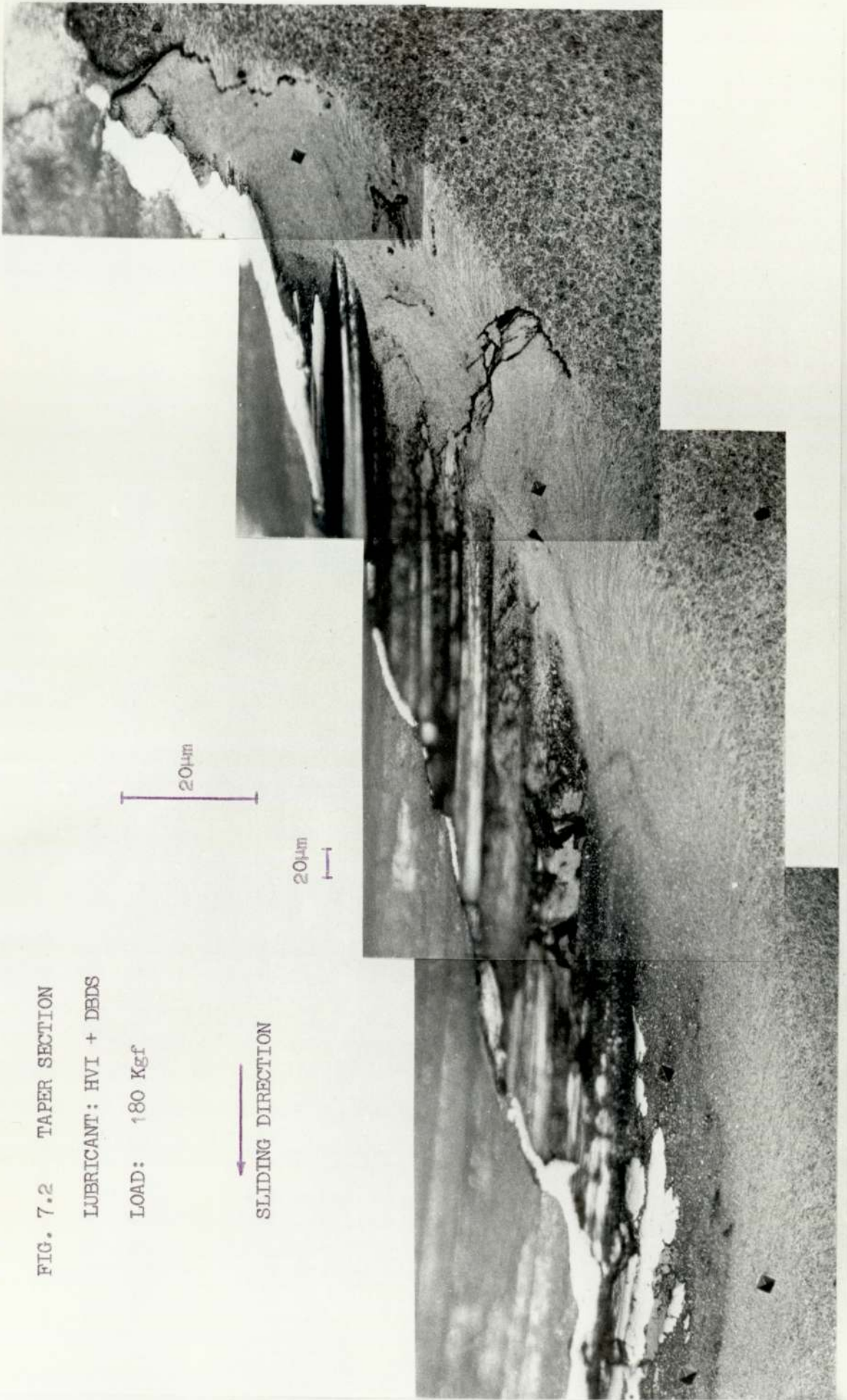
illustrated in Figure 7.1, with micro-indentations visible at various points. The indentations above the cracks near the leading edge indicated a hardness of 640 V.P.N., the one below the crack 610 V.P.N. and the three indentations on the left of Figure 7.2 gave hardness values of 460, 480 and 460 V.P.N. The region under the leading edge of the scar is the hardest area and would be expected to have had a high temperature. The hardness of the darker layer near the surface was the same as the light coloured layer. The hardness of the tempered martensite increased from 490 V.P.N. near the light layer to 860 V.P.N. when the ordinary martensite was reached at a depth of about 100μm. The hardness of the sulphide film was not obtained as the film cracked even under lighter loads than 100 gms. The hardness of the layers under the scar increased with increasing depth. This was observed for scars formed with both DBDS and DTBDS additives in the e.p. region and gives weight to the results presented in Table 7.1. In Figure 7.2 flow lines can be observed in the light surface layer. These flow lines follow the direction of sliding.

Figure 7.3 shows a taper section of a scar formed at a load of 140 Kgf with HVI + DPDS as lubricant. A thick white layer has been formed under most of the scar and is particularly thick at the leading edge. A dark layer of tempered martensite has formed below the white layer. Micro-indentation hardness tests were made at a number of points. Figure 7.4 shows a series of these indentations in the white layer formed with Risella 29 + DPDS at a load of 140 Kgf. The four indentations on the left of Figure 7.4 give hardness values, taken from top to bottom, of 1070, 910, 830, 450 V.P.N. The two other indentations give values of 910 V.P.N. on the right and 875 V.P.N. in the centre. The hardness of the tempered martensite increases from 450 V.P.N. below the white layer to 910 V.P.N. in the ordinary martensite. The streaked darker area near the trailing edge of the scar has a hardness of 675 V.P.N. The white layer is very hard and has not reacted with Nitol, the

SLIDING
DIRECTION

20μm

20μm
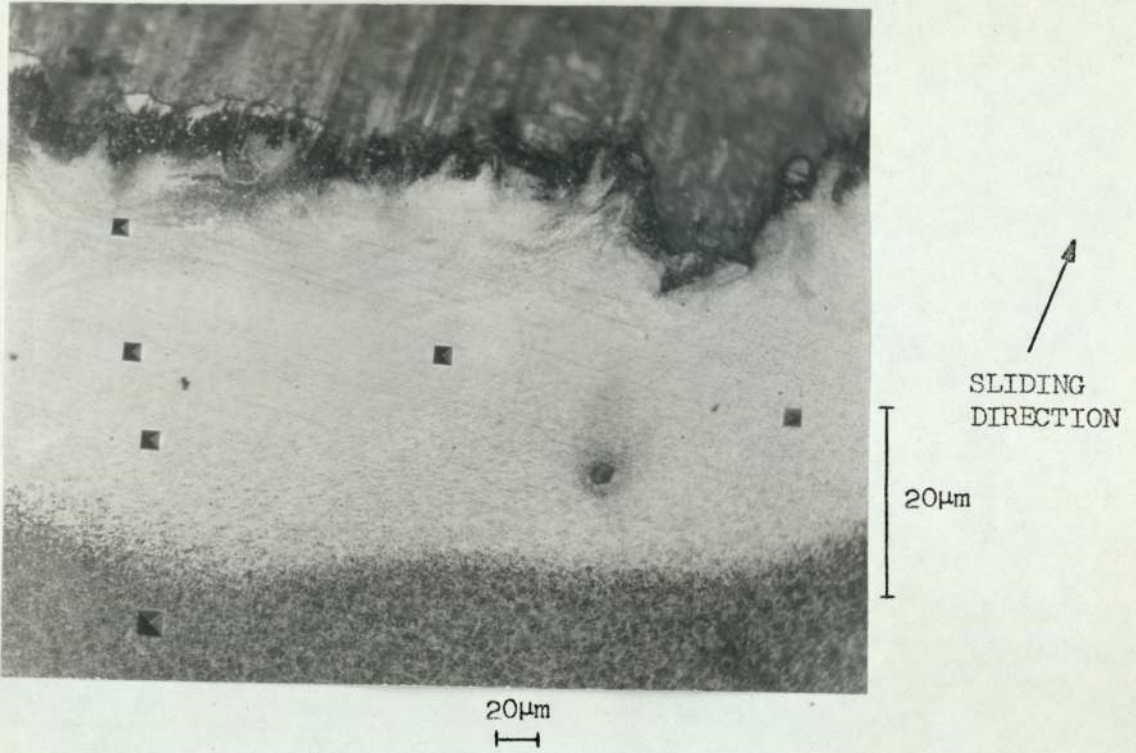
FIG. 7.4

LUBRICANT: RISELLA 29 + DPDS

LOAD: 140 Kgf

SLIDING
DIRECTION

100μm

100μm
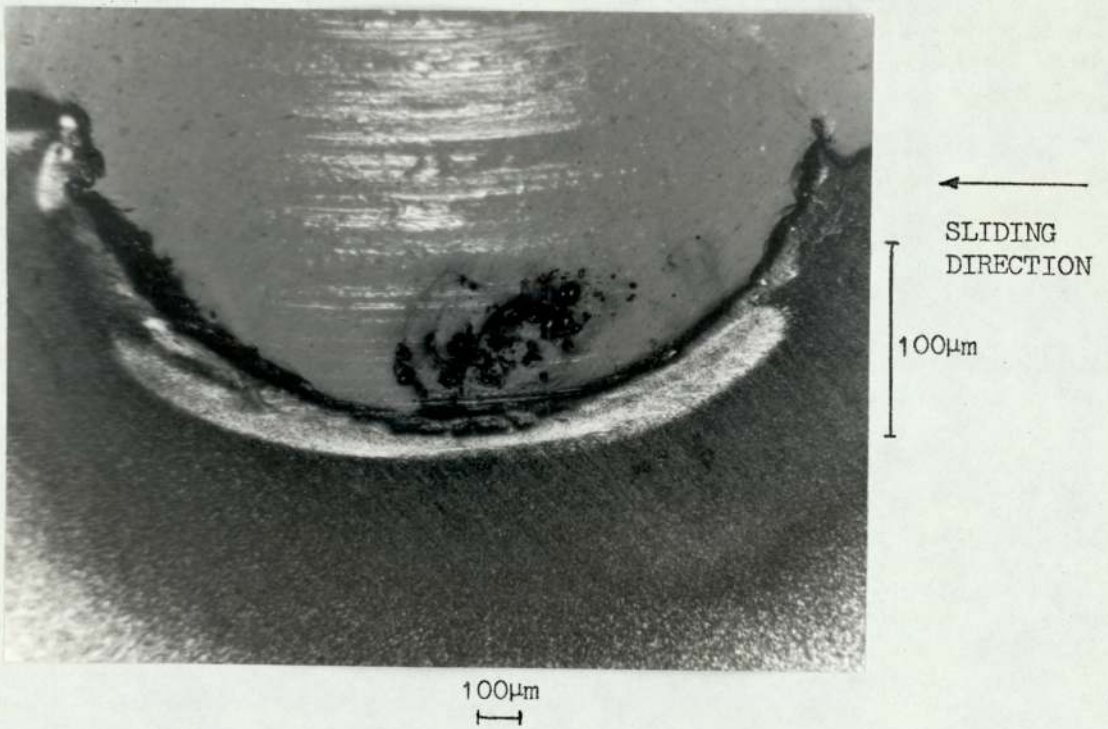
FIG. 7.5

LUBRICANT: HVI + ZDP

LOAD: 120 Kgf

etching agent, and consequently does not appear to be the type of formation conducive to good e.p. lubrication as the e.p. additive will also have difficulty reacting with this structure.

Similar results to those obtained with DPDS additive were observed with ZDP and Lubrizol 1395 additives. Figure 7.5 shows a taper section of a scar formed at a load of 120 Kgf with HVI + ZDP as lubricant. Again a thick white layer was formed under the scar, being thickest at the leading edge. The white layer was surrounded by a dark tempered martensite area above the ordinary martensite. Figure 7.6 shows a series of indentations made near the leading edge of the scar. The hardness of the material to the right of the white layer was 580 V.P.N. whereas just within the white layer the hardness was 910 V.P.N. The four indentations on the left of Figure 7.6 give hardness values taken from top to bottom of 1050, 940, 860 and 500 V.P.N. The hardness of the tempered martensite increased from 500 V.P.N. to 860 V.P.N. with increasing depth the value of 860 V.P.N. being that of the ordinary martensite. The white layer was again hard and unreactive, reinforcing the results obtained in section 7.1, that the surfaces of the scars formed in the e.p. region with poor e.p. additives are hard compared to those obtained with DBDS and DTBDS additives.

Savitskiy and Kogan (66) established that white layers arising on friction surfaces of steels may originate by quenching or diffusion. Type I layers were formed by quenching, had hardness values in the range 900 - 1100 Kg/mm^2, and had austenitic - martensitic structures with some carbide phase. Type II layers were formed by diffusion of carbon, had hardness values greater than 1200 Kg/mm^2, and by X-ray diffraction only iron carbide (mainly Fe_3C) and α-Fe lines were observed. They used an alkaline solution of sodium picrate to etch the white layers and show their structure. Two specimens (formed with HVI + DPDS lubricant at 140 Kgf and HVI + ZDP lubricant at 120 Kgf) were etched in a boiling solution of alkaline sodium picrate for

SLIDING
DIRECTION

20μm

20μm

FIG. 7.6

LUBRICANT: HVI + ZDP

LOAD: 120 Kgf

five minutes. The resultant etched specimens showed up carbide particles distributed randomly through the matrix and through the white layers. In one case the white layer was darker than the matrix and in the other lighter than the surrounding matrix. From this evidence it was not possible to ascertain whether the white layers were enriched with carbides. Further work in this area is necessary to elucidate the types of structures under the wear scars.

7.3 Results using Electron Spectroscopy for Chemical Analysis (ESCA)

Towards the end of the period of research a new ESCA machine was installed at Shell Research Limited to replace a hand-built model used previously. The limited amount of work conducted on the hand-built model showed the necessity of using masks to blank off the unworn part of the rollers. Using this instrument a roller worn with DBDS as additive at 200 Kgf load revealed that two forms of sulphur were present in the scar. The peaks were obtained by stacking 10 slow scans in a multichannel analyser. These two peaks were tentatively identified as sulphide and sulphate. When a roller formed at a load of 140 Kgf with Lubrizol 1395 as additive was observed, zinc, phosphorus and sulphur peaks were obtained. These results were obtained near the limit of resolution of the instrument.

On the new commercial instrument an area of approximately 2mm x 10mm is irradiated. Platinum masks were used to cover all but the wear scars. Unfortunately, lead and sulphur peaks were observed when irradiating only the mask. Fine gold (99.98% pure) masks were used instead of platinum but again two sulphur peaks were observed when irradiating only the mask. These peaks were of similar intensity to those observed when a small scar was irradiated. It was not possible to overcome these problems in the time available, but the work is continuing and these problems will be solved.

7.4 Summarizing Remarks

The hardness of the wear scars is very similar to that of the unworn EN31 steel in most cases. The exceptions are the wear scars formed with DBDS and DTBDS additives in the e.p. region. For these scars much lower hardness values were obtained indicating that the sulphide film is much softer than the steel. The micro-indentation hardness tests on the taper section show that the structures under the wear scars formed with DBDS and DTBDS additives, in the e.p. region, have a lower hardness value than the ordinary unworn steel and that no thick white layer has been formed. For the other additives used, the structures under the wear scars consist of a thick, hard white layer, thickest at the leading edge, supported on a softer tempered martensite layer.

The ESCA results at present do not give much information about the chemical environment of the atoms present on the worn surfaces but work is in progress to overcome the initial problems encountered and obtain some very useful results.

C H A P T E R   8

DISCUSSION

8.1   Comparison of Results with other Published Work

The results of the wear tests show the differing effects of the various additives, geometries and base oils. When no additives were used Risella 29 oil had no e.p. activity whereas HVI oil did, especially when used with 3 flats geometry. HVI oil contains polar impurities and approximately 1% by weight sulphur and these can act as e.p. agents at higher loads.

The 4-ball results using the sulphur additives were similar to those obtained by Allum and Ford (39). Table 8.1 shows the initial and final seizure loads obtained by Allum and Ford with a 0.302% weight sulphur concentration (4.63 millimoles per 100 gms of blend) compared to 0.265% weight sulphur (4.06 millimoles per 100 gms of blend) in these tests, both using a highly refined paraffin oil. There is good agreement between the two sets of results both for initial seizure (I.S.) and final seizure (W.L.) loads. Also the form of the graphs are similar, both sets having intermediate regions or steps between the a.w. and e.p. regimes.

The results obtained with zinc di-butyldithiophosphate and Lubrizol 1395 additives are not so easily correlated with other published work. The nearest comparison found in the published literature was with the results of Allum and Forbes (54), who used a series of zinc dithiophosphates in a highly refined paraffin oil at a concentration of 0.236% weight sulphur (8.0 milliatoms of sulphur per 100 gms of blend) compared to 0.265% weight sulphur (8.12 milliatoms of sulphur per 100 gms of blend) with ZDP in this work. Table 8.2 shows the initial and final seizure loads for ZDP and

Table 8.1

Comparison of e.p. results for a series of disulphides at a
concentration of 0.302% weight sulphur (Allum and Ford) and
0.265% weight sulphur (Thesis) in paraffin oil

	THESIS		ALLUM AND FORD	
ADDITIVE	I.S. Kgf	W.L. Kgf	I.S. Kgf	W.L. Kgf
DBDS	55	260	60	240
DTBDS	45	240	50	220
DPDS	55	180	60	170

Table 8.2

Comparison of e.p. results for a series of zinc dithiophosphates
at a concentration of 0.236% weight sulphur (Allum and Forbes)
and 0.265% weight sulphur (Thesis) in paraffin oil

ADDITIVE	I.S. Kgf	W.L. Kgf
ZDP ⎫ Thesis	100	140
Lubrizol 1395 ⎭	90	150
Zn di-(4-methyl pentyl-2)dithiophosphate	60	155
Zn di-n-hexyl dithiophosphate	75	150
Zn -(2,2,dimethyl(pentyl)dithiophosphate	85	140
Zn di-n-dodecyl dithiophosphate	100	150

Lubrizol 1395 compared to those of Allum and Forbes. These results show that all the additives have comparable final seizure loads indicating similar e.p. activity. The variations in initial seizure loads show different a.w. activities. Both ZDP and Lubrizol 1395 compare favourably in their a.w. activity with the additives used by Allum and Forbes.

When the one-ball-on-3-flats geometry was used there were small variations in initial and final seizure loads compared to those obtained with 4-ball geometry. Also when HVI oil was used there were again small differences compared to the results using Risella 29 base oil. The main purpose of using the rollers was to extend the use of physical analytical techniques. As the wear test results for the two types of geometry are similar, the results of the physical analyses, whether on ball or roller, can be used in direct comparisons with the results of other published work.

The 4-ball tests cannot be used to explain the action of the additives. Physical and chemical analytical techniques must be used in conjunction with other tests and the 4-ball results to get a complete picture. The interactions during the rubbing process in the 4-ball machine must be considered as this is a dynamic test where several variables are changing continually. Dorinson (67) considered the inter-relations of these variables and states that qualitatively, "the interaction of the following factors can be recognised (a) primary generation of heat at the rubbing surfaces, (b) breakdown of the elastohydrodynamic film with the possible concomitant formation of a protective coating or the occurrence of an anti-seizure reaction with the additive, (c) penetration of heat into the body of the ball from the rubbing surface, (d) wear at the rubbing interface with additional generation of heat and (e) relaxation of the contact pressure as the area of the contact zone increases through wear, secondary effects being decreased rate of depth wear, decreased heat flux and partial or full re-establishment of a fluid lubricant film". Because of these complex inter-

relations the behaviour of lubricant additives in the 4-ball tests must continue to be viewed empirically. Consequently, the analysis of specimens formed in the 4-ball machine must be placed in the context of the test procedure and any inferences to more generalised applications of the additives must be treated with considerable circumspection. For instance, it is particularly relevant to remember that in the e.p. region the mean pressure has been reduced considerably by the wear. Typically at 15 Kgf load (a.w. region) the mean pressure on a ball with a scar of 0.3mm diameter is 87 Kgf/mm^2, whereas the mean pressure at a load of 140 Kgf with a scar diameter of 2.5mm (DPDS, ZDP and Lubrizol 1395 additives) has decreased to 11.7 Kgf/mm^2. For a scar diameter of 1.8mm at 140 Kgf load (DBDS and DTBDS additives) the mean pressure is 22.5 Kgf/mm^2. These are macroscopic pressures the load being carried by the real areas of contact. From the above 'macro-pressures' the percentage of the apparent area of contact which actually constitutes the real area of contact is greater in the a.w. than in the e.p. region assuming the same pressure can be born by the real areas of contact in both regimes. In practice this will not be the case because of the different temperatures involved under the two sliding conditions.

The X-ray diffraction analyses show that in the a.w. region for all oils and additives no film can be detected on the wear scars. This obviously does not preclude the presence of thin and/or non-crystalline films. In the e.p. region increasing amounts of cementite Fe_3C were found in the scars formed with DPDS, ZDP and Lubrizol 1395 additives and with DBDS and DTBDS additives FeS, Fe_3O_4, α-Fe_2O_3 and Fe_3C were detected. Godfrey (27) showed that for sulphurised mineral oil run in the S.A.E. machine there were several constituents to the e.p. film formed. He showed by X-ray and electron diffraction of stripped films from the worn surface, that Fe_3O_4 was the major constituent and an iron carbide, FeC, and iron sulphide were also present.

By emission spectroscopy he found concentrations of silicon significantly greater than in the base metal. Because of these structures in the worn film he suggested that several mechanisms occur during e.p. lubrication. The fact that oxides are only detected when appreciable amounts of iron sulphide are present, and that these are only found on surfaces where good protection was afforded up to high loads confirms the ideas of several authors [Greenhill(21); Simard, Russell and Nelson (20); Godfrey (27); Toyoguchi, Takai and Kato (38)] namely that oxygen and active sulphur compounds complement each other in e.p. lubrication. Godfrey (27) suggests that Fe_3O_4 is the major constituent and FeS the minor, whereas the reverse appears to be true from the diffraction and E.P.M.A. results of specimens worn with DBDS and DTBDS additives.

Sakurai and Sato (68) found from X-ray diffraction studies of specimens formed using Barcroft's (69) hot-wire corrosion technique that when DPDS additive was used in white oil the corrosion rate at 490°C was very similar to that obtained with white oil alone. The wire was of pure iron and the corrosion product on the surface was Fe_3O_4. When they used DBDS as additive the corrosion rate was extremely high and iron sulphide FeS was the main reaction product. They also used a 0.5% weight concentration of zinc di-isobutyldithiophosphate in white oil and found that at 380° and 480°C the corrosion rate was slower than with white oil alone. They suggest that zinc di-isobutyldithiophosphate forms a polymer product which retards oxidation of the iron.

The observation that large amounts of Fe_3C were detected with DPDS, ZDP and Lubrizol 1395 additives in the e.p. region and that no oxides were detected suggests that the rate of formation of oxides and sulphides at these loads is insufficient to form an effective thick film lubricant. The large quantities of Fe_3C may be due to breakdown of the lubricant and formation of Fe_3C at the high contact temperatures and preferential wear of the steel leaving an excess of carbides in the surface layers.

The E.P.M.A. results are consistent with the X-ray diffraction results in several ways. The elements detected on the surface of the scars (sulphur in the case of the sulphur additives and zinc, phosphorus and sulphur for the zinc dithiophosphate additives) in the a.w. region formed a sufficiently thin layer to leave the iron X-ray image unaffected. This was also true in the e.p. region when DPDS, ZDP and Lubrizol 1395 were used as additives. When DBDS and DTBDS additives were used the iron X-ray image was increasingly affected by the sulphur as the load was increased. Figures 5.7 (a), (b) and (c) show that the highest concentrations of sulphur are associated with decreases in the iron X-ray intensities. The highest concentrations of sulphur detected (31% weight) suggest that a thick film of FeS (36.5% weight sulphur) has been formed in these areas and is consistent with the X-ray diffraction results.

From the quantitative electron probe analyses (Figures 5.8 to 5.13) the amount of sulphur detected in the scars decreases to a minimum at and after initial seizure. Also the sulphur that is observed at initial seizure is concentrated in the pitted areas (Figures 5.4(a) and 5.4(c)) and not the load bearing areas. Figures 5.1(a) and 5.1(c) show that, in the a.w. region, the sulphur is concentrated mainly in the load bearing areas, note the dark lines across the sulphur X-ray image where polishing scratches cross the scar. Similarly, Figures 5.5(a) and 5.5(c) show the same effect in the e.p. region. This indicates that at initial seizure the additive is not providing good protection to the rubbing surfaces. This is consistent with the hypothesis that there are two distinct modes of action of these sulphur additives under the a.w. and e.p. conditions. When the transition from the a.w. mode occurs there is a range of loads at and above initial seizure where neither mechanism gives adequate protection to the rubbing surfaces. The increasing amounts of sulphur detected when DBDS and DTBDS show that the e.p. mode of action is functioning, whereas the very limited amount of

sulphur detected in the e.p. region when DPDS was used suggests that the e.p. activity of DPDS is too slow to give good protection.

When ZDP and Lubrizol 1395 were used as additives the distribution of the elements in the a.w., and to a lesser extent in the e.p. region, showed that zinc and phosphorus were always closely associated spatially. The sulphur distributions were different and more localised than zinc and phosphorus in both regimes. The three elements were mostly restricted to the load bearing areas of the scars in the e.p. region and not in the torn, welded areas. The atomic ratios (Tables 5.3 and 5.4) show that the trend is for the sulphur to increase with increasing load relative to the zinc content, while the phosphorus decreases with increasing load.

In the E.P.M.A. results of Allum and Forbes (28) they also detected increasing amounts of sulphur with increasing load in the e.p. region for a series of disulphides. They infer that the oxygen content (by the difference method) decreases with increasing sulphur content whereas in these analyses the difference, which as they state can be oxygen and carbon, varies considerably from point to point within one scar and with load. The general trend is for the difference (oxygen and carbon) to increase slightly at the highest loads but no great weight can be placed on the accuracy of the oxygen and carbon contents because of the method used to obtain these results. The X-ray diffraction analyses of scars formed with DPDS as additive suggest that the main difference is in fact carbon as very intense Fe_3C lines were observed. Fe_3C does however only contain 7% by weight carbon compared to 28 and 30% by weight oxygen in Fe_3O_4 and $\alpha-Fe_2O_3$ respectively, thus there would be four times more Fe_3C than either of the oxides for the same weights of carbon and oxygen. When FeS, Fe_3C, Fe_3O_4 and $\alpha-Fe_2O_3$ were detected by X-ray diffraction with DBDS and DTBDS additives there was more oxygen than carbon as the difference (the sum of oxygen and carbon) was still approximately 8% by weight as measured by E.P.M.A. This is the same amount

detected when DPDS additive was used but now the oxide lines are clearly distinguished, the Fe_3C lines being much less intense than those observed with DPDS additive. Thus the main constituent found in the wear scars when DBDS and DTBDS additives were used was FeS, the oxides and carbide being minor constituents. No quantitative analysis of the X-ray diffraction patterns was attempted because the diffraction lines were fine and a large number of them on each pattern were faint. Micro-densitometer traces only gave reasonable peak intensities for a small number of lines, a considerable number were unresolved.

The quantitative E.P.M.A. results obtained with the zinc dithio-phosphate additives highlight the difficulty of looking at thin films where the quantities involved are very small leading to large statistical errors in the results. Forbes, Allum and Silver (29) show that in the a.w. region the average atomic ratios Zn:P:S are 1:1.9:0.3 for zinc di-4methyl pentyl dithiophosphate additive and in the e.p. region 1:2:2.2 showing that there is more sulphur compared to zinc in the e.p. region than the a.w. region. However, they indicate that the zinc, phosphorus and sulphur are accumulated in the pitted areas of the scars in the e.p. region whereas Figures 5.17 and 5.18 indicate that the elements are concentrated in the smooth tracked areas of the scar. Only around initial seizure were similar distributions obtained (Figure 5.15). It must be remembered that the concentrations were extremely low and that the chemical structures of the zinc dithiophosphates were different.

The similar zinc and phosphorus distributions indicate that possibly zinc phosphate and iron phosphate are adsorbed on the metal surface to form the load bearing film in the a.w. region, the small amount of sulphur playing only a minor role. The concentrations of sulphur (Figure 5.17(c)) on the load bearing areas of the scars and the increased ratio of sulphur suggest that the limited e.p. activity of the zinc dithiophosphates is due

to the presence of sulphur in the molecules.

Scanning electron microscopy reinforces the results so far discussed. The sulphur additives give smooth finely scored wear scars in the a.w. region and optically visible thin films. At initial seizure, there are noticeable differences in the scars formed with the sulphur additives when Risella 29 and HVI oils are used. The polar impurities in the HVI oil may give a limited protection in this region where neither a.w. nor e.p. modes of action of the sulphur additives are functioning adequately. In the e.p. region the surfaces formed with DBDS and DTBDS as additives are covered with thick reacted layers whereas with DPDS as additive a torn welded surface was observed with very little evidence for the presence of a reacted film. The reacted layers on the scars formed with DBDS and DTBDS are thick (2 to 4 μm) and crack across the direction of sliding before being removed from the surface as debris. This indicates that a brittle fracture mechanism may be operating and causing the break-up of the film. The load bearing areas are generally very smooth even on the scars formed with DPDS as additive. Using ZDP and Lubrizol 1395 additives the wear scars formed in the a.w. region are very smooth and are covered, particularly in the central region of the scar (Figure 6.14), by a dark film. In the e.p. region the scars are similar to those obtained with DPDS as additive showing that there has been very little e.p. activity.

Micro-indentation hardness testing of a range of rollers worn with the various lubricants showed that the surface hardness of the unworn part of the rollers was around 1000 V.P.N. (300 gm load) compared to 855 V.P.N. (30 Kgf load) for the normal hardness test. This difference shows that no direct comparison can be made between macro- and micro-indentation tests unless calibration procedures have been carried out. The hardness of the scars were all similar to or just below the unworn hardness except those formed in the e.p. region with DBDS and DTBDS additives. The hardness of

the unworn part of the rollers was also reduced to around 800 V.P.N. at the

highest loads while the hardness of the scar was down to 400 V.P.N. Mott (70)

quotes micro-indentation hardness values for pyrrhotite FeS, 214 V.P.N. and

for pyrites FeS_2, 840 to 1130 V.P.N. Pyrrhotite was identified in the wear

scars formed with DBDS and DTBDS as additives by X-ray diffraction and is

by far the softer of the two iron sulphides. The hardness of the worn

surfaces formed under e.p. conditions with DBDS and DTBDS additives can be

explained in terms of an iron sulphide layer.

The optical micrographs of taper sections reveal that for the scars

worn with DBDS and DTBDS additives in the e.p. region there were only thin

white layers formed under the scars compared to the thick layers observed

with DPDS, ZDP and Lubrizol 1395 additives. The hardness of the various

structures formed under the scars with DBDS and DTBDS additives showed that

the hardness increased from the surface downwards until the ordinary marten-

sitic hardness was reached (860 V.P.N.). With the other additives a thick

white layer was formed which was hardest immediately below the surface of

the scar. The white layer was supported on a softer layer of tempered

martensite. These results suggest that the good e.p. film does not allow

the metal to get as hot as the metal in the poor e.p. case and consequently

a hard white layer is not allowed to form. If a thick white layer has

formed an e.p. additive is less likely to function adequately as this layer

is hard and unreactive.

8.2 Discussion of the Mode of E.P. Action of the Disulphides

Having compared the results of the present work, where possible,

with other published research, the mechanisms of action of the additives in

the e.p. region have to be explained. To explain the results the mode of

action in the a.w. region must be considered first. With the disulphide

additives a visible film containing sulphur is formed and is sufficiently

thin to leave the iron X-ray image, obtained in the electron probe,
unaffected by the film. There is a decrease in the amount of sulphur at
initial seizure suggesting that the film has broken down and been removed.
This indicates that the film was not bound to the surface tightly enough to
withstand the severe conditions of temperature and load and in fact may
desorb at initial seizure. Davey and Edwards (36) suggest that initially
the disulphides are adsorbed on the surfaces and then form iron mercaptides.
Groszek (71) showed that in his adsorption tests disulphides adsorbed at a
greater rate on iron oxide than on pure iron. Sakurai, Ikeda and Okabe (26)
suggested that some iron sulphide was formed initially and that this had an
adsorption activity greater than iron oxide and consequently the disulphide
molecules can chemisorb more easily on the iron sulphide. Allum and Forbes
(40) hypothesised that scission of the sulphur - sulphur bond to form iron
mercaptides was the mechanism involved in the a.w. region. However, in a
later paper Forbes and Reid (41) modify this mechanism and state that the
scission of the sulphur - sulphur bond is not a prerequisite to explain the
differences in the a.w. properties of organic disulphides. They indicate
that the differences can be explained by the physical properties of the
film formed by adsorption of the disulphides onto the metal surface. It is
not possible to indicate the exact mechanisms involved in the light of the
present work but it is clear that the film is chemisorbed as the lack of
sulphur at initial seizure suggests that the film is removed very quickly
and has not formed an inorganic layer. Also at initial seizure a difference
due to the base oils is apparent whereas at all other loads no difference
due to base oil can be detected. This indicates that at initial seizure
the conditions change and a different mode of action is required. The polar
impurities and sulphur in the HVI oil gave a smoother less pitted surface
than when Risella 29 was used as the base oil. The pitting of the surface
at initial seizure may well be due to a fatigue mechanism. When a film

gives good protection the stresses produced at the asperities are spread through the film and distributed over a wider area. If, however, there is considerable metal to metal contact there will be higher stressing of the surfaces locally and concomitant thermal stressing which could lead to large areas cracking up and being removed.

Spikes (72) suggests that for DBDS additive in oil below 80°C there is no irreversible chemical action with steel, between 80 and 110°C there is a chemically adsorbed film, probably of iron mercaptide and above 110°C there is scission of the carbon - sulphur bond to form iron sulphide. This reaction is quite slow until a temperature of around 150°C is reached. This may explain the poor protection afforded at initial seizure where there is break-down of the adsorbed film and the formation of iron mercaptide and possibly iron sulphide. It is not until more severe conditions are reached that the temperature is sufficiently high for the reaction rate to increase so that a thick film of iron sulphide can be formed. The intermediate step between the onset of initial seizure and the e.p. region can be thought of as the region where adsorption of the molecules has failed, but the reaction rate for iron sulphide formation is still low and iron mercaptide, iron sulphide films are the load bearing layers. Once more severe conditions have been reached the e.p. activity of the disulphides is determined by the ease of scission of the carbon - sulphur bond to form iron sulphide. The order of increasing e.p. activity is the same as that observed by Allum and Ford (39), namely,

diphenyl $\ll$ di-tert-butyl $\leqslant$ dibenzyl
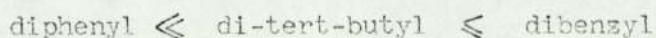
and follows the order of ease of scission of the carbon - sulphur bond.

The thick film formed by the two good disulphide e.p. additives (DBDS and DTBDS) consists of mainly iron sulphide and iron oxide with some iron carbide. Llopis et alia (37) has shown that oxygen enhances the rate of formation of iron sulphide from disulphides but suppresses the action of

mercaptans. This again supports the results that there is poor protection afforded at initial seizure and then increasing amounts of iron sulphide are produced in the e.p. region giving good protection.

Having formed these thick films of iron sulphide and iron oxide with the good e.p. additives, why do they afford good protection? Bowden and Tabor (73) say that only a solid film properly interferes with potentially damaging asperity contacts, whereas a liquid film allows high friction and wear. Godfrey (74) states that the important physical properties of the solid film lubricant are (a) melting point, (b) shear strength and (c) hardness, with adhesion, lack of cohesion and rates of formation as other major factors involved. Russell, Campbell, Burton and Ku (75) showed that there was a sudden increase in friction when the melting point of a number of hydrocarbons had been reached. Peterson (76) showed that for high temperature lubrication thermal softening is one of the predominant factors affecting failure. Thus a high melting point film is required for a good e.p. surface. Bowden and Tabor (77) proposed that the frictional force is given by

$$F = A \left\{ \alpha\, S_{metal} + (1 - \alpha)\, S_{lubricant} \right\}$$

where A = Area which supports the load; α = Fraction of A over which breakdown of the film occurs and S_{metal} and $S_{lubricant}$ are the shear strengths of the metal and lubricant junctions respectively. Thus a low shear strength film is required for low friction and low running temperature. Piggott and Wilman (78) used Fe_3O_4, $\alpha\text{-}Fe_2O_3$ and FeS films on mild steel discs lubricated with paraffin oil. They observed abrasive wear due to the relatively hard oxide and sulphide particles abrading the softer mild steel. Thus the hardness of the films has to be kept as low as possible to avoid abrasive wear. From the Handbook of Physics and Chemistry (79) the melting points of the following materials were obtained:

Material	Melting Point °C
FeS	1195
Fe_2O_3	1565
Fe_3O_4	1540

Godfrey (74) quotes shear strengths for the following materials as:

Material	Shear Strength Kgf/mm^2
FeS	20
Fe_2O_3	23
Steel	~90
FeS_2	23

Mott (70) gives the micro-indentation hardnesses of the following materials as:

Material	Hardness V.P.N.
FeS	214
Fe_2O_3	1100
Fe_3O_4	480
FeS_2	840 - 1130

The above properties show that for a film consisting mainly of iron sulphide with a measured hardness of 400 V.P.N., compared to 1000 V.P.N. for EN31 steel, the criteria that a good e.p. film has high melting point and moderately low shear strength and hardness have been fulfilled. Appeldoorn, Goldman and Tao (80) use the Pilling and Bedworth rule (81) that the integrity of a film is strongest if the volume quotient $\emptyset$ is the same as the metal from which the film was formed. They quote values of $\emptyset$ for the oxides of $\emptyset_{FeO}$ = 1.72, $\emptyset_{Fe_2O_3}$ = 2.15 and $\emptyset_{Fe_3O_4}$ = 2.1. They say that it would be expected from the values of $\emptyset$ that these oxides would be quite easily rubbed off, even under mild conditions. Hauffe (82) quotes a value for FeS of $\emptyset_{FeS}$ = 2.57 and thus the sulphide film would be less adherent than the oxide films. The cohesion between iron sulphide and iron is also much lower than between iron

and iron. Also the reaction rates are high at the high sliding temperatures occurring in the e.p. region. Tao (83) developed a mathematical model for oxidative wear. He used a parabolic rate law and predicted a higher rate constant and a lower activation energy for oxidation in corrosive wear than in static corrosion at the same 'hot spot' temperature. Stafford and Manifold (84) state that the formation of iron sulphide on iron was also a diffusion controlled process following a parabolic law. Fe cations diffuse many times faster than S anions in the FeS lattice. Indeed the rate of Fe cation diffusion is very high in the FeS lattice thus the rate of oxidation and sulphidation is enhanced by the presence of the iron sulphide. The oxides play a vital part in the load bearing film as instanced in the case of the mild dry wear of steels (85). The combination of FeS and Fe_3O_4 thus gives greater reaction rates and better load bearing properties than either one on their own. Because the formation of the film is an Fe cation diffusion process it might be expected that a porosity would develop at the iron - iron sulphide interface due to the greater rate of outward diffusion of the Fe cations compared to the inward diffusion of the S anions. The film may plastically deform back onto the retreating metal or form a void. Stafford and Manifold (84) show that a duplex scale is formed in their corrosion tests. The thick outer friable layer had a coarse grain structure (Figure 6.13 shows the worn film has this structure) and the thin inner layer a finely crystalline structure which was mechanically strong. The boundary between the two layers was the original iron surface. In the light of this evidence and that from the dry wear work of Quinn (86) a limiting film thickness can be hypothesised which was reached at the highest loads with DBDS and DTBDS as additives. The cracking across the direction of sliding would then be brittle fracture because of the lack of adhesion with the underlying metal. Also because of the friable or crumbly nature of the film the large blocks of debris that

broke off the surface would break up quickly to form small wear particles as
evidenced by the debris shown in Figure 6.10. Further the micro-indentation
tests did break the film up (Figure 6.12). Thus the criteria suggested by
Godfrey (74) for the functioning of a good e.p. film are satisfied by the
properties of the iron sulphide, iron oxide film formed in these 4-ball
tests with DBDS and DTBDS as additives. However, as Godfrey points out data
concerning the melting points, shear strengths and hardness values, need to
be obtained under high pressure, high shear rates and high temperatures before
a complete understanding of e.p. lubrication can be found.

When the data on the poor e.p. disulphide additive is examined the
explanations for the mode of action up to initial seizure load are the same
for the other disulphides but from there onwards the similarities end. Sato
and Sakurai (68) found no iron sulphide formed in their hot wire experiments
at a temperature of 490°C with DPDS and Forbes and Reid (41) with their
adsorption tests on iron powder found very little sulphur present on the
iron even after 24 hours at 150°C. They state that DPDS does not break down
via the scission of the carbon - sulphur bond and consequently has a very
low reaction rate with iron. Thus in the e.p. region there is no thick film
formed and welding or metal to metal contact occurs at relatively low loads.
Only Fe_3C was detected, other than α-Fe, by X-ray diffraction and small
amounts of sulphur using E.P.M.A. Taper sections reveal that a hard white
layer has been formed immediately below the surface of the wear scar. This
layer may be formed as a consequence of poor e.p. protection that leads to
high running temperatures and welding of the surfaces. However, once this
layer has been formed it may further inhibit the reaction which was taking
place and thus hasten the approach of final seizure.

8.3 Discussion of the Mode of Action of the Zinc Dithiophosphates

When the mode of action of zinc dialkyldithiophosphate additives in

the a.w. region is considered there is evidence to support a number of

mechanisms, none of which has been proved conclusively. The present work

does indicate that the zinc and phosphorus act together in some way possibly

forming an adsorbed zinc phosphate and / or phosphate layer on the iron

surface. The ratio of the elements Zn:P:S in the a.w. region was similar to

that obtained by Loeser et alia (25) and Allum et alia (29),namely that there

was a low sulphur ratio compared to the ratio of the elements in the original

additive molecule. The explanation of Barton et alia (55) that both

phosphorus and zinc containing polar impurities are preferentially adsorbed

on the worn surface to form the load bearing film is similar to the ideas

put forward for the mechanism of action of tricresyl phosphate. Barcroft

and Daniels (56), Beiber, Klaus and Tewksbury (57), and Forbes, Upsdell and

Battersby (58) all indicate that for tricresyl phosphate additive, the

additive molecule decomposes on the metal surface to give acid phosphates;

these may further decompose to give inorganic metal salts. Similarly,

Barton et alia proposed that the polar impurities in zinc dithiophosphate are

preferentially adsorbed on the surface and asperity contacts then produce

high temperatures and chemical action with the bearing metal takes place to

produce a metal phosphate surface film. This hypothesis does not explain

why the pure ZDP additive, which has very few polar impurities, behaves in a

similar manner to Lubrizol 1395, which does have polar impurities, in these

tests. Furey (45) suggested that varnish or lacquer deposits containing

physically or chemically bound phosphorus could be formed on the load-bearing

areas when zinc dithiophosphate additives were used. Feng et alia (51)

proposed that a polymer was produced from zinc dithiophosphates with structure

$$\left[\begin{array}{c} O \\ \parallel \\ - P - S - Zn - S - P - S \\ \mid \\ OR \end{array} \quad \begin{array}{c} O \\ \parallel \\ \\ \mid \\ OR \end{array} \right]_n$$
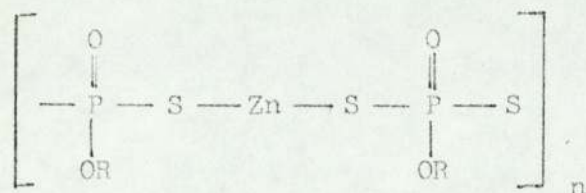
Gallopoulos (50) throws doubt on the actual mechanism of formation of the polymer proposed by Feng but Sakurai and Sato (68), in their "hot-wire" experiments found evidence for the formation of a polymer product. The atomic ratios of Zn:P:S are 1:2:3 in the polymer which goes some way towards explaining the low concentrations of sulphur found by Loeser et alia (25) and Allum et alia (29). The Scanning Electron Microscope prints (Figures 6.14 and 6.15) show a thick dark film, the blackness being attributable to low atomic number elements. This film has the appearance of a varnish or lacquer and further reinforces the idea that polymers are produced in the a.w. region with zinc dithiophosphate additives.

After initial seizure very small amounts of the three elements zinc, phosphorus and sulphur were found on the load bearing regions. Loeser et alia (25) found metal sulphides, using sulphur printing, in localised high pressure areas of the worn specimens used in his tests. Forbes (87) considered that metal dithiophosphates act primarily as a.w. additives with moderate e.p. activity due to the presence of sulphur atoms in the zinc dithiophosphate molecule. Table 8.2 supports this idea as the final seizure loads for all the zinc dithiophosphates listed are similar showing that the various structures of the molecules have very little effect on the e.p. performances. Streaks of sulphur found in the load bearing regions of the wear scars support this idea that it is primarily the sulphur in the additive that gives the e.p. activity. The small amounts of zinc, phosphorus and sulphur in the load bearing region may mean that to a limited extent the additive was able to act as a boundary lubricant once a sufficiently large scar had been formed. The type of surface formed in the e.p. region with the zinc dithiophosphate additives was very similar to that formed with DPDS as additive. Also the taper sections showed that the same structures were formed under the scars. The thick white layer could have the same

effect as stated for e.p. activity of DPDS additive, that is to further reduce the limited activity that was taking place.

8.4 Areas for Future Work

From the discussion of the results obtained in this thesis there are several areas where further work would be useful. These areas fall into two broad groups, physical properties of the films and the chemical mode of formation of these films. The actual physical properties of the films formed under rubbing e.p. conditions of high pressure, shear rate and temperature, rather than static test data, are important in learning what exactly happens during the sliding process. E.S.C.A. has a great potential in obtaining understanding about the chemical environment of the elements detected. The role of oxygen, and to a lesser extent carbon, in the sliding process needs further consideration. An electron probe microanalyser that can detect the very light elements such as oxygen and carbon will shed light on the relative abundance of oxides and carbides and their positions relative to the load bearing surface. Metallographic studies of the structures formed under worn surfaces would help understand the interaction of the lubricant with the metal and the sorts of temperatures involved in the sliding process.

8.5 Conclusions

The following conclusions can be drawn from the work presented.

(i)   There is no difference in the results due to the type of base oil except at initial seizure when the sulphur additives are used. Then the HVI oil affords slightly better protection.

(ii) The disulphides form adsorbed films in the a.w. region.

(iii) At initial seizure this mode of action fails and there is no

really effective lubrication.

(iv) The e.p. activity of the disulphides follows the order of the ease of scission of the carbon - sulphur bond, namely

diphenyl $\ll$ di-tert-butyl $\leqslant$ dibenzyl

(v) The good e.p. additives (DBDS and DTBDS) form thick solid iron sulphide films (with a small amount of oxide) which are relatively soft and sit on a softened metal substrate.

(vi) These good e.p. films have the properties required for e.p. lubrication.

(vii) The poor e.p. sulphur additive (DPDS) does not form a thick film and welds at a low load.

(viii) There is very little sulphur in this film and it is hard and sits on a thick, hard, unreactive metal substrate.

(ix) The zinc dithiophosphate additives are extremely good a.w. additives and possibly form a polymer on the worn surface.

(x) The zinc dithiophosphates are poor e.p. additives and do not form a thick film under e.p. conditions.

(xi) Their e.p. activity is due to the sulphur in the additive molecule.

(xii) The scars formed in the e.p. region are similar to those formed with DPDS additive and the substrate has the same structure, namely a thick white layer.

ACKNOWLEDGEMENTS

A P P E N D I X

The work presented in this section consists of a report on the research carried out at Shell Research Limited, Thornton, Cheshire, during the summer of 1972 as part of the C.A.P.S. Studentship.

Introduction

This research was carried out as a basic study of the action of some oils on the wear of two bronzes, lead and phosphor, worn against steel. The wear tests were conducted on a 4-ball machine and using "Physical Methods of Analysis" on the worn surfaces, an understanding of the inter-actions that occurred during sliding can be obtained.

Experimental Procedure

The basic experiments were carried out on a Stanhope 4-Ball Machine. The ball pot assembly was modified to take three 0.25 x 0.25 inch bronze rollers, against which the top steel ball was rotated. The bronze rollers were clamped in position when the locking nut was tigtened, forcing the cone against the sides of the bronze rollers (see Chapter 2).

Loads up to 500 Kgf were applied in all the tests and the coefficient of friction measured. The tests were of one minute duration, the top ball rotating at 1500 revolutions per minute.

Both balls and rollers were cleaned in a vapour bath of SBP 2 before and after each test and the specimens stored in a desiccator.

Materials

The upper ball was of EN31 steel. The two bronzes used for the lower rollers were:-

Phosphor Bronze BS369
(94.5% Cu; 5.25% Sn; 0.1% P)

Lead Bronze LB1

(8-10% Sn; 13-17% Pb; Balance Cu).

The flat ends of the rollers were machined with a diamond tool to give a surface finish of the order of 15 microinches c.l.a.

The following oils were used:- Risella 29 (SPL 758/70)

HVI   (SPL 77/65)

plus the following additives at a concentration of 1% by weight:-

Dibenzyl Disulphide (DBDS)

Lubrizol 1395 (SPL 122/77)

Tritolyl Phosphate (TTP)   (SPL 768/71)

Two fully formulated oils were also tested.

Theory

An estimate of the Hertzian diameter for a steel ball on a bronze flat

Radius of Hertzian contact 'a' $= \sqrt[3]{\dfrac{3\pi P}{4} \cdot \dfrac{(K_1 + K_2) \cdot R_1 R_2}{R_1 + R_2}}$

where $K_i = \dfrac{(1 - \nu_i^2)}{\pi E_i}$ $\left.\begin{array}{l} \nu_{steel} = 0.30 \\ \nu_{bronze} = 0.38 \end{array}\right\}$ Ref. A.1

$E_{steel} = 2.125 \times 10^4 \ Kg/mm^2$

$E_{p.b.} = 1.125 \times 10^4 \ Kg/mm^2$

$E_{l.b.} = 0.914 \times 10^4 \ Kg/mm^2$

$R_{steel} = 6.35 \ mm$

$R_{bronze} = \infty$

$P = $ the normal load at each of the three contacts, and

$P = 0.4082 \ W$, where W is the applied load.

Diameter of contact $= 2a = \sqrt[3]{\dfrac{3\pi}{4} \ 0.4082 \ W. (K_1 + K_2) \ R_{steel}} \ \times 2.$

$$\underline{\text{Diameter}_{p.b.} = 0.123 \, W^{1/3} \, \text{mm}} \quad (\text{W in Kgf}) \quad (\text{p.b.} = \text{Phosphor Bronze})$$

$$\underline{\text{Diameter}_{l.b.} = 0.129 \, W^{1/3} \, \text{mm}} \quad (\text{W in Kgf}) \quad (\text{l.b.} = \text{Lead Bronze})$$

<u>An estimate of the maximum Hertzian pressure q_o</u>

$$q_o = \frac{3P}{2\pi a^2} = \frac{3P}{2\pi} \left(\frac{4}{3\pi P (K_B + K_S) R_{steel}} \right)^{2/3}$$

$$\underline{(q_o)_{\text{Phosphor Bronze}} = 51.75 \, W^{1/3} \, \text{Kg/mm}^2} \quad (\text{W in Kgf})$$

$$\underline{(q_o)_{\text{Lead Bronze}} = 47.21 \, W^{1/3} \, \text{Kg/mm}^2} \quad (\text{W in Kgf})$$

(The Mean Pressure $P = \frac{2}{3} q_o$ the maximum pressure).

<u>Results</u>

Figures A.1 to A.4 are plots of the load versus mean wear scar diameter plotted on a log - log scale for all the oils and the two bronzes.

Figure A.5 shows a typical friction versus time plot.
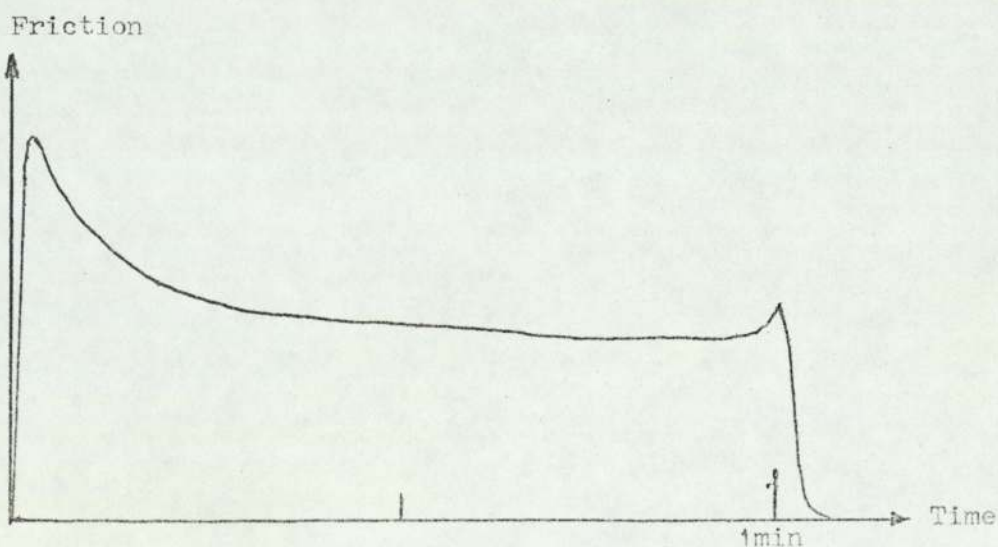
Fig. A.5
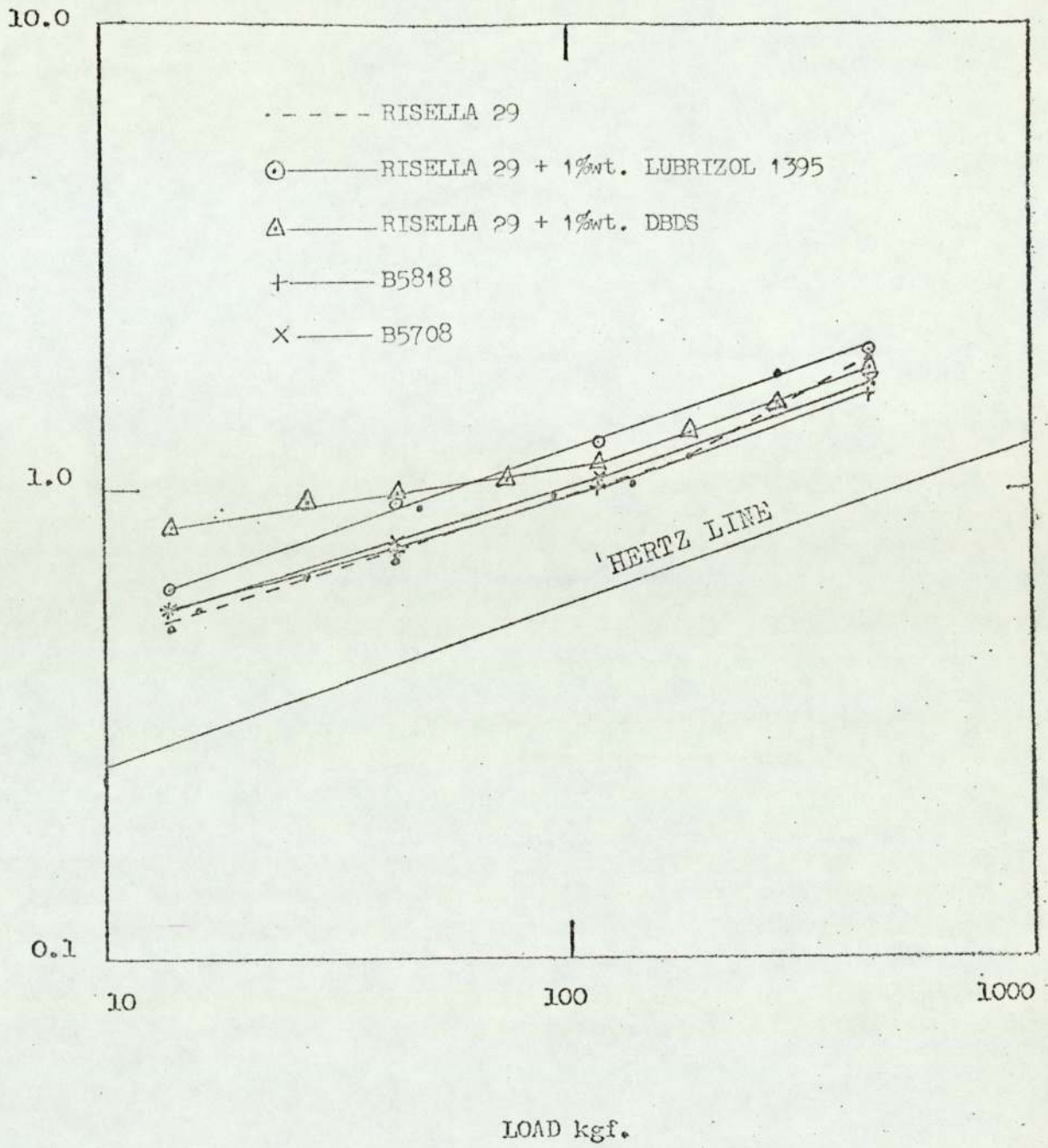
FIG. A.1

Load Versus Mean Wear Scar Diameter -

Phosphor Bronze Rollers
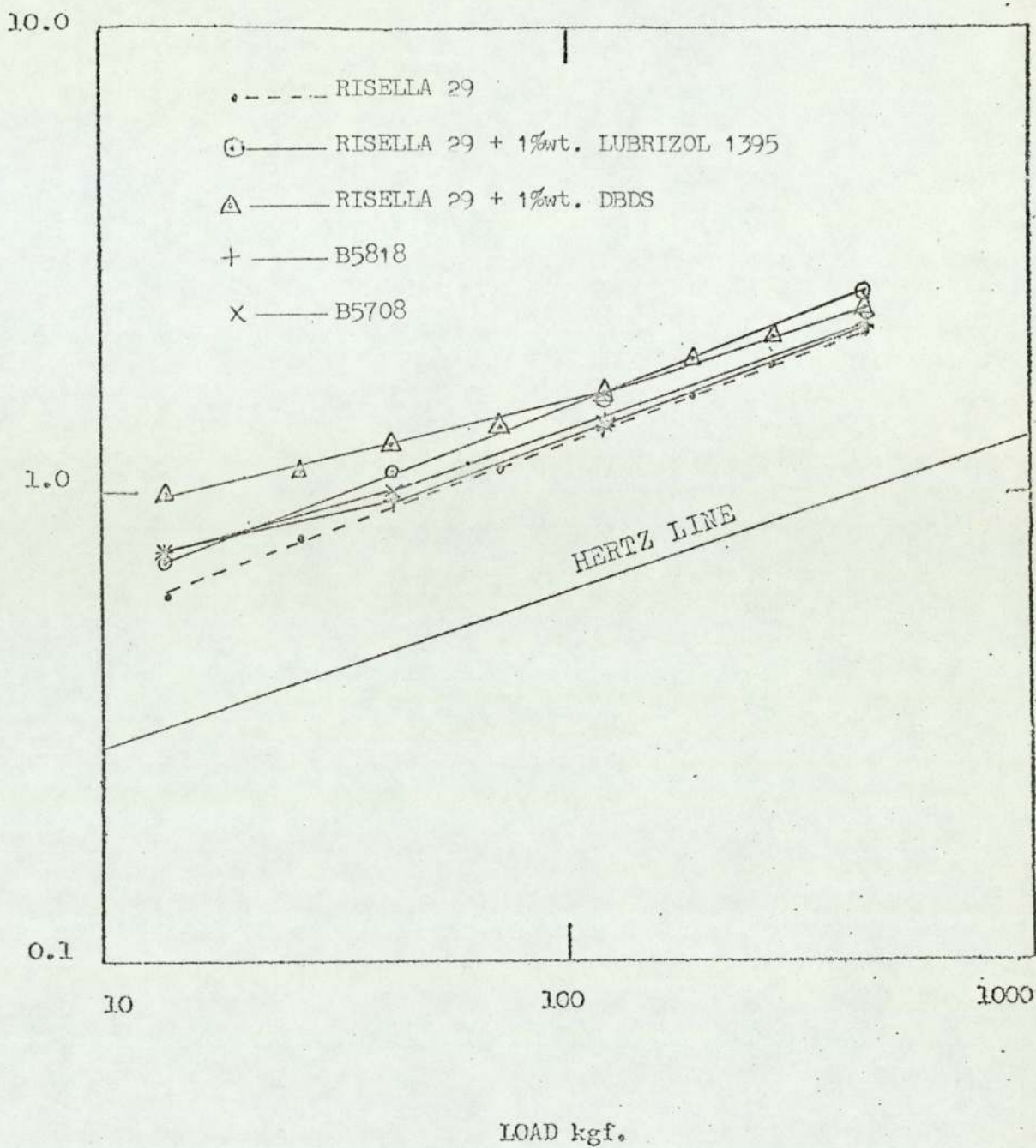
FIG. A.2

Load Versus Mean Wear Scar Diameter -

Lead Bronze Rollers

LOAD kgf.
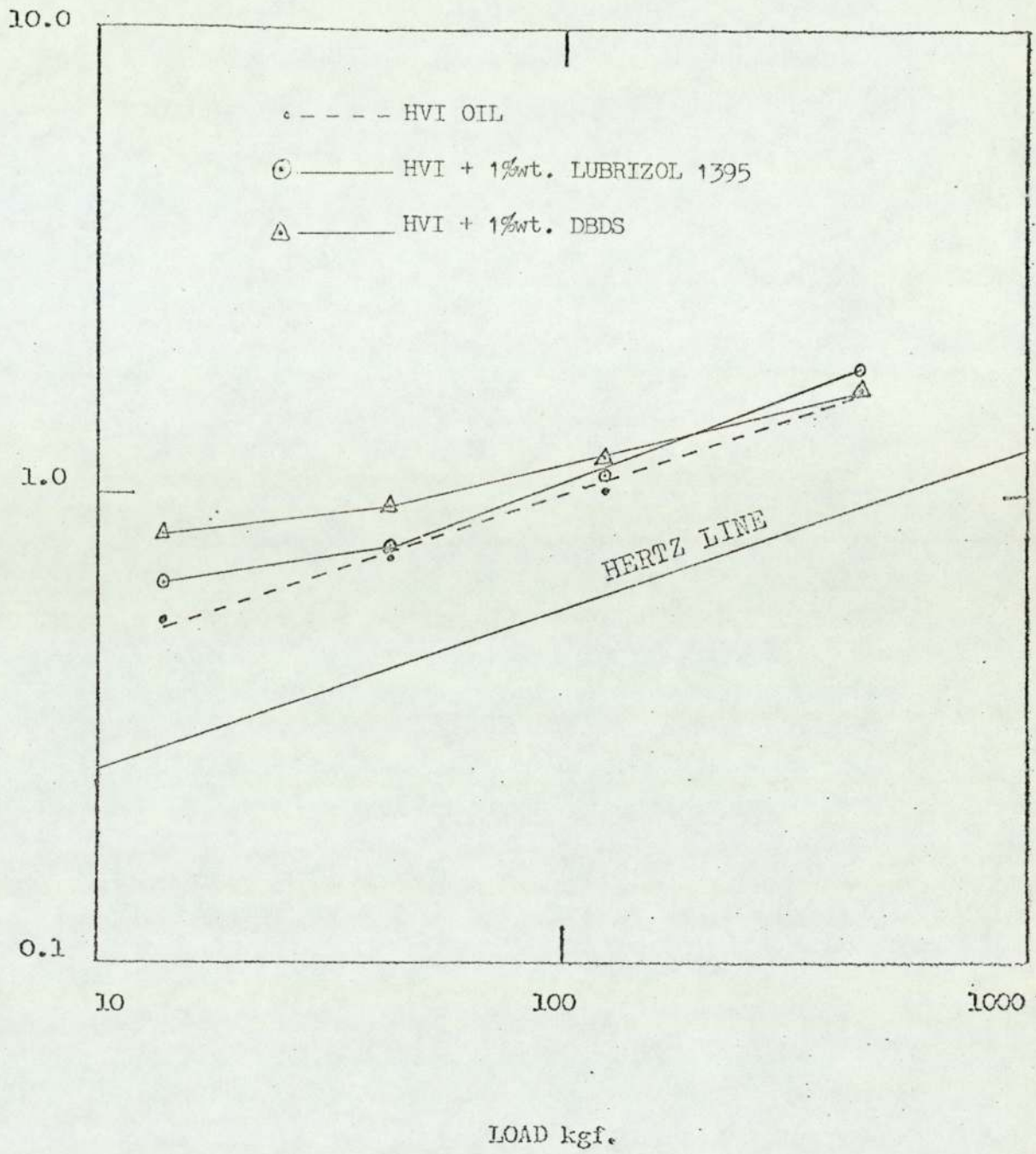
FIG. A.3

Load Versus Mean Wear Scar Diameter –
Phosphor Bronze Rollers
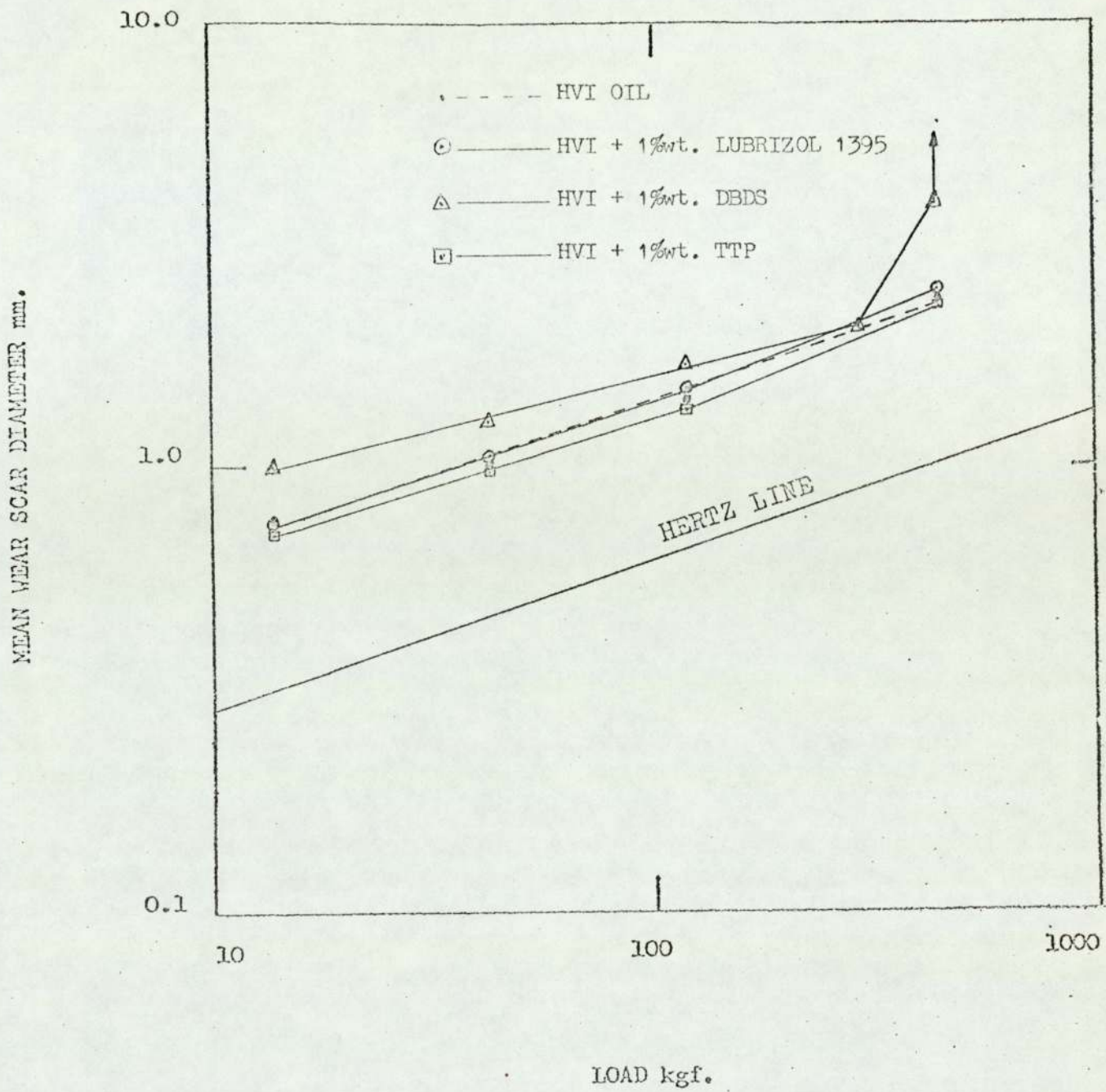
FIG. A.4

Load Versus Mean Wear Scar Diameter -

Lead Bronze Rollers

After the initial seizure the friction holds steady and decreases very slowly as the run proceeds. The friction increased slowly with load, starting at $\sim$0.02 at 14 Kgf and increasing to $\sim$0.08 at 500 Kgf for most tests. The coefficient of friction was calculated using the average value of the friction in the steady region.

The specimens obtained from the 4-ball tests were analysed using the following techniques:-

1. Optical Microscopy

2. Glancing Angle X-Ray Diffraction

3. Electron Probe Microanalysis (EPMA)

4. Scanning Electron Microscopy (SEM)

5. Electron Spectroscopy for Chemical Analysis (ESCA)

Optical Microscopy

Figure A.6 shows a cross-section of the phosphor bronze indicating a single phase structure. Figure A.7 shows a coarse grained lead bronze structure. Both prints are x 1000 magnification and are etched cross-sections through the wear scars, the section plane being parallel to the direction of sliding. Both micrographs show that the worn surfaces do not produce any marked deformation of the underlying bronze matrix. The surfaces are disturbed to a depth of a few micrometres only.

Depletion and deformation of the matrix only occurred in one case; namely lead bronze lubricated with HVI + 1% weight DBDS at a load of 500 Kgf. Figures A.8 and A.9 show cross-sections through the worn surface parallel to the direction of sliding. Figure A.8 shows the central area of the scar, where to a depth of the order of 100 micrometres the bronze has been depleted and deformed. The trailing edge of the wear scar is shown in Figure A.9. The dark grey areas are lead and above these, near the surface, a layer of copper is visible. The wear in this specimen was catastrophic and consequently
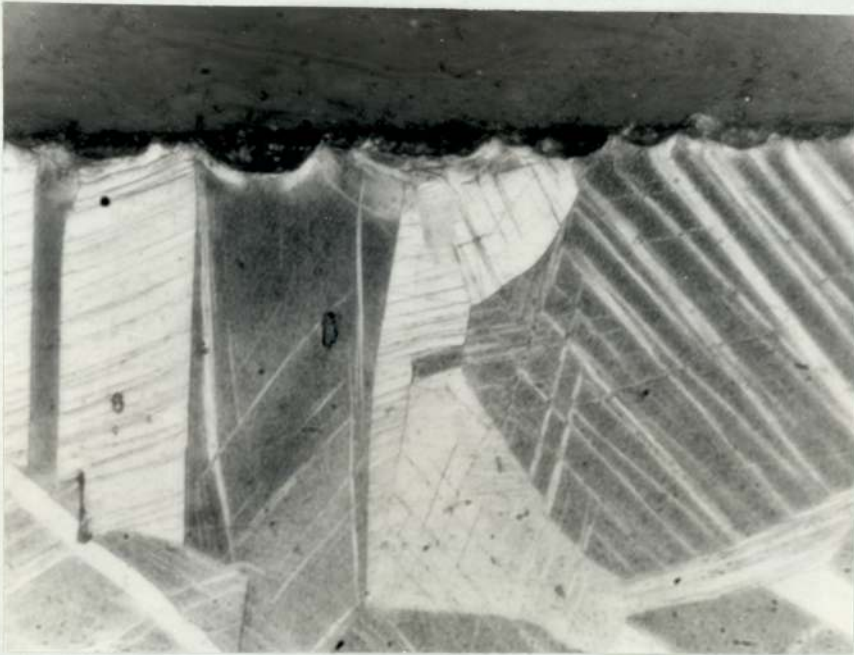
FIG. A.6

Worn surface.

Etched cross-section
of worn surface of
phosphor bronze roller
cut along the direction
of sliding.

LOAD : 315 Kgf

OIL : RISELLA 29

MAGNIFICATION : x 1000
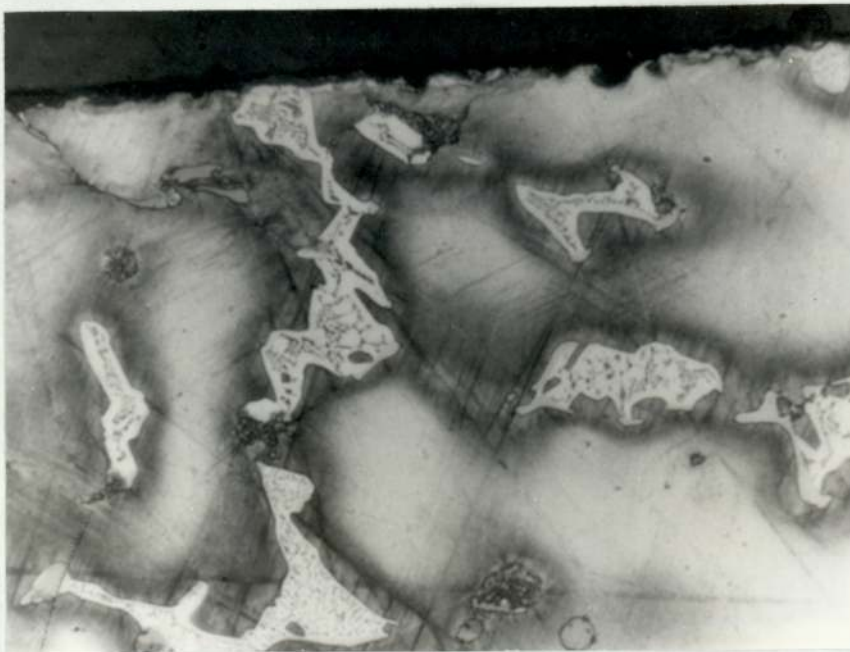
FIG. A.7

Worn surface.

Etched cross-section
of worn surface of
lead bronze roller
cut along the direction
of sliding.

LOAD : 14 Kgf

OIL : RISELLA 29

MAGNIFICATION : x 1000

◄─────── Worn surface.

Etched cross-section
of worn surface of
lead bronze roller
cut along the
direction of sliding.
LOAD: 500 Kgf
OIL: HVI + 1%wt. DBDS
MAGNIFICATION: x 500

◄─── sliding
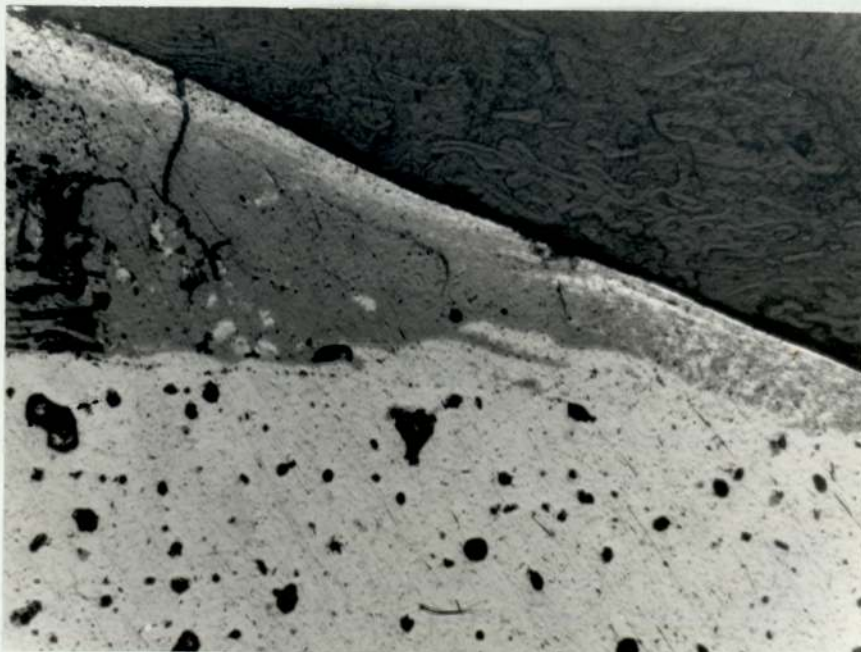
Etched cross-section
of worn surface of
lead bronze roller
cut along the directio
of sliding (trailing
edge).
LOAD::500 Kgf
OIL: HVI + 1%wt. DBDS
MAGNIFICATION: x 200

◄─── sliding

the temperatures at the surfaces were high enough to melt the bronze.

The surface of the wear scars have a thin overlay of material (Figure A.10), apart from a thin coating of oxide over all the surface, which is thickest in the centre of the scar. This overlay of material has a thickness of several micrometres at the higher loads.

Observations of the steel balls showed increasing amounts of bronze being smeared on the wear tracks as the load was raised (Figure A.11). In general there appeared to be more bronze smeared near the sides of the wear track than directly in the centre. Also, there was more transfer of leaded bronze than phosphor bronze.

Micro-hardness tests on the Vickers Microscope were inconclusive as the curvature of the wear scars reduced the accuracy of the measurements, thus giving a wide scatter to the results and no systematic variation of the hardness across the surface of the scars could be detected.

Glancing Angle X-Ray Diffraction

This technique gave very little information about the surfaces of the wear scars. Initially the whole face of the wear scar was irradiated using Cobalt radiation (Figure A.12). Only the lines associated with the bronzes appeared on the film. The exposure times were two to three hours using a one kilowatt tube and a Debye-Scherrer powder camera and using a 300 watt tube with a 3 cm diameter single crystal camera exposures up to 60 hours were used. In each case a one millimetre diameter collimator was used.

Some of the rollers were sectioned so that the X-ray beam could penetrate through the central area of the wear scars (Figure A.13). Looking through these cross-sections produced no further lines.

Another technique was to carefully scrape the surface of the wear scar and stick the material removed onto a fibre. The fibre was then placed
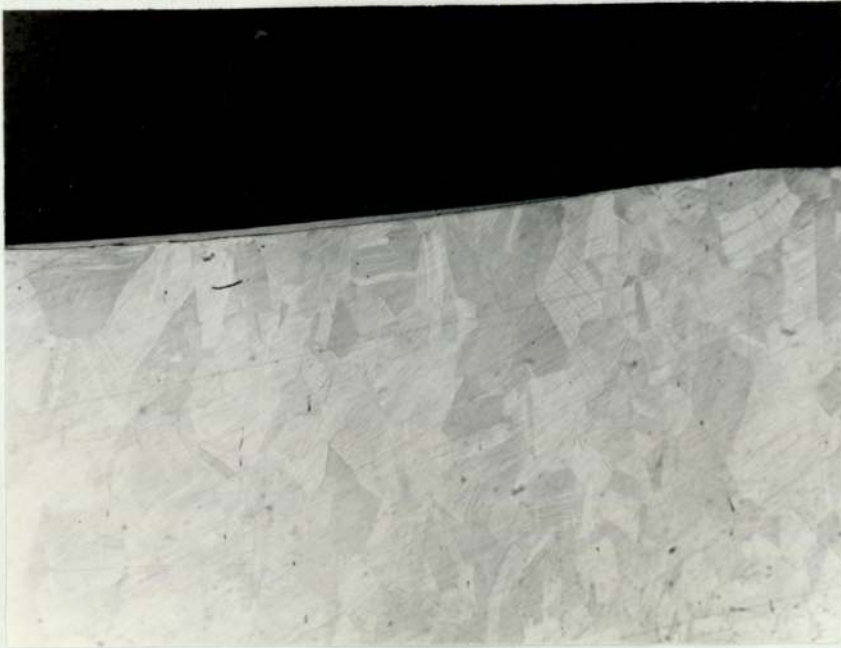
FIG. A.10

← —— Worn surface.

Etched cross-section of worn surface of phosphor bronze roller cut along the direction of sliding.

LOAD: 500 Kgf

OIL: RISELLA 29 + 1%wt. DBDS

MAGNIFICATION: x 100

sliding ——▶

FIG. A.11

Transfer of phosphor bronze to EN 31 steel ball.

LOAD: 500 Kgf

OIL: RISELLA 29 + 1%wt. DBDS

MAGNIFICATION: x 120

sliding

BRONZE ROLLER

WEAR SCAR

X-RAY

BEAM
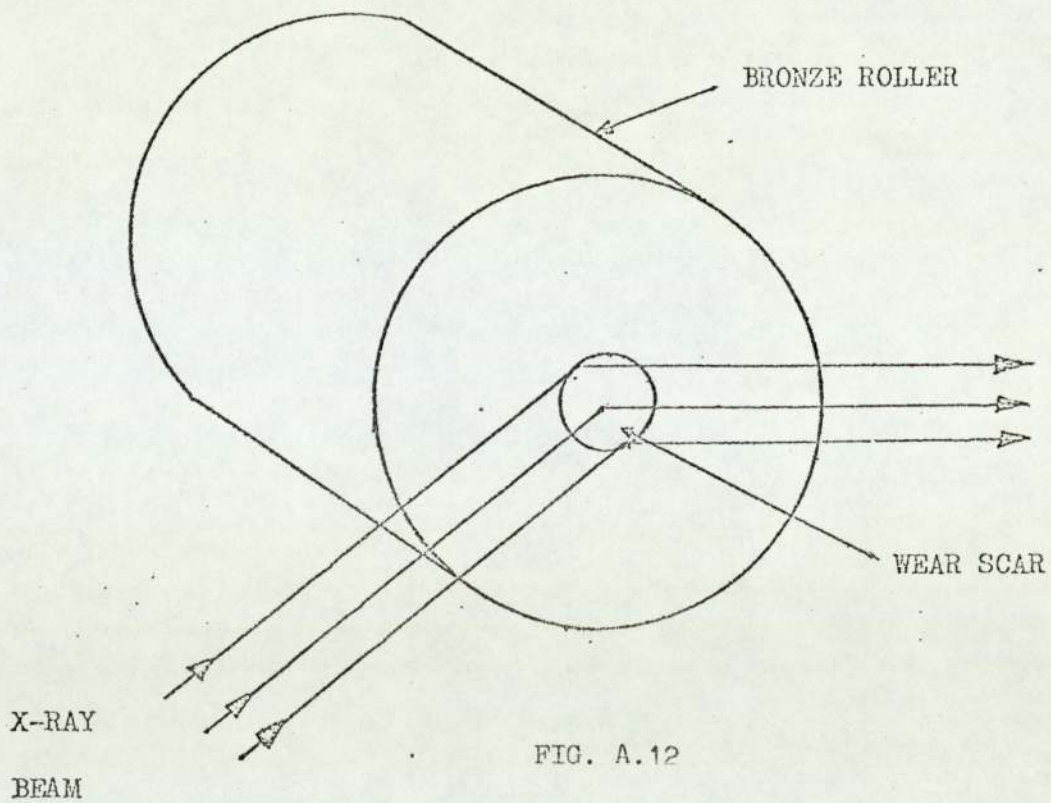
FIG. A.12

Glancing Angle X-Ray Diffraction From The Whole Face Of A Bronze Roller

SECTIONED BRONZE ROLLER

WEAR SCAR

X-RAY

BEAM
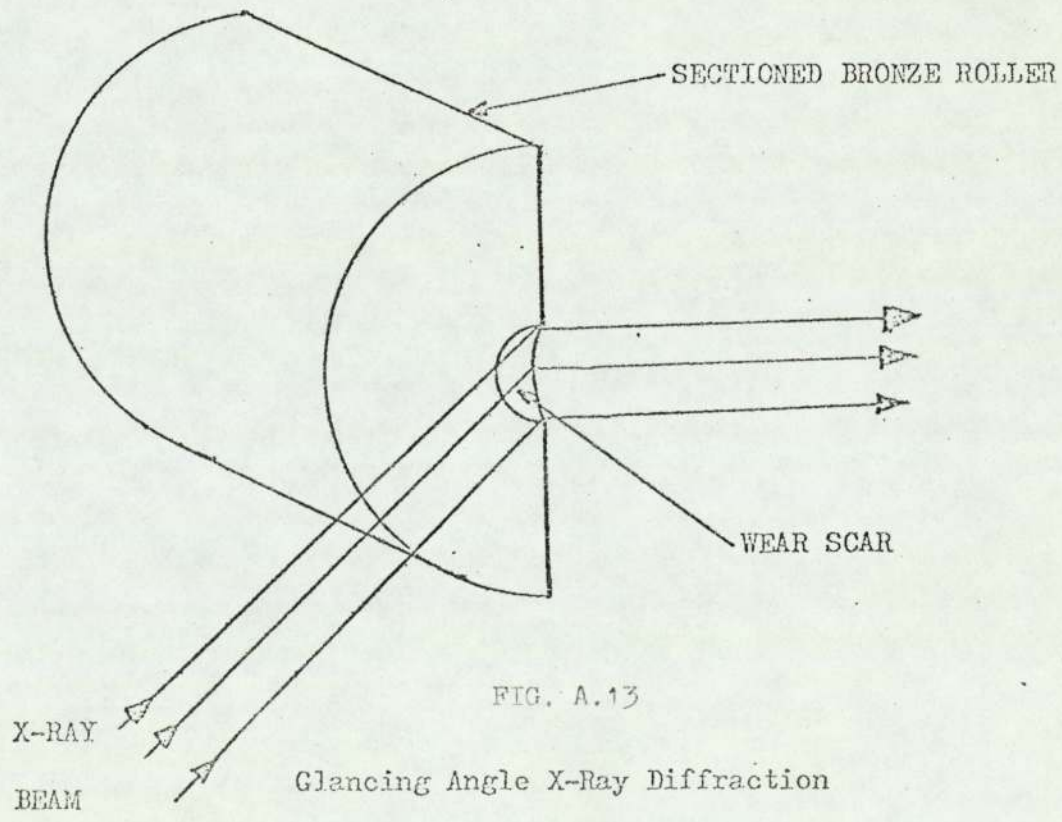
FIG. A.13

Glancing Angle X-Ray Diffraction

Through A Cross-Section Of A Wear Scar.

in a powder camera and rotated whilst being irradiated. Again only the
bronze lines were observed.

Glancing angle diffraction from the wear tracks of the steel balls
was attempted. The resultant patterns indicated the presence of iron (4 lines),
bronze (5 lines) and α-Fe_2O_3 (7 lines).

Black particles were observed in the oil when lead and phosphor
bronzes were run at loads of 14, 28, 77 and 126 Kgf in Risella 29 + 1% weight
DBDS as lubricant. These particles were centrifuged out of the oil and
stuck on a fibre and then irradiated in a powder camera. The resultant
pattern showed that these particles contained bronze and Copper Sulphide
$Cu_{1.96}S$.

Electron Probe Microanalysis

A range of specimens have been analysed using the electron probe
microanalyser. The quantities of the elements present in the surface layers
were quite small, up to about 5% by weight. Because of these low levels of
concentration, no systematic quantitative analysis was carried out on the
specimens.

Figure A.14 (a), (b) and (c) represent the electron, sulphur X-ray
and copper X-ray images respectively, of the trailing edge of the wear scar
on a phosphor bronze roller worn under a load of 500 Kgf with Risella 29 +
1% weight DBDS as lubricant. The area of high sulphur concentration on the
sulphur X-ray image appeared as a bluish-black rough area, when viewed under
an optical microscope, indicating that the area may be covered with copper
sulphide. Similar prints were obtained at loads of 45, 126 and 200 Kgf.
The quantity of each element present cannot be directly compared as the
count rates for each element are different for the same concentration, hence
the "whiteness" of the prints will be dissimilar for different elements even
if exposure time, specimen current, etc. are held constant. However, if the

(a) Electron image of
phosphor bronze roller
(trailing edge of scar).

Sliding Direction

(b) Sulphur X-ray image
of phosphor bronze roller.
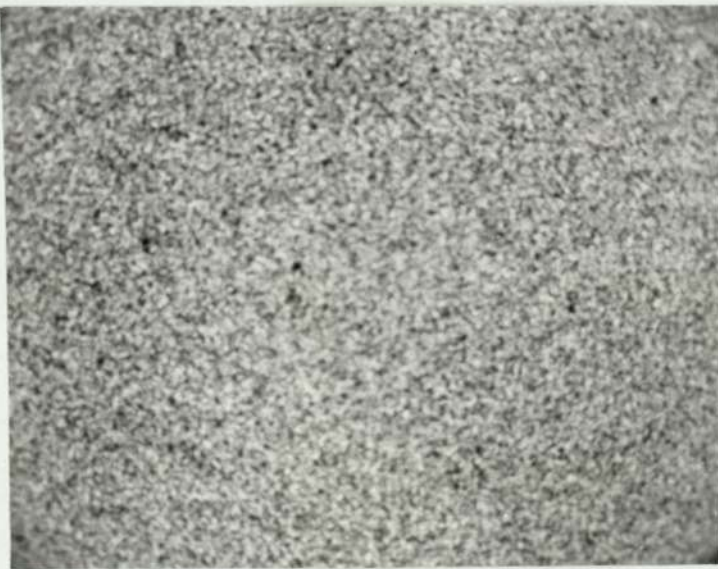
(c) Copper X-ray image of
phosphor bronze roller.

FIG. A.14   LUBRICANT: RISELLA 29 + 1%wt. DBDS

LOAD: 500 Kgf

MAGNIFICATION: x 200

exposure times, specimen current, etc. are held constant for a particular element then a good qualitative estimate of the variation in the concentration of an element with load can be obtained. Using the above and some spot counts, it was apparent that the quantity of sulphur on the surface of the wear scars increased with increasing load. A similar analysis was carried out on lead bronze rollers worn with HVI + 1% weight DBDS as lubricant and again the quantity of sulphur in the surfaces of the wear scars increased with increasing load.

Analysis of the lead bronze rollers worn with HVI + 1% weight TTP as lubricant did not show the presence of phosphorus in the scars at any load. The non-detection indicates that the quantity of phosphorus present is extremely small and if present at all, it is in the form of a thin film.

Figure A.15 (a), (b), (c), (d) and (e) represent the electron image and the sulphur, phosphorus, zinc and copper X-ray images respectively of the same area of the wear scar on a phosphor bronze roller worn under a load of 500 Kgf with Risella 29 + 1% weight Lubrizol 1395 as lubricant. As there is 0.1% phosphorus in the bronze, the phosphorus X-ray image does not give a reliable indication of the amount of phosphorus present in the surface film due to the phosphorus from the additive. The sulphur and zinc X-ray images show that they are present in the wear scar and in the debris. The quantities of zinc and sulphur varied considerably with load and with position on the wear scars. From the analysis it was not possible to establish whether the quantities of these elements varied consistently with load as in the case of dibenzyl disulphide additive.

Scanning Electron Microscopy

At low loads (up to 126 Kgf) smooth, finely scored scars were obtained for all the oils (Figure A.16) on both bronzes, but as the load was increased most of them exhibited a "tiled roof" effect around the edges of
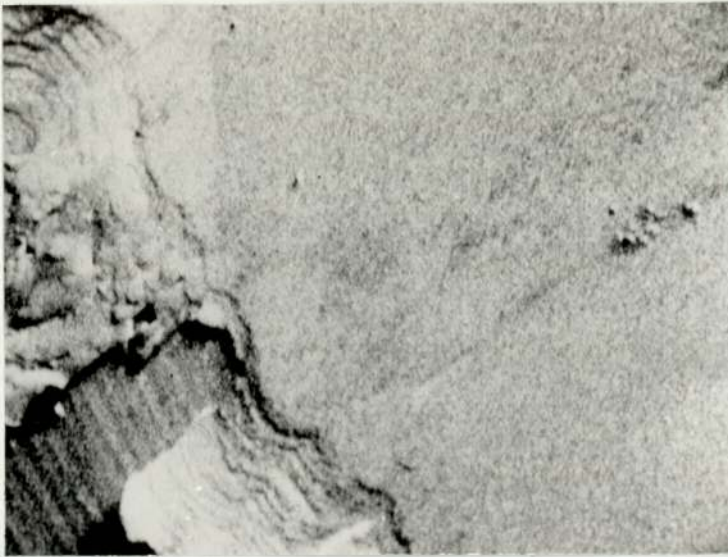
(a) Electron image of phosphor bronze roller (trailing edge of scar).

sliding direction
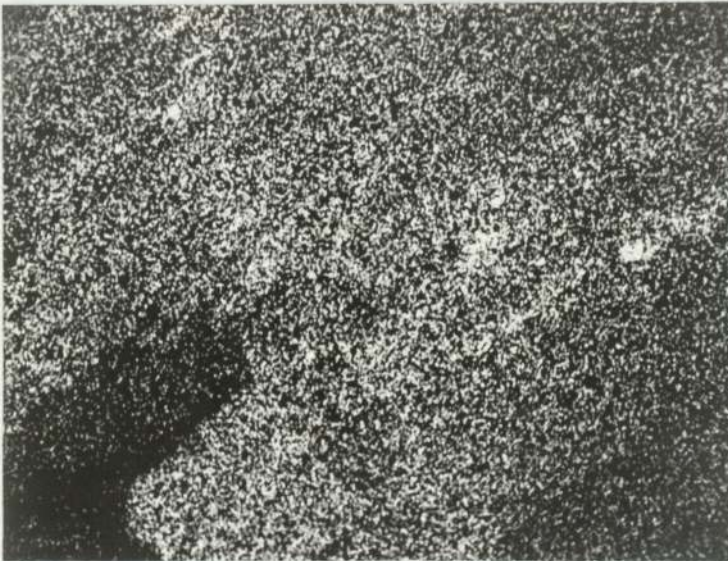
(b) Sulphur X-ray image

(c) Phosphorus X-ray image

FIG. A.15   LUBRICANT: RISELLA 29 + 1%wt. LUBRIZOL 1395

LOAD: 500 Kgf

MAGNIFICATION: x 200

(d) Zinc X-ray image

(e) Copper X-ray image

FIG. A.15

FIG. A.16

Scanning electron micrograph of a wear scar formed on a phosphor bronze roller.

LOAD: 50 Kgf

OIL: RISELLA 29

MAGNIFICATION: x 150

sliding

FIG. A.17

Scanning electron micrograph of part of a wear scar formed on a phosphor bronze roller.

LOAD: 315 Kgf

OIL: RISELLA 29

MAGNIFICATION: x 1.35K

sliding

the scars (Figure A.17). This effect is in the same direction on all parts of the scars where it is observed. The direction in which all this material appears to be squeezed is towards the centre of the holder, that is towards the axis of rotation. This can be explained if one considers the motion of the ball whilst rotating. As the bronze is worn away the ball moves down (Figure A.18) the face of the roller and the centre of the wear scar moves across the face of the roller towards the axis of rotation. This movement, if associated with the flow of the bronze, is in one direction only, hence the "tiled roof" effect in one direction.

From optical micrographs of cross-sections through wear scars, the centre of the scars at high loads (over 126 Kgf) appear to have rough over-lays of material. This was confirmed using the Stereoscan (Figure A.19), where the rough areas appear to be on top of the tracked region. This over-lay also appears less conducting (white areas on print) suggesting that it is not bound to the surface very firmly and / or that it contains oxides, sulphides, etc. which have been formed during sliding. There appears to be no satisfactory explanation for this phenomenon. It may be formed when the ball has stopped rotating at the end of the run, when material is transferred back to the bronze from the ball.

When dibenzyl disulphide was used as the additive the wear scars had a much more reacted, flaked appearance (Figure A.20) when compared to the scars obtained with the base oils and the other additives. This indicates that the sulphur has reacted readily with the bronze under extreme pressure conditions.

Electron Spectroscopy for Chemical Analysis

Two steel specimens were used in this preliminary study, one worn in Risella 29 + 1% weight Lubrizol 1395, and the other in Risella 29 + 1% weight DBDS. The surface of the rollers was masked off using aluminium foil,

BRONZE
ROLLER

EN 31 STEEL BALL

CENTRE OF

SCAR

CENTRE OF

SCAR

EN 31 STEEL BALL

HAS MOVED DOWN

DUE TO WEAR OF
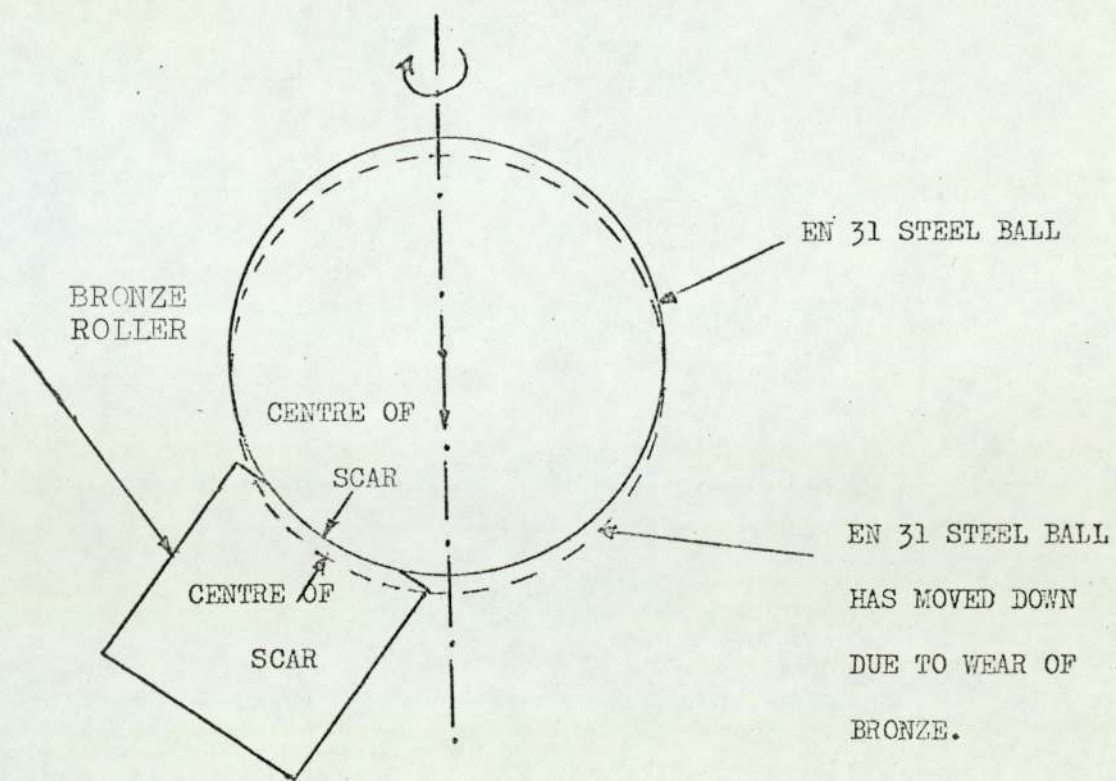
BRONZE.

FIG. A.18

Movement of the Centre of the Wear Scar down the Face
of the Roller as the Roller is worn away.
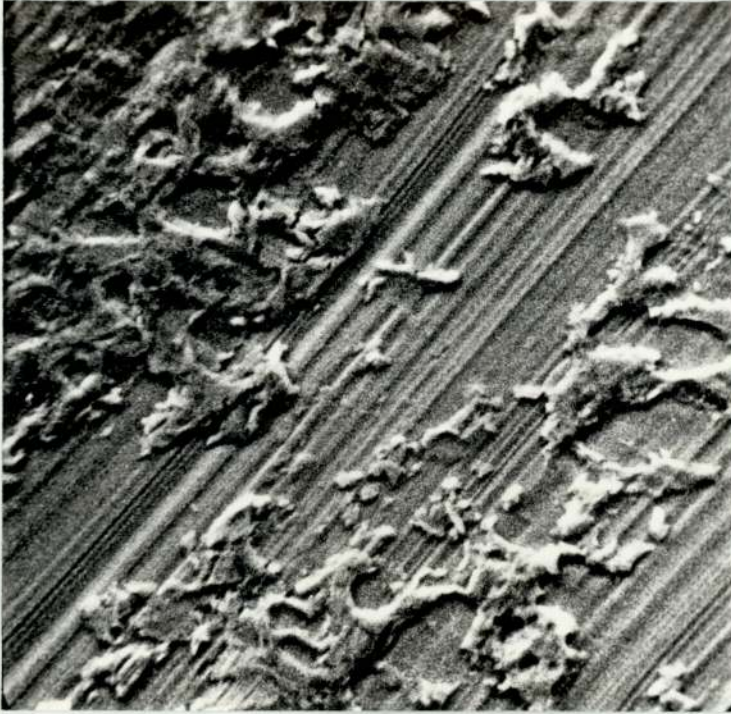
FIG. A.19

Scanning electron micrograph of part of a wear scar formed on a phosphor bronze roller.

LOAD: 500 Kgf

OIL: RISELLA 29 + 1%wt. LUBRIZOL 1395

MAGNIFICATION: x 650

sliding
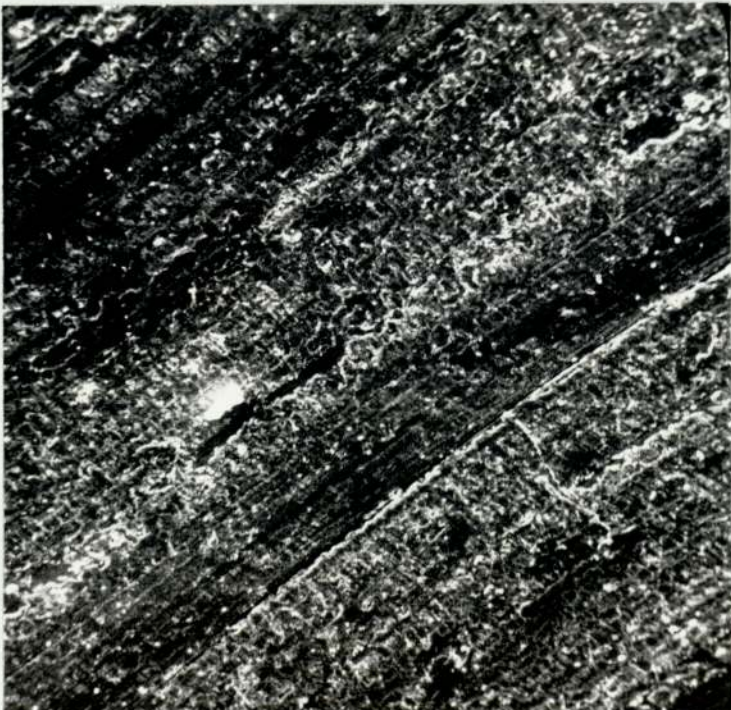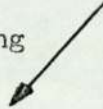
FIG. A.20

Scanning electron micrograph of part of a wear scar formed on a lead bronze roller.

LOAD: 500 Kgf

OIL: RISELLA 29 + 1%wt. DBDS

MAGNIFICATION: x 640

sliding

leaving only the wear scar exposed. Carbon, sulphur and oxygen peaks were found on the DBDS scar, the sulphur lines showing the presence of sulphide and sulphate components. Similarly, for the Lubrizol scar, carbon, sulphur, phosphorus and zinc were detected.

During a short visit to K/SLA with Mr. G.D. Galvin in August two specimens were examined using a Varian ESCA. A holder had been adapted to take the specimens. The first specimen had been heated in Risella 29 + 1% weight Lubrizol 1395 for two hours at 150°C. No iron peak was observed but zinc, sulphur and phosphorus were all detected indicating that the specimen was covered by a layer thicker than the X-rays could penetrate ($>$100 Å). The second specimen was a wear scar approximately 1.0mm in diameter on one face of the roller worn in Risella 29 + 1% weight Lubrizol 1395. The scar presented less than 1% of the irradiated area. Again, no iron peaks were detected but sulphur, phosphorus and zinc were all present. When the wear scar was blanked off approximately the same amount of zinc was found, indicating that the film covered the whole surface of the roller and not just the wear scar.

No examination of the bronze specimens was carried out in the time available, but this technique can be applied in the future.

Conclusions

A.W.J. de Gee et al. (A.2) found that there were critical loads for various bronzes and oils. Interpolating from his data to the 4-ball machine indicates that the anti-wear region will occur at loads below a few hundred grammes, hence all the tests were carried out in the extreme pressure region. From Figures 1 to 4 it is apparent that only DBDS additive gives appreciably greater wear scars than the base oils particularly at lower loads.

The slope of a number of the graphs of load versus mean wear scar diameter changes between 50 and 126 Kgf. One explanation for this could be

the difference in activation energies between monoclinic CuO ($\sim$20 Kcals) and cubic Cu_2O ($\sim$40 Kcals) when the transition temperature ($\sim$500°C) is reached (A.3).

There was very little deformation of the bulk material around the wear scars even at the highest loads used except in the one case (HVI + DBDS and lead bronze) where extreme deformation occurred. The amount of transfer of bronze to the steel balls was greater for the lead bronze than the phosphor bronze. A recent paper by Vaessen and de Gee (A.4) suggests that effective boundary films are formed on a thin transferred film of bronze on the steel, rather than on the steel itself. Also, the formation in the bronze of finely dispersed tin oxide particles is beneficial, surplus phosphorus inhibiting the formation of such particles.

X-ray diffraction indicates that if any surface films are formed, they are extremely thin. Copper sulphide was detected in the wear particles using DBDS as additive showing that some reactions had taken place.

Electron probe microanalysis of the surfaces indicates that both DBDS and Lubrizol 1395 reacted with the surfaces, whereas TTP did not appear to although this is not conclusive. The amount of sulphur in the wear scars for DBDS increased with increasing load, whereas no such pattern could be established for the Lubrizol 1395. Also very high concentrations of sulphur, when DBDS was used, were associated optically with blue-black areas which were most probably copper sulphide.

The Stereoscan pictures show that smooth wear scars are obtained at low loads (up to 126 Kgf) and at higher loads the centre of the wear scars have an overlay of material, which may be deposited, from the transferred material on the balls, at the end of the tests when the balls have stopped rotating and before the load is removed. Also the "tiled roof" effect can be explained in terms of the flow of bronze at extreme pressures at the centre

of the wear scar moves towards the axis of rotation.

Electron spectroscopy for chemical analysis can give valuable information about the surface elements and the chemical reactions that have taken place.

As a preliminary study of the wear of bronzes on steel using various oils and additives, the above conclusions show that the mechanisms involved are complex and further work is required to elucidate them.

References

A.1   Kempes Eng. Year Book, p.301

A.2   de Gee, A.W.J., Vaessen, G.H.G. and Begelinger, A.,
      A.S.L.E. Trans. 12, 1969, pp. 44-54

A.3   Kubaschevski and Hopkins, Oxidation of Metals and Alloys, p.89

A.4   Vaessen, G.H.G. and de Gee, A.W.J., A.S.L.E. Conference,
      New York, October 1972

Acknowledgements

Bibliography

1. NAYLOR, H., The Evolution of Engineering: Bearings and Lubrication. The Chartered Mechanical Engineer, December 1965, pp 642-649.

2. DA VINCI, LEONARDO, "Notebooks". Translated into English by E. MacCurdy, Jonathon Cape, London 1938.

3. AMONTONS, G., De la résistance causée dans les machines (Frictional resistance in machines), Acad. Roy. des Sci., Memoires de math. et de phys., 1699, pp 259-286.

4. NEWTON, I., Philosophiae naturalis principia mathematica (Mathematical principles of natural philosophy), Lib.11, Sec.IX, London, 1687.

5. COULOMB, C.A. de, Théorie des machines simples, en ayant égard au frottement de leur parties (Theory of simple machines, taking into account the friction of their parts), Acad. Roy. des Sci., Memoires de math. et de phys.,t.10, 1785, pp 161-332.

6. ADAMS, W.B., "Railway Axle Lubrication", Proc. Inst. Mech. Engrs., 1853, pp 57-60.

7. PETROFF, N., Friction in machines and the effect of the lubricant
    (a) In Russian: Eng. Jour., St. Petersb., 1883; No.1, pp 71-140; No.2, pp 228-279; No.3, pp 377-436; No.4, pp 535-564.
    (b) German trans. by L. Wurzel, Hamburg: L. Voss, 1887, p.187

8. TOWER, B., First report on friction experiments., Proc. Inst. Mech. Engrs., (a) 1883, pp 632-659; (b) 1884, pp 29-35.

9. REYNOLDS, O., On the theory of lubrication and its application to Mr. Beauchamp Tower's experiments, including an experimental determination of the viscosity of olive oil, (a) Phil. Trans. Roy. Soc., Vol.177, Pt.1, 1886, pp 157-234; (b) Papers on Mechanical and Physical Subjects, Macmillan, Vol.2, 1901, pp 228-310.

10. THURSTON, R.H., Friction and lubrication, New York, The Railroad Gazette, 1879, p.212.

11. KINGSBURY, A., Experiments on the friction of screws, Trans. A.S.M.E. Vol.17, 1895-6, pp 96-116.

12. KAPFF, S., Wertbestimmung von Schmierölen, besanders von Spindelölen, mit emem neuen Oelprüfer (Evaluation of lubricating oils, spindle oils in particular, with a new oil tester), Zeit. V.D.I., Bd.42, 1898, pp 553-558.

13. HARDY, W.B., Boundary conditions in lubrication, Dict. Applied Physics, Glazebrook, Vol.1, 1922, pp 572-579 (Macmillan).

14. MOUGEY, H.C. and ALMEN, J.O., Extreme pressure lubricants, Bull.A.P.I., Refining Div., December 1931, pp 76-94.

15. MURISON, C.A., Phil. Mag. 17, 1934, p 201.

16. CLARK, G.L., STERRETT, R.R. and LINCOLN, B.H., Industr. Engng. Chem. 28, 1936, p 1318.

17. GERMER, L.H. and STORKS, K.H., Phy. Rev. 55, 1939, p 648.

18. BEECK, O., GIVENS, J.W. and SMITH, A.E., On the mechanism of boundary lubrication: 1. The action of long-chain polar compounds, Proc. Roy. Soc., 1940, A177, pp 90-102.

19. FINCH, G.I. and SAHOORBUX, F.D., The study of wear and lubrication by electron diffraction, The Inst. Mech. Engrs., Vol.2, 1937, pp 295-301.

20. SIMARD, G.L., RUSSELL, H.W. and NELSON, H.R., Extreme Pressure Lubricants Film forming action of lead napthenate and free sulphur, Ind. Eng. Chem. Vol.33, 1941, pp 1352-1359.

21. GREENHILL, E.B., The lubrication of metals by compounds containing sulphur, J. Inst. Pet., Vol.34, 1948, p 659.

22. CLARK, G.L., GALLO, S.G. and LINCOLN, B.H., Radiosulfur Tracer Study of Sulfurized Lubrication Addition Agents, Journal of Applied Physics, Vol.14, 1943, pp 428-434.

23. BORSOFF, V.N. and WAGNER, C.D., Studies of formation and behaviour of an e.p. film, Lub. Eng., 1957, p.91.

24. LOESER, E.H., WIQUIST, R.C. and TWISS, S.P., Cam and tappet lubrication. III - Radioactive study of phosphorus in the e.p. film, Trans. ASLE, Vol.1, No.2, 1958, pp 329-35.

25. LOESER, E.H., WIQUIST, R.C. and TWISS, S.P., Cam and tappet lubrication. IV - Radioactive study of sulfur in the e.p. film, Trans. ASLE, Vol.2, 1959, pp 199-205.

26. SAKURAI, T., IKEDA, S. and OKABE, H., The mechanism of the reaction of sulphur compounds with steel surfaces during boundary lubrication using S^{35} as a tracer, Trans. ASLE, Vol.5, 1962, pp 67-74.

27. GODFREY, D., Chemical changes in steel surfaces during extreme pressure lubrication, Trans. ASLE, Vol.5, 1962, pp 57-66.

28. ALLUM, K.G. and FORBES, E.S., The load carrying mechanism of organic sulphur compounds - application of E.P.M.A., Trans. ASLE, Vol.11, 1968, pp 162-173.

29. FORBES, E.S., ALLUM, K.G. and SILVER, H.B., Load carrying properties of metal dialkyl dithiophosphates: application of electron probe micro-analysis, Proc. Instn. Mech. Engrs., Vol.183, Pt.3P, 1968-9, pp 35-49.

30. CZICHOS, H. and KIRSCHE, K., Investigations into film failure (transition point) of lubricated contacts, Wear, Vol.22, 1972, pp 321-33

31. QUINN, T.F.J. and WOOLLEY, J.L., The unlubricated wear of 3% Cr - $\frac{1}{2}$% Mo steel, Lubrication Engineering, September 1970, pp 312-321.

32. EVANS, E.A., Extreme pressure lubricants, The Inst. of Mech. Engrs., Vol.2, 1937, pp 55-59.

33. BEECK, O., GIVENS, J.W. and WILLIAMS, E.C., On the mechanism of boundary lubrication: II Wear prevention by additive agents, Proc. Roy. Soc., 1940, A177, pp 103-118.

34. PRUTTON, C.R., TURNBULL, D. and DLOUGHY, G., Mechanism of action of organic chlorine and sulphur compounds in extreme pressure lubrication, J. Inst. Pet., 32, 1946, p.90.

35. HAMILTON, L.A. and WOODS, W.W., Reaction of iron with organic sulphur compounds, Ind. and Eng. Chem., 42, 1950, p.513.

36. DAVEY, W. and EDWARDS, E.D., The extreme pressure lubricating properties of some sulphides and disulphides in mineral oil as assessed by the 4-ball machine, Wear, Vol.1, 1957, pp 291-309.

102

37. LLOPIS, J., GAMBOA, L., ARIZMENDI, L. and GOMEZ-MINANA, J.A.
Surface reactions of iron with hydrocarbon solutions of organic
sulphides, Corrosion Science, Pergamon Press Ltd., vol.4, 1964,
pp.27-49.

38. TOYOGUCHI, M., TAKAI, Y. and KATO, M. Reaction between iron and
sulfur compound with S-35 as a tracer, J. of Japan Petrol Inst.,
vol.2, 1960, pp.50-56.

39. ALLUM, K.G., and FORD, J.F. The influence of chemical structure on
the load carrying properties of certain organo-sulphur compounds,
J. Inst. Pet., 51, 1965, p.145.

40. ALLUM, K.G., and FORBES, E.S. The load carrying properties of
organic sulphur compounds. Influence of chemical structure on the
antiwear properties of organic disulphides. J. Inst. Pet., 53, 1967,
p.173.

41. FORBES, E.S. and REID, A.J.D. Liquid phase adsorption/reaction
studies of organo-sulphur compounds and their load carrying mechanism,
ASME/ASLE International Lubrication Conference, New York, 1972,
preprint no. 72LC-3C-1.

42. LOESER, E.H., TEAGUE, D.M., WILLSON, P.J. and TWISS, S.B. Cam and
Tappet test for lubricants. I - Antiscuff Evaluation, Lubrication
Engineering, vol. 13, no.4 April 1957, pp.191-6.

43. LOESER, E.H., TWISS, S.B. and TEAGUE, D.M. Cam and tappett test
for lubricants. II - Wear Evaluation, Lubrication Engineering
vol.13, No. 5, May 1957, pp.269-74.

44. LARSON, R.   The performance of zinc dithiophosphates as lubricating
     oil additives, Scientific Lubrication, August 1958, pp.12-19.

45. FUREY, M.J.   Film formation by an antiwear additive in an
     automotive engine, presented at ASLE-ASME Joint Lubrication Conference,
     Los Angeles, October 1958.

46. ANTLER, M.   Discussion of reference 45.

47. BENNETT, P.A.   A surface effect associated with the use of oils
     containing zinc dialkyl dithiophosphates, presented at ASLE-ASME
     Joint Lubrication Conference, Los Angeles, October 1958.

48. ASSEFF, P.A.   Discussion of reference 47.

49. FRANCIS, S.A. and ELLISON, A.H.   Reflection infra-red studies of
     zinc dialkyl dithiophosphate films adsorbed on metal surfaces, Journal
     of Chemical and Engineering Data, Vol.6, No.1, January 1961, pp.83-86.

50. GALLOPOULOS, N.E.   Thermal decomposition of metal dialkyldithiophosphate
     oil blends, presented at ASLE Lubrication Conference, Rochester,
     New York, October 1963.

51. FENG, I.M., PERILSTEIN, W.L. and ADAMS, M.R.   Solid film deposition
     and non-sacrificial boundary lubrication, ASLE-ASME Lubrication
     Conference, Pittsburgh, Pennsylvania, October 1962, Preprint No.62LC-11;
     and ASLE Trans. 6, 1963, pp.60-66.

52. ROWE, C.N. and DICKERT, J.J.   The relation of anti-wear function to
     thermal stability and structure for metal O, O-dialkylphosphorodithioates
     ASLE Trans. 10, 1967, pp.85-90.

53. ROWE, C.N.   The role of additive adsorption in the mitigation of wear, ASLE Trans. 13, 1969, pp.179-183.

54. ALLUM, K.G. and FORBES, E.S.   The load-carrying properties of metal dialkyl dithiophosphates: The effect of chemical structure, Proc. Instn. Mech. Engrs. Vol.183, Pt.3P, 1968-69, pp.7-14.

55. BARTON, D.B., KLAUS, E.E., TEWKESBURY, E.J. and STRANG, J.R. Preferential adsorption in the lubrication process of zinc dialkyl-dithiophosphate, ASME-ASLE International Lubrication Conference, New York, 1972, preprint No.72LC-3C-3.

56. BARCROFT, F.T. and DANIEL, S.G.   The action of neutral organic phosphates as e.p. additives, ASME Trans., September 1965, p.761.

57. BIEBER, H.E., KLAUS, E.E. and TEWKESBURY, E.J.   A study of TCP as an additive for boundary lubrication, ASLE Trans. 11, 1968, pp.155-161.

58. FORBES, E.S., UPSDELL, N.T. and BATTERSBY, J.   Current thoughts on the mechanism of action of tricresyl phosphate as a load-carrying additive, Inst. of Mech. Eng. Tribology Convention, Keele, September 1972.

59. AMERICAN SOCIETY FOR TESTING AND MATERIALS,   Designation D2783-69T.

60. INSTITUTE OF PETROLEUM,   Designation 239/69.

61. TIMOSHENKO, S. and GOODIER, J.N.   Theory of Elasticity, McGraw Hill, New York, 1951.

62. ISHERWOOD, B.J. and QUINN, T.F.J.   British Journal of Applied Physics, 18, 1968, p.717.

63. QUINN, T.F.J.   Journal of Physics, D, Applied Physics, Vol.3, 1970.

64. SALTER, W.J.M.   A manual of quantitative electron probe microanalysis, Structural Publications Ltd., London, 1970.

65. BIRKS, L.S.   Electron Probe Microanalysis, Interscience Publishers [a division of John Willey and Sons], New York/London, 1963, p.113.

66. SAVITSKIY, K.V. and KOGAN, Yu.I.   The nature of white layers. Fizika Metallov i Metallovedenie, Vol.15, No.5, 1963, pp.664-672.

67. DORINSON, A.   The additive action of some organic chlorides and sulphides in the four-ball lubricant test, ASME-ASLE International Lubrication Conference, New York 1972, preprint No.72LC-3C-2.

68. SAKURAI, T. and SATO, K.   Study of corrosivity and correlation between chemical reactivity and load-carrying capacity of oils containing e.p. agents, ASLE Trans. 9, 1966, pp.77-87.

69. BARCROFT, F.T.   A technique for investigating reactions between e.p. additives and metal surfaces at high temperatures, Wear 3, 1960, p.440.

70. MOTT, B.W.   Micro-indentation hardness testing, Butterworths Scientific Publications, London 1956.

71. GROSZEK, A.J.   Heats of preferential adsorption of boundary additives at iron oxide/liquid hydrocarbon interfaces, ASLE, Trans.13, 1970, pp.278-287.

72. SPIKES, H.A.   Physical and chemical adsorption in boundary lubrication, Ph.D Thesis, London 1972.

73. BOWDEN, F.P. and TABOR, D.   The friction and lubrication of solids, Oxford University Press, 1950, p.202.

74. GODFREY, D.   Boundary lubrication.   Interdisciplinary approach to friction and wear.   NASA.SP-181.

75. RUSSELL, J.A., CAMPBELL, W.E., BURTON, R.A. and KU, P.M.   Boundary lubrication behaviour of organic films at low temperatures, ASLE Trans. 8, 1965, p.48.

76. PETERSON, M.B.   High temperature lubrication.   Proc. International Symp. on Lubrication and Wear, D. Muster and B. Sternlicht, eds., McCutchan Publ. Corp., Berkeley, 1965, p.941.

77. BOWDEN, F.P. and TABOR, D.   The friction and lubrication of solids, Oxford University Press, 1950, p.222.

78. PIGGOTT, M.R. and WILMAN, A.   Nature of the wear and friction of mild steel on mild steel and the effect of surface oxide and sulphide layers, Proc. Conf. on Lubrication and Wear, Inst. Mech. Engrs., 1957, p.613.

79. HANDBOOK OF CHEMISTRY AND PHYSICS, 48TH EDITION, published by The Chemical Rubber Company, 1967, p.B-185.

80. APPELDOORN, J.K., GOLDMAN, I.B. and TAO, F.F.   Corrosive wear by atmospheric oxygen and moisture, ASLE Trans. 12, 1969, pp.140-150.

81. PILLING, N.B. and BEDWORTH, R.E.   J. Inst. Metals, 29, 1923, p.529.

82. HAUFFE, K.   Oxidation of Metals, Plenum Press, 1964, p.366.

83. TAO, F.F.   A study of oxidation phenomena in corrosive wear, ASLE Trans. 12, 1969, pp.97-105.

84. STAFFORD, K.N. and MANIFOLD, R.   The corrosion of Fe and some Fe-based alloys in S vapour at 500°C, Corrosion Science, Vol.9, 1969, pp.489-507.

85. QUINN, T.F.J.   Oxidational wear, Wear, 18, 1971, pp.413-419.

86. QUINN, T.F.J.   The dry wear of steel as revealed by electron microscopy and X-ray diffraction, Tribology Convention, Pitlochry, Scotland, 1968. Proc. Inst. Mech. Engrs. 182, (3N), 1967/68, pp.201-213.

87. FORBES, E.S.   Antiwear and extreme pressure additives for lubricants. Tribology, August 1970, pp.145-152.

C94/72 AN APPLICATION OF ELECTRON PROBE MICROANALYSIS AND X-RAY DIFFRACTION TO THE STUDY OF SURFACES WORN UNDER EXTREME PRESSURE LUBRICATION

R. C. COY*   T. F. J. QUINN*

Electron probe microanalysis and a glancing-angle, edge-irradiated X-ray diffraction film technique have been used to examine the topographies, compositions and structures formed in the surfaces of En 31 steel specimens which have been slid against each other under conditions of extreme pressure lubrication. Various sulphur and phosphorus compounds were used as additives in the lubricant.

1 INTRODUCTION

THIS PAPER describes some *preliminary investigations* into the mechanisms of extreme pressure lubrication using oils containing sulphur and phosphorus compounds as additives. Most of the specimens were kindly supplied by Mr E. S. Forbes (B.P. Research Centre, Sunbury-on-Thames). Each of these specimens had been one of the lower three balls in a typical four-ball test machine run for 1 min at a load beyond the initial seizure load for the particular lubricant and additive concentration, and at an angular speed of 1500 rev/min. A few specimens were produced under the same running conditions in the authors' laboratory on a modified version of the four-ball tester. In this modification the central ball was rotated against the flat ends of three roller bearings ($\frac{1}{4}$ in diameter and $\frac{1}{4}$ in long) held as shown in Fig. 94.1. This '1-ball-on-3-flats' geometry readily allows the wear scar to be viewed in the electron probe microanalyser without having to carry out the difficult task of cutting a very hard specimen into a suitable size.

Both types of specimen were analysed for the sulphur, phosphorus and iron distribution within the wear scar using the microanalyser. This instrument provides an 'electron picture' of the topography of the wear scar and a corresponding picture of the relative concentrations of the particular element in question within the same area as that covered by the 'electron picture'. Selected specimens were also examined with a glancing-angle, edge-irradiated X-ray diffraction film technique to determine some of the compounds present in the wear scars.

The results are discussed in terms of their relevance to current ideas regarding the mechanism of extreme pressure lubrication with additives containing sulphur and phosphorus compounds.

2 EXPERIMENTAL DETAILS

The lubricants used in these experiments were liquid paraffin to which 1 per cent by weight of the following compounds had been added:

Phosphorus additives

1. Cyclohexylammonium dibutyl phosphate (c.d.b.p.a.)
2. Dibutyl phosphite (d.b.p.i.)
3. Dibutyl phosphate (d.b.p.a.)
4. Tricresyl phosphate (t.c.p.)

Sulphur additives

5. Di-*n*-butyl disulphide (d.n.b.d.s.)
6. Diallyl disulphide (d.a.d.s.)
7. Dibenzyl disulphide (d.b.d.s.)

Electron probe microanalysis was carried out on the wear scar formed on one of the lower balls of the four-ball machine for each of the extreme pressure experiments with the above compounds as additives. A limited amount of analysis was also carried out on the wear scar formed on one of the flats used in the t.c.p. and d.b.d.s. additive experiments with the modified specimen geometry mentioned earlier. The analyser was set to detect X-rays originating from phosphorus, sulphur or iron in the specimens. Copper phosphide (Cu_3P), cadmium sulphide (CdS) and iron (Fe) were used as standard specimens for the quantitative analysis. 'X-ray pictures' were used to indicate areas of high concentration of these three elements in each of the wear scars, and spot analyses were then carried out in these regions.

The glancing-angle, edge-irradiated X-ray diffraction film technique [1]† is particularly relevant to the analysis of surface structures present in worn surfaces. It imposes no restrictions upon specimen geometries. With this technique, one must ensure that the general surface of the

† *References are given in Appendix 94.1.*

0·5 in dia.EN 31 ball

0·25 in×0·25 in EN 31 roller
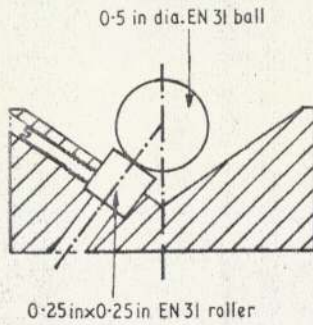
Fig. 94.1. The specially designed '1-ball-on-3-flats' modification of the normal four-ball machine

Wear scar   Diffraction line

Cylindrical film   Shadow edge

2θ

X-ray beam   Incident beam

20

0·5 in dia.EN 31 ball
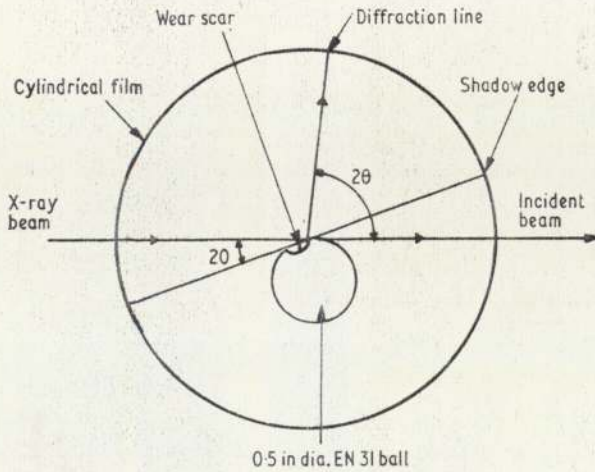
Fig. 94.2. Diagram of the irradiation geometry used for obtaining the glancing-angle, edge-irradiated X-ray diffraction patterns (wear scar size exaggerated for the sake of illustration)

wear scar lies at about 20° to the incident X-ray beam and that the *edge* of the wear scar is *exactly* in the centre of the cylindrical camera used to record the diffraction maxima. This is shown in Fig. 94.2. Provided one uses a fine collimator (say 0·5 mm diameter), a well-resolved diffraction pattern will be obtained. For example, Fig. 94.3 shows a typical pattern obtained by irradiating with X-rays the surface of a wear scar formed on one of the lower balls of the four-ball machine lubricated with the d.b.d.s. additive. The X-rays originated from a cobalt tube, and the exposure time was about 60 h.

3 RESULTS

3.1 Electron probe microanalysis

Analysis of the scars formed under extreme pressure conditions with c.d.b.p.a., d.b.p.i. and d.b.p.a. as additives, showed about 15, 5 and 5 per cent phosphorus respectively, while *no* phosphorus could be detected for the t.c.p. specimen. The amounts of iron in these four scars were 70, 80, 80 and 75 per cent respectively. The remainder, in each case, could possibly be oxygen, but the particular instrument used for this investigation is unable to detect such a low atomic number element. In the next section, it will be shown that this limitation can be overcome to some extent by the use of an X-ray diffraction technique to determine the *structure* of the surface compounds.

Analysis of the d.n.b.d.s., d.a.d.s. and d.b.d.s. additive specimens showed that sulphur concentrations of about 20 per cent were present in the surfaces formed under extreme pressure conditions. Fig. 94.4 is a typical example of a 'sulphur picture' (magnification ×150) obtained with the microanalyser set to scan the wear scar formed on one of the lower balls of the 'four-ball' geometry using d.a.d.s. as the additive. The bright streaks show the presence of

Fig. 94.3. Glancing-angle, edge-irradiated X-ray diffraction pattern from a surface worn under extreme pressure conditions with dibenzyl disulphide (d.b.d.s.) as the additive
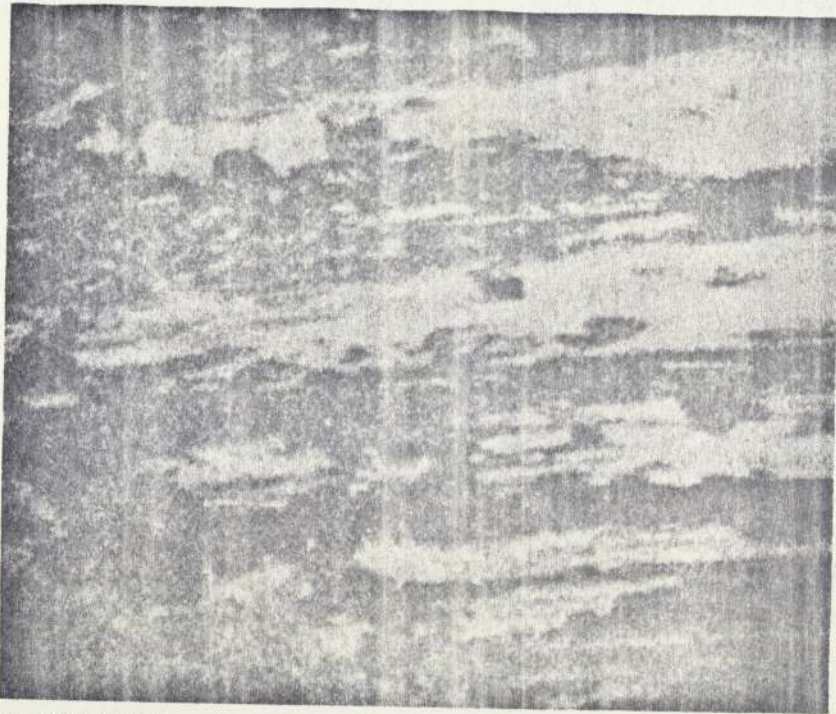
Fig. 94.4. 'Sulphur picture' of part of the wear scar formed under extreme pressure conditions with diallyl disulphide (d.a.d.s.) as the additive ('four-ball' geometry)
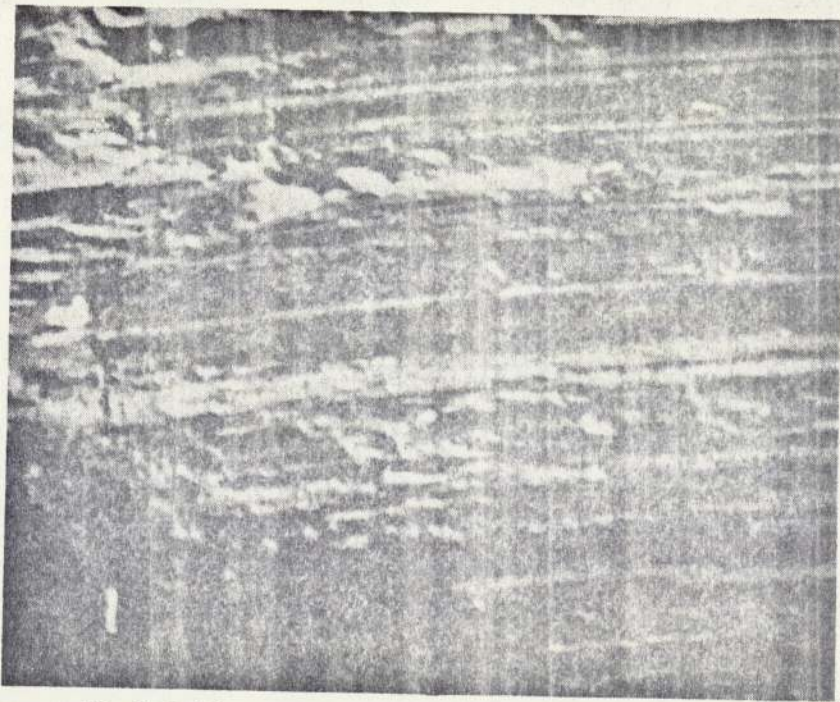
Fig. 94.5. 'Electron picture' of the region shown in Fig. 94.4

sulphur in the surface. Fig. 94.5 is the 'electron picture' for the same area. Comparison reveals that the sulphur lies in the raised grooved regions comprising the *real areas of contact*. This was confirmed by the 'iron pictures' (not shown here) in which the areas of high sulphur concentration in Figs 94.4 and 94.5 were shown to be areas of apparently low iron concentration, thereby indicating the

presence of a thick (i.e. > 1 μm) sulphur-containing film above the iron. Figs 94.6 and 94.7 respectively show the 'sulphur picture' and the 'electron picture' for a region very close to the edge of the scar formed on one of the flats in the '1-ball-on-3-flats' geometry, using d.b.d.s. as the extreme pressure additive. Once again, the presence of sulphur in the contact areas is most evident.
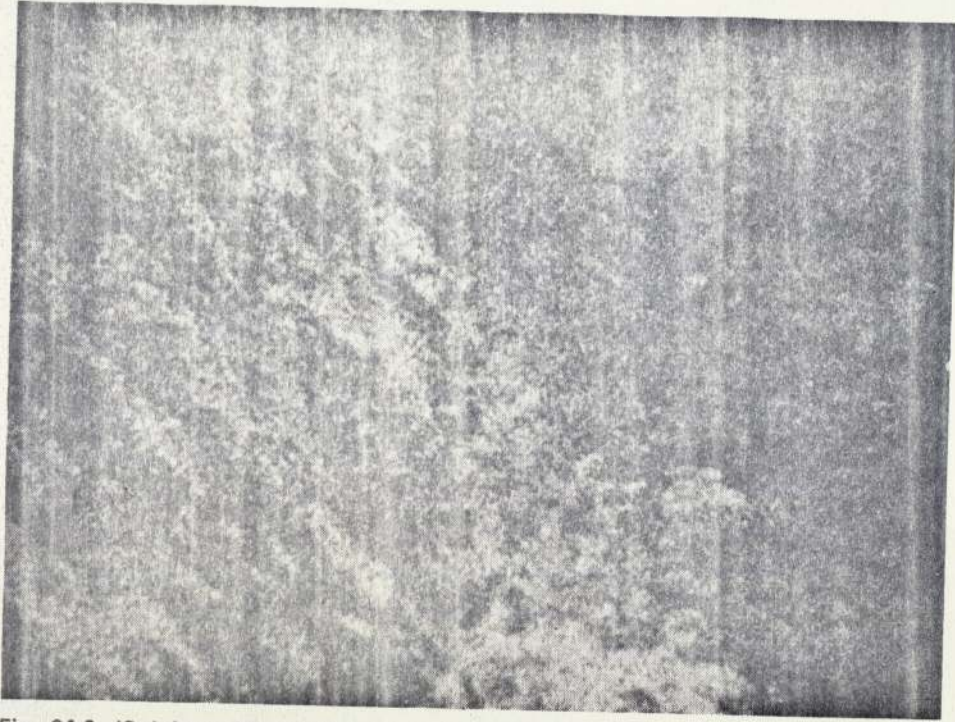
Fig. 94.6. 'Sulphur picture' from a region near the edge of the wear scar formed under extreme pressures with dibenzyl disulphide (d.b.d.s.) as the additive ('1-ball-on-3-flats' geometry)
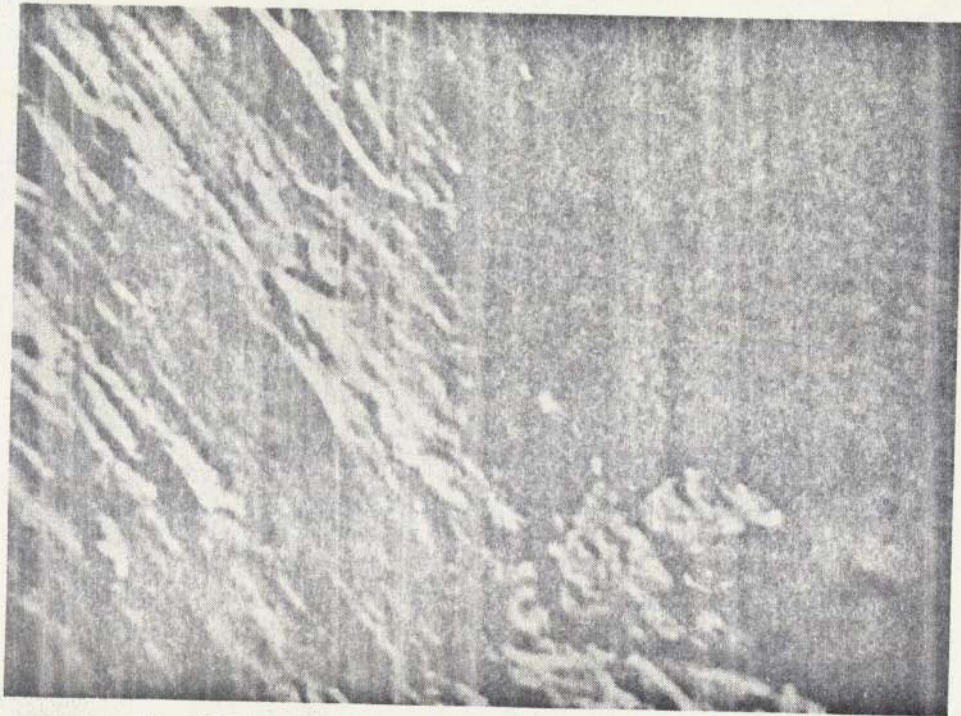
Fig. 94.7. 'Electron picture' of the region shown in Fig. 94.6

3.2 X-ray diffraction analysis

One would not expect the phosphorus and sulphur found in extreme pressure surfaces to be present in their elemental forms. Using X-ray diffraction it should be possible to determine the particular form in which the sulphur or phosphorus exists, as well as finding out which other compounds are present in the worn surfaces. A full

X-ray diffraction analysis of all the specimens used in this investigation is beyond the scope of this paper. For the present, it is sufficient to describe just two X-ray diffraction analyses, namely that relating to the pattern shown in Fig. 94.3 (from the wear scar formed with d.b.d.s. as additive) and that relating to the pattern from a wear scar formed with t.c.p. as additive.

Table 94.1. Identification of the compounds giving rise to
the glancing-angle X-ray diffraction patterns

Dibenzyl disulphide scar	Tricresyl phosphate scar
α-Fe	α-Fe
α-Fe$_2$O$_3$	α-Fe$_2$O$_3$
Fe$_3$O$_4$	Fe$_3$O$_4$
FeCr$_2$O$_4$	FeCr$_2$O$_4$
FeS	

There were 38 diffraction lines in the X-ray diffraction pattern from the d.b.d.s. scar and 17 lines in the pattern from the t.c.p. scar. Both patterns contained the four broad white lines corresponding to the 2·03, 1·43, 1·17 and 1·01 Å interplanar spacings of α-iron. These were used for calibrating the pattern (1). About 15 of the lines in the d.b.d.s. pattern correlated strongly with α-Fe$_2$O$_3$, about 12 with Fe$_3$O$_4$ and about 7 lines with FeCr$_2$O$_4$. FeS correlated strongly with 15 of the lines not fully
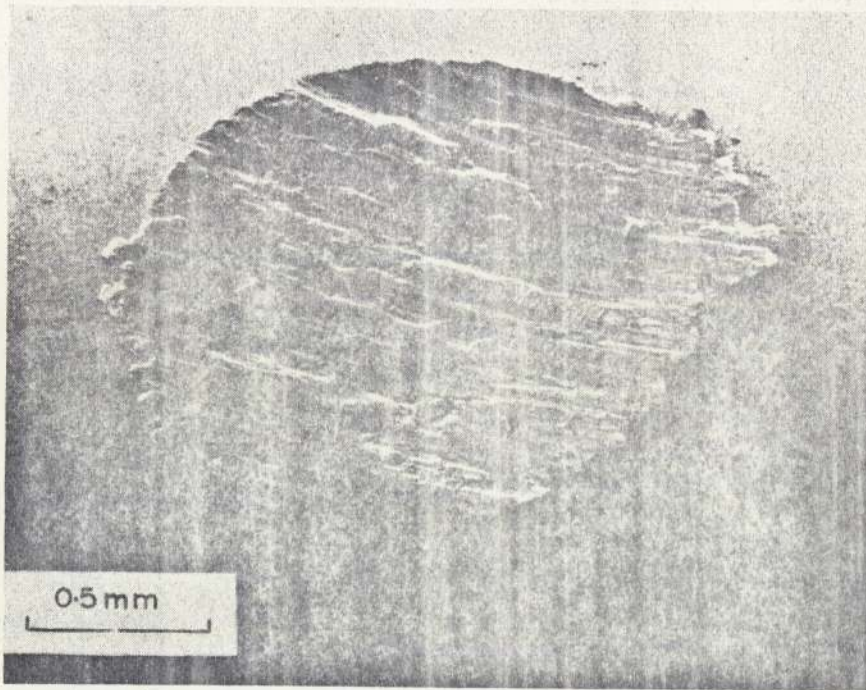
Fig. 94.8. Scanning electron micrograph of the wear scar on a ball worn with tricresyl phosphate (t.c.p.) as additive
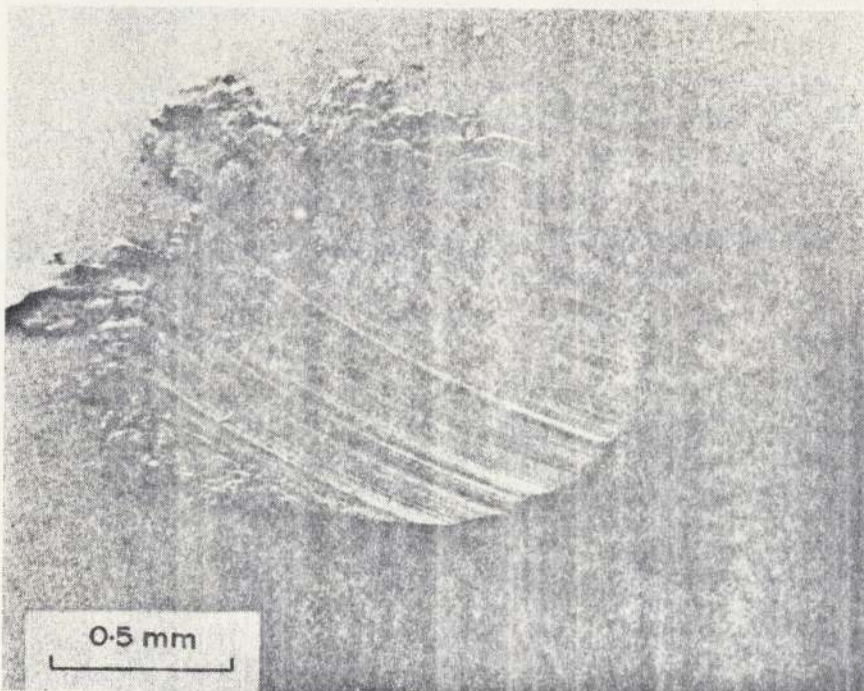
Fig. 94.9. Scanning electron micrograph of the wear scar on a ball worn with dibenzyl disulphide (d.b.d.s.) as the additive

explained by the other identifications. The 13 lines in the pattern from the t.c.p. scar not attributable to α-iron could, in fact, be explained in terms of a mixture of α-Fe_2O_3, Fe_3O_4 and $FeCr_2O_4$. It is interesting to note that no phosphorus compounds were detectable in the X-ray diffraction pattern obtained from the t.c.p. scar.

The analyses of the diffraction patterns from these two specimens are summarized in Table 94.1. Thus, one can see that the use of X-ray diffraction analysis has

(a) confirmed the presence of a sulphur compound in the d.b.d.s. surface,

(b) confirmed the non-detection of phosphorus by electron probe microanalysis of the t.c.p. worn surfaces, and

(c) indicated the presence of oxygen (in the form of oxides) which is normally beyond the detection limits for a conventional electron microprobe.

It is interesting to compare the worn surface topographies of these two specimens. Figs 94.8 and 94.9 are low-magnification scanning electron micrographs of the t.c.p. and the d.b.d.s. scars respectively. Clearly, the t.c.p. scar is much rougher and more severely worn than the d.b.d.s. scar.

4 DISCUSSION

This study of the surfaces formed during wear under conditions of extreme pressure lubrication has revealed that the combined use of electron probe microanalysis and the glancing-angle, edge-irradiated X-ray diffraction film technique can provide useful information not readily available by more conventional techniques. Furthermore, if one supplements the 'electron picture' (which one obtains with the microprobe and which is of fairly low resolution) with a few micrographs from the scanning electron microscope, the information is even more reliable and useful. For instance, scanning electron microscopy indicates that the worn surface topography is much smoother when using d.b.d.s. as an extreme pressure additive than when t.c.p. is used. The sulphur additive provides a scored, smooth surface with large flat plateaux, much like the surface obtained under mild dry wear (e.g. see Quinn (2)), whereas the phosphorus additive appears to provide a much rougher surface. Clearly, any further work along the lines of this investigation must include much more scanning electron microscopy.

The electron probe microanalysis of the scars formed with the sulphur additives has confirmed the findings of Allum and Forbes (3) that large percentages of sulphur are present. The present results, however, suggest that the sulphur is in the real areas of contact, i.e. the raised smooth islands, and in the debris, whereas Allum and Forbes (3) tend to detect sulphur mainly in the debris. These authors detected very little sulphur in the raised areas of contact (e.g. see Fig. 5(b) of reference (3)). This apparent difference in distribution may not be significant if the mechanism of extreme pressure lubrication involves the continuous formation and removal of the load-carrying film formed on the real areas of contact.

Most of the previous work on the action of organic phosphorus compounds as additives (4)–(6) tends to be concerned mainly with their antiwear properties, especially in the case of t.c.p. Electron probe microanalysis appears

to have been carried out in very few instances. Forbes et al. (7), reporting some work on the application of electron probe microanalysis to surfaces formed under extreme pressure lubrication using metal dialkyl dithiophosphates as additives, have shown that the metal, the sulphur and the phosphorus are all present in the same regions of the wear scar, in particular, in the rough areas below the smooth real areas of contact. The present results indicate that c.d.b.p.a., d.b.p.i. and d.b.p.a provide small amounts of phosphorus-containing layers within the scars, while the t.c.p. additive provides an undetectable amount of phosphorus within the immediate surface of the scar. This could mean that the phosphorus-containing layers are formed with much smaller film thicknesses than those occurring in extreme pressure lubrication with sulphur additives. In fact, this could be the source of the inferiority as extreme pressure additives of some phosphorus compounds compared with the sulphur compounds. Clearly, further work is required to elucidate the role of the phosphorus compound formed at the real areas of contact in protecting the surfaces under extreme pressure conditions. Such work must involve a technique (such as Auger spectroscopy) that has the ability to resolve the presence of elements in the uppermost layers of the worn surfaces. For example, the non-detection of phosphorus X-rays in the electron probe microanalysis of the t.c.p. scar does not preclude the possibility of an extremely thin film of a phosphorus compound being present. Unfortunately, the technique of Auger spectroscopy does not have the spatial resolution necessary to determine whether or not the phosphorus is in the real areas of contact within the scar.

The same criticism applies to the results obtained using the glancing-angle, edge-irradiated X-ray diffraction technique. Although the technique failed to detect any phosphorus compounds in the t.c.p. scar, this does not preclude the possibility of a thin film (say less than about 1 μm) being present. Also, the X-ray diffraction technique does not have the spatial resolution mentioned in the last paragraph. Nevertheless, the X-ray diffraction analyses of the d.b.d.s. scar has revealed the presence of FeS which, with the electron probe microanalysis, enables one to postulate that the sulphur in the additive has reacted with the iron, or iron oxides, in the real areas of contact to form iron sulphide.

In conclusion, it is obvious that more work is required in order to determine which compounds are formed in the surfaces of the wear scars formed with various sulphur and phosphorus compounds as extreme pressure additives. The role of the oxide films in extreme pressure lubrication also needs further elucidation.

APPENDIX 94.1

REFERENCES

(1) ISHERWOOD, B. J. and QUINN, T. F. J. 'The application of a glancing-angle X-ray diffraction film technique to the study of the low-temperature oxidation of iron–chromium alloys', Br. J. appl. Phys. 1967 18, 717.

(2) QUINN, T. F. J. 'The dry wear of steel as revealed by electron microscopy and X-ray diffraction', Proc. Instn mech. Engrs 1967–68 182 (Pt 3N), 201.

(3) ALLUM, K. G. and FORBES, E. S. 'The load-carrying mechanism of organic sulphur compounds—application of electron probe microanalysis', ASLE Trans. 1968 11, 162.

(4) BARCROFT, F. T. and DANIEL, S. G.   'The action of neutral organic phosphates as e.p. additives', *Trans. Am. Soc. mech. Engrs* 1965 **87**, 761.

(5) GODFREY, D.   'The lubrication mechanism of tricresyl phosphate on steel', *ASLE Trans.* 1965 **8**, 1.

(6) BIEBER, H. E., KLAUS, E. C. and TEWKESBERY, E. J.   'A study of tricresyl phosphate as an additive in boundary lubrication', *ASLE Trans.* 1968 **11**, 155.

(7) FORBES, E. C., ALLUM, K. G. and SILVER, H. B.   'The load-carrying properties of metal dialkyl dithiophosphates. Application of electron probe microanalysis', *Proc. Instn mech. Engrs* 1968–69 **183** (Pt 3P), 35.